Exploring and mapping the functional chemical space of amorphadiene synthase with non-canonical farnesyl diphosphate analogues

A thesis submitted to Cardiff University
for the degree of Doctor of Philosophy by:

Melodi Demiray

Supervisor: Rudolf K. Allemann

2016

Declaration

This work has not been submitted in substance for any other degree or award at this or any other university or place of learning, nor is being submitted concurrently in candidature for any degree or other award.

Signed …… (candidate) Date……

STATEMENT 1

This thesis is being submitted in partial fulfilment of the requirements for the degree of Doctor of Philosophy.

Signed …… (candidate) Date……

STATEMENT 2

This thesis is the result of my own independent work/investigation, except where otherwise stated, and the thesis has not been edited by a third party beyond what is permitted by Cardiff University's Policy on the Use of Third Party Editors by Research Degree Students. Other sources are acknowledged by explicit references. The views expressed are my own.

Signed …… (candidate) Date……

STATEMENT 3

I hereby give consent for my thesis, if accepted, to be available online in the University's Open Access repository and for inter-library loan, and for the title and summary to be made available to outside organisations.

Signed …… (candidate) Date……

STATEMENT 4: PREVIOUSLY APPROVED BAR ON ACCESS

I hereby give consent for my thesis, if accepted, to be available online in the University's Open Access repository and for inter-library loans **after expiry of a bar on access previously approved by the Academic Standards & Quality Committee.**

Signed …… (candidate) Date……

Abstract

Malaria is a threat to approximately 40% of the world's population. Artemisinin and its derivatives in combination therapy are the world's number one treatment against malaria. Agricultural production remains the primary source of artemisinin, however alternative methods are constantly being seeked to combat the unreliable and fluctuating processes present today. In addition, reported cases of parasitic resistance to the combination therapies emphasise the urgent need to produce novel and active analogues to replace the existing first line treatments.

Artemisinin is a terpenoid extracted from *Artemisia annua*. Terpenes constitute one of the largest families of natural products that boast a substantial degree of chemical diversity and functionality. The broad diversity of biological applications of terpenes has found several uses, particularly in medicine.

Terpene synthases convert linear isoprenyl diphosphates into complex hydrocarbon structures that exhibit exquisite stereochemistry. Amorphadiene synthase converts farnesyl diphosphate to amorpha-4,11-diene. This bicyclic frame, with four stereocenters is the first precursor found in the biosynthesis of artemisinin. Terpene synthases are studied extensively by scientists, because of their ability to generate complex structures that require several synthetic steps to reproduce the same complexity.

This project focuses on studying the promiscuity of amorphadiene synthase. By using the recombinant protein *in vitro* gives the advantage of feeding the enzyme with novel FDP analogues, in attempt to introduce new functionalities in the resulting amorphadiene structure. These added functional groups then serve as platforms to carry out further chemical steps or can be carried forward to the respective artemisinin derivative, and consequently tested for antimalarial activity. A library of FDP analogues were designed, synthesized and incubated with ADS to test for enzymatic activity. In addition to the search for new amorphadiene derivatives, one of the synthesized FDP analogues, 12-hydroxy FDP, was converted to dihydroartemisinic aldehyde. Dihydroartemisinic aldehyde is a precursor found further down the schematic pathway to artemisinin. A three-step chemo-enzymatic approach to producing dihydroartemisinic aldehyde was established, providing an alternative method to sourcing artemisinin.

Acknowledgements

I would like to take the time to thank quite a few people for their roles in supporting me during my Ph.D. The last four years have taught me that having a big team around you, both in and outside of work, make milestones such as this one achievable.

First and foremost I would like to thank my supervisor, Professor Rudolf Allemann, for giving me the opportunity to work on this amazing project. I am very grateful for your continued support and guidance throughout my Ph.D. It has been a pleasure to work under your supervision and in the Allemann group.

I would like to give a special thanks to Dr. Veronica Gonzalez, for her constant belief that I was capable of achieving this Ph.D, especially at times when I thought I was at a dead end. Her endless help, ideas, support and magic hands in the bio lab definitely helped me to finish my research. I am eternally grateful for everything that you do for me.

I would like to thank Dr. Juan Faraldos, for his in-depth conversations about terpenes, his crazy ideas that gave results and his overall enthusiasm to chemistry. You were a joy to learn from and you showed me the importance of always seeing the lab as a fun place to work.

I would like to thank Dr. David Miller for his extensive reading of my thesis and all reports, posters and presentations that I have made in the last four years. I have definitely learnt how to be a better scientific writer under your supervision.

I would like to thank Dr. Sabrina Touchet for her patience and guidance in my first year. She taught me all of the protein expression and molecular biology techniques that came across like a foreign language when I first started. She was an excellent teacher and gave a lot of her time to me so for that I am very grateful.

I would like to thank Dr. Xiaoping Tang and Marianna for keeping me sane, for making the office and lab enjoyable to work in and for always being up for a gin night to either drink away our problems or celebrate our successes of the day.

I would like to thank Dr. Robert Mart and Dr. Dan Grundy for their great chemistry knowledge, whenever I needed to brainstorm off one of them, they were always around to help and offer their opinion.

Thank you to Dr. Louis Luk for his daily supply of Haribo's and jokes, and to Antonio for his perfect coffee whenever we requested. Of course I would like to thank the rest of the Allemann group, especially Louis, Ryan, Will, Vicky, Zulfa, Antonio, Oscar and Stella for making my Ph.D enjoyable.

Lastly, in Cardiff University I would like to give a special thanks to Tom Williams and the rest of the technical staff for their advice and guidance when I had problems with the NMR or GC machines. Thank you Tom for always taking the time out to answer all of my questions and help me whenever needed.

Next I would like to thank everyone outside of work for all of their support, especially since for them I often think my stories from the chemistry lab made no sense but they continued to humour me and sound interested.

Firstly I would like to thank Hannah. My best friend who would always be on the other side of a phone to cheer me up when my research was plummeting, and at the same time sound completely ecstatic when I was on a high. Thank you for being you and always having a story to put a smile on my face. I promise to not bore you so much with my chemistry stories anymore, or at least less often?

Thank you to the boys from home (including the girls) for just being their usual selves and reminding me not to take things so seriously. They are the best group of friends to have around you when you want to de-stress and I'm lucky to have them as my best friends. Now that I finally finish this Ph.D they can stop with the 'Malaria never sleeps' joke!

A big thank you to the basketball girls, for providing lovely weekends away where we can all escape work and catch up on each other's lives. Thank you for always encouraging me to do my best and being there whenever I need one of you to talk too.

I would like to give my sincere gratitude to my aunty Belma and uncle Naeem. You both support and push me to excel in everything I put my mind too. You show me that nothing is impossible and your confidence in me gives me motivation to conquer all challenges. Thank you for being excellent role models to me.

I would like to thank dearly my mum and brother. Without your support and love, I would not be where I am today. You are my rocks that keep me going and you encourage me everyday to be the best I can. Thank you for always being there, whenever I have needed you. I am eternally grateful for having you as my mum and brother.

Lastly I would like to dedicate my thesis to my dad. Thank you for teaching me the biggest life lesson, that giving up is never an option no matter how hard the obstacle infront may be. I promise to remember all of the life lessons you tried to teach me and move them along with me to my next work place. Thank you for the late phone calls, for your endless advice and for your wise words.

Table of Contents

List of Figures

List of Schemes

List of Tables

List of Abbreviations

3,4-DHP	3,4-Dihydro-2*H*-pyran
9-BBN	9-Borabicyclo [3.3.1] nonane
ACT	Artemisinin based combination therapy
ADP	Adenosine diphosphate
ADS	Amorphadiene synthase
AMU	Atomic mass unit
ATP	Adenosine triphosphate
BL21 RP	BL21-(DE3)-Codon Plus RP cells
BOS	α-Bisabolol synthase
BPPS	(+)-Bornyl diphosphate synthase
CD	Circular dichroism
CDC	Centers for Disease Control and Prevention
MeI	Methyl iodide
MeMgI	Methyl magnesium iodide
CMP	Cytidine monophosphate
CoA	Coenzyme A
CTP	Cytidine triphosphate
DCM	Dichloromethane
DCS	δ-Cadinene synthase
DEAE	Diethylaminoethanol
DHFR	Dihydrofolate reductase
DHP	Dihydropyran
DHPS	Dihydropteroate synthase
DIBAL-H	Diisobutyl aluminium hydride
DMADP	Dimethylallyl diphosphate
DMF	Dimethylformamide
DNA	Deoxyribonucleic acid
DTT	Dithiothreitol
DXP	Deoxyxylulose phosphate
EBFS	(*E*)-β-Farnesene synthase
E. coli	*Escherichia coli*
EDTA	Ethylenediaminetetraacetic acid
FDP	Farnesyl diphosphate
FMOC-Cl	Fluorenylmethyloxycarbonyl chloride
FPS	Farnesyl diphosphate synthase
GAS	Germacrene A synthase
GC-FID	Gas chromatography flame ionisation detection

GC-MS	Gas chromatography mass spectrometry
GDP	Geranyl diphosphate
GDS	Germacrene D synthase
GGDP	Geranylgeranyl diphosphate
HEPES	4-(2-Hydroxyethyl)-1-piperazineethanesulfonic acid
HMG-CoA	Hydroxymethylglutaryl coenzyme A
HPLC	High pressure liquid chromatography
IDP	Isopentenyy diphosphate
IPTG	Isopropyl β-D-1-thiogalactopyranoside
β-ME	β-Mercaptoethanol
MEV	Mevalonate
MsCl	Methane sulfonyl chloride
MVA	Mevalonic acid
$NADP^+$	Nicotinamide adenine dinucleotide phosphate, oxidised form
NADPH	Nicotinamide adenine dinucleotide phosphate, reduced form
NBS	N-Bromosuccinimide
NDP	Nerolidyl diphosphate
NIST	National Institute of Standards and Technology
NMR	Nuclear magnetic resonance spectroscopy
NTA	Nitrilotriacetic acid
OD	Optical density
PCR	Polymerase chain reaction
PMSF	Phenylmethane sulfonyl fluoride
PPi	Diphosphate
PPTS	Pyridinium *para*-toluenesulfonate
SDM	Site-directed mutagenesis
SDS-PAGE	Sodium dodecyl sulfate polyacrylamide gel electrophoresis
TEAS	5-*Epi*-aristolochene
THF	Tetrahydrofuran
THP	Tetrahydropyran
TLC	Thin layer chromatography
TMSCl	Trimethylsilyl chloride
Tris	Trisaminomethane
TsOH	*para*-Toluene sulfonic acid
WHO	World Health Organisation
WT	Wild type

Chapter 1. Introduction

1. 1 Malaria

1.1.1 Overview of the disease

Malaria is a parasitic disease that is a threat to over 40% of the world's population. It is passed to a human through the bite of an infected female *Anopheles* mosquito.[1,2] In 1907, Charles Louis Alphonse Laveran was awarded the Nobel Prize in Physiology or Medicine for his research carried out in 1880 determining that it was protozoa that caused diseases such as malaria. Following his work, Ronald Ross identified female mosquitos as the host vectors for the parasites in 1897. He was awarded a Nobel Prize in Physiology or Medicine in 1902.[3]

The parasites responsible for this deadly disease are collectively termed as *Plasmodium* with *Plasmodium falciparum* causing the most severe and deadly infections. There are three other *Plasomodium* species known to cause malaria in humans, *P. vivax*, *P. malariae* and *P. ovale*. The symptoms seen in a patient can vary; uncomplicated malaria will cause fevers and chills that can be treated with no major complications. Severe malaria will result in anaemia, kidney failure, seizures, and even lead to death if left untreated. Children and pregnant women are the most vulnerable to catching this parasitic disease.[4]

The fight to control malaria has been an on-going struggle for over a century. Currently, the disease remains a major and growing threat to the public health and economic development of many countries. The regions that are affected by malaria are the sub tropical countries that lie on the equator, they possess the hottest and driest climates with low terrains. These optimal conditions enable mosquitos to successfully multiply and allow the *Plasmodium* mosquito to complete their growth cycle in their hosts. It is estimated that 90% of all malaria deaths occur on the African continent.[5,6] In 2015 the Centers for Disease Control and Prevention (CDC) stated that 214 million cases of malaria occurred worldwide, spread across 106 countries.[7]

When a mosquito feeds off a human for blood, she injects sporozoites into the human's blood stream. These sporozoites rapidly invade the liver cells where they develop during asexual reproduction to form merozoites. Depending on the class of *Plasmodium*, some of these liver stage parasites can remain dormant in the liver for years, allowing initiation of a cycle of asexual reproduction in the absence of a new mosquito bite. When the liver cells rupture due to the intensive replication of merozoites, which typically takes 5-10 days, the parasites are released back into the blood stream where they invade the red blood cells. Similarly, they begin to asexually reproduce in the red blood cells, eventually causing the destruction of each cell they infect. This is what causes the clinical symptoms of malaria, such as high fevers and chills.[8,9]

A small proportion of these merozoites will further develop into male and female gametocytes, and it is in this form that the parasites are taken back by a mosquito that feeds off that human. Whilst in the mosquito, the fusion of the male and female gametocytes forms diploid zygotes, which in turn become ookinetes. These migrate to the midgut of the mosquito; pass through the gut wall and form oocysts. Meiotic division of the oocysts lead to the formation of sporozoites which migrate to the salivary glands, ready to start another cycle of transmission (Figure 1.1).[10,11]

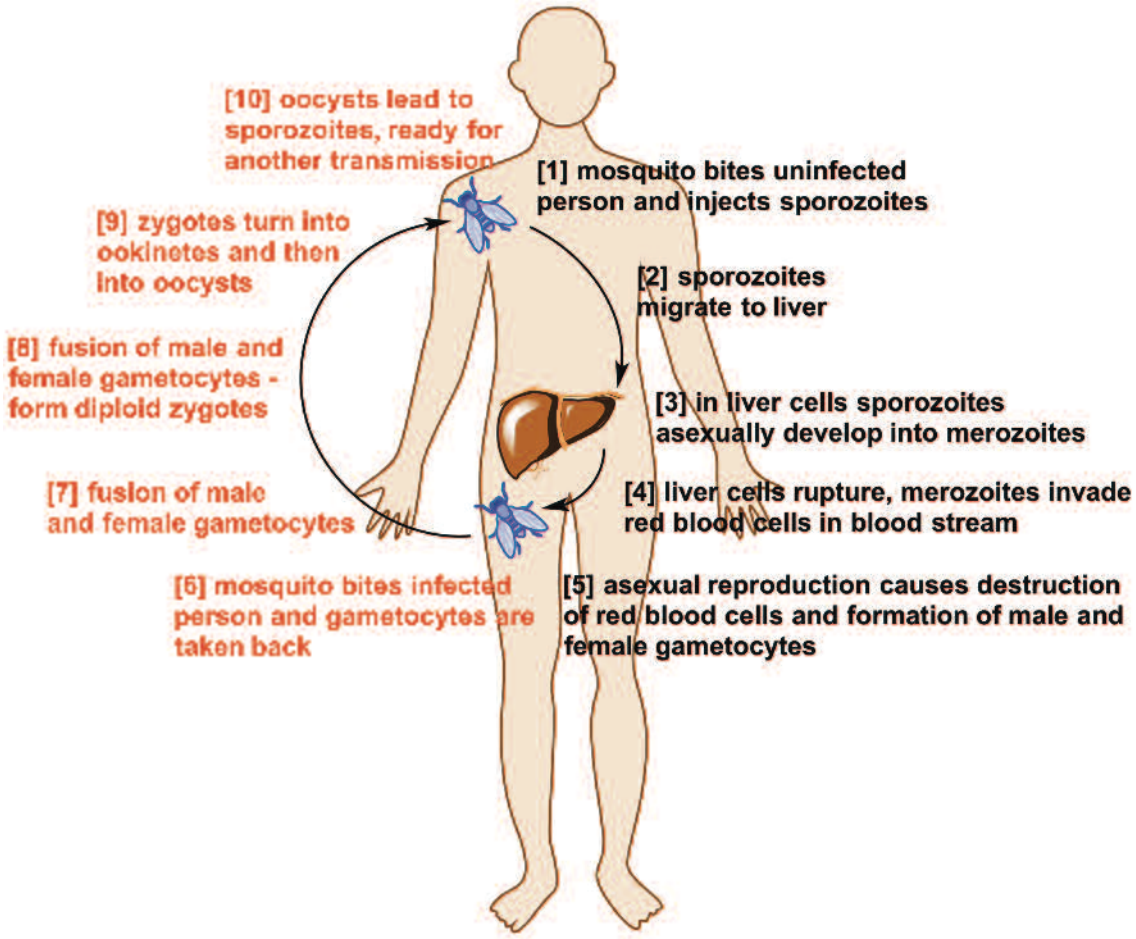

Figure 1.1 Cartoon representation of the life cycle of *Plasmodium* in an infected human (Black) and in a mosquito (Red).

1.1.2 Traditional chemotherapy for malaria

Quinine (**1**, Figure 1.2) was the first successful chemical compound that was found to treat malaria, and its use is reported as far back as the early 1600s. Quinine is a component of the bark of the cinchona tree originally found in Peru, South America. It is an alkaloid compound and due to its basic nature, is always presented as a salt, most commonly the dihydrochloride salt.[12] In 1820 French scientists, Pierre Pelletier

and Joseph Caventou, extracted the compound from the bark and isolated the pure alkaloid to be administered to patients. Before then it was simply dried, ground and mixed into some liquid such as wine or a spirit for administration, possibly the source of origin for the gin and tonic partnership that is still popular today. It remained the mainstream antimalarial drug for another century before more efficient, synthetic antimalarials became available.[13] While there are many other antimalarials that have been discovered to date, quinine continues to play a role in the management of malaria, and today is still recommended as the second line of treatment for the disease.[1]

Chloroquine (**2**, Figure 1.2) was the next major antimalarial drug that replaced quinine. Bayer AG synthesized the compound in 1934 as a result of the German government commissioning a search for a quinine alternative.[14] At first its properties were identified as too toxic to start clinical trials, and so it wasn't until 1942 that it was found to be active against malaria and there were no serious problems found with the toxicity.[15] More importantly it was found to be far superior compared to its derivatives that were being used at the time.[12] Chloroquine rapidly became available for all blood stage human malaria infections.[16] In addition, it was also used as a prophylactic drug after Mario Pinotti introduced the medicated salt program 'Pinotti's method'. Chloroquine was mixed into common cooking salt as a way of distributing it to everyone.[17] Chloroquine resistance in *Plasmodium falciparum* was first observed in the early 1960s and eventually the resistance grew until chloroquine could not be used as the first line treatment for malaria any longer.[18]

Pyrimethamine (**3**) and sulfadoxine (**4**, Figure 1.2) were the next major antimalarials to replace chloroquine.[19,20] After antifolates were found to be a successful treatment of leukemia and tumours, scientists started to focus on treating other rapidly dividing cells such as parasites with these antifolates.[21] The combination of the two drugs was introduced in the 1970s. Pyrimethamine and sulfadoxine are antifolate agents used synergistically, acting together to inhibit enzymes important in the parasites folate biosynthesis pathway. Dihydrofolate reductase (DHFR) is inhibited by pyrimethamine and dihydropteroate synthase (DHPS) is inhibited by sulfadoxine.[22] Neither of these antifolates is efficient enough to act alone as monotherapy treatment so the combination of the two is crucial.[23] Studies show that resistance to this duo is associated with point mutations in DHFR and DHPS.[24]

Mefloquine (**5**, Figure 1.2) was discovered by researchers at the Walter Reed Army Institute of Research in attempts to find a replacement for the first antimalarial, quinine. Initially the synthesis of this compound was very expensive, and so with the partnership of the 'UNICEF-UNDP-World Bank-WHO' special program for research and training in tropical diseases, and the pharmaceutical company Hoffmann-La Roche, a

cheaper synthetic pathway led to the product registration of mefloquine in 1984.[25] In 1986, mefloquine was combined with the sulphadoxine-pyrimethamine combination to treat malaria stricken patients. This trio of drugs was found to be effective until resistance developed for this combination, which led to their abandonment in 1989.[12,14]

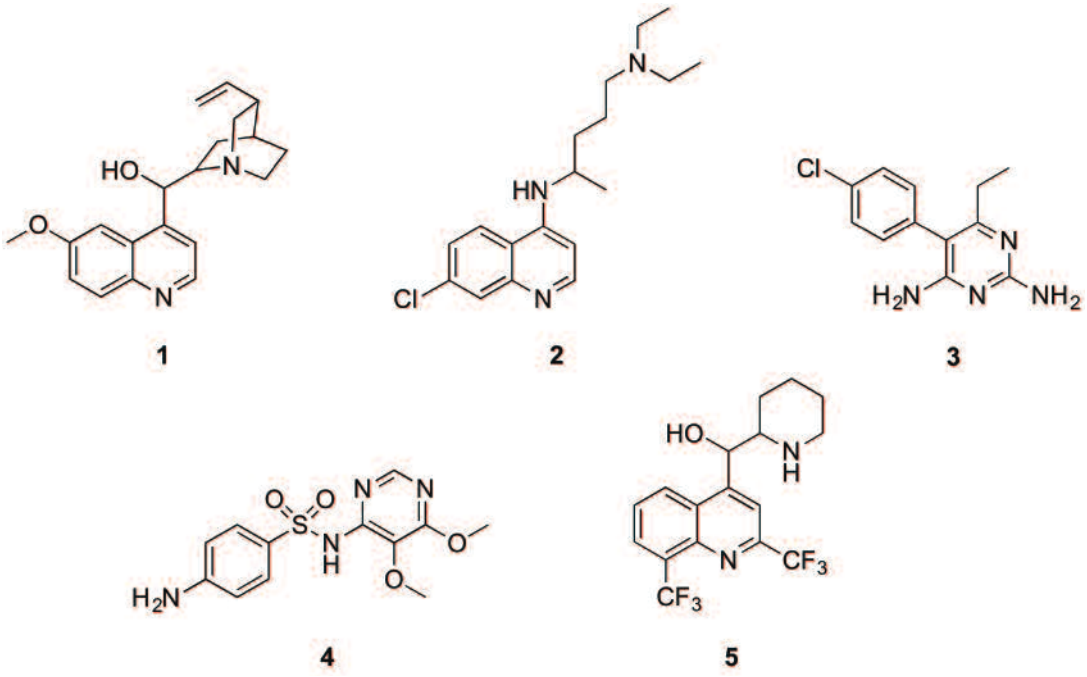

Figure 1.2 Quinine (1), chloroquine (2), pyrimethamine (3), sulfadoxine (4) and mefloquine (5).

1.1.3 Artemisinin and its derivatives

In the 1990s resistance to available antimalarial drugs worsened across the globe, and as a consequence, morbidity and mortality rates increased. The majority of deaths reported were those of African children.[26] In an attempt to reduce the death rate and control the parasitic disease, artemisinin based combination therapies (ACTs) were introduced. The success of the ACTs at a time where resistance had caused a fear of untreatable malaria was seen as a positive development. In 2005, the World Health Organisation (WHO) recommended that ACTs should be used as first line treatment for all severe malaria in countries where malaria was endemic.[27]

Artemisinin (**6**) (Figure 1.3) is derived from the herb *Artemisia annua*, also known as sweet wormwood, originally found in China. Although artemisinin was only introduced in the 1990s, the herb itself has been used for centuries in traditional Chinese medicine.[28] The earliest report of its use appears in Chinese books dating back to 168 BC, where the use of *A. annua* was reported to treat haemorrhoids, chills

and fevers.[14] The re-discovery of sweet wormwood came after the Chinese government set up a program named 'Project 523' in 1967 to screen traditional remedies in search for a new antimalarial drug. Professor Tu Youyou extracted the active ingredient artemisinin from the sweet wormwood herb into cold ether and this, when tested, exhibited antimalarial activity.[29,30] Professor Tu Youyou received the 2011 Lasker Award in clinical medicine[31] and was awarded a Nobel Prize in Physiology or Medicine in 2015.[32]

In 1972 the active ingredient, artemisinin, was extracted and purified.[33] This isolation of the compound led to the identification of its sesquiterpene trioxane lactone structure.[34] Artemisinin was proven to be an antimalarial of rapid action, high efficiency and low toxicity that gave quicker parasite clearance than all formerly used antimalarials.[33] The disadvantages of artemisinin are poor solubility in water and oil and the high recrudescence rate of *Plasmodium* when artemisinin is used to treat malaria. This led to the synthesis of artemisinin derivatives. Water-soluble derivatives of artemisinin included artesunate (**7**) and artelinate (**8**), and the oil-soluble derivatives saw the creations of artemether (**9**) and arteether (**10**) (Figure 1.3).[35,36]

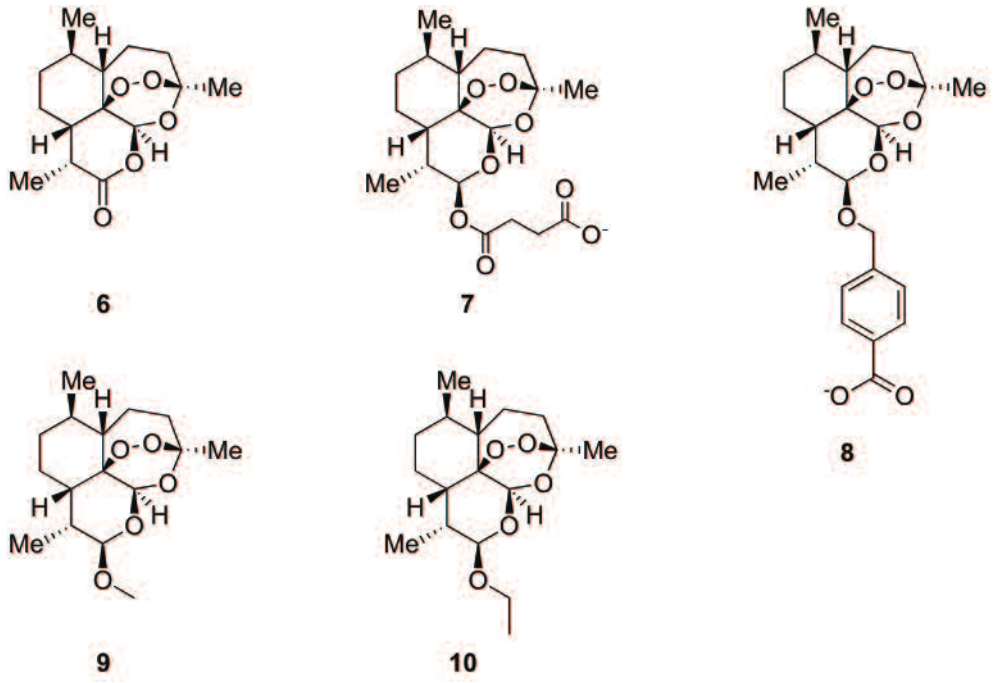

Figure 1.3 Artemisinin (6), artesunate (7), artelinate (8), artemether (9) and arteether (10).

The concept of ACTs presents the idea that by giving two drugs, the chances of a parasite developing resistance to both drugs at the same rate are reduced.[37,38] In addition to this, since artemisinin and its derivatives have a very short elimination half-life after being administered into a patient, this precludes the possibility of using it on its

own as monotherapy treatment. Combining the artemisinins with other antimalarial drugs that have a longer half-life, grants a more effective method for treating the parasitic disease with a reduced possibility of recrudescence.[39,40]

The discovery of artemisinin introduced an entirely new class of drugs for treatment of malaria. Unlike the former antimalarials, artemisinin and its derivatives all contain a unique 1,2,4-trioxane ring structure which is believed to be responsible for the antimalarial activity.[41,42] Another difference from the other antimalarial drugs is that artemisinin lacks nitrogen containing heterocyclic ring systems. Despite the artemisinins being a unique class of molecules and to date, the only group of antimalarials that have not received an excessive amount of parasitic resistance, there is still a lot to learn about them. Although there are several theories on their mode of action, the precise nature of how the drug inhibits malarial growth is still to be established.[43–47]

Antimalarials are among the most commonly used medications in tropical regions of the world. Unfortunately their extensive misuse has caused human-hosted malaria parasites to evolve mechanisms of resistance and so there is a continuous race to provide alternative antimalarials that are efficient and cost effective.[37,48] To continue using the existing artemisinins without appreciating that resistance unfortunately will alter the success of these drugs would be irresponsible. Therefore there is always a constant duty for scientists to find an alternative; to create a new drug that will be ready to take over as the next first line of treatment to contribute to global malaria control.

1. 2 Terpenes

Terpenes and terpenoids constitute one of the largest families of natural products that boast an amazing degree of chemical diversity and functionality. To date, there are more than 60,000 known terpenes, mainly found in plants, but they are also found in fungi, bacteria and humans.[49] This thesis however will solely focus on terpenes derived from plants.

In plants, not only do terpenes exist as primary metabolites, serving purposes such as membrane structure and function (*e.g.* campesterol, **11**)[50] and photosynthetic pigments (*e.g.* β-carotene, **12**)[51], they also exist as a product of secondary metabolism.[52,53] Secondary metabolites in plants have properties that include repelling herbivorous insects (*e.g.* 7-epizingiberene, **13**)[54] and attracting pollinators (*e.g.* β-phellandrene, **14**)[55].

The broad diversity of biological applications of terpenes is of great interest to scientists, particularly in medicine and agriculture. The use of oils isolated from plants in traditional medicine dates back over 4500 years ago, many of which are still in use

today.[56] At present times, terpenes are used as anti-cancer drugs (*e.g.* taxol, **15**) and antimalarials (*e.g.* artemisinin, **6**) as well as for non-medicinal use, such as fragrance ingredients (*e.g.* (-)-menthol, **16**) and flavourings (*e.g.* (*R*)-limonene, **17**), to name but a few (Figure 1.4).[57]

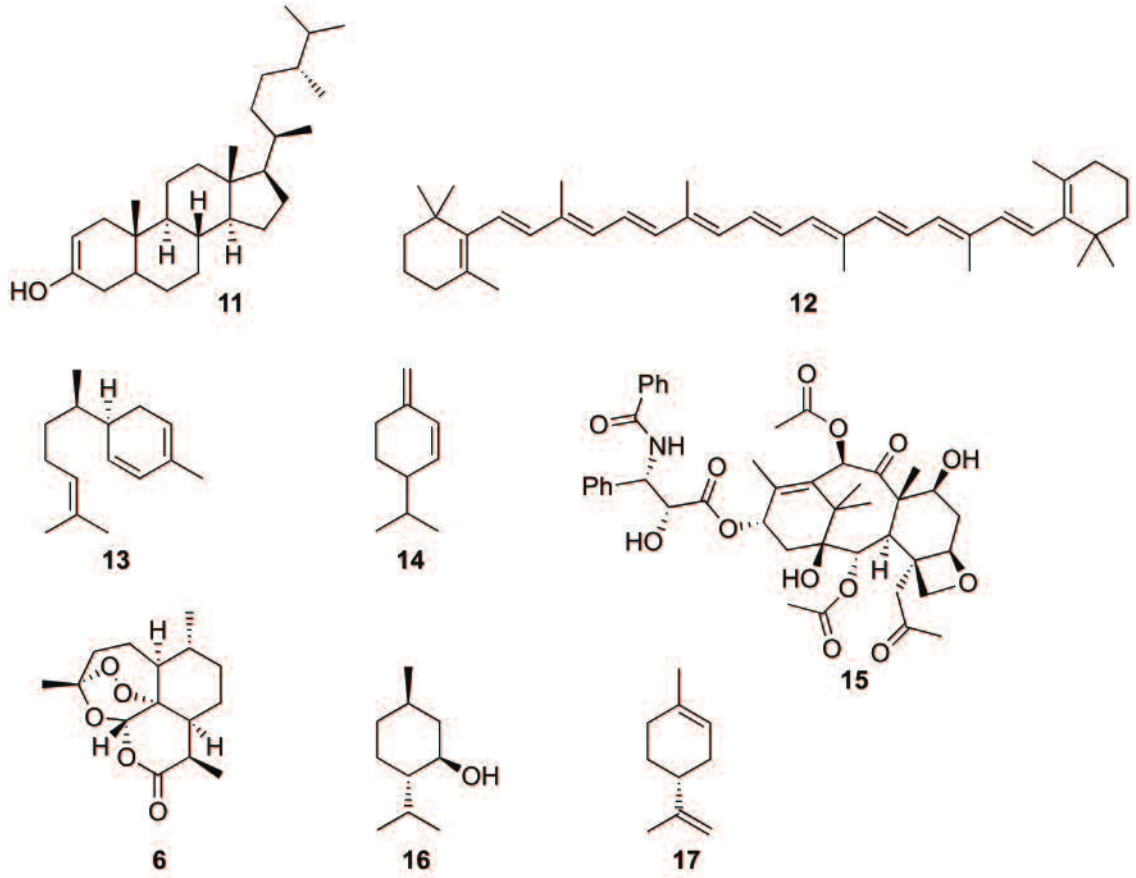

Figure 1.4 Campesterol (11), β-carotene (12), 7-epizingiberene (13), β-phellandrene (14), taxol (15), artemisinin (6), (-)-menthol (16), and (*R*)-limonene (17).

All terpenes are constructed by the repetitive coupling of the branched five-carbon building blocks, isopentenyl diphosphate (IDP, **18**) and dimethylallyl diphosphate (DMADP, **19**).[58] The resulting terpenes are classified into groups depending on how many isoprene units (**20,** Figure 1.5) the terpene skeleton is comprised of (Table 1.1). Otto Wallach presented the concept of an empirical isoprene rule in 1887. Initially, the 'empirical isoprene rule' was used to define terpenes as compounds that were composed of one or more isoprene units, with an empirical formula of C_5H_8 (**20**, Figure 1.5).[59] Research by Leopold Ruzicka in 1953 led to the rule being modified. Renaming it the 'biogenetic isoprene rule' added the possibility of the fused, acyclic terpene skeleton cyclizing and undergoing rearrangements to form the final product.[60,61]

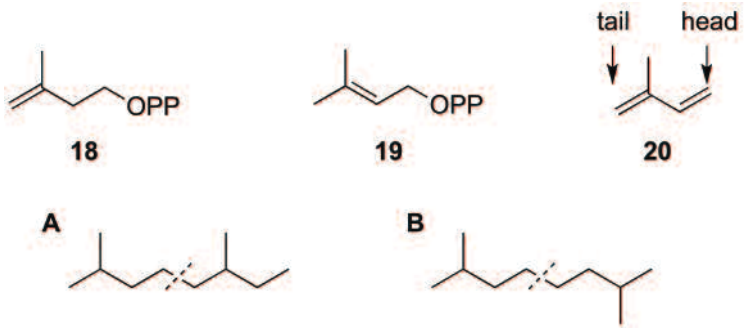

Figure 1.5 IDP (18), DMADP (19) and isoprene (20). A: Regular 'head to tail' coupling of IDP and DMADP. B: Irregular 'head to head' coupling of IDP and DMADP.

Table 1.1 Classification of terpenes

Class	C_x	Precursor	Example
Hemiterpenes	5	dimethylallyl diphosphate (DMADP)	isoprene
Monoterpenes	10	geranyl diphosphate (GDP)	limonene
Sesquiterpenes	15	farnesyl diphosphate (FDP)	amorpha-4,11-diene
Diterpenes	20	geranylgeranyl diphosphate (GGDP)	taxol
Sesterterpenes	25	geranylfarnesyl diphosphate (GFDP)	cheilanthatriol
Triterpenes	30	(2) x farnesyl diphosphate	gossypol
Tetraterpenes	40	(2) x geranylgeranyl diphosphate	β-carotenoid

1.2.1 Biosynthesis of terpenes

In plants the precursors to all terpenes, IDP and DMADP, are biosynthesized *via* two different pathways, depending on the subcellular compartment of the plant they are generated in.[62] The mevalonate (MEV) pathway is found in the cytosol whereas the deoxyxylulose phosphate (DXP) pathway (also known as the non-mevalonate pathway) is found in the plastids.[63] In addition to this, different groups of terpenes are also produced in different compartments of a plant. Monoterpenes and diterpenes tend to be made in the plastid compartments of plants, whereas sesquiterpenes and triterpenes tend to be synthesised in the cytosol compartments.[64]

Mevalonate pathway

The mevalonate pathway (Scheme 1.1) starts with a Claisen condensation of two molecules of acetyl-coenzyme A (acetyl-CoA, **21**) to form acetoacetyl-CoA (**22**). An addition of a third acetyl-CoA molecule affords 3-hydroxy-3-methylglutaryl-CoA (HMG-

CoA, **23**). This aldol reaction is catalysed by HMG-CoA synthase.[65] HMG-CoA reductase, with two equivalents of NADPH, converts HMG-CoA to mevalonic acid (**24**). Two sequential ATP-dependent phosphorylations follow to form 5-diphosphomevalonic acid (mevalonic acid diphosphate, **25**) with the use of mevalonate kinase and 5-phosphomevalonate kinase.[66] Mevalonic acid diphosphate undergoes an ATP-dependent decarboxylation and an elimination of water, catalysed by diphosphomevalonate decarboxylase, to afford IDP (**18**). Lastly, IDP isomerase catalyses an isomerisation to DMADP (**19**).[67]

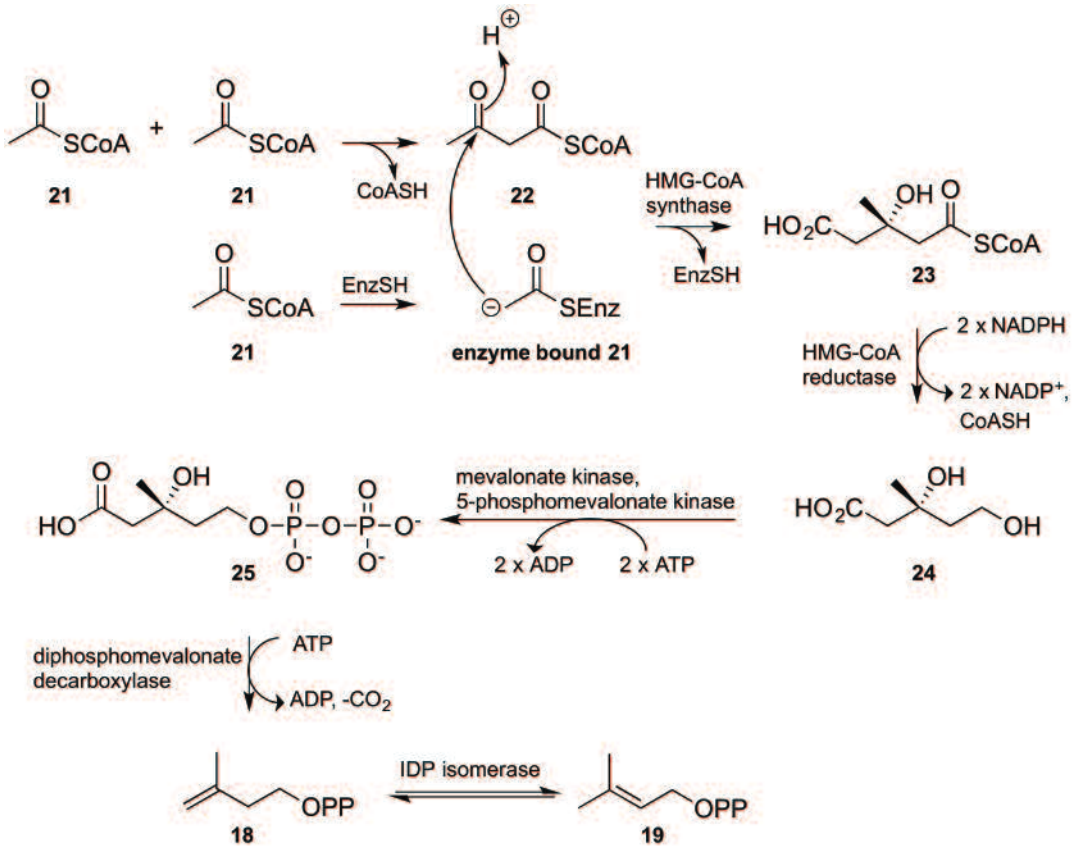

Scheme 1.1 Biosynthesis of IDP (18) and DMADP (19) *via* the mevalonate pathway.

Deoxyxylulose phosphate pathway

The alternative deoxyxylulose pathway (Scheme 1.2) begins with the addition of an 'activated acetaldehyde', generated from pyruvate (**26**) and thiamine diphosphate (TDP), to glyceraldehyde 3-phosphate (**27**) to form 1-deoxy-D-xylulose 5-phosphate (**28**).[68] 1-Deoxy-D-xylulose 5-phosphate (**28**) is converted to 2C-methyl-D-erythritol 4-phosphate (**29**) catalysed by 1-deoxy-D-xylulose 5-phosphate reductoisomerase (IspC) in a NADPH-dependent reaction. The next step involves the addition of cytidine monophosphate (CMP) on to the terminal phosphate group of **29** to form 4-diphosphocytidyl-2C-methyl-D-erythritol (**30**), which then follows with an ATP-

dependent phosphorylation to produce 4-diphosphocytidyl-2C-methyl-D-erythritol 2-phosphate (**31**). This intermediate cyclises to 2C-methyl-D-erythritol 2,3-cyclodiphosphate (**32**) with the loss of CMP.[69] A reductive ring opening of the cyclic diphosphate forms 1-hydroxy-2-methyl-2-(*E*)-butenyl diphosphate (**33**). The final step of the deoxyxylulose phosphate pathway consists of two stepwise single-electron transfers from an iron-sulfur cluster and a cleavage of the hydroxyl moiety to yield an allylic carbanion. Deprotonation of the carbanion affords either IDP or DMADP.[70]

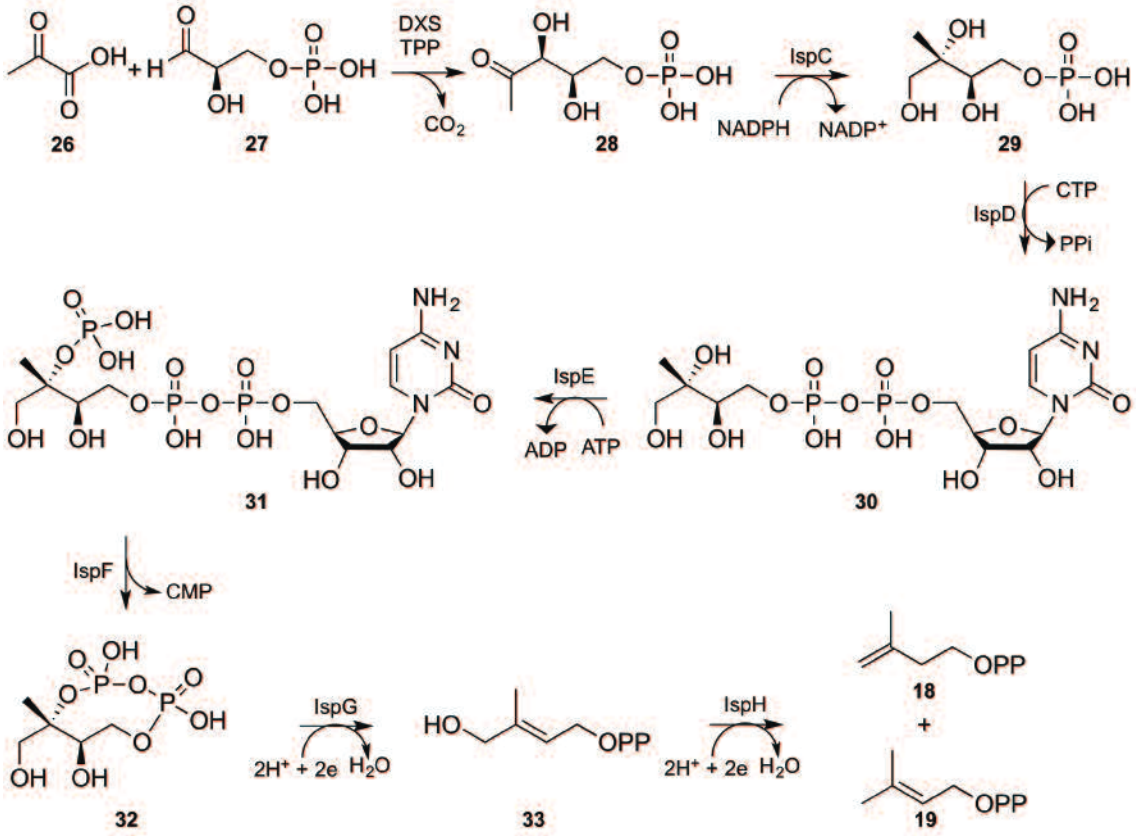

Scheme 1.2 Biosynthesis of IDP (18) and DMADP (19) *via* the deoxyxylulose phosphate pathway.

Isoprenyl diphosphate elongation

A family of enzymes called isoprenyl diphosphate synthases catalyse the chain elongation reactions that involve sequential condensations of IDP and DMADP (Scheme 1.3). Geranyl diphosphate synthase carries out the most simple chain elongation reaction involving a condensation of IDP and DMADP to produce GDP (**34**).[71] The isoprenyl diphosphate synthase directs the condensation by initiating a Mg^{2+} dependent cleavage of the diphosphate moiety from DMADP. The resulting cation is attacked by the electron rich double bond on a molecule of IDP resulting in a tertiary carbocation (**35**) (Scheme 1.3). A deprotonation of **35** at C2 results in the formation of

GDP.[72] The formation of FDP (**36**), catalysed by FDP synthase, adds a second molecule of IDP onto GDP to create a C_{15} hydrocarbon chain. Subsequent elongations occur with additional units of IDP to create GGDP (**37**, C_{20}) and increasingly longer isoprenyl chains.[73]

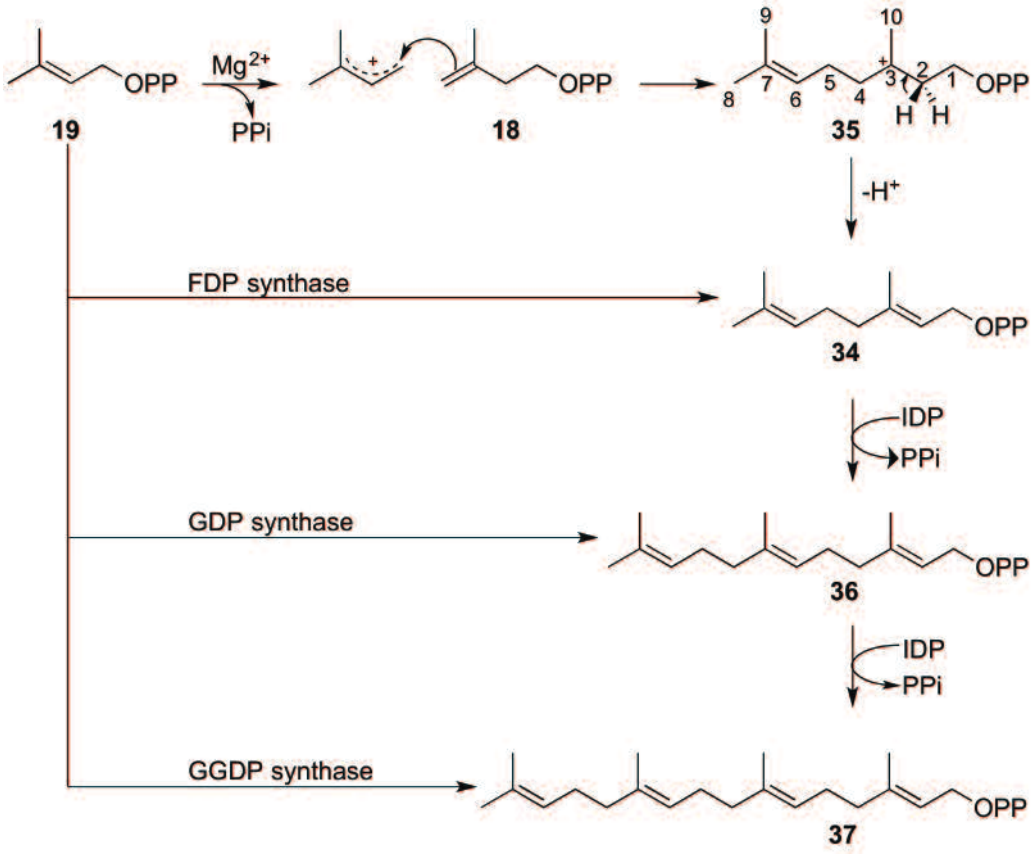

Scheme 1.3 Biosynthesis of isoprenyl diphosphates catalysed by prenyltransferases.

Isoprenyl diphosphates are converted to mature terpenes by terpene synthases (Section 1.3). They often then undergo further redox modifications mediated by a series of cytochrome P450s and other oxidoreductases to produce the many thousands of different terpenoid metabolites of plants (Figure 1.6).[74] Examples are found across all classes of terpenes. Monoterpene precursor GDP (**34**) is cyclised to α-pinene (**38**) by α-pinene synthase and further converted to (+)-verbenone (**39**) for example. Verbenone is used by bark beetles as a dispersal pheromone to modulate the attack density on conifers.[75–77] FDP (**36**) is converted to the sesquiterpene germacrene A (**40**), catalysed by germacrene A synthase and then further converted to costunolide (**41**), an insect deterrent produced in lettuce and chicory.[78,79] An example for the C_{20} precursor, GGDP (**37**), is seen in the conversion to the diterpene abietadiene (**42**), which is further oxidised to ferruginol (**43**), the major constituent of

resin which is secreted from the miro tree (*Podocarpus ferrugineus*) as a chemical defense against any cuts or incisions made to the tree bark (Figure 1.6).[80–82]

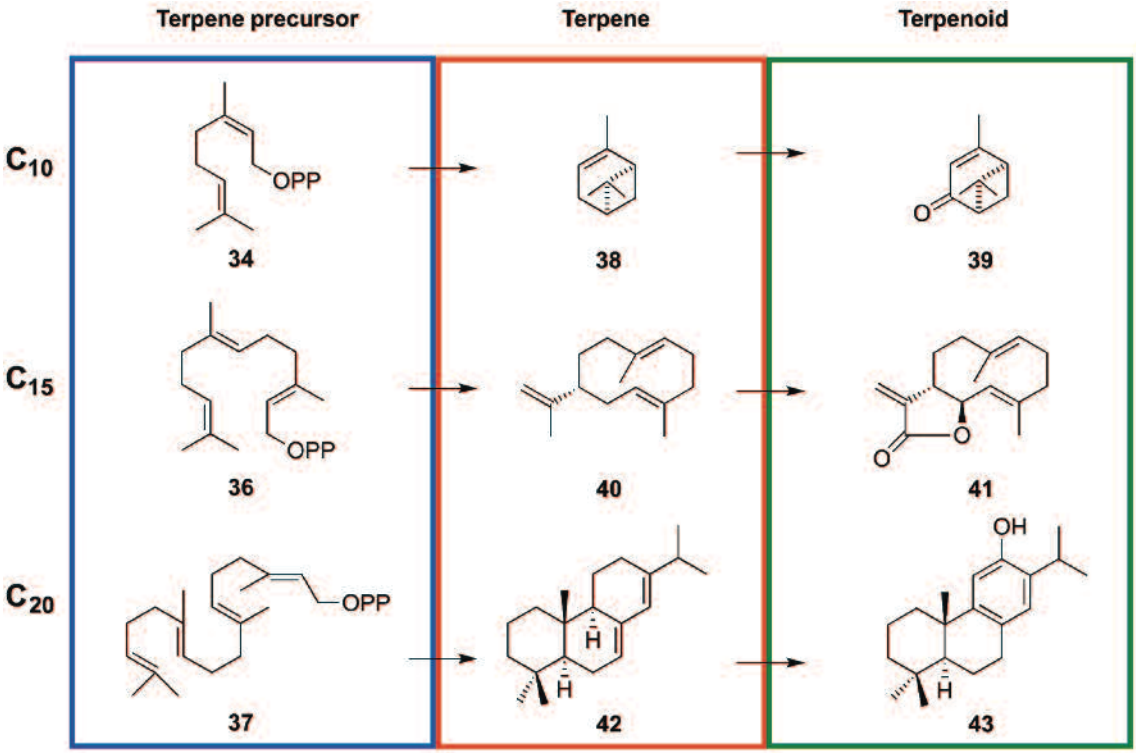

Figure 1.6 Examples of conversions of isoprenyl diphosphates to the terpenoids (+)-verbenone (39), costunolide (41) and ferruginol (43).

1. 3 Terpene synthases

Terpene synthases are crucial for catalysing the stereoselective conversion of acyclic isoprenyl diphosphates into a vast number of chiral terpenes. Tens of thousands of natural terpene products have been identified to date, all stemming from a small number of precursors.[83] This draws attention to the complex nature of the chemical reactions taking place in the active site of these synthases, and their ability to create unique compounds with structural and stereochemical precision. Terpene synthases guide substrates through changes in bonding, hybridization, and configuration in series of precise cascades.[84] Terpene synthases exhibit a high degree of functionality for the active site to control all these rearrangements. They are also specifically composed to handle the highly reactive intermediates formed in the cascade of reactions. The hydrophobic active site effectively mimics an inert organic solvent in a normal cyclisation reaction and the presence of fixed and protected dipoles and aromatic residues with ring π-electrons stabilise the carbocation intermediates formed.[85–87]

One example of a terpene synthase that boasts remarkable precision is lanosterol synthase. This is used in the biosynthesis of cholesterol and produces only 1 out of a possible 128 stereoisomers of lanosterol.[88] There are, however, terpene synthases that show more promiscuity in their product profile, generating multiple terpenes. An example of a more promiscuous synthase is γ-humulene synthase, which generates an astonishing 52 products from FDP as its sole substrate.[89]

There are two different mechanisms for initiating the polycyclisation cascade that leads to the formation of terpenes; therefore terpene synthases can be divided into two classes. Class I terpene synthases require three magnesium ion co-factors to co-ordinate to the diphosphate group, resulting in a cleavage of the group and ionisation of the isoprenyl chain.[86,90] Class II terpene synthases differ in their initial catalytic step. Instead of dephosphorylating the isoprenyl diphosphate they generate the initial carbocation via a protonation of the distal C=C bond or an epoxide derivative thereof.[91,92]

The terms 'terpene' and 'terpenoid' are used interchangeably in the literature with no consensus on their definitions. For clarity in this work however, a terpene is defined as the hydrocarbon or alcohol product specifically arising as a product from terpene synthase catalysis, whereas terpenoids are defined as the downstream biosynthetic derivatives of the initial terpene.

1.3.1 Sesquiterpene synthases

Sesquiterpene synthases catalyse the metal dependent conversion of FDP to generate a rich diversity of sesquiterpene scaffolds. Most plant sesquiterpene synthases consist of two α-helical domains and belong to the family of class I synthases. The C-terminal α-domain is known as the catalytically active domain as it holds the active site where FDP enters and is converted to a sesquiterpene.[93] The function of the N-terminal domain is still unclear, as it appears to lack catalytic activity, however it is proposed that, in some cases at least, it is crucial for desolvating the substrate and ensuring the correct folding of the C-terminal domain.[94–96]

Common to all sesquiterpene synthases, the active site contains two metal binding regions that bind three Mg^{2+} ions, necessary for the initiation of the catalytic cycle. The first motif is an aspartate rich 'DDXXD/E' motif, which binds Mg_A^{2+} and Mg_C^{2+} and the second, a 'DTE' motif that binds Mg_B^{2+}.[97] There are a few exceptions, for example (+)-δ-cadinene synthase from *Gossypium arboreum* does not possess a DTE motif and instead has a second DDXXD motif, and (+)-germacrene D synthase from *Solidago canadensis* has a NDTYD motif to replace the first DDXXD motif.[98,99] These highly conserved motifs were first observed when the X-ray crystal structure of farnesyl

diphosphate synthase (FPS) was solved.[100] Even with the slight differences, the metal binding motifs are all used for the same purpose. They bind to three Mg^{2+} ions, which in turn co-ordinate with the diphosphate moiety of FDP. The carbon-phosphoester bond breaks through ionisation and generates a highly reactive carbocation. The binding of the trinuclear magnesium cluster to the diphosphate triggers closure of the active site, shielding the carbocation from water.[101,102] Following the cleavage of the diphosphate group, sesquiterpene synthases chaperone the reaction through a series of reactions that culminate in the quenching of a final carbocationic species.[103] 5-*Epi*-aristolochene synthase (TEAS) from *Nicotiana tabacum* was one of the first sesquiterpene synthases to have its crystal structure solved.[104] In later work by creation of a complex with TEAS and an FDP analogue that acts as an inhibitor, 2-fluoro-farnesyl diphosphate (2F-FDP, **44**), a clear view of how the FDP substrate is positioned in the active site of a sesquiterpene synthase was revealed (Figure 1.7).[101]

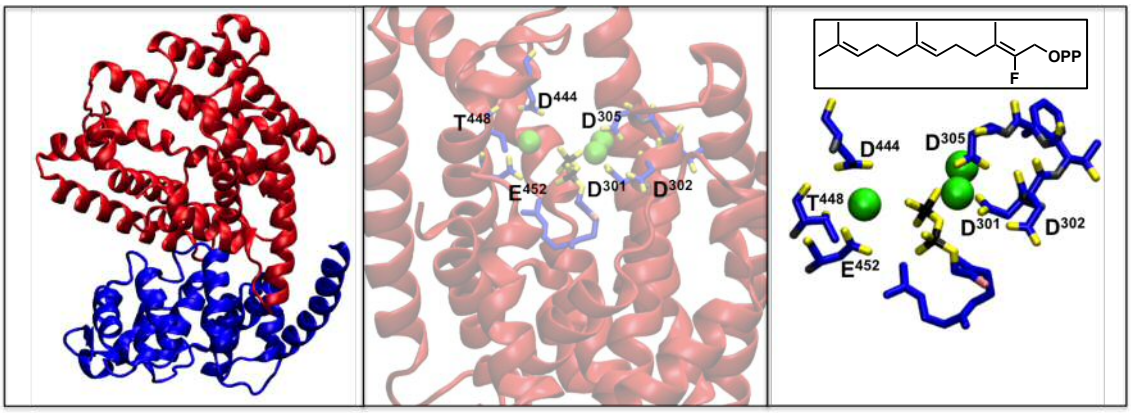

Figure 1.7 Left: Cartoon representation of the crystal structure of 5-*epi*-aristolochene synthase from *Nicotiana tabacum* (PDB 3MO1), showing the N-terminal domain in blue and the catalytic C-terminal domain in red. Middle: Schematic view of the TEAS:2F-FDP complex. Right: simplified representation of the coordination of $[Mg^{2+}]_3$-2F-FDP. D444, T448 and E452 coordinate to one Mg^{2+} ion and D301 and D305 coordinate the other two Mg^{2+} ions. Mg^{2+} ions are shown as green balls and 2F-FDP (44, inset picture) is represented where the black denotes phosphorus and the yellow denotes oxygen.

1.3.2 Amorpha-4,11-diene synthase and artemisinin

Amorpha-4,11-diene synthase (ADS) (Figure 1.8) from *A. annua* is a 571 residue sesquiterpene synthase that catalyses the conversion of FDP (**36**) into amorpha-4,11-diene (hereafter referred to as amorphadiene, **45**). ADS catalyses the first committed step of artemisinin biosynthesis in *A. annua* (Scheme 1.4).[105,106]

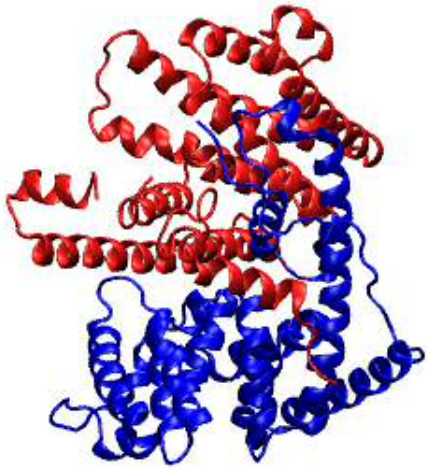

Figure 1.8 Cartoon representation of ADS. The homology model is based on the crystal structure of α-bisabolol synthase from *A. annua* (4GAX.pdb) with 82% sequence identity to ADS.[107] Blue denotes the N-terminal domain and red denotes the catalytic C-terminal domain. The homology model was constructed using SWISS-MODEL (http://swissmodel.expasy.org/).[108–110]

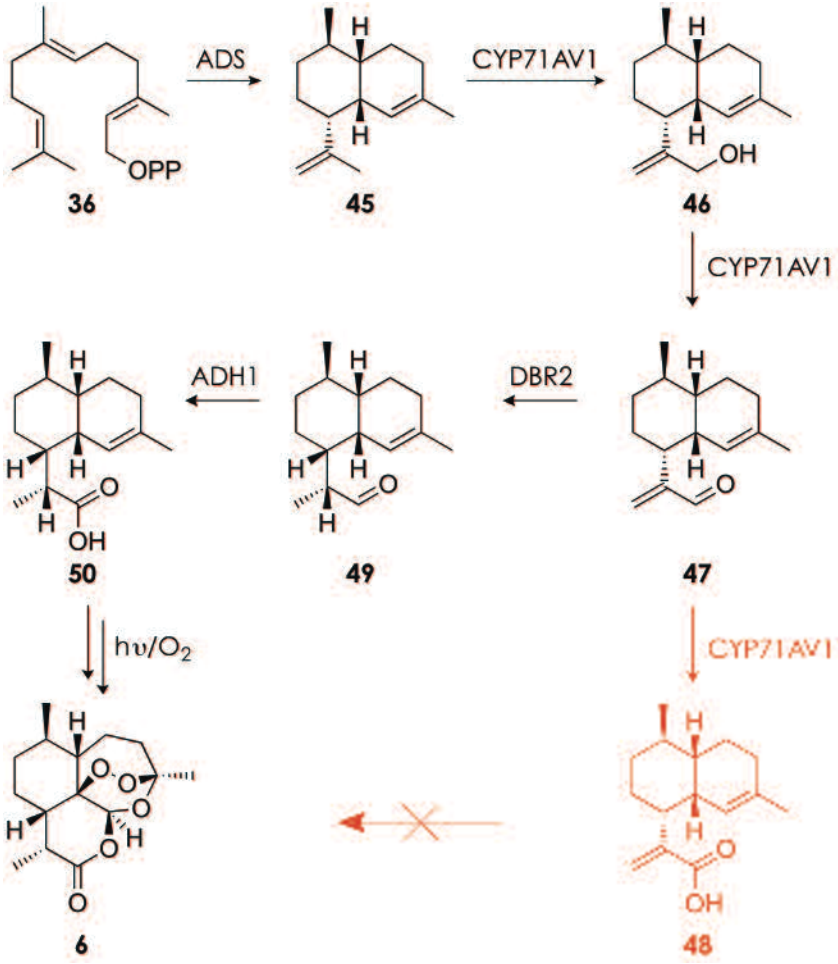

Scheme 1.4 Biosynthesis of artemisinin (6).

After the initial ADS dependent cyclisation of FDP to amorphadiene, a cytochrome P450 dependent hydroxylase (CYP71AV1) oxidises amorphadiene to artemisinic alcohol (**46**) and then further to artemisinic aldehyde (**47**).[111] The same hydroxylase can further oxidise **47** to artemisinic acid (**48**), however this compound has been shown not to be a precursor to artemisinin, despite earlier reports claiming otherwise.[112] Artemisinic aldehyde is reduced by a reductase (DBR2) to form dihydroartemisinic aldehyde (**49**), which is then oxidised to dihydroartemisinic acid (**50**) by aldehyde dehydrogenase 1 (ADH1).[113,114] The conversion of dihydroartemisinic acid to artemisinin is believed to be non-enzymatic.[115–118]

Interestingly, the intermediates and enzymes involved in the biosynthesis of artemisinin were not discovered in sequential order. By extracting from *A. annua*, the structural elucidation of artemisinic acid was determined by IR and ^{1}H NMR spectroscopy, in addition to biogenetic considerations, prior to the discovery of amorphadiene.[119,120] Initially named cadina-4,11-diene, the structure of amorphadiene was first determined in 1984 by NMR spectroscopy and gas chromatography-mass spectrometry (GC-MS). The structure was elucidated when it was discovered as an unknown terpene in the plant *Viguiera oblongifolia gardner.*[121,122]

Franssen and co-workers[123] were the first group to identify amorphadiene in *A. annua* and proposed its presence as an early intermediate in the biosynthesis of artemisinin. Leaf extracts of *A. annua* were analysed by GC-MS and 14 sesquiterpene compounds were found. The identity of amorphadiene was demonstrated by comparison of its peak in the GC with that of an authentic sample that had been prepared from artemisinic acid. The structure and configuration of amorphadiene made it a suitable candidate to be the terpene precursor to artemisinin. Furthermore, the formation of amorphadiene from FDP was the major sesquiterpene synthase activity in *A. annua*. Although there was a high amorphadiene synthase activity found in the plant, the small quantities of amorphadiene detected suggested that there were further modifications to the sesquiterpene, such as oxidations to produce oxygenated artemisinin precursors, and that the initial synthase activity of ADS was the rate-determining step in the biosynthesis of artemisinin.[124]

The catalytic mechanism of amorphadiene synthase has been studied and reported by numerous groups and is fully established. The first question to address was the order of cyclisations that occur in the catalytic mechanism of ADS. After an isomerisation of FDP to nerolidyl diphosphate (NDP, **51**), a 1,6 cyclisation occurs affording bisabolyl cation **52**, followed by a hydride shift to form (**53**) and then a 1,10-cyclisation to yield amorphyl cation (**54**). Alternatively the 1,10 cyclisation is achieved first, resulting in a germacradienyl cation (**55**), subsequently undergoing a hydride shift

to **56** and then a 1,6-ring closure to form cation **57** (Scheme 1.5).[125] After identification of minor enzymatic products arising from an incubation of ADS with FDP, Brodelius and co-workers proposed that the framework of amorphadiene was built *via* a 1,6-cyclisation followed by a 1,10-cyclisation.[126] In the array of sesquiterpenoids generated by ADS, all the monocyclic compounds, assumed to be a result of premature quenching, were various isomers of bisabolene. Further to this, none of the minor products contained a germacrene based structure (**55**), implying that no initial 1,10-cyclisation occurs (Scheme 1.6).[127] The presence of γ-humulene (**58**) did however indicate that a 1,11-cyclisation was achievable through ADS catalysis. (*E*)-β-farnesene (**59**) also demonstrated that acyclic sesquiterpene production occurs. The remaining minor products were either a result of quenching of intermediates by water, yielding (*E*)-α-bisabolol (**60**), amorpha-4-en-11-ol (**61**) and amorpha-4-en-7-ol (**62**), or through deprotonation, producing β-sesquiphellandrene (**63**), amorphadiene (**45**) and amorpha-4,7(11)-diene (**64**).

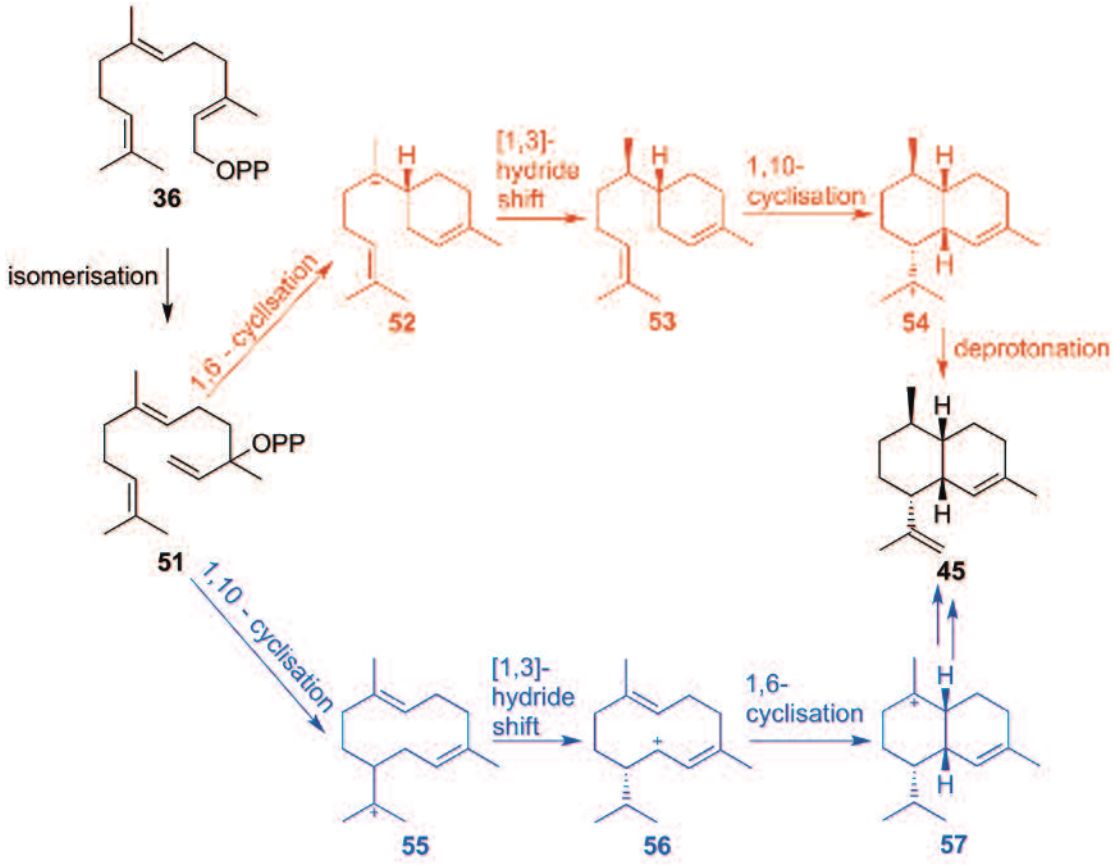

Scheme 1.5 Formation of amorphadiene (45) from FDP (36) via an initial 1,6 cyclisation (red) or a 1,10 cyclisation (blue).

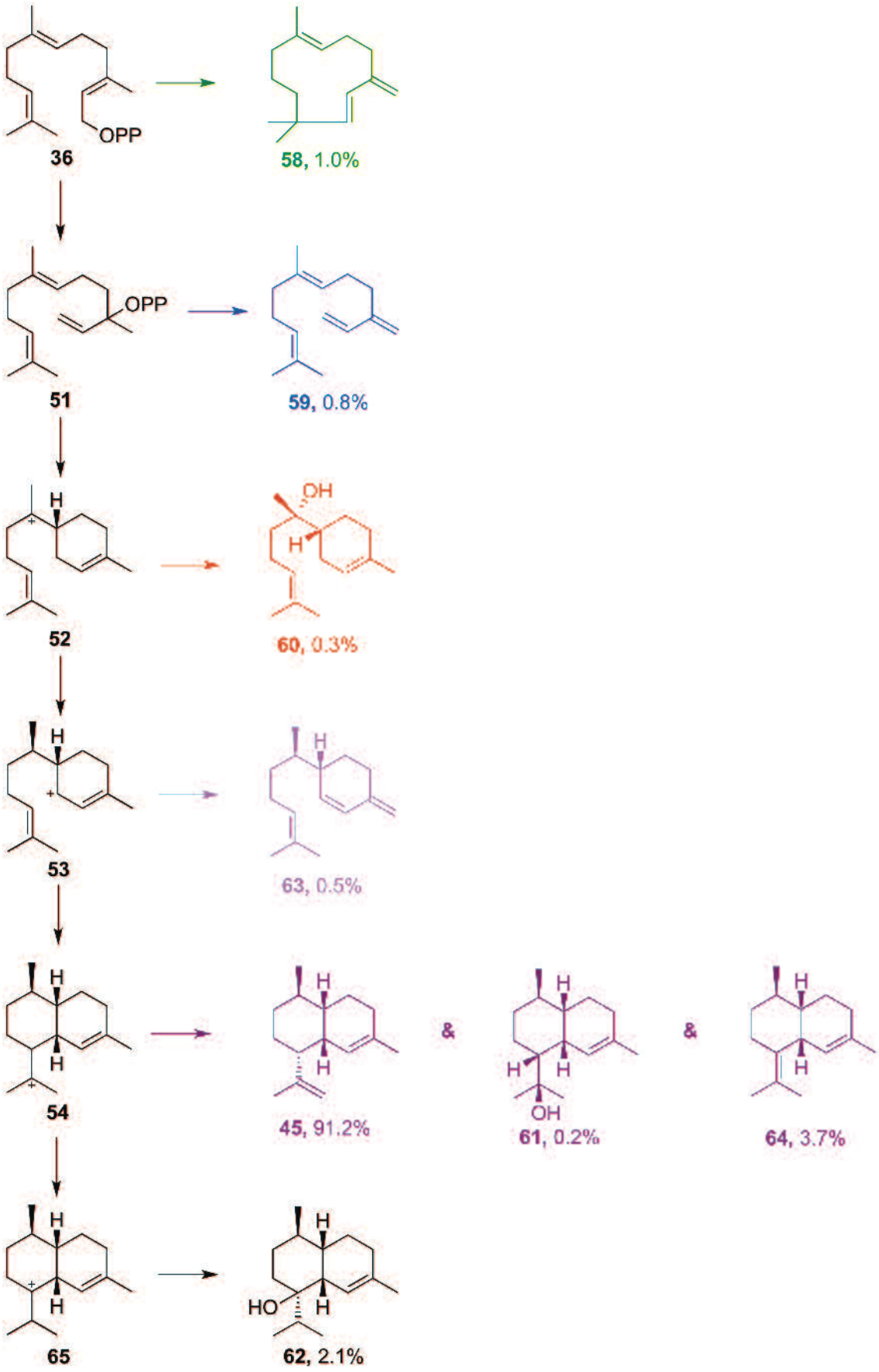

Scheme 1.6 Enzymatic products arising from incubation of ADS and FDP (36) reported by Brodelius and co-workers.[126]

Furthermore, Brodelius and co-workers[128] report that ADS is capable of converting GDP (**34**), the precursor of monoterpenes, into cyclic products; limonene (**17**), α-terpineol (**66**) and terpinen-4-ol (**67**) (Scheme 1.7). These products support the proposition of ADS carrying out an initial 1,6-cyclisation, when compared to TEAS, a sesquiterpene synthase that carries out an initial 1,10 cyclisation. An incubation of TEAS with GDP only forms acyclic products, linalool (**68**) and myrcene (**69**).

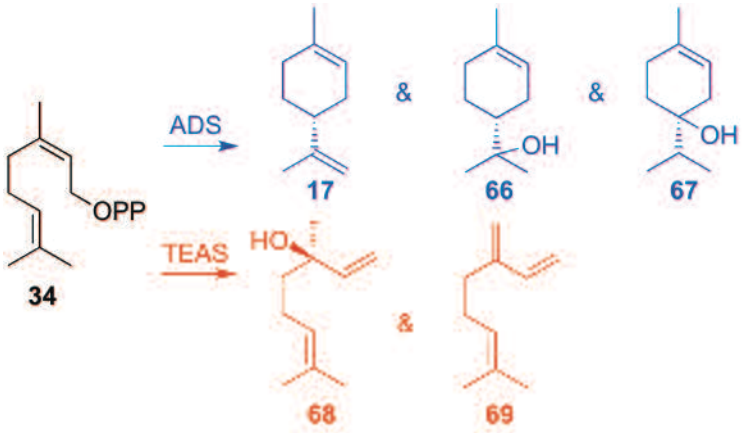

Scheme 1.7 Enzymatic products arising from incubation of ADS (blue) and TEAS (red) with GDP (34).

Determining the exact catalytic mechanism of ADS was accomplished through the use of deuterium labelled substrate analogues. This not only identified the stereochemistry of the enzymatic product but also enabled identification of the intermediate carbocations.

Brodelius and co-workers reported the use of single deuterated FDP; (1*R*)-[1-^{2}H]-FDP (**70**) and (1*S*)-[1-^{2}H]-FDP (**71**), and double deuterated FDP; [1,1-$^2H_2$]-FDP (**72**), to solve the catalytic mechanism of ADS (Figure 1.9).[128] It was observed by GC-MS that the molecular ion $[M]^+$ (**73**) of amorphadiene shifts by 1 and 2 atomic mass units (AMUs) when both single and double deuterated FDP is incubated with ADS, respectively. In addition to this, the $[M\text{-}CH_3]^+$ ion (**74**) also was shown to shift 1 and 2 AMUs, showing that none of the three methyl groups (C13, C14 and C15) contained any deuterium. Cation **75** observed at *m/z* = 121, the product when amorphadiene is cleaved at C1/C10 and C7/C8, retains the deuterium ions of both single and double deuterated FDP. However cation **76** observed at *m/z* = 93, formed by the cleavage of C1/C10 and C6/C7, only shows a shift in 1 AMU when ADS is incubated with (1*R*)-[1-^{2}H]-FDP but does not retain any deuterium label from an incubation of ADS with (1*S*)-[1-^{2}H]-FDP (Figure 1.9 and Table 1.2).

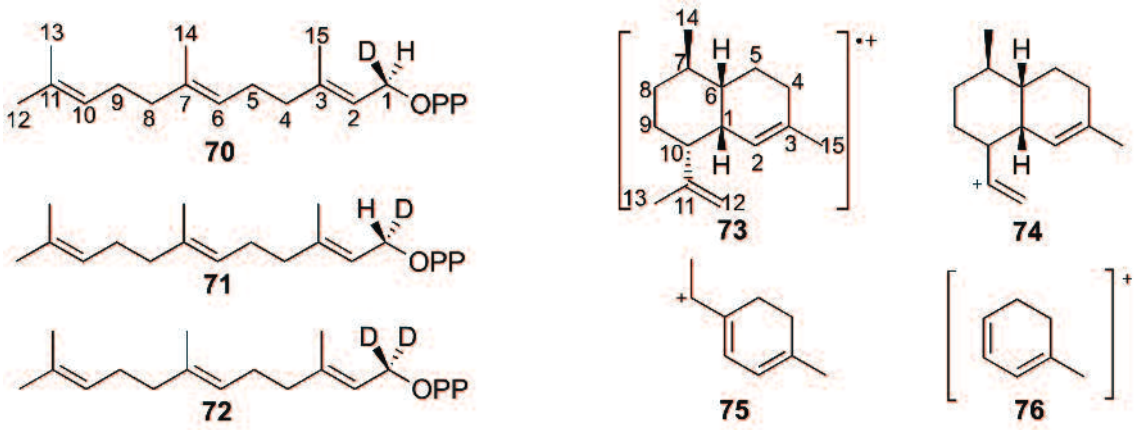

Figure 1.9 Single deuterated (70 and 71) and double deuterated (72) FDP. Ions 73-76 are observed in a mass spectrum of amorphadiene (45).

Table 1.2 Mass spectrometric parent and fragment ions from unlabelled and labelled amorphadiene.

Substrate	Ions (*m/z*) of amorphadiene product			
	73	**74**	**75**	**76**
36	205	189	121	93
70	205	190	122	94
71	205	190	122	93
72	206	191	123	94

The information observed from fragment ions **75** and **76** show that the 1-pro-S hydrogen of FDP (**36**) shifts from C1 to C7, during the catalytic mechanism. In addition, this observation also implies that the mechanism goes through a 1,3-hydride shift instead of two consecutive 1,2-hydride shifts. If two consecutive hydride shifts took place, the 1-pro-S hydrogen of FDP would shift to C6 and in the deuterium labelled tests, this deuterium would still be observed in fragment ion **76** (Scheme 1.8).

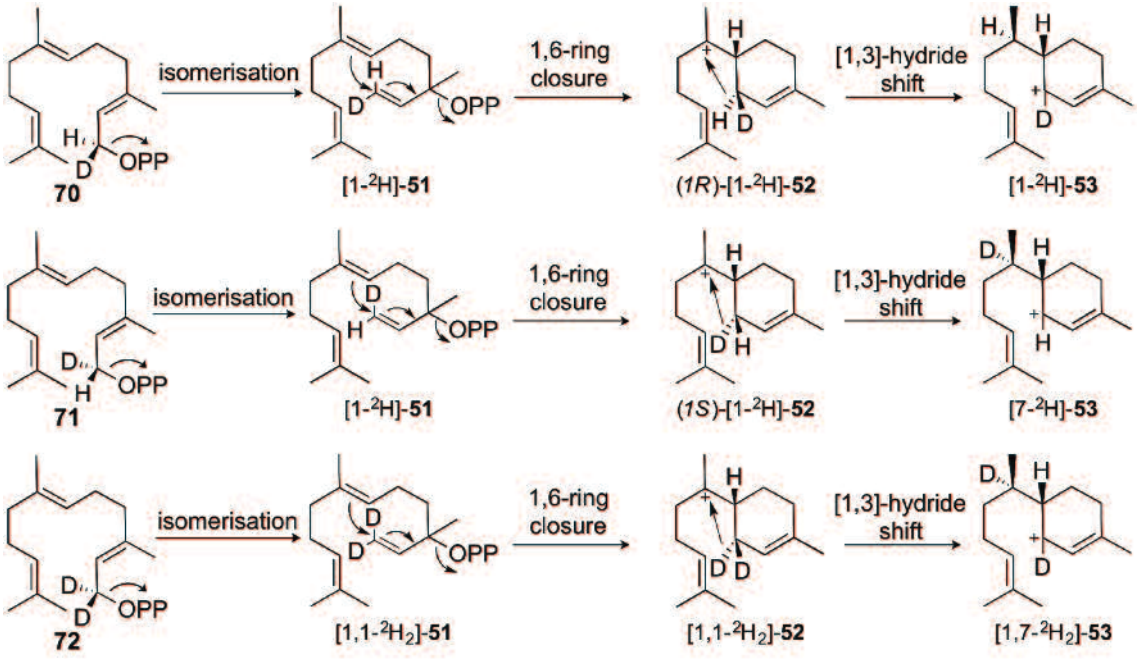

Scheme 1.8 Proposed mechanistic steps to illustrate the fragmentation patterns observed in the mass spectra resulting from single (70 and 71) and double (72) deuterated FDP.

The mechanism of ADS has also been studied by ^{1}H and ^{2}H NMR spectroscopy. Kim and co-workers also synthesised compounds **70**, **71** and **72** to incubate with ADS. On observation of the ^{2}H NMR spectra, when double deuterated **72** was incubated with ADS, there were two signals at δ_H = 1.38 and 2.60 corresponding to the deuterium signals of D-7 and D-1 respectively. When using only (1*R*)-[1-^{2}H]-FDP (**70**) the incubation yielded a single labelled product with a signal at δ_H = 2.60, whereas when (1*S*)-[1-^{2}H]-FDP (**71**) was used, a single signal appeared at δ_H = 1.38. To support this data additional spectra were measured using ^{1}H NMR spectroscopy. Firstly the ^{1}H NMR spectrum for a double labelled amorphadiene lacked the characteristic signals at δ_H = 1.40 and 2.55 showing the presence of deuterium at H-7 and H-1 respectively. When using only (1*R*)-[1-^{2}H]-FDP with ADS, the ^{1}H NMR spectrum lost the signal at δ_H = 2.55, characteristic of H-1. Similarly the incubation with (1*S*)-[1-^{2}H]-FDP generated a compound that lacked the signal at δ_H = 1.40. Both of these NMR spectroscopic techniques confirmed the same findings; the proton in the 1*S* position migrates to C7 showing that the mechanism must undergo a 1,6 ring closure, while the 1*R* proton remains at C1.[125]

With the deuterium labelling studies, the catalytic mechanism of ADS has been fully elucidated; a Mg^{2+}-dependent expulsion of the diphosphate moiety of FDP (**36**), followed by isomerisation yields NDP (**51**). This allows rotation to give the cisoid

conformer necessary for a 1,6-cyclisation to form the bisabolyl cation (**52**). A highly stereoselective [1,3]-hydride shift to cation **53**, followed by a 1,10-cyclisation, leads to the bicyclic amorphyl cation (**54**). Finally a deprotonation to quench the amorphyl cation from C12 or C13 generates amorphadiene (**45**) (Scheme 1.9).

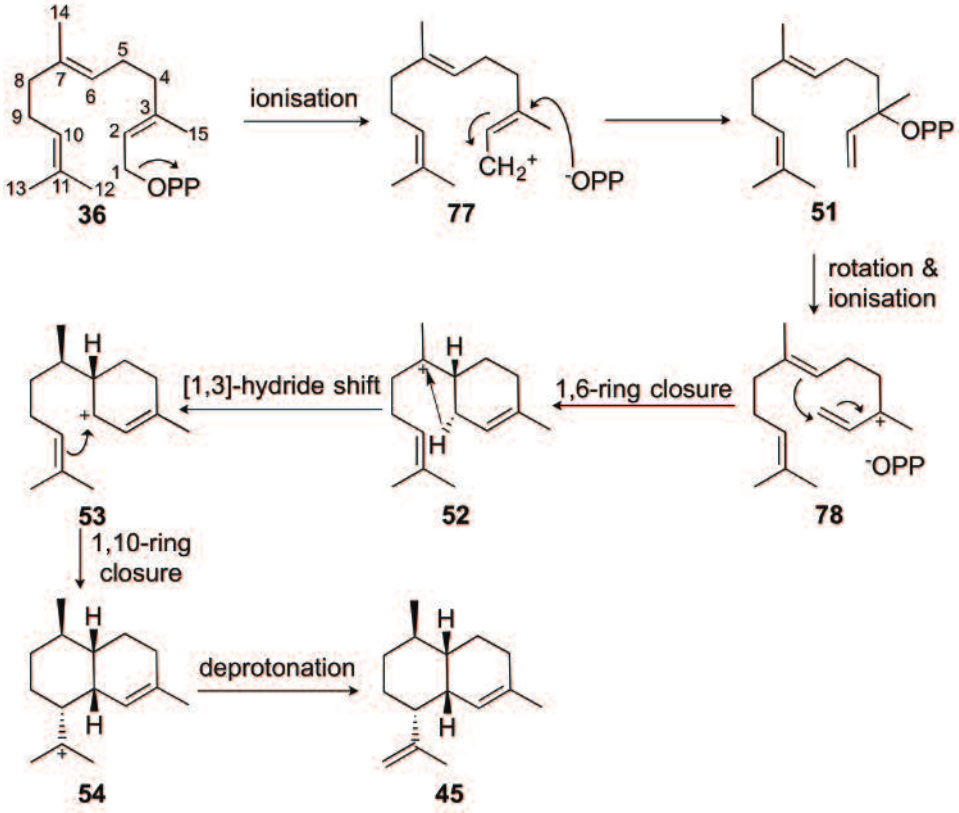

Scheme 1.9 ADS catalysed conversion of FDP (36) to amorphadiene (45).

1.3.3 Commercial production of artemisinin

There are various methods for probing artemisinin, with the majority of world production arising from extraction of the compound from dry plant material.[129] Screening for plant lines that can be bred with the existing *Artemisia* plant to enhance the yield of artemisinin is an active area of research.[130–132] *A. annua* is mostly cultivated in China, Vietnam, India and Africa. The plant takes around 8 months to fully grow, after which the dried leaves are sent to artemisinin-extraction facilities. The extracted artemisinin is commonly sent to a third contractor which oversees the conversion of artemisinin into its derivatives. The long cultivation periods, in addition to few manufacturers at some stages of the production cycle, and too many at others leads to an unstable supply of the artemisinins as well as a constant fluctuation in the price of the antimalarials.[133,134] Elegant total syntheses of artemisinin have also been carried out as an alternative approach to this drug.[135,136] Srihari and co-workers reported a total synthetic route,

starting with commercially available (*R*)-citronellal (**79**). The synthesis of artemisinin (**6**), was achieved in 11 steps with an overall yield of 5% (Scheme 1.10).[135]

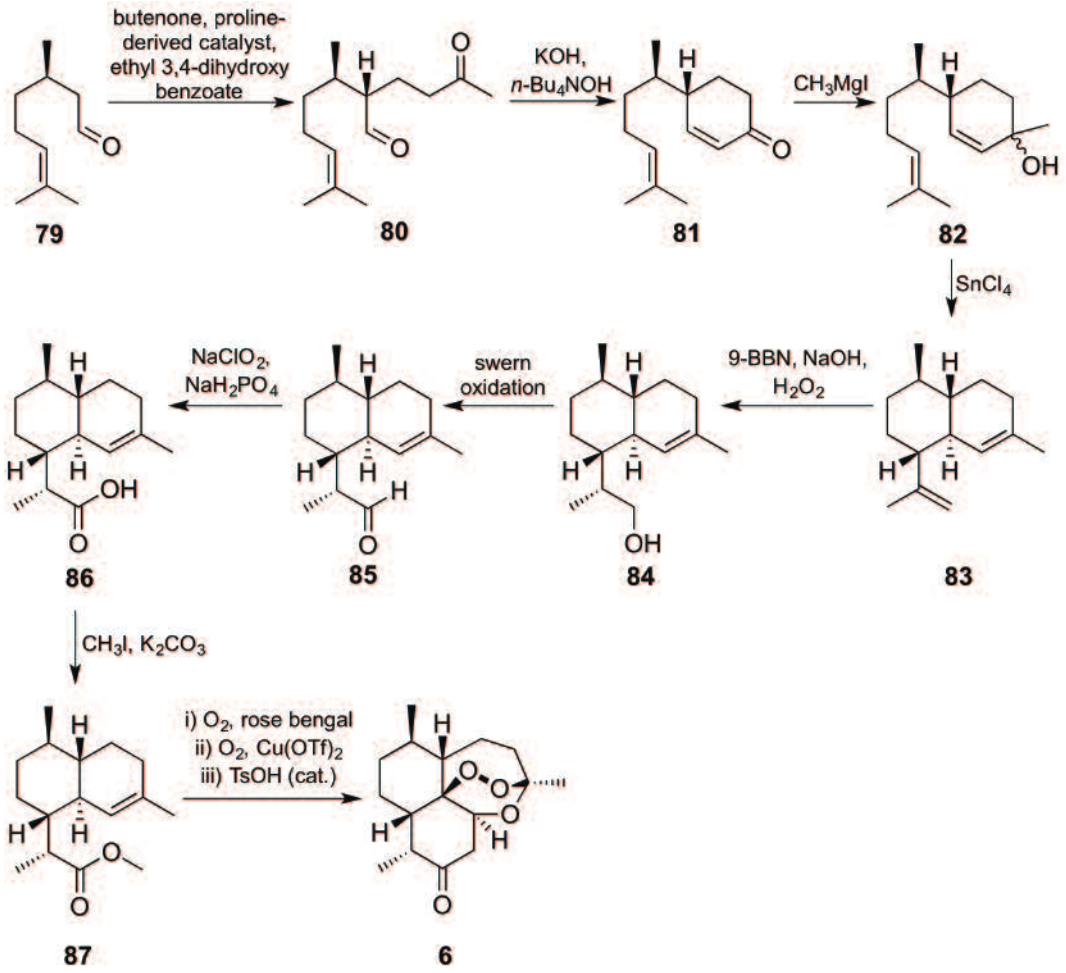

Scheme 1.10 Total synthesis of artemisinin (6) starting with (*R*)-citronellal (79) reported by Srihari and co-workers.[135]

An effective, and arguably a more reliable and efficient, route for sourcing artemisinin has been achieved using a biosynthetic approach. Strains of *Saccharomyces cerevisiae* have been developed to produce artemisinic acid (**48**, Scheme 1.11), a precursor to artemisinin.[137,138] This is then extracted from the yeast and converted to artemisinin through a series of chemical procedures.[139–141] There are four steps required for the chemical conversion. First, artemisinic acid is reduced to dihydroartemisinic acid (**50**). An esterification of the carboxylic acid moiety of **50** yields the methyl ester derivative, **88** and subsequent generation of a singlet oxygen produces the hydroperoxide moiety on **89**. This is followed by an acid catalysed Hock cleavage and rearrangement to form artemisinin (**6**) in the presence of molecular oxygen (Scheme 1.11).

The esterification of dihydroartemisinic acid was required, as explained by Newman and co-workers,[139] to prevent the formation of a five-membered lactone containing compound, dihydroepideoxyarteannuin B (**90**) which is a side reaction blocked by the formation of the ester **88** (Scheme 1.12). However, Levesque and Seeberger[141] report the synthesis of artemisinin *via* flow chemistry where they form hydroperoxide **91** directly from dihydroartemisinic acid (**50**). They state that with the formation of ester **88**, the formation of another side product, the six-membered lactone ring **92** is increased (Scheme 1.12). To our knowledge, there has not been a reported synthesis where the synthesis of both side products, **90** and **92,** have both been prevented.

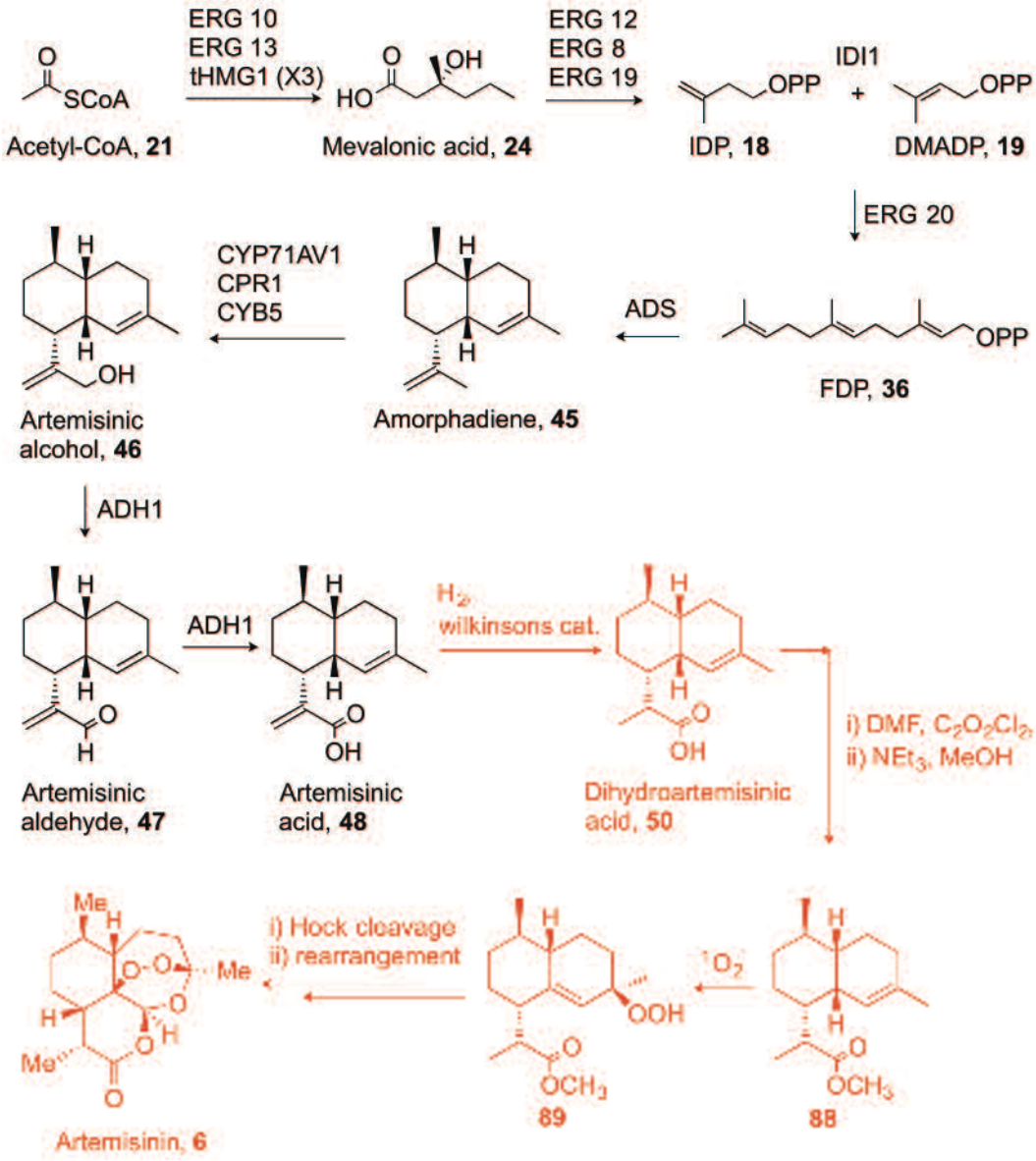

Scheme 1.11 Biosynthetic approach to the synthesis of artemisinin (6) reported by Newman and co-workers.[139] The intermediates in red are synthesised chemically once artemisinic acid (48) has been extracted from the yeast.

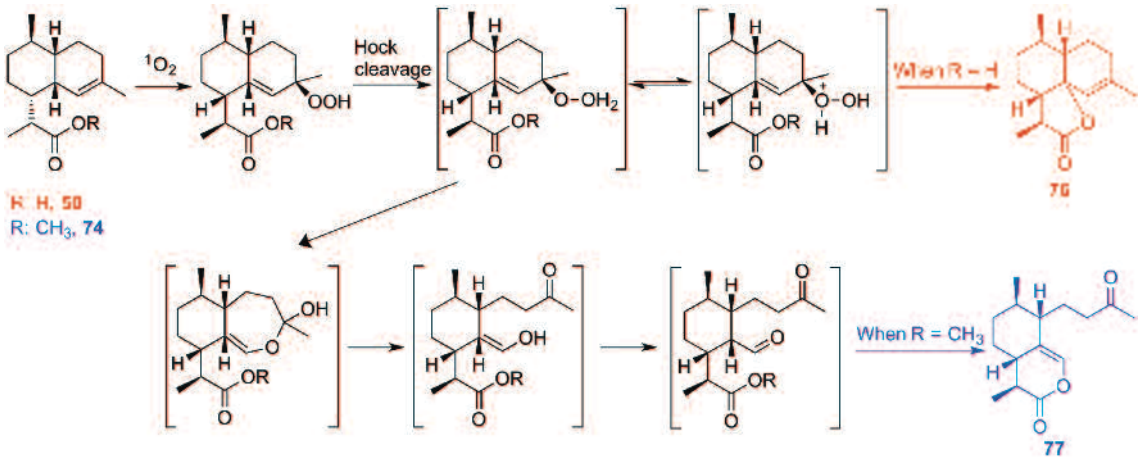

Scheme 1.12 Formation of side products 90 and 92 during the Hock cleavage.[142]

1. 4 Exploiting the promiscuity of sesquiterpene synthases

The promiscuity of sesquiterpene synthases has been studied and recorded by several research groups. Novel analogues of the natural substrate, FDP (**36**), have been synthesised and incubated with various sesquiterpene synthases to test their ability of catalysing an unnatural substrate into corresponding novel terpenoids. This area of research is of great interest as it provides the opportunity to introduce a heteroatom molecule into the terpene scaffold without the need of additional chemical steps. Novel analogues have also been used as mechanistic probes for elucidating the mechanistic steps of sesquiterpene synthases.

Allemann and co-workers[143] explored the biosynthetic utility of two plant sesquiterpene synthases, germacrene A (GAS) and germacrene D synthase (GDS). These enzymes catalyse the Mg^{2+}-dependent conversion of FDP (**36**) to germacrene A (**40**) and germacrene D (**93**), respectively (Scheme 1.13). Germacrene D is an important semiochemical that is responsible for affecting the olfactory response of insects.[144–147]

Based on the biological significance of germacrene A and germacrene D, a selection of methylated and fluorinated FDP analogues were synthesised to study the efficiency of the GAS and GDS catalysed conversions to produce non-natural germacrenes, with the potential of creating more potent semiochemicals. GAS and GDS were both capable of producing fluorinated germacrenes (6-fluoro germacrene A **94,** 6-fluoro germacrene D **95,** 14-fluoro germacrene A **96** and 14-fluoro germacrene D **97**) from 6-fluoro FDP (**98**) and 14-fluoro FDP (**99**). In addition, methylated germacrenes, 14-methyl germacrene A (**100**) and 14-methyl germacrene D (**101**) were yielded when both enzymes were incubated with 14-methyl FDP (**102**) (Figure 1.10).

GC-MS and NMR spectroscopy was used to identify the production of the novel germacrene products.

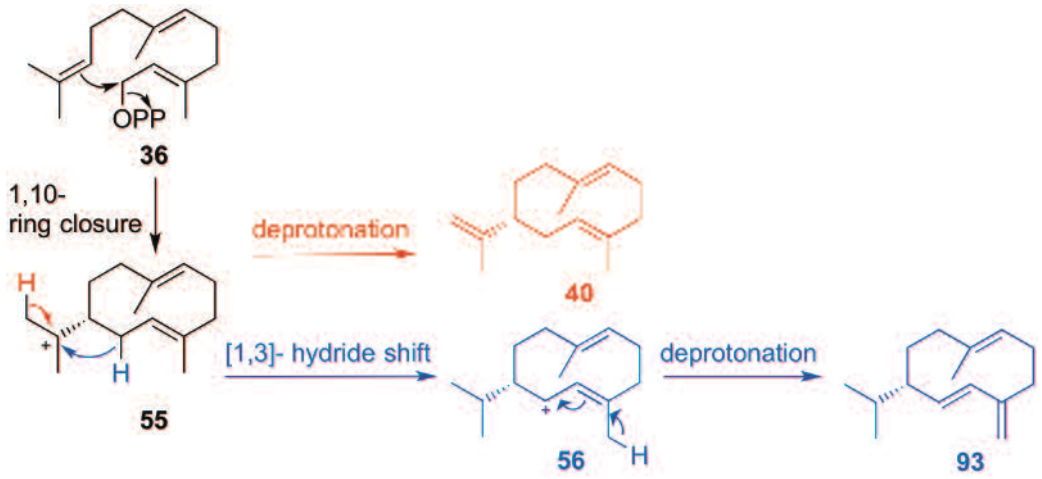

Scheme 1.13 GAS (red) and GDS (blue) catalysed conversion of FDP (36) to germacrene A (40) and germacrene D (93).

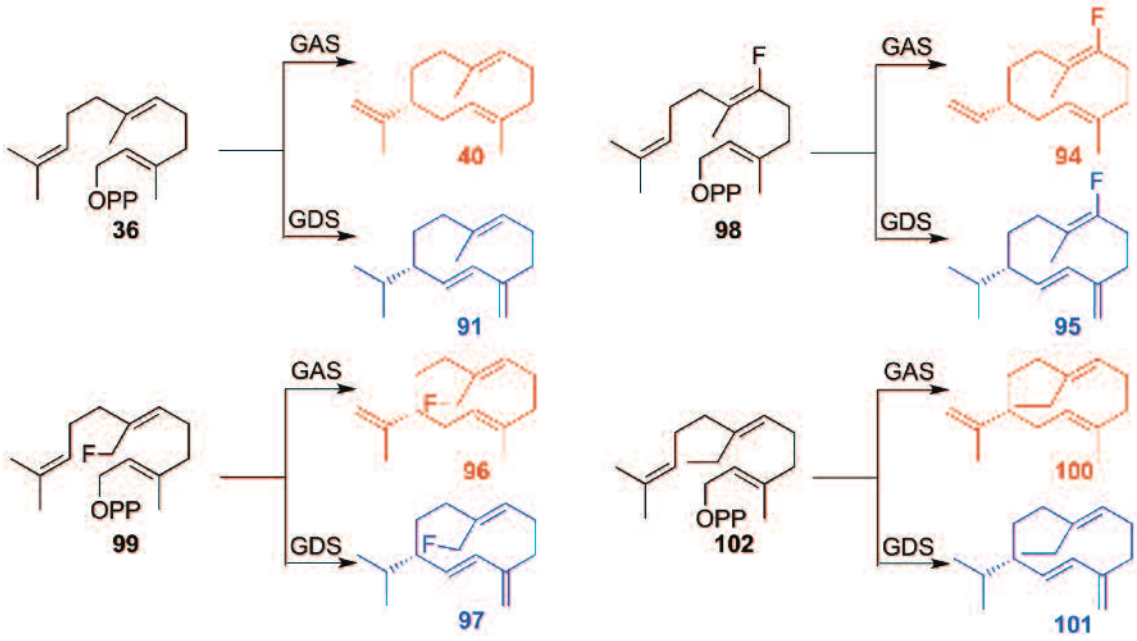

Figure 1.10 GAS and GDS catalysed conversions of fluorinated (98 and 99) and methylated (102) FDP analogues to produce novel germacrene A (red) and germacrene D (blue) derivatives.

Chappell and co-workers[148] showed that the plant sesquiterpene synthase, tobacco 5-*epi*-aristolochene (TEAS), also exhibited certain substrate promiscuity. TEAS catalyses

the conversion of FDP (**36**) into the bicyclic sesquiterpene, aristolochene (**103**) (Scheme 1.14).

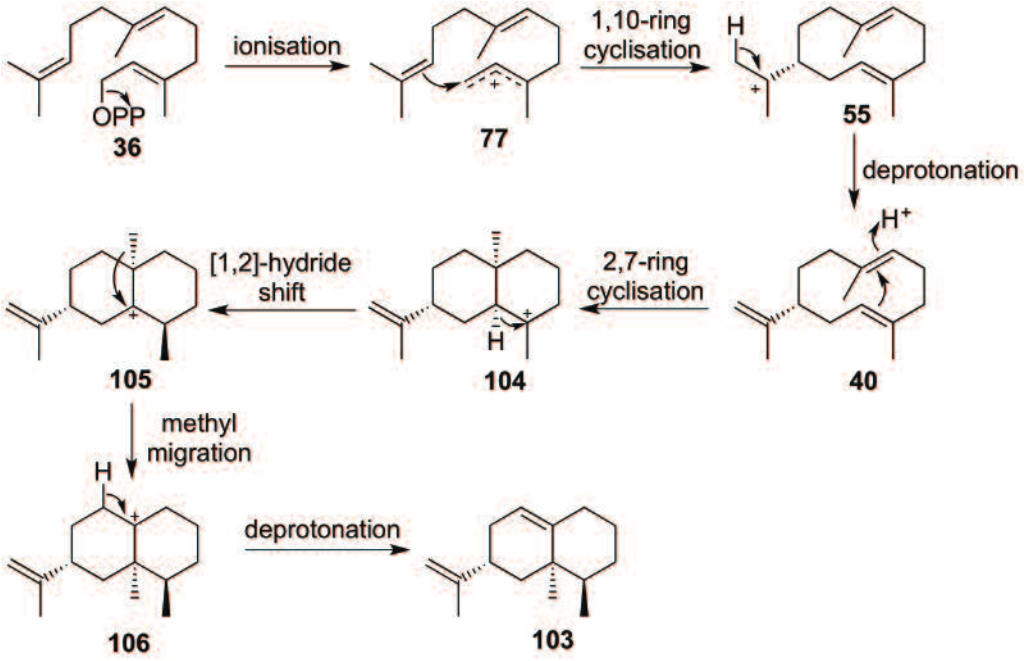

Scheme 1.14 TEAS catalysed conversion of FDP (36) to aristolochene (103).

An aza-analogue of GDP, 8-anilino GDP (**107**), was synthesised and incubated with TEAS because it was predicted that if the analogue bound to the active site and inhibited the catalytic mechanism of TEAS, then this substrate could be used to help refine the structural features of the enzyme in crystallographic studies. Although 8-anilino GDP is an analogue of the 10-carbon monoterpene precursor, GDP, the length of the isoprenyl chain is more consistent with that of FDP (Scheme 1.15). 8-Anilino GDP can be considered a structural analogue of FDP, where an aniline group replaces the terminal isoprene unit. 8-Anilino GDP was characterised as a non-competitive inhibitor of TEAS by measuring the conversion rate of [1-^{3}H]-FDP to [1-^{3}H]-5-epi-aristolochene in the presence of varying concentrations of 8-anilino GDP. Upon studying the crystal structure of the TEAS-8-anilino GDP complex, the Fo-Fc electron density map of the model exhibited a region of electron density in the active site. This observation suggested that ionization and macrocyclization of the novel substrate within the TEAS active site had occurred. NMR spectroscopy was used to identify the hexane extractable product generated by an incubation of 8-anilino GDP with TEAS as a novel 13-membered alkaloid (**108**) (Scheme 1.5).[148]

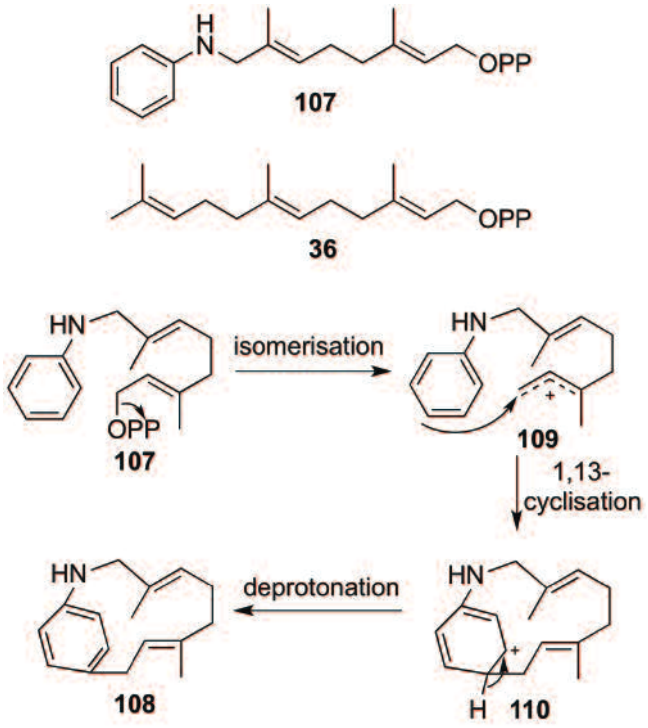

Scheme 1.15 Top: 8-anilino GDP (107) and FDP (36). Bottom: Proposed mechanism for the formation of alkaloid 108.

1. 5 Aims of project

Malaria is the most common and damaging parasitic disease worldwide, killing millions of people every year. Unfortunately the countries that suffer from this dreadful disease are those that have typically less than $10 per capita annually to spend on healthcare. Therefore the treatment of malaria in these countries must come at a price that is not prohibitive.[149] The wrong usage of antimalarials, for example in the dosage that a patient receives, or incompletion of a treatment cycle, contributes to the rise of parasitic resistance. Today, the artemisinins are used in ACTs as the first line treatment for malaria, but if parasitic resistance to these antimalarials worsens before a new alternative is available, it would be a great global disaster. Therefore there is a constant race to not only find the most cost effective and reliable way to supply artemisinins to the world, but also to find an alternative that will be ready to serve as the next first line treatment.

This project was divided into two parts. The first aim was to explore the promiscuity of the recombinant enzyme ADS. With previous knowledge of sesquiterpene synthases catalysing the conversion of FDP analogues into novel sesquiterpenoids,[143,148] the objective was to synthesise FDP analogues and test the enzymatic activity of ADS with them. Any amorphadiene derivatives produced can then be further converted to new corresponding derivatives of artemisinin and tested for

antimalarial activity. ADS is a very important enzyme for this approach in creating new artemisinins because it is responsible for generating the scaffold of artemisinin, which exhibits 4 stereocenters. If amorphadiene was synthesised chemically, many chemical steps would be required to replace the one enzymatic step catalysed by ADS. Furthermore, the synthesis would be complicated by the necessary construction of the correct stereochemistry.[135,136] For this reason, using ADS to produce analogues of artemisinin is advantageous.

The second aim of this project focuses on finding a route to produce artemisinin in a reliable and cost effective manner. ADS has been used previously *in vivo* to provide an improved production of artemisinin.[139] Carrying out incubations with the enzyme *in vitro* gives the advantage of employing substrate analogues that may be converted by the enzyme to, ultimately, artemisinin analogues. Both the biosynthetic pathway observed in plants,[111] and the chemical synthesis used by several groups,[137] show the necessity of oxidising amorphadiene to form artemisinin, and more importantly, in which position the initial oxidation occurs. A hydroxylated analogue of FDP was designed, and incubated with ADS to potentially form a precursor further down the schematic pathway to artemisinin (Section 5), thus reducing the overall steps required to produce the antimalarial.

Chapter 2. Characterisation of amorphadiene synthase

2. 1 Preface

The aim of the work described in this chapter was to fully characterise ADS. Experimental procedures were optimised to provide an efficient method for efficient heterologous expression of the amorpha-4,11-diene synthase gene in *E. coli* and to purify the recombinant ADS protein. In addition, it was planned to study the stability and structure of the enzyme by the means of pH studies and size exclusion chromatography. Steady-state kinetics were performed with the use of tritiated FDP to characterise the catalytic efficiency of ADS and compare the activity with kinetic parameters reported in the literature. The enzymatic product of ADS was confirmed, not only by comparing the GC-MS data to reported literature but also by characterising the product by NMR spectroscopy. Lastly, this chapter describes the production of ADS mutants to aid in the investigation of the contribution of the N-terminal domain to the catalytic mechanism.

2. 2 Subcloning the ADS gene into pET21d vector

The ADS gene was obtained from GenBank (Acc. No. JF951730.1). The gene was supplied in a pTrc99a expression vector (pTrc99a-ADS). After transforming the plasmid into competent *E. coli* BL21-(DE3)-Codon Plus RP (BL21 RP) cells, the gene was expressed. This was carried out by culturing the transformed cells at 30 °C until the optical density at 600 nm (OD_{600}) reached 0.7, at which time the expression was induced with IPTG (0.5 mM) and the cells were grown for 4 h at 37 °C prior to harvesting the cells. After extracting the recombinant protein from the cells by sonication, purification of the enzyme was attempted. A pre-packed Q-Sepharose Fast Flow anion exchange column was used in an attempt to purify ADS. Cell lysis buffers (buffer 1: 20 mM Tris base, 5 mM EDTA, 2 mM β-ME, pH 8; buffer 2: buffer 1 with 1 M NaCl) were set up to create a gradient with increasing sodium chloride concentrations to elute bound protein from the anion exchange column. SDS polyacrylamide gel electrophoresis (SDS PAGE) was used to analyse the fractions collected from the Q-Sepharose column. Analysis of the resulting gel demonstrated that ADS did not bind to the column and had eluted from the column with the initial low salt wash. In attempts to overcome this problem, purification was repeated at pH 9, 10 and 11 and also using anionic resin (DEAE Sepharose fast flow) at pH 6, 7, and 8. SDS PAGE verified that the protein did not bind to any of these resins at any given pH, and therefore that the purifications attempted using these methods had been unsuccessful.[98,150]

In an attempt to find another way to purify ADS, a hexahistidine-tag (His-tag) motif was introduced to the C-terminus of the protein. The addition of a His-tag motif should enable purification of ADS *via* nickel affinity chromatography. Before introducing a His-tag motif, the ADS gene was subcloned into a different expression vector,

pET21d. The pET21d vector contains an out of frame sequence for encoding a His-tag motif, which the pTrc99a vector does not possess.

The plasmid pET21d-GDS, present in the Allemann group library and containing the gene for germacrene D synthase, was used as the source of the required pET21d vector. pTrc99a-ADS and pET21d-GDS were digested with *Nco*I and *BamH*I restriction endonucleases to give the desired, isolated ADS gene and empty pET21d vector (Figure 2.1). The digestions were monitored using agarose gel electrophoresis and the desired fragments were cut out of the gel and purified using a QIAquick gel extraction kit protocol (Figure 2.2). These two complimentary, open fragments were ligated using T4 DNA ligase to give the new plasmid, pET21d-ADS.

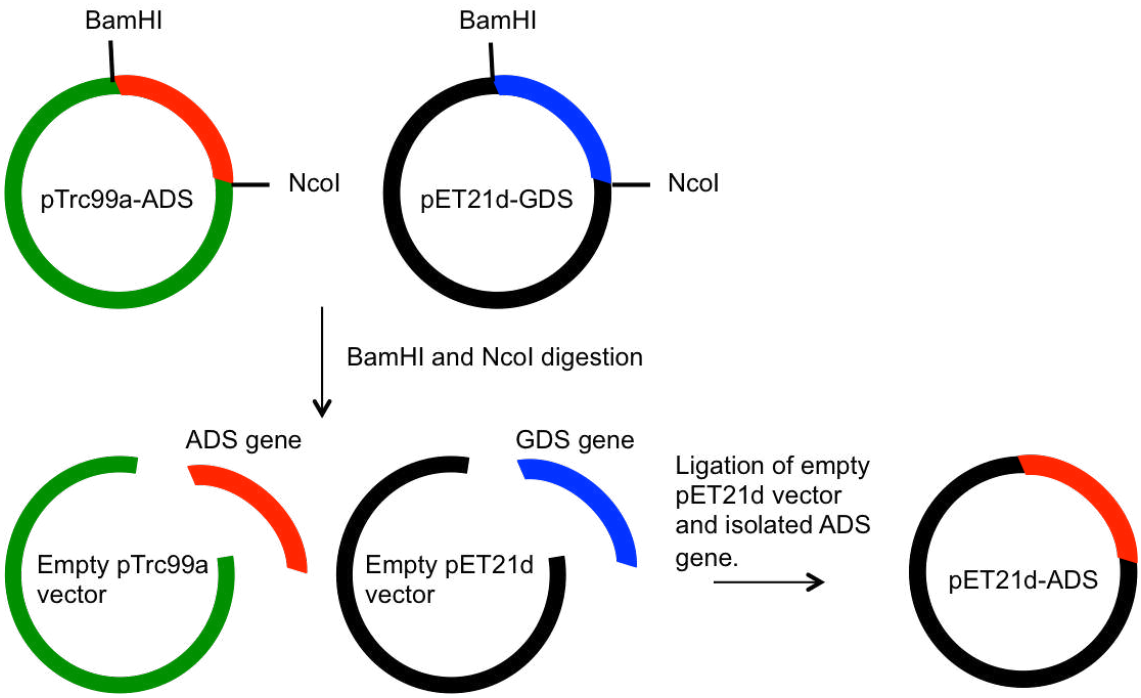

Figure 2.1 Cartoon representation of the insertion of the ADS gene into a pET21d vector.

Competent *E. coli* XL1 Blue cells were transformed with the resulting plasmid and colonies were grown on an agar plate containing ampicillin (100 μg/mL) in order to then inoculate LB medium with a single colony. The newly ligated plasmid was extracted using a QIAprep Spin Miniprep Kit Protocol and tested for successful ligation through the means of re-digestion. pET21d-ADS was digested with *Bgl*II because there are two *Bgl*II sites in the newly ligated plasmid, absent in the two parent plasmids, yielding a 1041 base pair fragment when digested. In addition to this, *Nco*I and *BamH*I were also used to re-digest pET21d-ADS. This digestion yielded a 1649 base pair fragment, the isolated ADS gene (Figure 2.2). Digested samples were analysed by agarose gel

electrophoresis. Samples that showed evidence of digestion were sequenced to demonstrate that the formation of pET21d-ADS was successful.

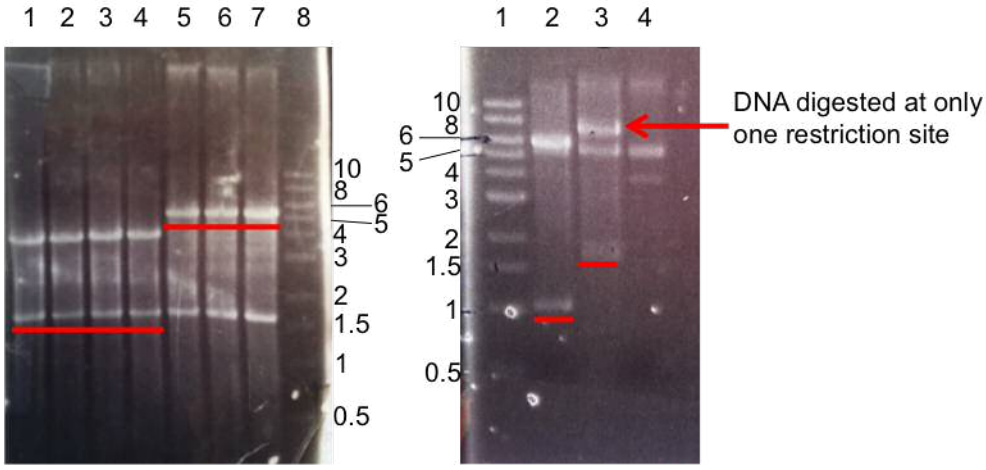

Figure 2.2 Agarose gels showing the results from digestion of DNA during the preparation of pET21d-ADS. Left: Results from digestions with *BamH*I and *Nco*I. Lanes 1-4) Ptrc99a-ADS, Lanes 5-7) pET21d-GDS, Lane 8) DNA ladder measured in kilobase pairs. Right: Results from re-digestions of pET21d-ADS. Lane 1) DNA ladder measured in kilobase pairs, Lane 2) *Bgl*II, Lane 3) *Nco*I and *BamH*I, Lane 4) uncut pET21d-ADS.

2. 3 Introducing a C-terminal hexa-histidine motif into the pET21d-ADS plasmid

Once the formation of the plasmid, pET21d-ADS, was confirmed by DNA sequencing, site directed mutagenesis was performed to introduce a single nucleotide deletion into the nucleotide sequence at the 3'-end. This deletion was required to bring the C-terminal hexa-histidine coding sequence of pET21d in frame with the ADS coding sequence. The ADS gene was followed by a stop codon that preceded the out of frame His-tag sequence, therefore a pair of primers were designed to eliminate the original stop codon, shift the His-tag in frame with the ADS coding sequence and create a new stop codon that followed after the His-tag (Figure 2.3).

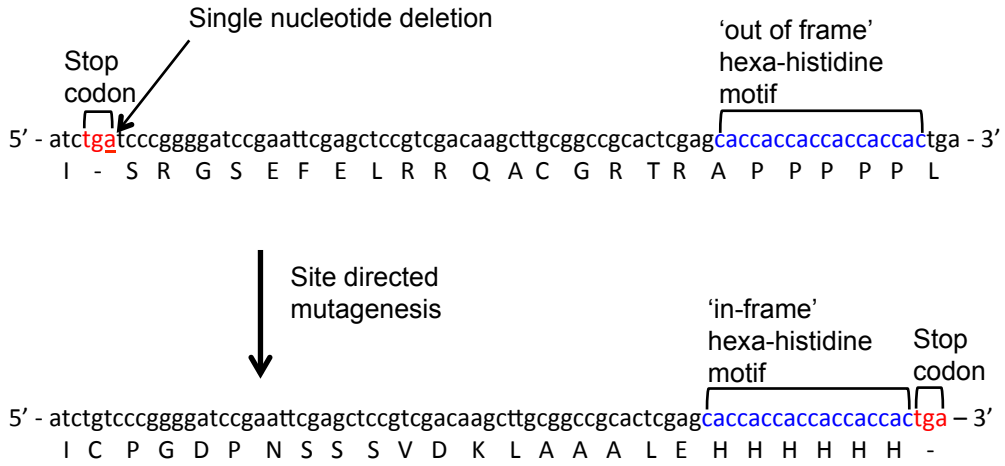

Figure 2.3 Nucleotide coding sequence and deduced amino acids involved in introducing an 'in-frame' his tag motif.

During the SDM reaction, the mutagenic primers were integrated into the newly synthesised plasmid and the His-tag was shifted in frame with the ADS coding sequence. Once the SDM reaction was complete the resulting plasmids were digested with a *Dpn*I restriction enzyme.[151] This was required to remove the original plasmid, which served as a template.[152] *Dpn*I only digests the template plasmid because only this plasmid is methylated on the adenine residues in the sequence GATC, as a result of being purified from a dam^+ strain in *E. coli*. The newly synthesised plasmids do not have this methylation and therefore are left intact.[153]

After site directed mutagenesis was performed, the resulting PCR product was transformed into *E. coli* XL1 Blue cells to clone the plasmid, after which sequencing confirmed successful addition of the c-terminal His-tag motif (pET21d-ADS His).

2. 4 Heterologous expression of the ADS gene

In order to determine the optimal conditions for the heterologous expression of the ADS gene, *E. coli* BL21 RP cells were transformed with the gene and test expressions were carried out using different culture conditions to assess the optimum isopropyl β-D-1-thiogalactopyranoside (IPTG) concentration, temperature and duration of subsequent cell culture time (expression) (Figure 2.4). Test expressions were designed based on two different literature procedures. Brodelius and co-workers[127] cultured cells at 30 °C until the optical density at 600 nm (OD_{600}) reached 0.5 and induced with IPTG (0.2 mM). The cells were then cultured at 30 °C for another 4 h prior to harvesting the cells. Kim and co-workers[125] also cultured cells at 30 °C until optical density reached 0.5, but

instead cells were induced with double the amount of IPTG (0.4 mM). The cells were then cultured at 20 °C for 6 h.

In addition to following these two protocols, a third test was implemented which consisted of inducing the cells when the optical density reached 0.5 using IPTG (0.4 mM) and culturing them at 16 °C for 21 h. SDS PAGE was carried out to determine which protocol produced the most soluble protein. ADS has a relative molecular mass of 66400 and therefore was detected around the 66.2 k band visible in the protein marker ladder (Figure 2.4). Whereas the first two sets of expression conditions showed varying amounts of ADS, the third set did not show any evidence of ADS expression. Under the optimal conditions found, cells were cultured at 30 °C until the optical density reached 0.5, at which they were induced with IPTG (0.4 mM) and grown for 6 h at 20 °C prior to harvesting the cells. Resulting pellets were stored at -20 °C.

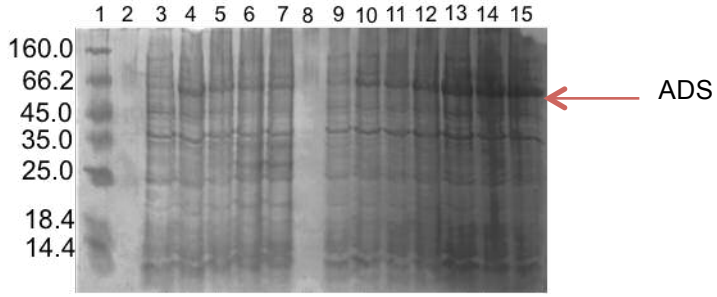

Figure 2.4 SDS-polyacrylamide gel showing the results from test expressions of ADS in BL21 RP cells. Lane 1) protein molecular weight ladder (x10^3 M_r), 2) empty, 3-7) samples taken at 0, 1, 2, 3 and 4 h after induction at 30 °C, 8) empty, 9-15) samples taken at 0, 1, 2, 3, 4, 5 and 6 h after induction at 20 °C.

2. 5 Extraction and purification of ADS

In order to purify ADS, pellets of harvested cells were defrosted and re-suspended in a Tris cell lysis buffer and sonicated. Sonication causes fragmentation of the cells, which are then centrifuged to separate the cell debris from the supernatant mixture. If the protein is successfully extracted into the supernatant solution it is further purified. If the protein is still encapsulated in the pellet, a basic extraction method is carried out to extract the protein from inclusion bodies by unfolding and refolding the protein's tertiary structure. The procedure involves increasing the pH of the re-suspended pellet to ~11 in attempt to unfold the protein's tertiary structure. The solution is left to stir for 30 min before the pH is returned back to pH 8, allowing for the tertiary structure to re-fold. The use of several cell lysis buffers have been reported in literature and three of those different buffers (cell lysis buffer 1[127], cell lysis buffer 2[125] and cell lysis buffer 3[154],

see Section 7.1.8) were tested for the extraction of ADS. When cell lysis buffer 1 (20 mM Na_xPO_4, 0.5 M NaCl, 5 mM $MgCl_2$, 10% v/v glycerol) was used, ADS did not extract into the supernatant solution after sonication or basic extraction. It is proposed that this could be due to protein aggregation and precipitation because the cell lysis buffer does not contain any reducing agents such as β-mercaptoethanol (β-ME) or dithiothreitol (DTT). No detergents such as TRITON, Tween 20 or CHAPS were used in the buffer either. Reducing agents are frequently used in cell lysate, purification and incubation buffers because it stops the formation of disulfide bonds between cysteine residues of neighbouring proteins, which can cause aggregation. Detergents can also be used to help solubilize membrane proteins and reduce the chance of the protein staying encapsulated in the pellet. When cell lysis buffer 2 (100 mM Tris-HCl, 1 mM PMSF, 5 mM $MgCl_2$, 10% v/v glycerol) was used, a slight improvement was observed with ADS protein present in the supernatant solution, but only after a basic extraction was carried out. The best results were found with the use of cell lysis buffer 3 (50 mM Tris-Base, 0.5 M NaCl, 5 mM imidazole, 20 mM β-ME 10% v/v glycerol). ADS protein was present in the supernatant solution after sonication, without the need for a basic extraction (Figure 2.5). This buffer was used subsequently for the extraction of ADS from the cell lysate. It is suggested that cell lysis buffer 3 resulted in the most efficient extraction of protein from the cell lysate because the buffer included a reducing agent, DTT, in addition to the detergent Tween 20.

The extracted ADS protein was then purified using a Ni^{2+}-NTA affinity column (Figure 2.6). Affinity resin with bound divalent nickel ions were used to coordinate with the His-tag motif. This resulted in the ADS protein solely binding to the column, as the other proteins that do not have a His-tag flowed through the column with the cell lysate. The column was washed with cell lysis buffer 3 consisting of increasing amounts of imidazole. This enabled fractionation from the column with an excess of imidazole displacing the histidine residues, allowing the free protein to elute from the column. ADS started to elute in buffer containing 40 mM imidazole but impurities were also observed. Pure protein eluted during a wash with cell lysis buffer 3 containing 60 mM imidazole. Fractions containing the desired protein were pooled and dialysed against a dialysis buffer (Section 7.1.4) to remove the imidazole. The resulting protein was concentrated with an Amicon ultrafiltration system (MWCO - 30,000). The protein concentration was determined by the Bradford method.[155,156]

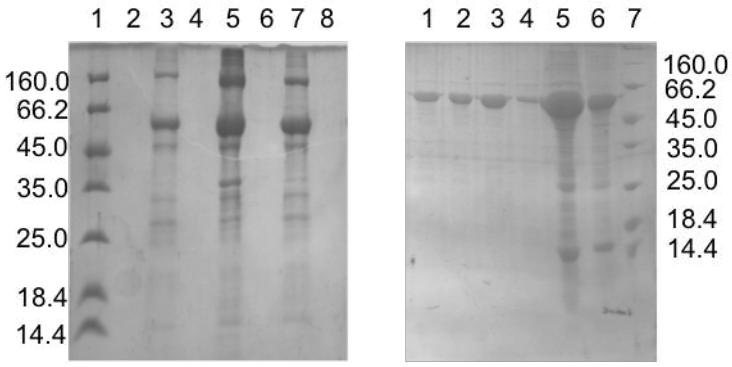

Figure 2.5 SDS-polyacrylamide gels of attempts to extract ADS from cell lysate. Left: Lane 1) protein molecular weight ladder (x10^3 M_r), 2) empty, 3-4) re-suspended pellet and supernatant solution after sonication using cell lysis buffer 1, 5-6) re-suspended pellet and supernatant solution after basic extraction using cell lysis buffer 1, 7-8) re-suspended pellet and supernatant solution after sonication using cell lysis buffer 2. Right: 1-2) supernatant solution after the first and second basic extraction using cell lysis buffer 2, 3-4) supernatant solution after basic extraction and sonication using cell lysis buffer 3, 5) re-suspended pellet after sonication using buffer 3, 6) re-suspended pellet after basic extraction using cell lysis buffer 2, 7) protein molecular weight ladder (x10^3 M_r).

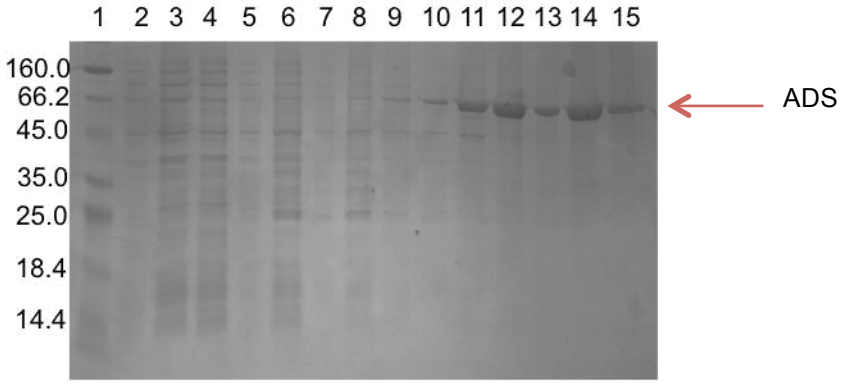

Figure 2.6 SDS polyacrylamide gel showing selected fractions from the Ni-NTA purification of ADS. 1) protein molecular weight ladder (x10^{-3} M_r), 2) empty, 3-4) flow through, 5) empty, 6-7) cell lysis buffer with 5 mM imidazole, 8) cell lysis buffer with 10 mM imidazole, 9-10) cell lysis buffer with 20 mM imidazole, 11) cell lysis buffer with 40mM imidazole, 12) cell lysis buffer with 60 mM imidazole, 13) cell lysis buffer with 80 mM imidazole, 14) cell lysis buffer with 100 mM imidazole, 15) cell lysis buffer with 300 mM imidazole.

2. 6 Characterisation of amorphadiene synthase and amorphadiene

2.6.1 Product analysis using GC-MS

Analytical incubations of ADS and FDP were carried out, not only to test activity of the purified ADS enzyme, but also to compare the product profile to those in reported literature. Incubations were left for 24 h and pentane extractable products were analysed using GC-MS (Figure 2.7). GC-MS analysis showed one major compound present, with a molecular ion at *m/z* = 204. The mass spectrum of the enzymatic product, amorphadiene (**45**) corresponds well with what is reported in literature.[124] As with previous reports, the most abundant peak is at *m/z* = 119. Depending upon the report used as the reference, the two second most abundant peaks, *m/z* = 189 (~ 90%) and *m/z* = 93 (~ 70%) either correlate[124] or are reversed.[123]

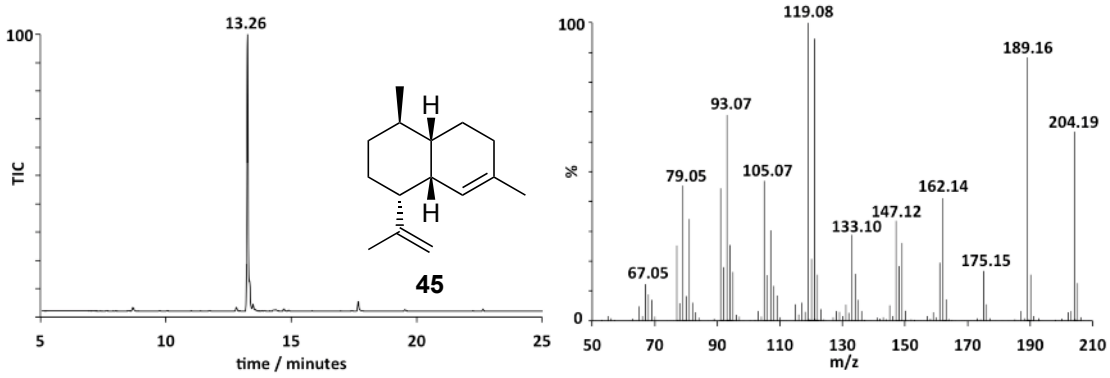

Figure 2.7 GC-MS analysis of pentane extractable products arising from incubation of ADS with FDP (36), Left: Gas chromatogram highlighting the formation of one major product, Right: The corresponding mass spectrum of the compound eluting at 13.26 min.

2.6.2 Size exclusion chromatography

Size exclusion chromatography (Superdex 75 10/300 GL) was used to determine whether ADS existed as a monomer, dimer or a bigger multi-subunit complex in solution.[157] The retention volumes of various proteins with known molecular mass were measured, in addition to the retention volume of ADS (Figure 2.8). Comparing the retention volumes of various proteins with the retention volume of ADS revealed that the protein existed as a monomer. In addition to comparing the retention volumes, the equation extrapolated from the calibration curve of molecular mass against retention volume also gave an estimate of the molecular weight of ADS. Using the equation (Figure 2.8), the molecular weight of ADS was calculated as 61000 compared to the actual molecular weight of 66400.

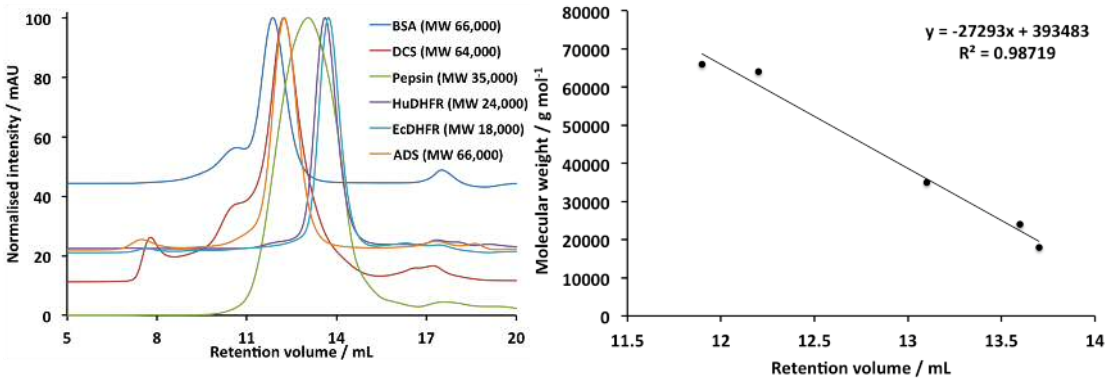

Figure 2.8 Left: Normalised and overlaid size-exclusion chromatograms of bovine serum albumin (BSA), δ-cadinene synthase (DCS), pepsin, human dihydrofolate reductase (HuDHFR), *E. coli* dihydrofolate reductase (EcDHFR) and amorphadiene synthase (ADS), Right: Calibration curve of protein molecular mass against retention time.

2.6.3 pH Stability profile

Circular dichroism (CD) spectroscopy was used in preliminary analysis to examine the effect of varying solution pH on the secondary structure of ADS. CD spectroscopy is a useful technique for this study because each secondary structure element, such as α-helices or β-sheets, has a specific CD signature spectrum measured in the UV region. This knowledge can be used when following changes in the structure of a molecule.[158] Greenfield provided an example of this by measuring the CD of polypeptides and proteins with representative secondary structures. All sesquiterpene synthases are composed of several antiparallel α-helices.[86,100,159] Proteins with an α-helical secondary structure, such as ADS, display distinctive minima at 208 nm and 222 nm, in addition to a maximum at 193 nm.[160]

CD spectra of ADS (10 μM) were recorded between 190 nm and 300 nm at room temperature (recorded as 22.7 °C). Between the values of pH 6 and pH 9, in a 20 mM Na_xPO_4 buffer, the folding of the enzyme was not affected as shown by an unchanging CD spectrum (Figure 2.9). Furthermore, the folding of the protein did not change over a period of 20 min.

Once this was established the steady state kinetics were determined using the same range of pH values in the assay buffers.

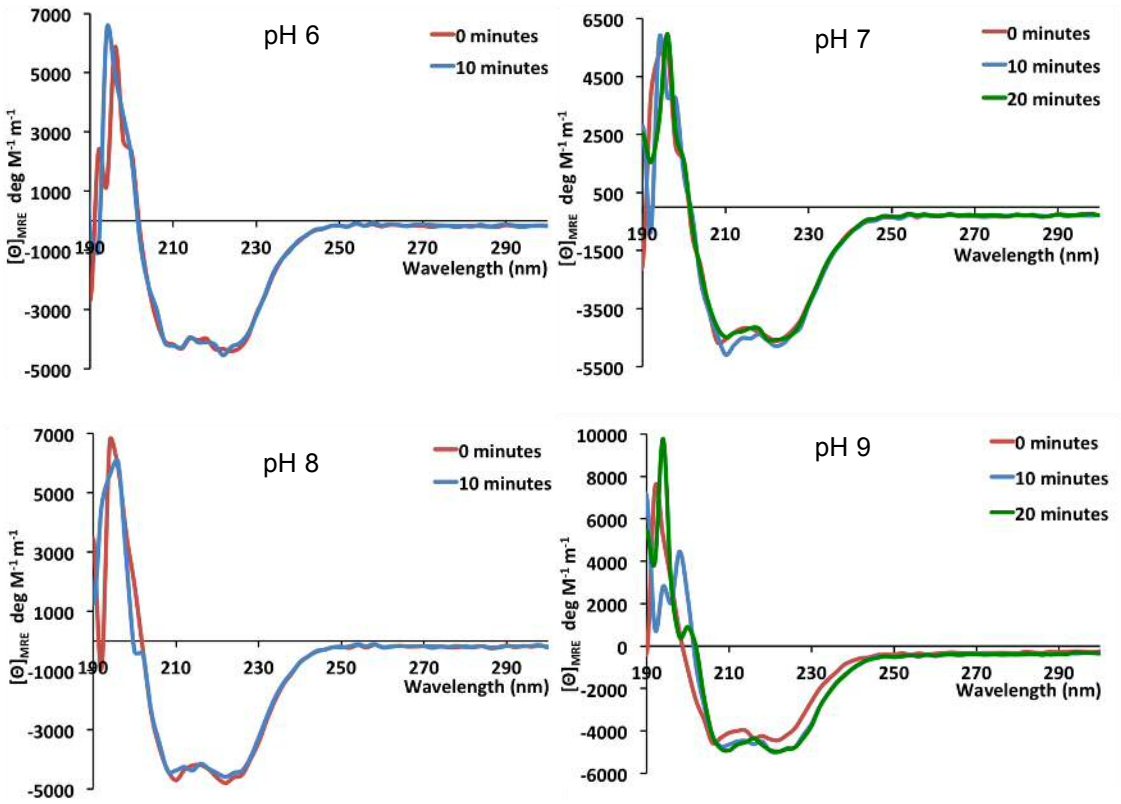

Figure 2.9 CD spectra of ADS at different pH values (pH 6-9). Spectra were recorded at 0, 10 and 20 min intervals.

2.6.4 Steady-state kinetics

The catalytic efficiency of a sesquiterpene synthase is commonly measured by the use of steady state kinetics. This technique involves incubating various concentrations of radiolabelled substrate (in this case [1-^{3}H]-FDP) with a set concentration of enzyme (ADS), for a specific length of time. An organic solvent, such as hexane, extracts the enzymatic-radiolabelled product and the radioactivity is measured through scintillation counting. The substrate is not soluble in the organic solvent and therefore only the radiolabelled product is present in the organic extracts. The results from the scintillation counting are used to obtain initial rates vs. substrate concentration, which is then re-plotted to give a Michaelis-Menten curve, $V = (V_{max}.[S]) / (K_M + [S])$, to determine the kinetic parameters K_M and k_{cat}. The Michaelis constant, K_M, is equal to the substrate concentration at which the rate of the reaction is half of the maximum. K_M is approximately the inverse of the substrates affinity to the enzyme. The catalytic constant, k_{cat}, measures the number of substrate molecules that are converted into products per unit of time. The ratio k_{cat}/K_M is a measure of the catalytic efficiency of the enzyme.

To perform steady state kinetics, all parameters that influence the catalytic incubation were first optimised. The factors that were considered to have an effect were: incubation time, enzyme concentration, magnesium ion concentration, and the pH of the incubation. Each of the factors, in turn, was varied in analytical incubations with tritiated FDP and ADS (Figure 2.10). The resulting radioactivity was measured and the conditions that gave a rate; proportional to enzyme concentration, linear with time, constant with saturated magnesium concentration, and lastly a pH value that gave the maximum rate, were carried further for all future steady state kinetics.

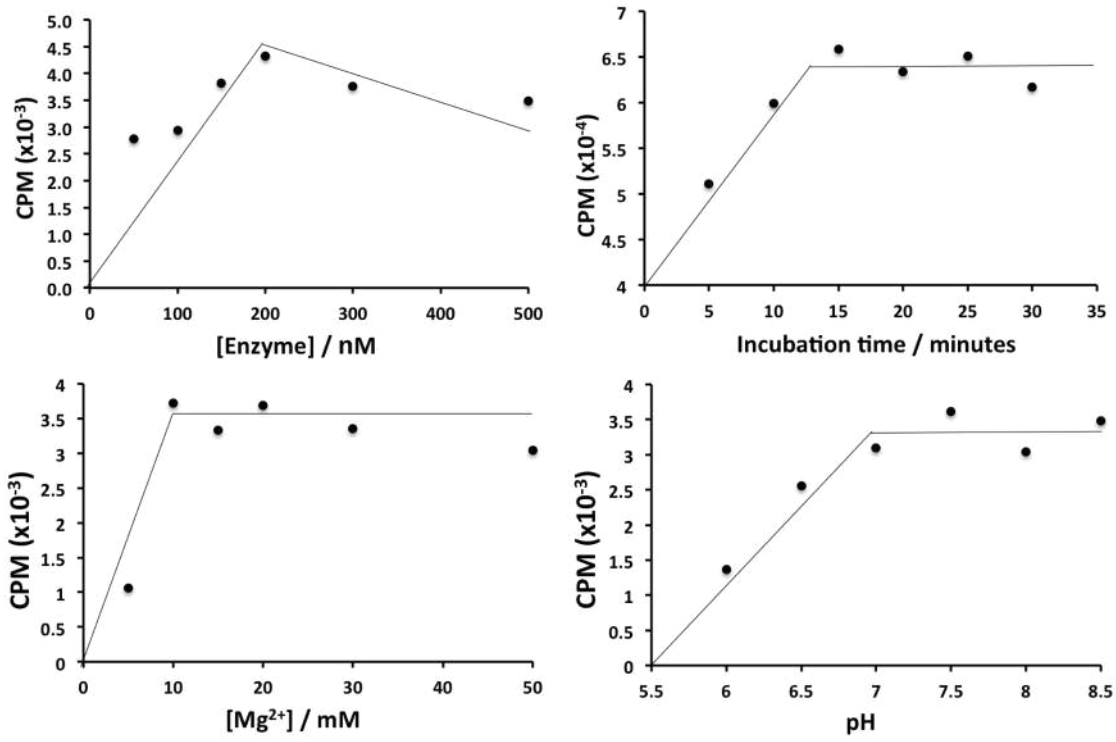

Figure 2.10 Graphs showing radioactivity counts per minute (CPM) against (top left) incubation time, (top right) enzyme concentration, (bottom left) magnesium concentration and (bottom right) pH for turnover of [1-^{3}H]-FDP (10 mM) with ADS in an incubation buffer (20 mM HEPES, 1 mM DTT, 10 mM $MgCl_2$).

Analytical incubations with tritiated FDP (10 μM) and ADS (100 nM) in incubation buffer (20 mM HEPES, 1 mM DTT, 10 mM $MgCl_2$, pH 7.5) were set up for the incubation time to be investigated. Incubations were performed between 0-30 min at 30 °C. Results showed that after 15 min, there was no increasing radioactivity observed in the hexane extracts. The incubation time of 10 min was chosen, as it was close to the maximum counts per minute (which is proportional to the product concentration), but still in the linear range. It is important to pick a value where time and counts follow a linear relationship because this assures that the initial rate is being measured. Enzyme

concentration was then varied between 50-500 nM. The rate of product formation was directly proportional to enzyme concentration up to 200 nM. 100 nM was chosen as the optimal enzyme concentration because the rate must be proportional to the enzyme concentration in order for the enzyme concentration to be the only limiting factor. Variation of Mg^{2+} concentrations showed that the rate was directly proportional to Mg^{2+} concentrations up to 10 mM whereupon increasing metal ion concentration had no increasing effect upon rate, indicating that they were at saturating conditions at this concentration and above; therefore 10 mM Mg^{2+} was used in all incubation buffers subsequently. The pH value for the incubations was varied between 6 and 9. The rate increased as the pH of the incubations increased to 7.5, whereupon increasing pH had no effect on the rate. Therefore the pH value of 7.5 was chosen for all further incubations.

The optimised conditions: 100 nM enzyme, 10 mM $MgCl_2$, pH 7.5 and an incubation time of 10 min were used to measure the steady state kinetics of ADS catalysed turnover of [1-^{3}H]-FDP. k_{cat} and K_M values, calculated as an average weighted mean from three separate experiments, were determined to be 0.016 ± 0.006 s^{-1} and 2.25 μM ± 0.30 μM respectively (Figure 2.11). The catalytic efficiency was calculated at 7.1 x 10^{-3} μM^{-1} s^{-1}. The measured K_M is consistent with that published by Brodelius and co-workers, (K_M was reported as 2.0 μM)[127] however the k_{cat} was found to be 3-fold higher. Furthermore the values measured for ADS are similar to those measured for other sesquiterpene synthases.[98,161]

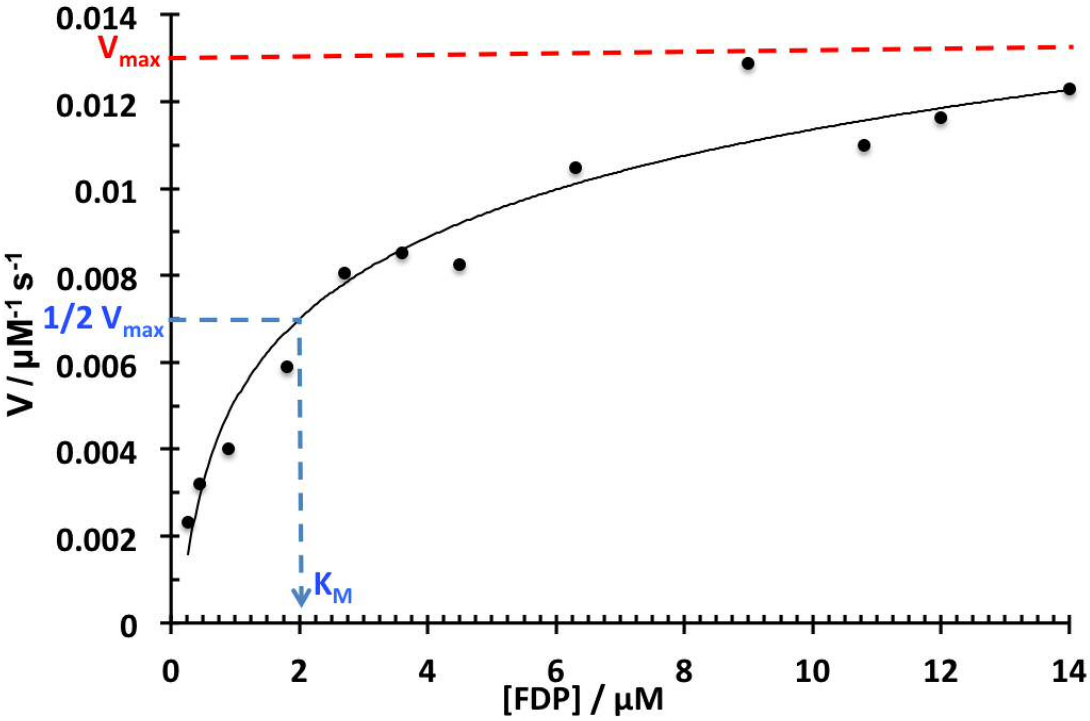

Figure 2.11 Representative Michaelis-Menten graph of steady-state kinetic parameters of ADS.

2.6.5 Product analysis using NMR spectroscopy

To confirm the production of amorphadiene (**45**, Figure 2.12), an incubation of ADS with FDP was carried out on a scale that produced enough material to be analysed by NMR spectroscopy (>2 mg of product). Preparative scale incubations were carried out using typically around 50-100 mg of FDP. Incubations were left for 24 h and pentane extractable products (~80% yield) were analysed using NMR spectroscopy (Figure 2.13). Both ^{1}H and ^{13}C NMR spectroscopy were used to carry out a series of 1D and 2D experiments and the enzymatic product was identified as amorphadiene (**45**), with the spectra corresponding to data previously published (Table 2.1).[124,162] The characteristic peaks of amorphadiene are found at δ_H = 5.05, 4.87 and 4.64 ppm, highlighting the presence of the alkene protons at C2 and C13, respectively. A doublet at δ_H = 0.88 ppm corresponds to the C14 methyl group, and further downfield there are two singlets observed at δ_H = 1.74 and 1.60 ppm corresponding to the allylic methyl groups, C12 and C15, respectively. The proton at C1 appears as a broad multiplet at δ_H = 2.55 ppm.

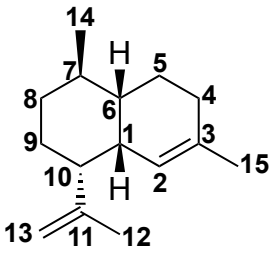

45

Figure 2.12 Structure of amorphadiene with the numbering system used in the assignment.

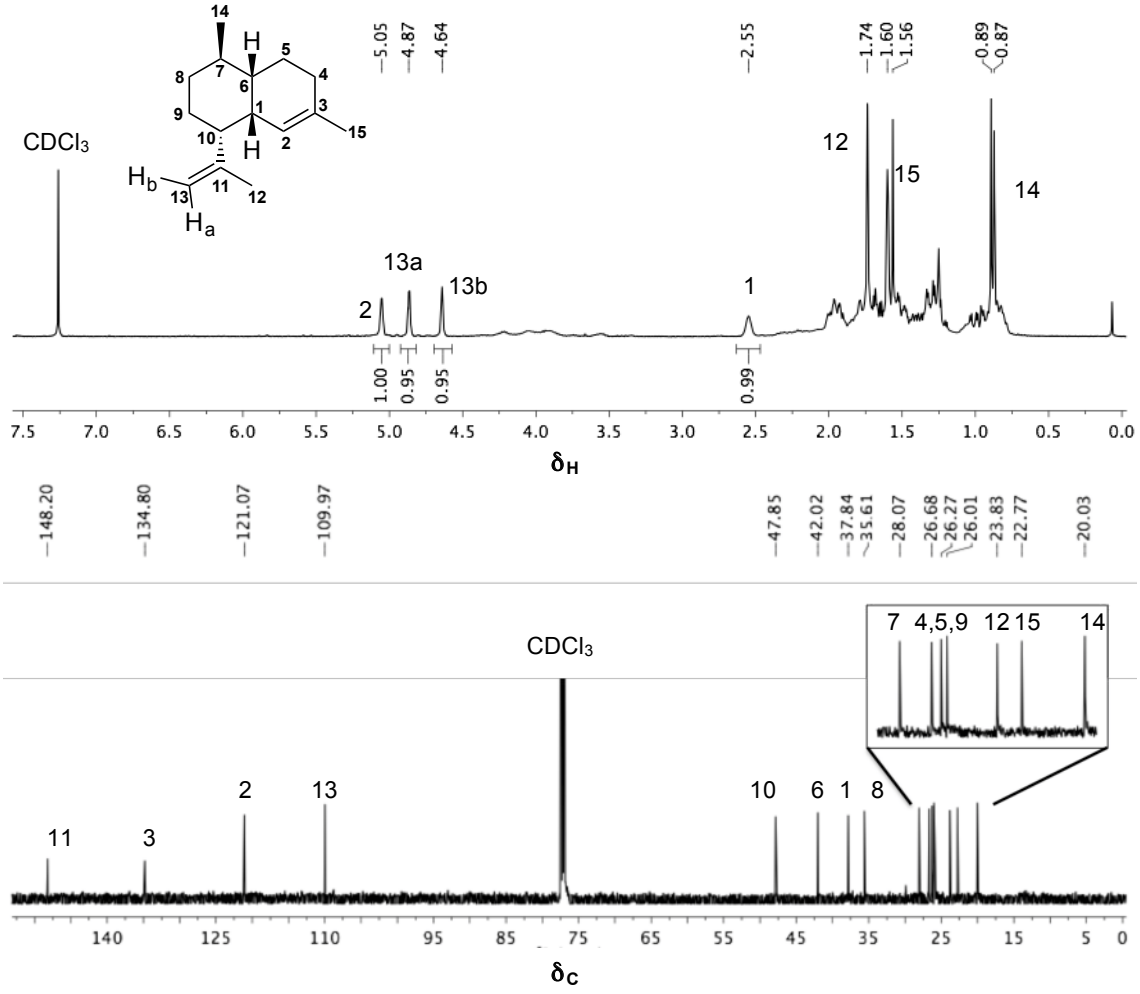

Figure 2.13 ^{1}H NMR spectrum (500 MHz, $CDCl_3$) (Top) and ^{13}C NMR spectrum (125 MHz, $CDCl_3$) (Bottom) of pentane extractable products from an incubation of ADS with FDP (36).

Table 2.1 Complete assignment of amorphadiene (45). Chemical shifts are reported relative to TMS in ppm.

	^{1}H	^{13}C
1	2.55 (1 H, m)	37.84
2	5.05 (1 H, bs)	121.1
3	-	134.8
4	1.5-1.7 (2 H, m)	26.68
5	1.5-1.7 (2 H, m)	26.27
6	1.79 (1 H, s)	42.02
7	1.40 (1 H, m)	28.07
8	0.8-1.1 (2 H, m)	35.61
9	0.8-1.1 (2 H, m)	26.01
10	1.9-2 (1 H, m)	47.85
11	-	148.2
12	1.74 (3 H, s)	23.83
13	4.86 (1 H, m, J = 2.0, 1.5 Hz), 4.64 (1 H, s)	110.0
14	0.88 (3 H, d, J = 6 Hz)	20.03
15	1.60 (3 H, s)	22.77

2. 7 Mutagenesis of ADS

Without a crystal structure of amorphadiene synthase, the identities of the specific residues that are involved in the catalytic mechanism remain elusive. Zhang and co-workers[107] tackled this by identifying a sesquiterpene synthase from *A. annua*, α-bisabolol synthase (BOS), which exhibits a high sequence identity with ADS (82%). BOS converts FDP into 5 monocyclic sesquiterpenoids: α-bisabolol (**60**), trans-α-bisabolene (**111**), β-bisabolene (**112**), cis-α-bisabolene (**113**) and cis-γ-bisabolene (**114**) (Scheme 2.1). The crystal structure of BOS was solved and due to the similarities in sequence and mechanism (Scheme 2.1), the crystal structure was a good candidate as a template for ADS. A homology model was created for ADS (Section 1.3.2) and several presumed plasticity residues (residues which are crucial for the catalysis of the enzymes natural product) were identified and studied. Among these residues, T399, located in the substrate-binding pocket was found to be crucial for the activity of ADS. When threonine was replaced with a hydrophobic amino acid, such as leucine (ADS-T399L), the product distribution changed considerably. Instead of amorphadiene (**45**) being the major compound of 92%, equal amounts of amorphadiene and amorpha-4,7(11)-diene (**64**) were observed, in addition to low amounts of β-sesquiphellandrene

(**63**) and zingiberene (**115**) (Scheme 2.1). The formation of these additional products suggested that the change from threonine caused the enzyme to lose regioselectivity at the deprotonation step, as well as allowing for premature quenching of the C1 on cation **53** (Scheme 2.1). Similar product profiles were observed when threonine was replaced with alternative neutral amino acids, alanine and asparagine. Replacing threonine with charged residues, aspartic acid and arginine, resulted in a loss of catalytic activity.

Mutant ADS-T399S showed a substantial increase in enzyme activity (k_{cat}/K_M increased by approximately 72%), and possessed a higher turnover rate of FDP (k_{cat} increased by approximately 83%). Zhang and co-workers[107] proposed that the increase in activity was likely a result of accelerated product release since by replacing a threonine with a serine, the hydroxyl side chain remained in position 399 but increased in polarity. This in turn creates a more hydrophilic environment that would result in a faster release of the hydrophobic product.

With all these findings combined, it was concluded that not only did the hydroxyl group on the side chain of threonine have an effect on the regioselective deprotonation step, but also on the rate of product release.

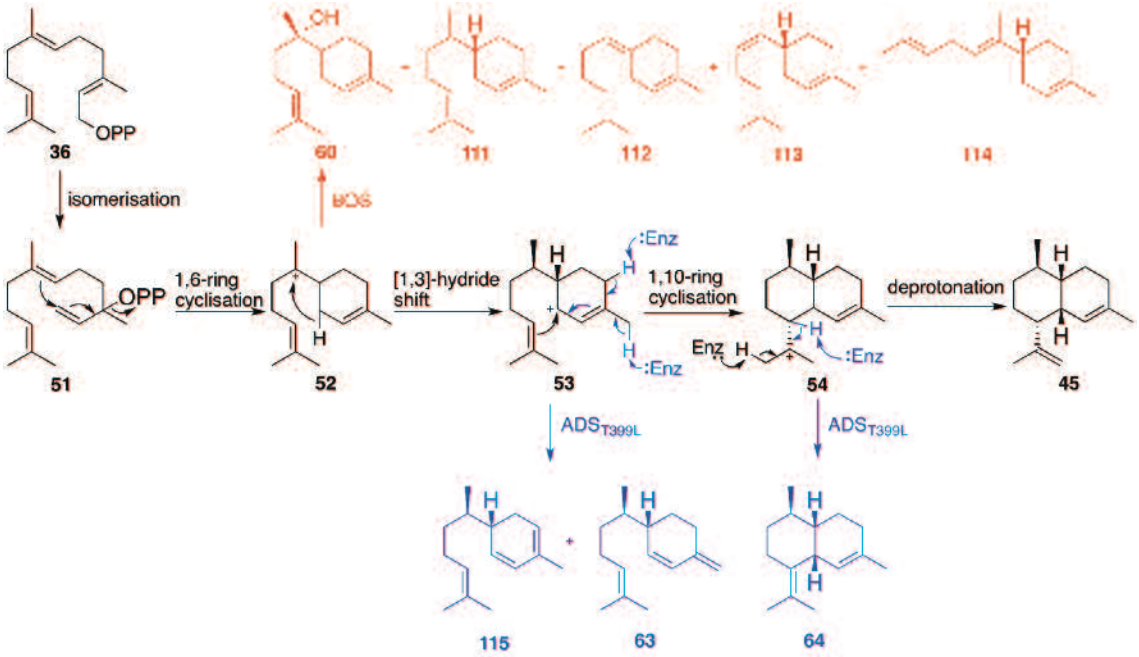

Scheme 2.1 Proposed mechanisms for the conversion of FDP into sesquiterpene products catalyzed by BOS (red), ADS, ADS-T399L and ADS-T399S (black), with the additional products generated by ADS-T399L (blue).

A different approach was taken in this project when performing site directed mutagenesis on ADS. Instead of focusing on the C-terminal domain, which is

responsible for the enzymatic catalysis, SDM was performed in the N-terminal domain. The function of the N-terminal domain is still unclear, however it was observed first with TEAS, and later with (+)-bornyl diphosphate synthase (BPPS) from *Salvia officinalis* that upon ligand binding to the C-terminal located active site, the N-terminus caps the active site of the enzyme to adopt a closed conformation, implying that it might be important for product release and desolvation of the active site.[104,163] By using SDM, purposely-engineered mutants can aid the mapping of the structure and function of the N-terminal domain.

Previous work carried out in the Allemann group[96] (and unpublished work) involved constructing truncated and single point mutation variants inside the N-terminal domain of *E*-β-farnesene synthase (EBFS)[161,164] and δ-cadinene synthase (DCS)[98,165]. EBFS and DCS catalyse the conversion of FDP to *E*-β-farnesene (**59**) and δ-cadinene (**116**), respectively (Scheme 2.2). To examine the contribution of the N-terminal domain to the active site closure and desolvation, truncated variants were designed in attempts to gradually impair the structure of the N-terminal domain. Deletions, starting at the N-terminus, of 14 (M14) and 24 (M24) residues in EBFS and 8 (M8), 20 (M20) and 30 (M30) residues in DCS were constructed.

It was found that with DCS, mutants M8 and M20 were reasonably functional synthases compared to the wild type, and the gradual deletion of residues led to a higher accumulation of germacradiene-4-ol (**117**), reaching 75% of total products by the M30 mutant (Scheme 2.2). This hydroxylated compound was proposed to be a result of premature quenching, by water, of the more stable allylic germacren-6-yl carbocation (**55**) due to an increase of solvation (Scheme 2.2). Steady state kinetics could not be recorded for M30 due to its very poor enzymatic activity.

Similarly, mutants M14 and M24 of EBFS showed efficient catalytic activity with M14, however no activity with M24 (Scheme 2.2). The inactivation of M30 (DCS) and M24 (EBFS) clearly indicates that the N-terminal domain has an effect on the catalysis by these synthases. The accumulation of increasing amounts of germacradiene-4-ol (**117**), as the truncation of DCS increases, is most likely due to premature quenching of water, which implies that the N-terminal domain is involved in the desolvation and active site closure of the enzyme. This further implies that the structural contribution of the N-terminal domain to catalysis resides mainly in a highly conserved inner polypeptide strand (M^{21}**RP**KAD**F**^{27}Q**PS**^{30} in DCS) and (R^{15}**PP**MTK**H**^{21}A**PS**^{24} in EBFS), despite the slightly different sequence of residues.

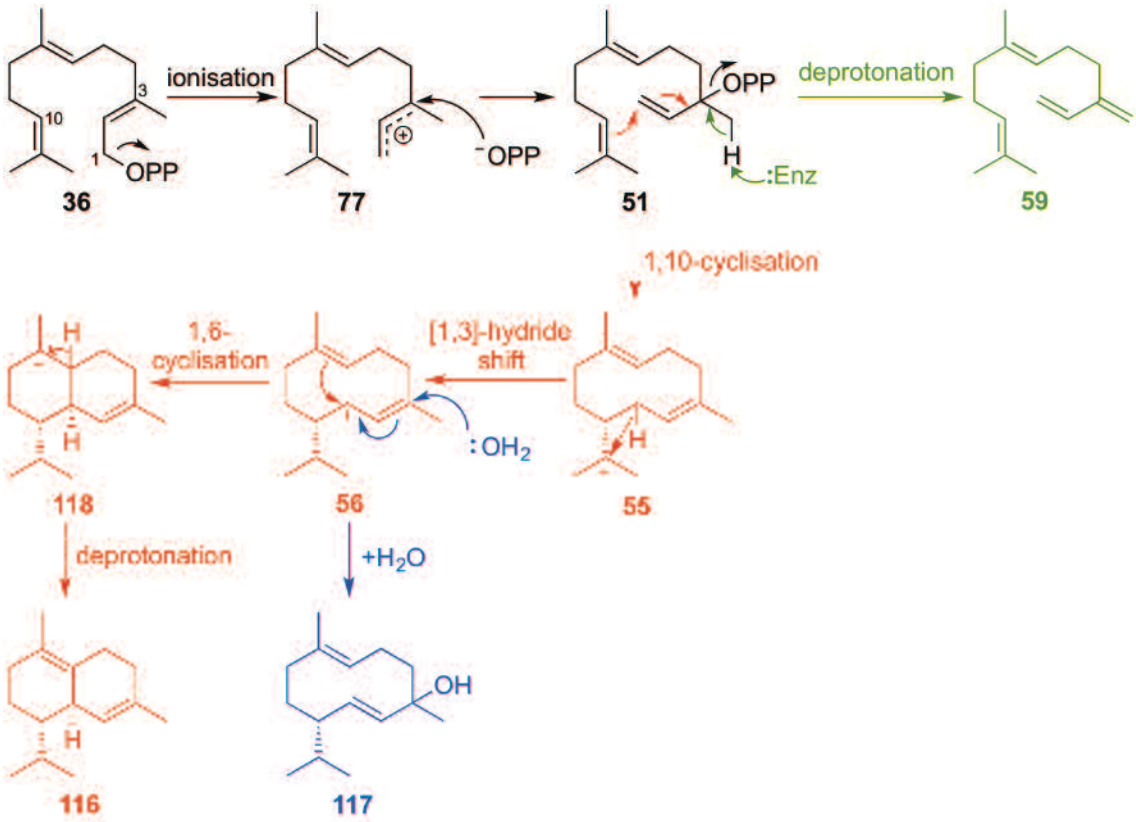

Scheme 2.2 Proposed catalytic mechanisms of EBFS (Black & Green) and DCS (Black & Red). Increasing truncations of DNA in DCS causes premature quenching of germacrene-6-yl cation (118) to form germacradiene-4-ol (117) (Blue).

To further investigate the role of the N-terminal domain, particularly after the conserved [X**RP/PP**XXX**F/H**X**PS**] motif, the X-ray crystal structure of DCS was compared to a homology model of EBFS (generated using the unrestricted algorithm of I-TASSER). The comparisons of both showed that aromatic residues, F30 in EBFS and F36 in DCS, were both positioned facing inwards towards the catalytic C-terminal domain. To explore whether they had any function towards catalysis, the phenylalanine residues were replaced with alanine residues. These single point mutations showed a substantial 4-fold increase in k_{cat} and a small reduction in K_M that combined, gave a 7-fold enhancement of the catalytic efficiency for both enzymes. This observation could imply that although this phenylalanine residue is too far (>12 Å) from the active site of both enzymes, it is likely to be part of the structural determinant responsible for the product release, which is suggested to be the rate limiting step during the catalysis of sesquiterpene synthases.[166]

With these interesting results for EBFS and DCS in mind, the same approach was taken with ADS to see if the results would be complementary. The amino acid sequence of ADS was aligned with EBFS and DCS and it was found that EBFS M14

and DCS M20 were equivalents to ADS M8 (Figure 2.14). ADS M8 was created to see if enzymatic activity was retained like the latter mutants. Additionally if ADS M8 produced any hydroxylated products, it would add further corroborating evidence for the postulate that the truncated segment causes an increase of solvation in the active site.

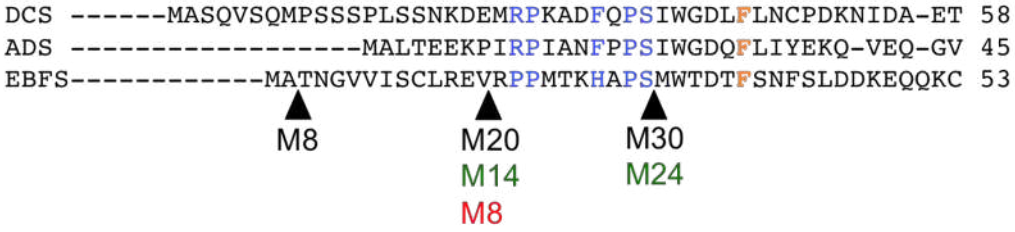

Figure 2.14 Amino acid sequence alignment of the N-terminal residues of DCS, ADS and EBFS. Blue residues highlight the [XRP/PPXXXF/HXPS] motif. Orange residues highlight the phenylalanine in all three enzymes that was replaced with an alanine. Black M8, M20 and M30 are truncated variants of DCS. Green M14 and M24 are truncated variants of EBFS. Red M8 is a truncated variant of ADS.

In order to truncate the first 8 residues of ADS, a primer was designed to introduce an *Nco*I restriction site in the corresponding point in the gene coding for the ninth residue. This resulted in mutant ADS-I9M/R10G (Figure 2.15). The unwanted mutation of R10G, required for the formation of the new *Nco*I site, was restored back to the original residue (G10R) with the use of another designed primer (Section 7.1.7) to form mutant ADS-I9M.

The gene coding mutant ADS-I9M/R10G possesses two *Nco*I restriction sites located on the first and ninth residue, and therefore was digested with *Nco*I restriction enzyme to enable the truncation of 24 base pairs that code for the first 8 amino acids. Agarose gel electrophoresis was carried out to separate the two resulting fragments of DNA. The open stranded plasmid was ligated back together using T4 DNA ligase, following the manufacturer's protocol, to form ADS-M8/R10G. The fourth mutant created was ADS-M8, achieved by changing the glycine (G10) back to the original arginine (Figure 2.15).

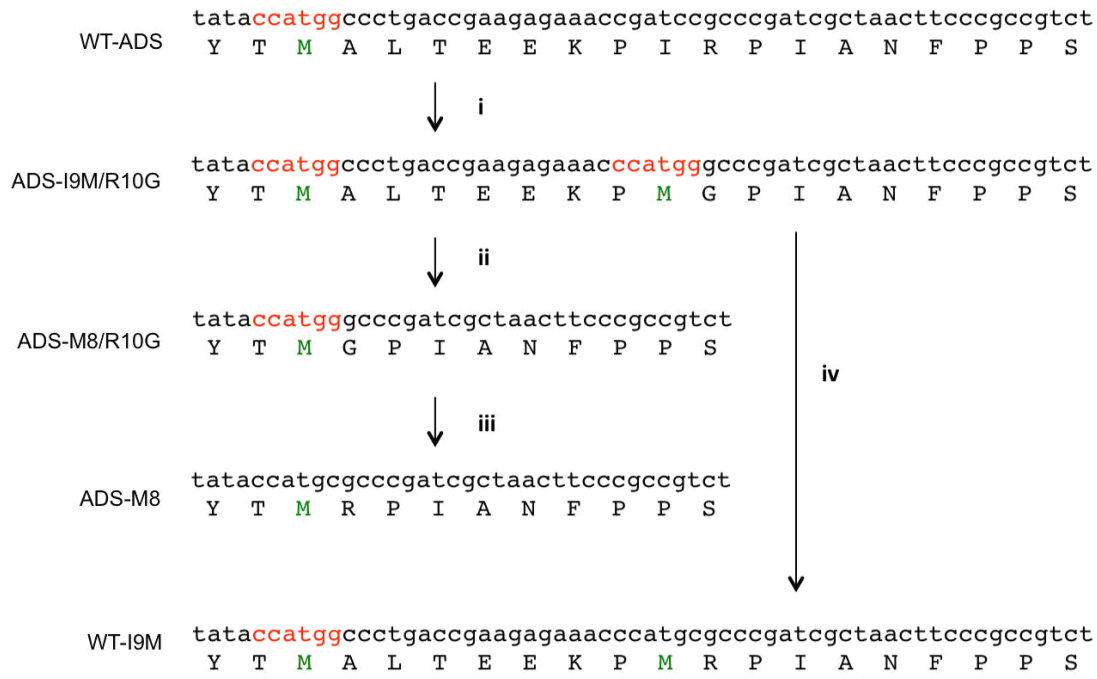

Figure 2.15 Design of mutants ADS-I9M/R10G, ADS-M8/R10G, ADS-M8 and ADS-I9M. Red residues denote *Nco*I sites; Green M's denote start codons. i) Introduction of a second *Nco*I site, ii) digestion with *Nco*I restriction enzyme to truncate 24 base pairs that code for the first 8 amino acid sequence, iii) mutation G2R, iv) mutation G10R.

The four new mutants produced by heterologous expression in *E. coli* proved to be active variants, as shown by observation of pentane extractable products by GC-MS (Figure 2.16). Each gas chromatogram of the products deriving from incubation of each mutant with FDP was compared with that generated from incubation of the wild-type ADS (ADS-WT) with FDP. GC chromatograms of all the ADS variants did not show any formation of hydroxylated products.

In addition to studying the target mutant ADS-M8, steady state kinetics were measured for all four variants, summarized below (Table 2.2). Mutant ADS-M8 retained good enzymatic activity, with k_{cat} and K_M values of 0.0051 ± 0.0001 s^{-1} and 1.25 ± 0.10 μM respectively (Figure 2.16). The catalytic efficiency was calculated at 4 x 10^{-3} μM^{-1} s^{-1}. Compared to ADS-WT, the Michaelis constant, K_M, was almost half the value and the catalytic constant, k_{cat}, was 3.2 fold less. This resulted in the catalytic efficiency of the enzyme, k_{cat}/K_M being almost half of that of ADS-WT. These results correlate with what was observed for DCS.[96] Although DCS-M20 had a larger K_M than DCS, the k_{cat} also decreased by 2.5 fold and the k_{cat}/K_M reduced by over 4 fold. The reduced catalytic constant and catalytic efficiency of ADS-M8 help conclude that although the specific function of the N-terminal domain remains unclear, it can be presumed that it plays a part in the structural contribution to the enzymes catalysis.

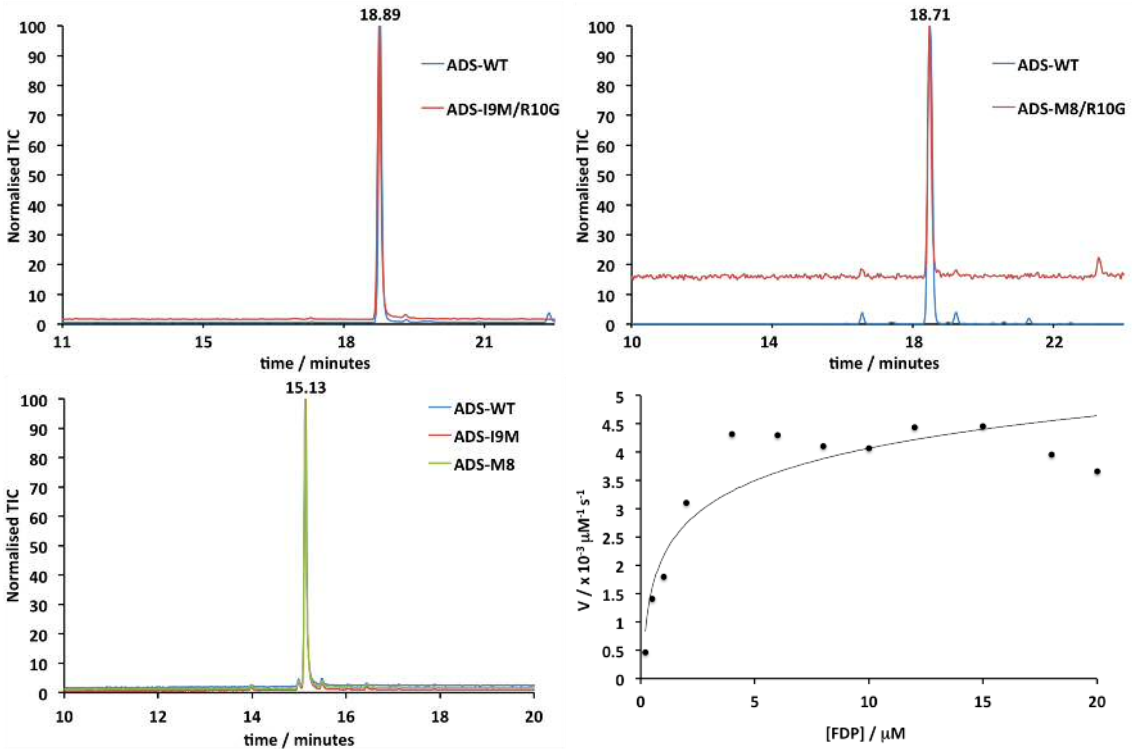

Figure 2.16 Top left: Overlaid gas chromatograms of ADS-WT and ADS-I9M/R10G. Top right: Overlaid gas chromatograms of ADS-WT and ADS-M8/R10G. Bottom left: Overlaid gas chromatograms of ADS-WT, ADS-I9M and ADS-M8. Bottom right: Representative graph for the calculation of steady-state kinetic parameters of ADS-M8.

Table 2.2 Steady state kinetics carried out on ADS, ADS-I9M/R10G, ADS-M8/R10G, ADS-I9M, ADS-M8 and ADS-F24A.

Enzyme	k_{cat} (x10^{-3} s^{-1})	K_M (μM)	k_{cat}/K_M (x10^{-3} $\mu M^{-1}s^{-1}$)
ADS-WT	16.03 ± 0.60	2.25 ± 0.30	7.1 ± 0.9
ADS-I9M/R10G	6.92 ± 0.10	13.20 ± 2.60	0.05 ± 0.01
ADS-M8/R10G	6.91 ± 0.80	9.37 ± 1.90	0.7 ± 0.2
ADS-I9M	9.48 ± 0.30	2.64 ± 0.30	3.6 ± 0.4
ADS-M8	5.06 ± 0.10	1.25 ± 0.10	4.0 ± 0.7
ADS-F24A	1.29 ± 0.10	2.67 ± 0.70	0.5 ± 0.2

Carrying out additional Michaelis-Menten kinetics on mutants I9M/R10G, M8-R10G and I9M, showed that the replacement of arginine 10 with glycine (R10G) had a larger effect on the catalytic efficiency than truncating the first 8 residues from ADS. In both I9M/R10G and M8-R10G, the k_{cat} was reduced to less than half of that measured for the WT and the binding constant, K_M, was increased by more than 5-fold. This set of results strongly correlate with the idea that the structural contribution of the N-terminal domain to enzymatic catalysis resides mainly in a highly conserved inner polypeptide strand (I^{9}**RP**IAN**F**^{15}P**PS**^{18}), as was proposed previously.[96]

Amino acid sequence alignment highlighted that ADS had a phenylalanine in the same position as EBFS and DCS, however due to the shorter DNA coding sequence for ADS, this phenylalanine was in position 24 in the amino acid sequence, compared to F30 in EBFS and F36 in DCS (Figure 2.14). SDM was performed on ADS to replace the phenylalanine with an alanine (ADS-F24A) and the new mutant produced by heterologous expression in *E. coli* led to be an active variant, as shown by observation of pentane extractable products by GC-MS (Figure 2.17). Measurement of the steady state kinetics of ADS-F24A surprisingly did not follow the trend shown by EBFS and DCS but instead a k_{cat} that had decreased by more than 10-fold (1.29×10^{-3} s^{-1}), and a slightly larger K_M (2.67 μM) was found. This combination resulted in a 14-fold decrease in catalytic efficiency (5×10^{-4} $\mu M^{-1}s^{-1}$), relative to wild type ADS (Figure 2.17).

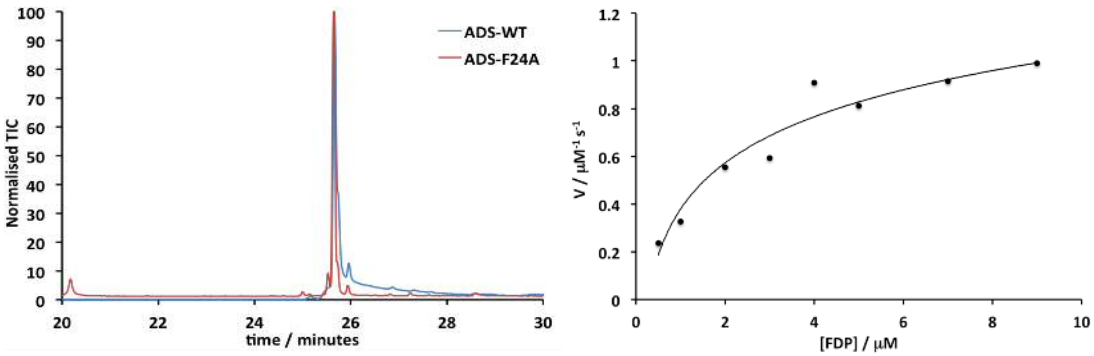

Figure 2.17 Left: Overlaid GC spectra of ADS-WT and ADS-F24A. Right: Representative graph for the calculation of steady-state kinetic parameters of ADS-F24A.

2. 8 Summary

To conclude, *E. coli* was successfully transformed with the ADS gene and heterologous expression of the gene in *E. coli* under optimal conditions produced the corresponding ADS enzyme. The gene was originally transferred from a pTrc99a

vector to a pET21d vector to allow for a hexa-histidine motif to be introduced into the C-terminus of the pET21d-ADS plasmid. The addition of a His-tag allowed for an efficient purification of the ADS protein *via* nickel affinity chromatography. The enzymatic product, amorphadiene, was characterised by the means of NMR spectroscopy and GCMS and was in agreement with reported literature.

Steady state kinetics were performed to determine the catalytic efficiency of ADS, and compare it to the catalytic efficiency of ADS reported in the literature. Parameters that influence the catalytic incubation were first optimised. Once the optimal conditions were determined; 100 nm ADS, 10 mM $MgCl_2$, pH 7.5 and an incubation time of 10 min, steady state kinetics were carried out. k_{cat} and K_M values were determined to be 0.016 ± 0.006 s^{-1} and 2.25 μM ± 0.30 μM respectively. The catalytic efficiency was calculated at 7.1 x 10^{-3} μM^{-1} s^{-1}. The measured K_M is consistent with that published by Brodelius and co-workers,[127] however the k_{cat} was found to be 3-fold faster.

Lastly ADS mutants were designed and created to assess the contribution of the N-terminal domain on the enzymes catalysis. Mutant ADS-M8 possessed a truncation of 8 amino acids from the N-terminus of the enzyme and the catalytic efficiency of the mutant was almost half of that reported for the wild type, indicating that the N-terminal domain can be presumed to play a part in the structural contribution to the enzymes catalysis.

Chapter 3. Synthesis of farnesyl diphosphate analogues

3.1 Preface

This chapter will cover the design and synthesis of each FDP analogue that was chosen to be tested as a substrate of ADS. A range of FDP analogues were designed and synthesised, including methylated, oxygenated and aza-derivatives with these alterations situated in various positions of the FDP backbone (Figure 3.1). This series of analogues enabled exploration of the scope of promiscuity displayed by ADS.

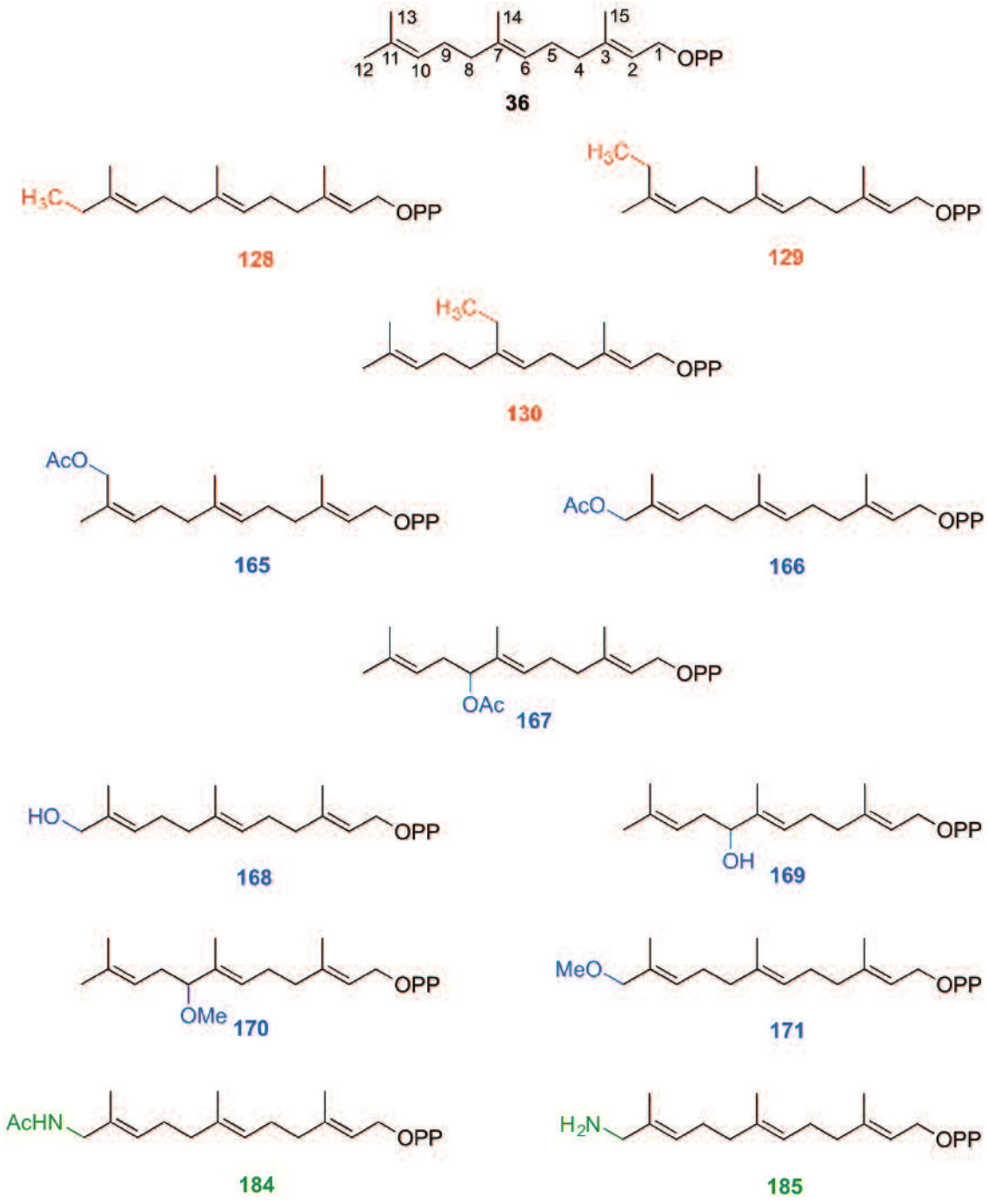

Figure 3.1 FDP analogues that were synthesised in this project. The numbering system shown on FDP (36) will be used throughout this report.

3.2 Diphosphorylation of farnesol analogues

To synthesise FDP analogues, the corresponding farnesol derivatives were first made, and then diphosphorylated. The diphosphorylation began with a halogenation of the alcohol on the farnesol derivative (**119**).[167,168] This was followed by a direct displacement of the halide (**120**) with tris(tetrabutylammonium) hydrogendiphosphate (**121**), to produce the corresponding diphosphate analogue **122** (Scheme 3.1) as described by Poulter and co-workers.[169]

Conversion of farnesol analogues to the corresponding allylic halide was carried out following two different procedures. The first yielded a farnesyl chloride analogue achieved by a nucleophilic substitution, *via* a mesylate intermediate, with lithium chloride.[167]

Alternatively, to prepare farnesyl bromide analogues, a direct nucleophilic substitution was carried out with phosphorous tribromide.[168]

The tris(tetrabutylammonium) hydrogendiphosphate salt was prepared by passing disodium dihydrogen diphosphate (**123**) through a Dowex AG 50W-X8 cation exchange resin (100-200 mesh, H^+ form). Deionized water was used to elute the free acid and the resulting solution was titrated to pH 7.3 with tris(tetrabutylammonium) hydroxide. The resulting solution was lyophilised to yield **121** in the form of a white powder that was freshly recrystallized from ethyl acetate immediately prior to use.

Once the farnesol derivatives were diphosphorylated, purification of the corresponding FDP analogues was carried out in two different manners, resulting in the FDP salt with two alternative counter ions. The first method required purifying the crude FDP tris(tetrabutylammonium) salt by flash chromatography on silica gel (eluting with 6:2.5:0.5, isopropanol: water: 30% ammonium hydroxide). TLC fractions that contained the diphosphate (6:3:1, isopropanol: water: 30% ammonium hydroxide, Rf: 0.3, visualisation with 4.2% ammonium molybdate and 0.2% ceric sulfate in 5% H_2SO_4) were pooled. The isopropanol was removed under reduced pressure and the remaining solution was lyophilized to give the FDP analogue possessing tris(tetrabutylammonium) counter ions (**124**).[170] The second purification method was performed by passing the crude FDP tris(tetrabutylammonium) salt through a column of DOWEX 50W-X8 cation exchange resin (ammonium form) to generate the FDP trisammonium salt, which was then further purified by reverse phase high performance liquid chromatography (HPLC – method used is stated in Section 7.2.1). Pure fractions were lyophilised to yield purified FDP analogues possessing ammonium counter ions (**125**).[169]

The advantage of exchanging the counter ions to ammonium ions was that, when exchanged, the form of the FDP analogue changes from an oil to a powder, making it easier to weigh as well as it possessing better chromatographic properties.

ADS was challenged with both forms of FDP (**36**)**.** The enzyme was able to convert both into amorphadiene. In addition to this observation, by keeping the tris(tetrabutylammonium) ions, the purification time was halved, from two days to one.

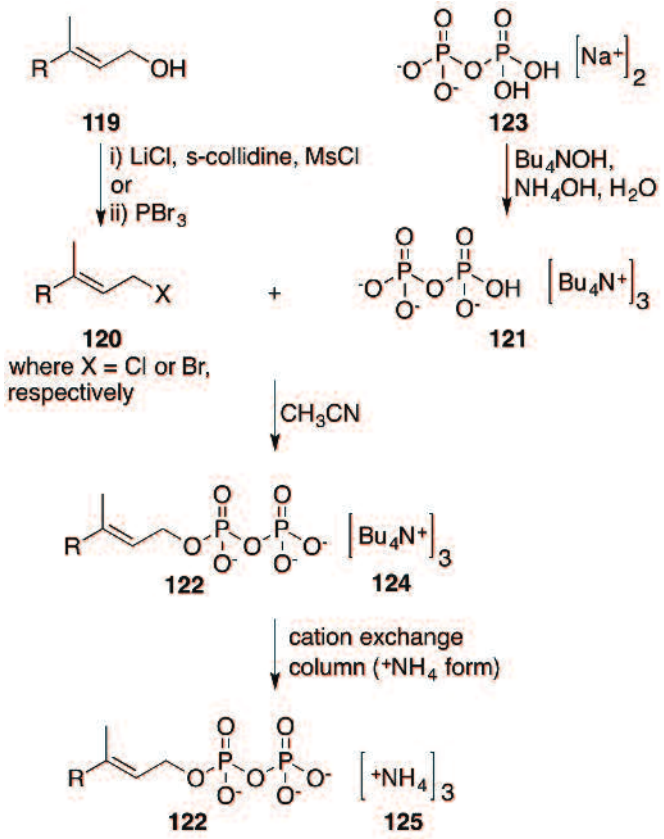

Scheme 3.1 Method of preparation of the FDP analogues synthesised in this work and purified to yield either tris(tetrabutylammonium) (124) or ammonium (125) salts.

3.3 Synthesis of FDP (36)

The synthesis of FDP (**36,** Scheme 3.2) was required to test the catalytic activity of ADS by GC-MS analysis, in addition to carrying out full kinetic analyses. The synthesis was performed following protocols reported by Meyers,[167] Poulter,[169] and Keller[170] Beginning with commercially available farnesol (**126**), farnesyl chloride (**127**) was synthesised via a mesylate intermediate.[167] Farnesyl chloride was diphosphorylated with the use of tris(tetrabutylammonium) hydrogen diphosphate (**121**). The 24 h reaction of **127** and **121** afforded FDP (**36**) with tris(tetrabutylammonium) counter ions (**124**), achieving an overall yield of 51%.

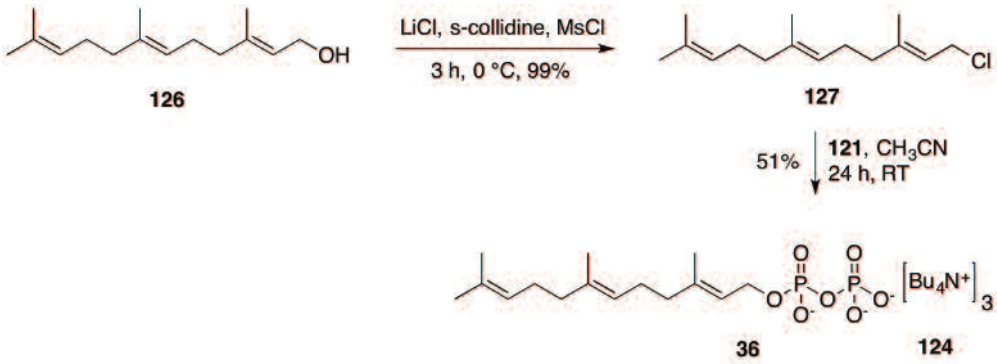

Scheme 3.2 Synthesis of FDP (36).

3.3.1 Methylated FDP analogues

Methylated analogues (12-methyl FDP, **128**, 13-methyl FDP, **129**, and 14-methyl FDP, **130**) were the first group of analogues chosen to test as substrates of ADS. The size of the functional group added to the FDP backbone was one of the concerns when designing this project. The dimensions of the enzymes active site and the extent to how big a substrate it can accommodate are unknown, and starting with a minimal change in size was seen as a good to start. Choosing a hydrocarbon group, instead of a heteroatom such as a hydroxyl group, also reduces the possibility of the novel analogue intercepting with the enzymatic mechanism, by either reacting with amino acid residues in the active site or with an intermediate carbocation during the catalytic cycle.

3.3.2 12-Methyl FDP (128)

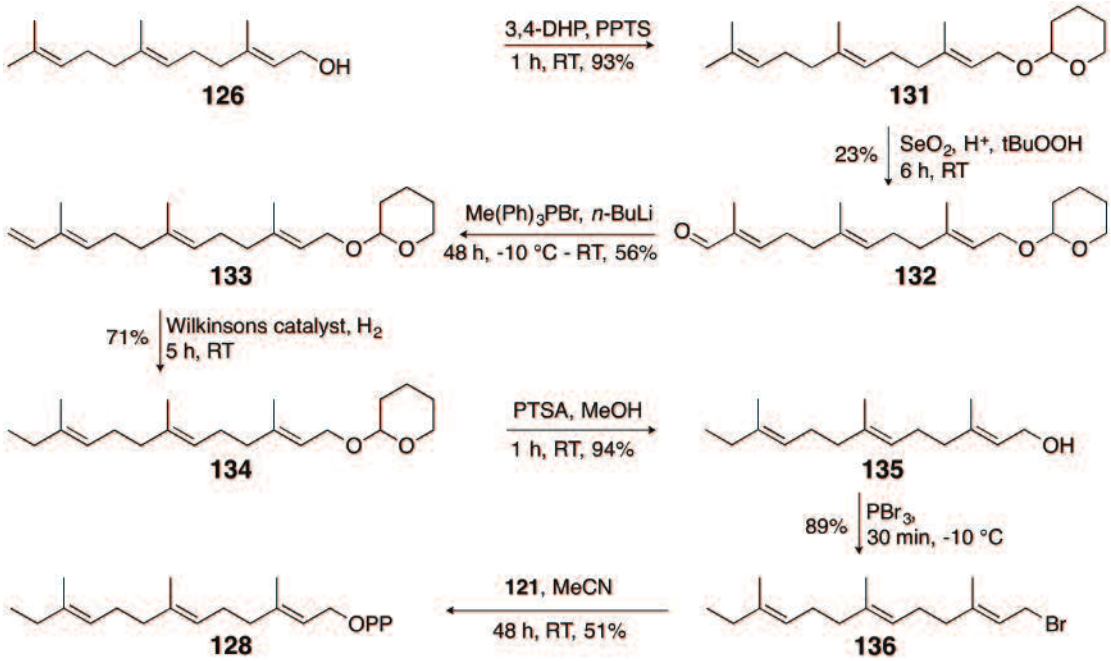

Scheme 3.3 Synthesis of 12-Methyl FDP (128).

12-Methyl FDP (**128**) was prepared *via* a seven step synthesis (Scheme 3.3). This analogue has been previously synthesised in the Allemann group following a different synthetic route.[171] The first step was an acid-catalysed protection of farnesol (**126**) to form the tetrahydropyran ether **131** (94% yield).[172] This was followed by an allylic oxidation using a combination of selenium dioxide, salicylic acid and *tert*-butyl hydroperoxide to produce aldehyde **132** (23% yield).[173,174] The limitations that selenium dioxide brings, such as forming the reduced form of selenium and organoselenium by-products, were prevented by using it in a catalytic quantity and using tert-butyl hydroperoxide as a co-oxidant to regenerate SeO_2 *in situ*. A Wittig olefination was carried out to convert **132** to **133** using methyl triphenyl phosphonium bromide and *n*-butyl lithium (56% yield).[175] The terminal unsaturated alkene in **133** was then hydrogenated with the use of a homogeneous catalyst chlorotris(triphenylphosphine)rhodium(I), also known as Wilkinson's catalyst, used because of its ability to selectively hydrogenate the terminal alkene without affecting the other carbon-carbon double bonds in the compound (71% yield).[176] Once **134** was prepared, a deprotection of the tetrahydropyran ether with *p*-toluene sulfonic acid and methanol afforded the resulting alcohol **135** (94% yield), which in turn was brominated with phosphorous tribromide to **136** (89% yield) and immediately diphosphorylated to the final product, **128**, with the use of salt **121**.[168,169,177] After a 24 h reaction, the crude product was directly purified using flash chromatography on silica gel (6:2.5:0.5,

isopropanol: water: 30% ammonium hydroxide)[170] and was used as the tris(tetrabutylammonium) salt (**124**) (51% yield).

3.3.3 13-Methyl FDP (129)

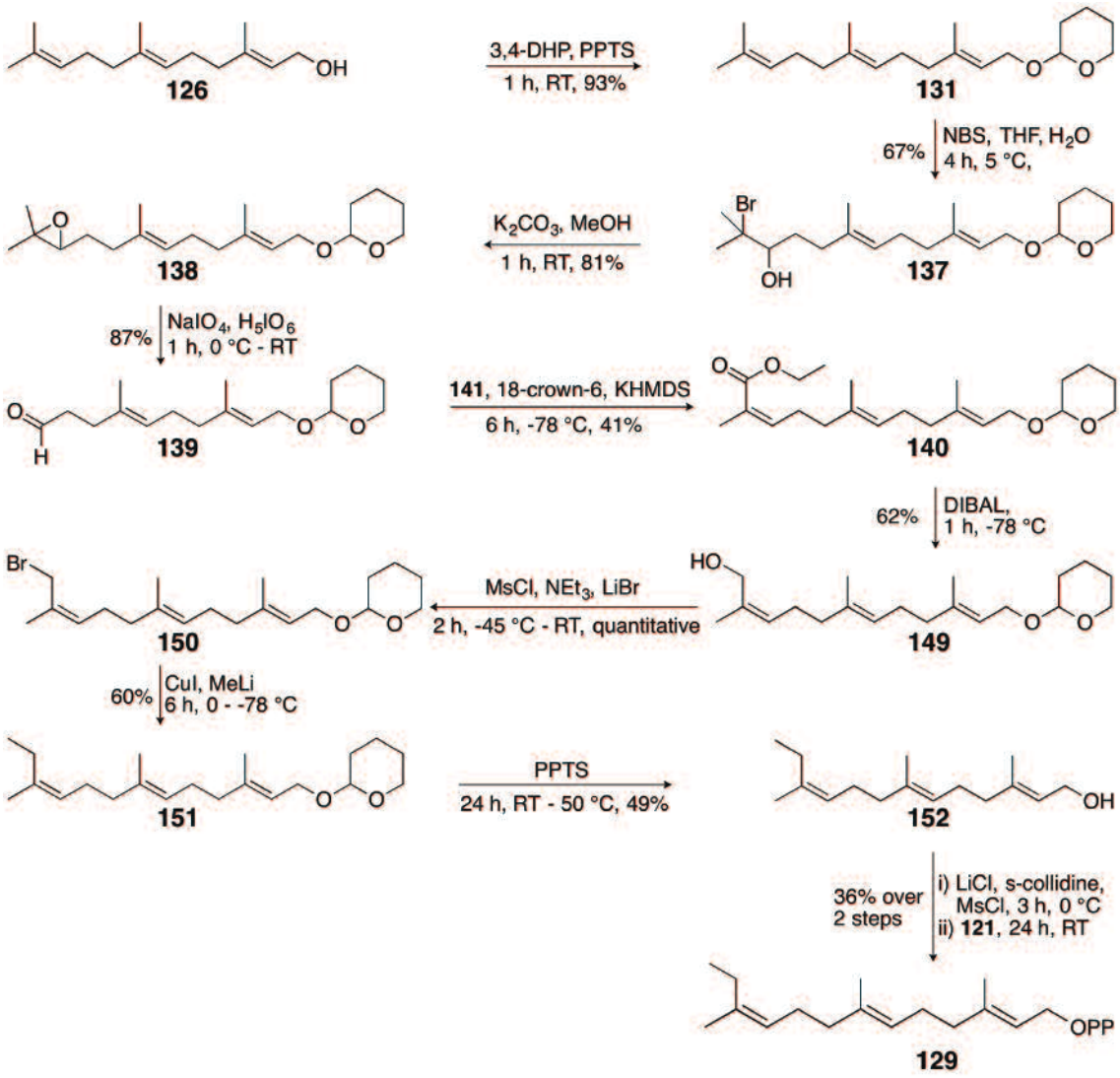

Scheme 3.4 Synthesis of 13-methyl FDP (129).

13-Methyl FDP (**129**), a novel analogue to our knowledge, was synthesised in ten steps (Scheme 3.4). With the use of *N*-bromosuccinimide in THF/H_2O, a bromohydrin was successfully created from the distal alkene group of **131** to give **137** (67% yield).[178] An intramolecular S_N2 reaction with potassium carbonate and methanol formed the epoxide **138** (81% yield),[178] which was cleaved with sodium periodate and periodic acid to form aldehyde **139** (87% yield).[179] Once aldehyde **139** had been prepared, the next step was to carry out an olefination reaction that favoured the formation of the *Z*-alkene **140**.

A Horner-Wadsworth-Emmons modification of the classic Wittig olefination was carried out to form an α, β-unsaturated ester (**140**). A typical phosphonoester, such as triethyl phosphonoacetate, could not be used in this synthesis, as it is commonly known that Horner-Wadsworth-Emmons reactions preferentially favours the formation of *E*-olefins.[145,180] To overcome this problem, triethyl phosphonoacetate had to be modified in a way that would yield *Z*-olefins stereoselectively. It has been reported by Still and Gennari,[181] by using a phosphonoester such as ethyl trifluoroethyl phosphonopropionate (**141**), electron-withdrawing groups are introduced to stabilize the formation of the erythro intermediate adduct. This in turn facilitates the elimination step to produce a *Z*-olefin (Scheme 3.5).

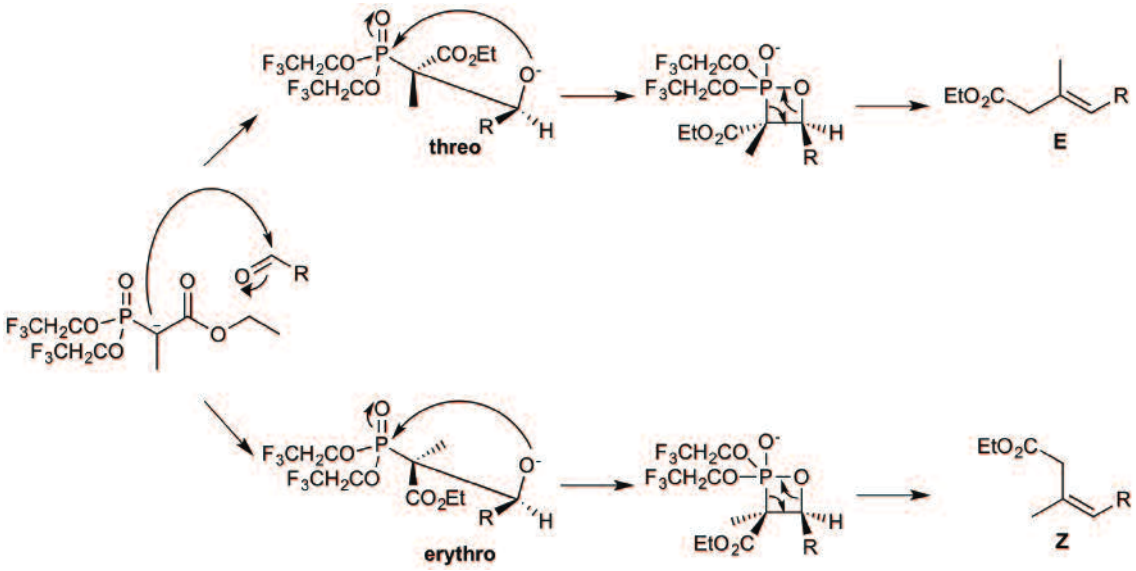

Scheme 3.5 Possible products that result from a Horner-Wadsworth-Emmons olefination. A threo adduct gives rise to *E*-isomers, whereas an erythro adduct will result in the production of *Z*-isomers.

Three different procedures were carried out for the production of **141** (Scheme 3.6). The first procedure consisted of a Michaelis-Arbuzov reaction.[182,183] This is a S_N2 reaction where a nucleophilic phosphite, in this case triethyl phosphite **142**, attacked an electrophilic alkyl halide, ethyl 2-bromopropionate **143**. The resulting anionic halide then underwent a second S_N2 reaction by attacking one of the alkyl groups attached to the phosphorous, forming a new alkyl halide and phosphonate **144** with a yield of 65%. Once **144** was synthesised, phosphorous pentachloride was used to yield **145** (61% yield).[184] The replacement of the alkyloxy groups with chlorides generated a highly reactive phosphoryldichloride ready for the following reaction. Trifluoroethanol, with the aid of diisopropylethylamine, was reacted with **145** to give **141** (22% yield).[181] After

each step the product was purified by fractional distillation under reduced pressure. The overall yield for this synthesis was poor, and was recorded as 9%.

The second approach to synthesising **141** was aimed at avoiding the use of the harsh reagent phosphorous pentachloride, which is corrosive, toxic and carcinogenic, in addition to finding better conditions for the last step with trifluoroethanol. Oberthur and co-workers[185] prepared the dichloride **145** *via* two steps, starting with triethyl phosphonopropionate (**144**). With the use of neat trimethylsilyl chloride, the reaction was carried out in screw-cap pressure tubes to afford **146.** The only side product formed in this reaction was chloromethane, and therefore no further purification was required as chloromethane was removed with evaporation under reduced pressure. **145** was prepared from **146** with the use of oxalyl chloride without the formation of any major side products, so again no purification was required. The final step was modified from the first approach as trifluoroethanol was added with the addition of triethylamine instead of diisopropylethylamine and with the addition of 4-dimethylaminopyridine (DMAP).[186] In contrast to the first approach, this synthesis only required one purification step, after all three reactions. The overall yield was 84%.

The final approach to the synthesis of **141** only consisted of one step. Ethyl-2-bromopropionate (**143**) was refluxed with trifluoroethyl phosphite (**147**) in the presence of potassium fluoride/alumina to yield **141** at 12%.[187]

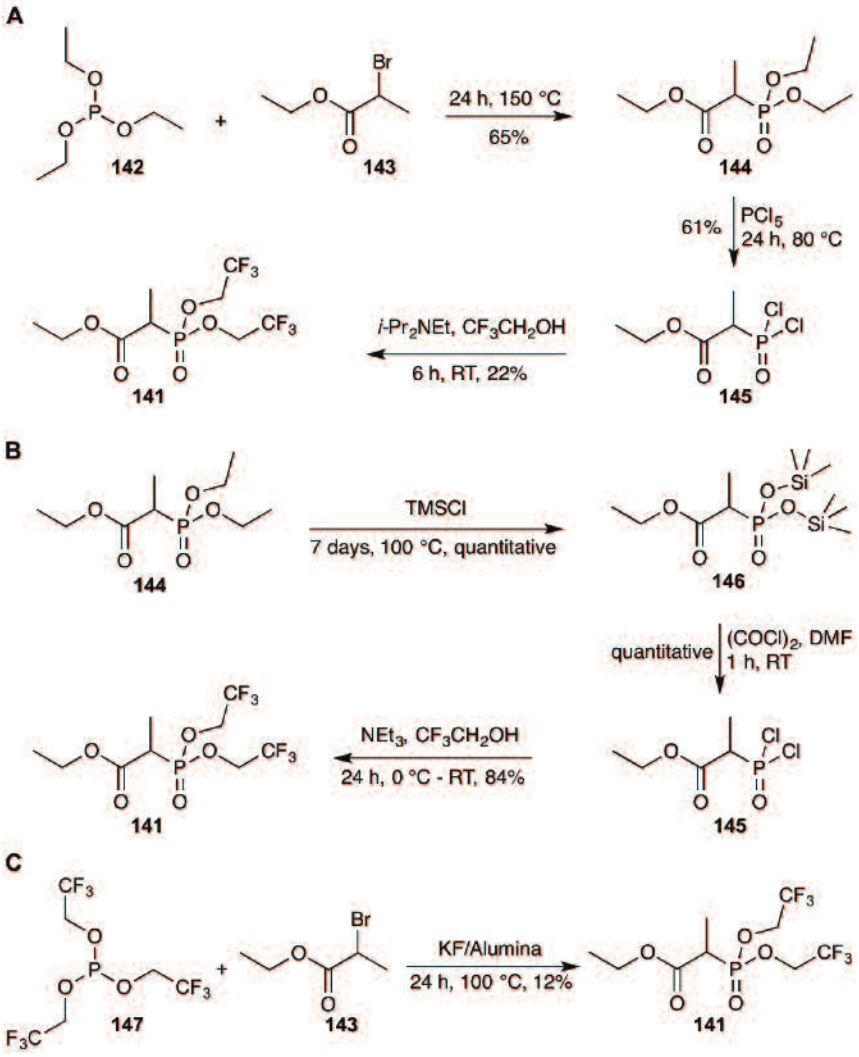

Scheme 3.6 Three alternative approaches for the synthesis of 141.

With both **139** and **141** synthesised, they were combined using the Still-Gennari olefination method to produce **140** (41%, 95:5, 11-*Z*:11-*E*). The olefination was carried out at -78 °C with the use of KHMDS/18-crown-6 as the base. Ando[188] states that in general, the vinyl protons of a *Z*-isomer exhibit signals in ^{1}H NMR spectra that are seen further up-field compared to those of a corresponding *E*-isomer. This can be observed clearly when comparing a ^{1}H NMR spectrum of **140** and its corresponding *E*-isomer **148** (Figure 3.2).

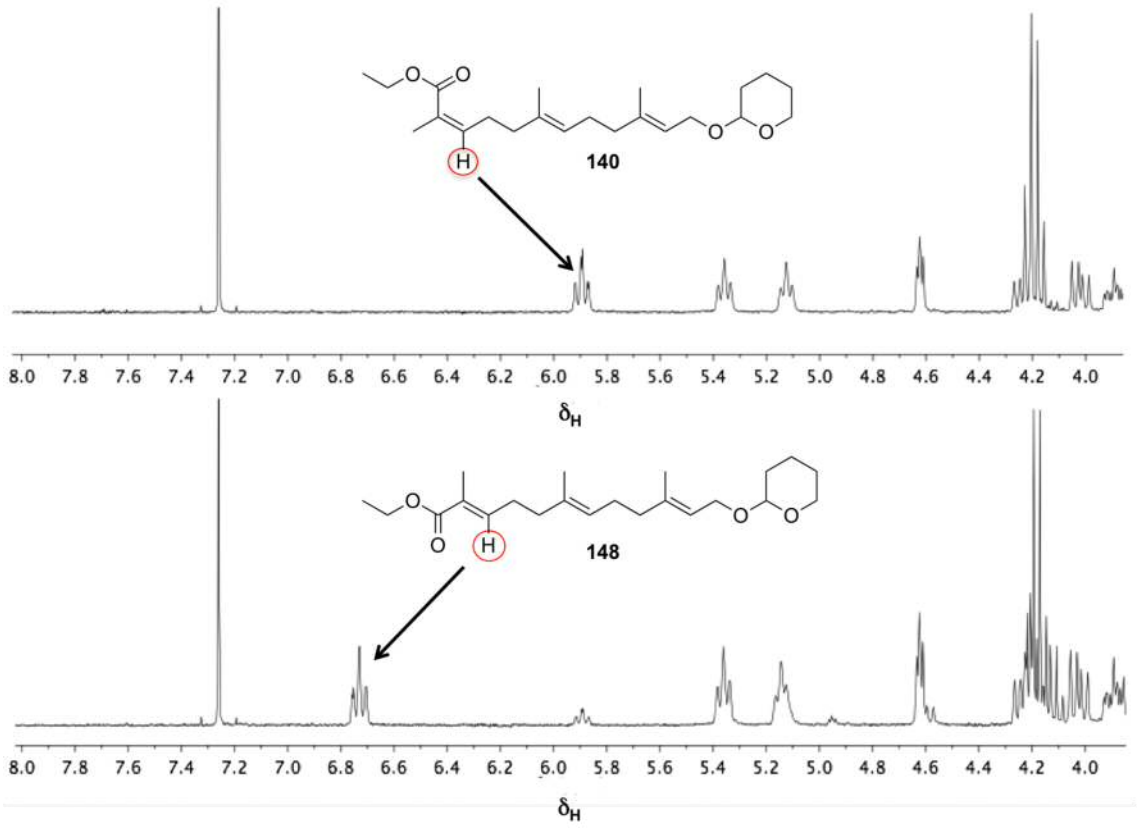

Figure 3.2 Top: ^{1}H NMR spectrum (300MHz, $CDCl_3$) of 10*Z*-140. Bottom: ^{1}H NMR spectrum (300MHz, $CDCl_3$) of 10*E*-148.

Once the Still-Gennari reaction had produced the desired α,β-unsaturated ester **140**, reduction with DIBAL gave alcohol **149** in a 62% yield.[189] The next functional group interconversion was challenging, as it required several steps. First, the alcohol moiety of **149** was converted to a mesylate using methanesulfonyl chloride (MsCl) and triethylamine (NEt_3), followed by a nucleophilic displacement of the mesylate group using lithium bromide. The resulting bromide **150** was displaced with a methyl group using lithium dimethyl cuprate to form **151** in a 60% yield. It was essential to carry out all three steps on the same day due to the instability of the bromide intermediate.

The final two steps required deprotection of the alcohol functionality and diphosphorylation. Deprotection was carried out by pyridinium *p*-toluenesulfonate in methanol to form alcohol **152** (49% yield).[177] Diphosphorylation of the resulting farnesol analogue was generated from the corresponding chloride as described earlier. The crude diphosphate was passed through a cation exchange column replacing the tris(tetrabutylammonium) ions with ammonium ions.[167,169,190] 13-Methyl FDP (**129**) was obtained in a 36% yield after purification by HPLC.

3.3.4 14-Methyl FDP (130)

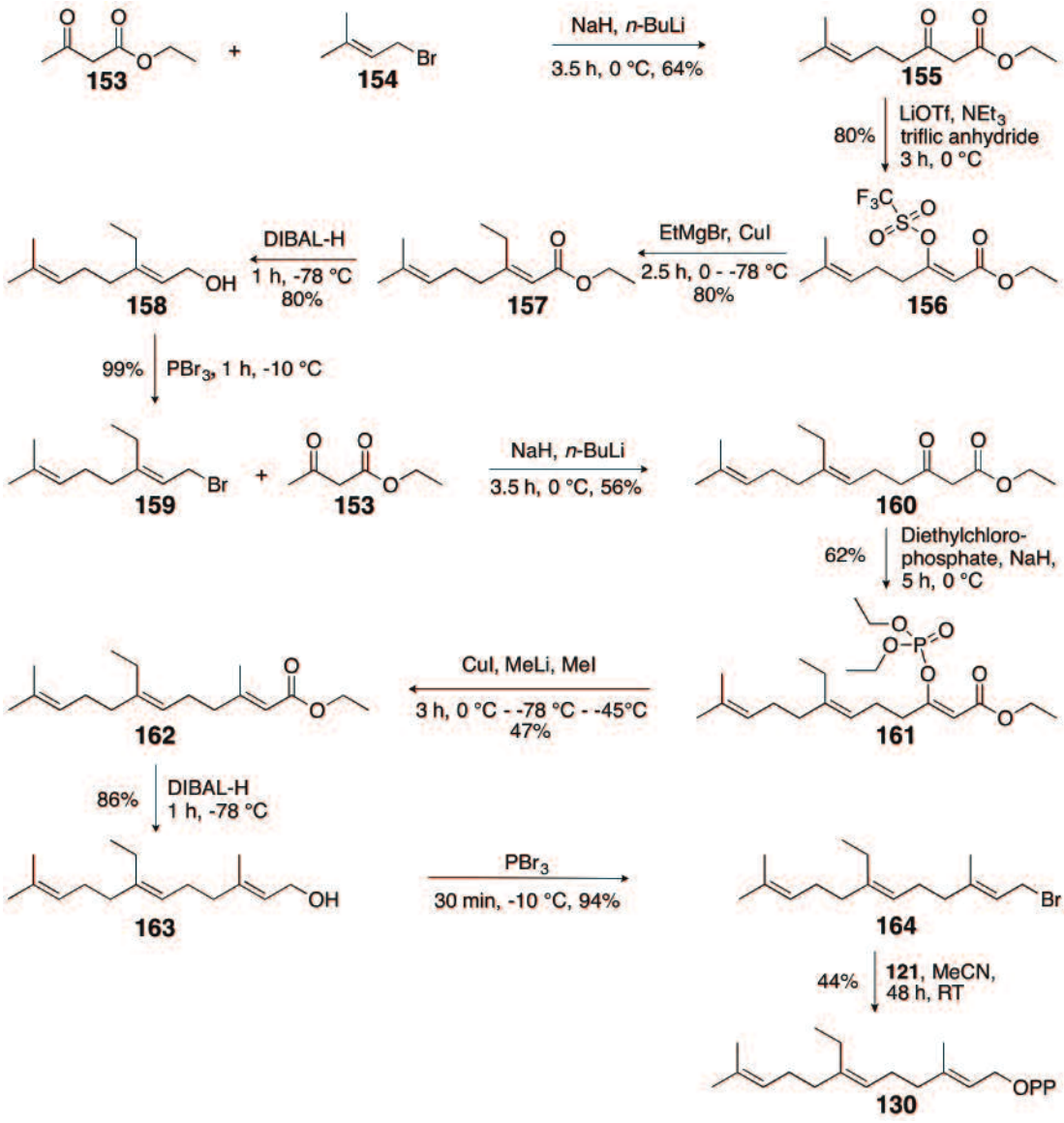

Scheme 3.7 Synthesis of 14-methyl FDP (130).

14-Methyl FDP was synthesised over a total of 11 steps (Scheme 3.7) following a synthetic route previously reported by Rawat and Gibbs.[191] The synthesis began with the formation of a dianion, prepared by treating ethyl acetoacetate (**153**) sequentially with sodium hydride and n-butyl lithium, and alkylating that dianion to dimethylallyl bromide (**154**) with a 64% yield.[192] The resulting product **155**, was transformed in a highly stereoselective manner to the vinyl triflate **156** (80% yield), the intermediate required for the formation of **157** (80% yield).[193,194] With the addition of an ethyl group on the α-isoprene unit of **157**, an additional chain elongation reaction was necessary to complete the synthesis of **130**. Compound **157** was reduced to the geranyl derivative

158 (80% yield), brominated to **159** (99% yield) and treated with a second dianion derived from ethyl acetoacetate, as described previously, to yield **160** (56% yield).[191]

160 was converted to an enol phosphate intermediate **161** (62% yield)**,** to allow for substitution of the phosphate group with a methyl group by stereoselective coupling with lithium dimethylcuprate to form **162** (47% yield).[195] Ester **162** was reduced with DIBAL to give farnesol derivative **163** (86% yield), brominated to **164** (94% yield), and diphosphorylated to the final compound **130**.[168,169] **130** was purified by flash chromatography on silica gel (6:2.5:0.5, isopropanol: water: 30% ammonium hydroxide) and was used as the tris(tetrabutylammonium) salt with a 44% yield.[170]

3.4 Oxygenated FDP analogues

Oxygenated FDP analogues were designed to introduce a variety of oxygenated functional groups in different positions of the FDP framework. These derivatives included the addition of acetoxy groups (13-acetoxy FDP, **165**, 12-acetoxy FDP, **166**, and 8-acetoxy FDP, **167**), alcohol groups (12-hydroxy FDP, **168**, and 8-hydroxy FDP, **169**) and methoxy groups (8-methoxy FDP, **170**, and 12-methoxy FDP, **171**).

Oxygenated FDP analogues were synthesised to investigate whether ADS could convert them into corresponding oxygenated amorphadiene analogues, with the oxygenated moiety providing a platform for further reactivity. It was also postulated that the use of heteroatom containing analogues might also enable premature quenching of carbocations hence competing with other nucleophiles present and giving insight into the catalytic mechanism.

Furthermore, looking at the biosynthesis of artemisinin (Section 1.3.2, Scheme 1.4), it is clear that amorphadiene is converted to artemisinin through a series of oxygenated intermediates as a result of cytochrome P450 oxidations. By introducing an oxygen into FDP before the cyclisation to amorphadiene, it was postulated that ADS might be capable of generating an oxygenated intermediate of artemisinin, bypassing the need for one or more of the P450 enzymes.

3.4.1 13-Acetoxy FDP (165)

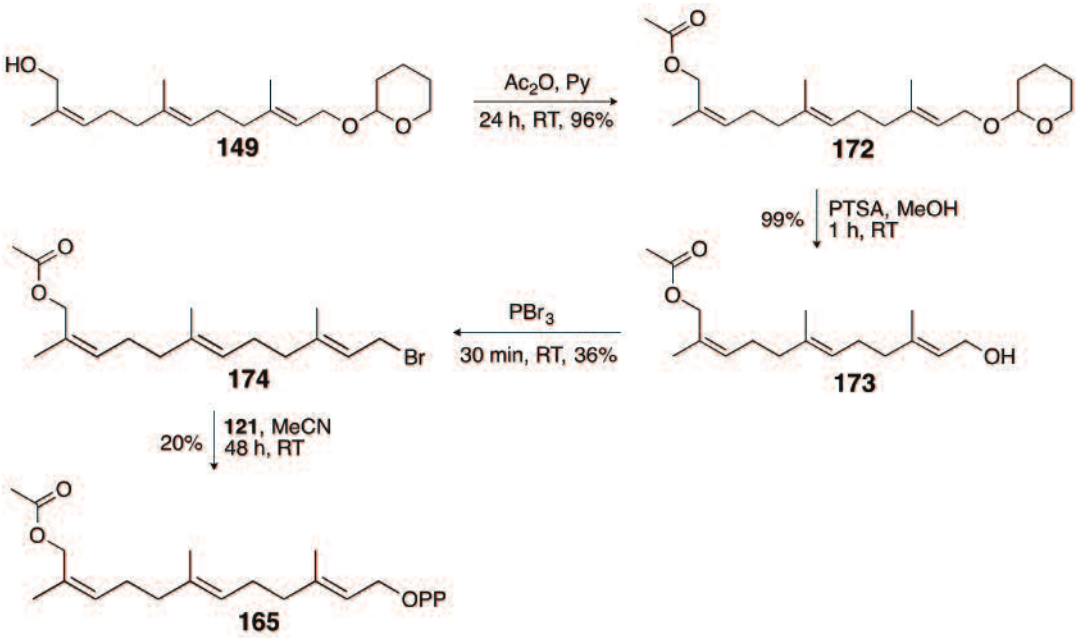

Scheme 3.8 Synthesis of 13-acetoxy FDP (165).

The synthesis of 13-acetoxy FDP (**165,** Scheme 3.8), a novel analogue to our knowledge, began in the same manner as 13-methyl FDP (**129**, Section 3.4.2). Once intermediate **149** was synthesised, the alcohol was reacted with acetic anhydride and pyridine to introduce the acetoxy functional group on C13, and produce **172** (96% yield).[196] The following steps to the final FDP analogue required a deprotection of the tetrahydropyran ether, to form 13-acetoxy farnesol **173** (99% yield), followed by a diphosphorylation *via* a bromide intermediate, **174** (36% yield), to form the final product, **165**.[168,169,177] **165** was purified by flash chromatography on silica gel (6:2.5:0.5, isopropanol: water: 30% ammonium hydroxide) and was used as the tris(tetrabutylammonium) salt with a yield of 20%.[170]

3.4.2 12-Acetoxy FDP (166) and 12-hydroxy FDP (168)

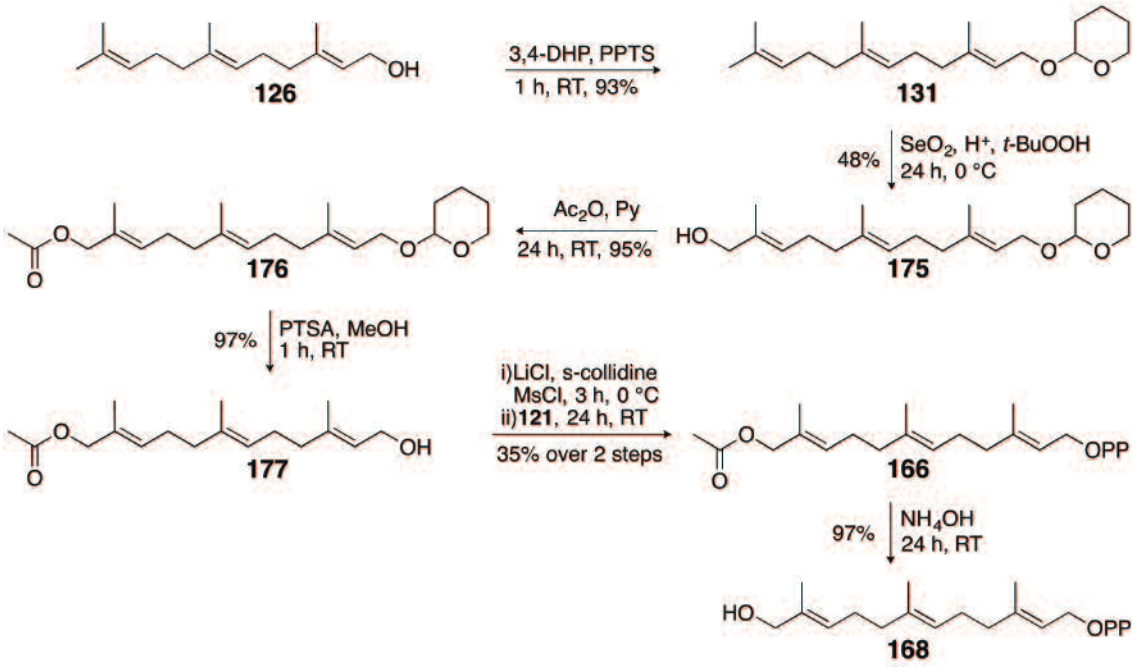

Scheme 3.9 Synthesis of 12-acetoxy FDP (166) and 12-hydroxy FDP (168).

The allylic oxidation of **131**, using a combination of selenium dioxide, salicylic acid and *tert*-butyl hydroperoxide (Section 3.4.1) not only produced aldehyde **132,** but in addition, alcohol **175,** which was actually the major product formed in this reaction, (**175** - 48% yield).[173,174] To add the acetoxy functional group at C12, alcohol **156** was treated with acetic anhydride in the presence of pyridine to form **176** (95% yield).[196] Acid catalysed deprotection of the THP ether resulted in **177** (97% yield) and diphosphorylation of **177** via a chloride intermediate produced 12-acetoxy FDP (**166**).[169,177] The crude product was passed through a cation exchange column, replacing the tris(tetrabutylammonium) ions with ammonium ions, and purified by HPLC to give a yield of 35% over the two last steps (Scheme 3.9).[190]

12-Hydroxy FDP (**168**, Scheme 3.9), a known analogue synthesised by Koyoma and co-workers[197], was synthesised by hydrolysis of the acetoxy group with the use of 30% ammonium hydroxide. The reaction was carried out in deuterated water (D_2O) to allow for easy monitoring of the reaction by ^1H NMR spectroscopy. The reaction was complete once the acetyl methyl group corresponding to a singlet at δ_H = 2.2 ppm, could no longer be observed. The protons on C12, corresponding to a singlet, shifted upfield from δ_H = 4.50 to 3.88 ppm (Figure 3.4). Once the reaction was complete, the solution was lyophilised to give **168** quantitatively as a white solid.

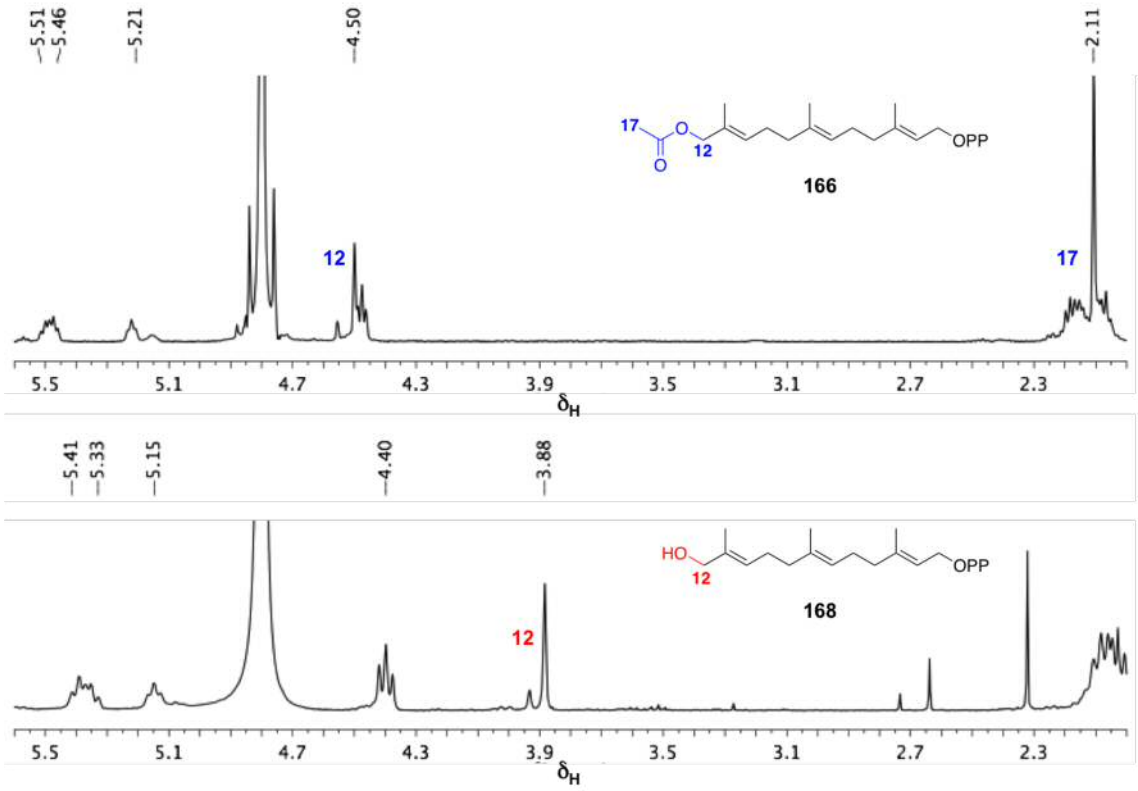

Figure 3.3 ^{1}H NMR spectrum (500 MHz, D_2O) of 12-acetoxy FDP 166 (top) and of 12-hydroxy FDP 168 (below). Expansion of the region from δ_H = 2.0 to 5.6 ppm.

3.4.3 8-Hydroxy FDP (169) and 8-acetoxy FDP (167)

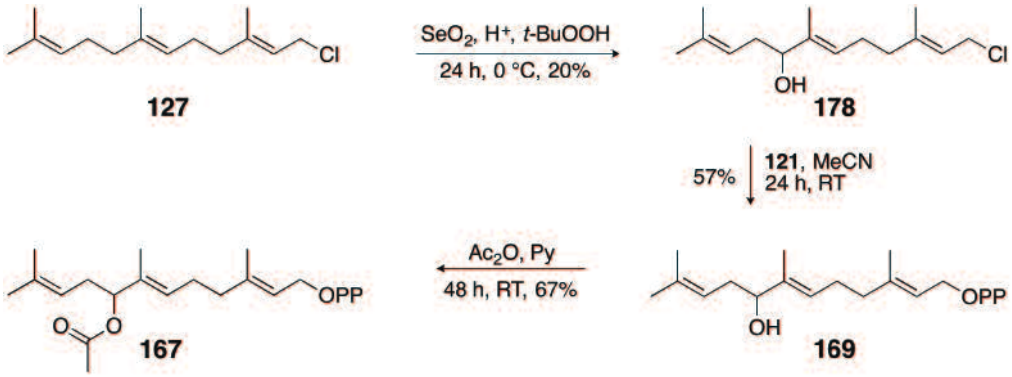

Scheme 3.10 Synthesis of 8-hydroxy FDP (169) and 8-acetoxy FDP (167).

The addition of a hydroxyl and acetoxy moiety on C8 of FDP was improved and shortened from the previous synthesis of analogues **166** and **168** (Section 3.5.2). The synthesis was optimised (Section 5) to reduce the overall steps to the desired analogues, and this was accomplished by starting with commercially available farnesyl

chloride (**127**). The allylic oxidation reaction, used previously for the synthesis of intermediates **132** and **175**, also, as an additional product generates an alcohol group on C8 of FDP to create **178** (20%).[173,174] Using farnesyl chloride instead of the THP ether **131**, conditions for the allylic oxidation were changed to accommodate the less stable intermediate. Instead of carrying out the reaction at room temperature, the reaction was left for 24 h at 0°C, and the workup that followed was maintained as cold as possible. This was achieved by using ice-cold diethyl ether for the extractions and storing each extract over ice. The resulting 8-hydroxy farnesyl chloride (**178**) was used immediately in the next step to avoid any decomposition of the chloride intermediate. The diphosphorylation was carried out in the same way as discussed for the previous analogues and the resulting product, 8-hydroxy FDP (**169**) was purified by flash chromatography on silica gel (6:2.5:0.5, isopropanol: water: 30% ammonium hydroxide) to result in a pure tris(tetrabutylammonium) salt with a yield of 57% (Scheme 3.10).[170]

8-Acetoxy FDP (**167**) was synthesised by treating FDP analogue **169** with acetic anhydride and pyridine (67% yield).[196] This reaction was carried out in deuterated chloroform ($CDCl_3$) to enable the easy monitoring of the product formation by ^1H NMR spectroscopy (Figure 3.5). The reaction was complete once the methyl group in the acetyl moiety, C17 of **167**, could be observed as a singlet at δ_H = 2.2 ppm in addition to the downfield shift of the proton on C8, seen as a triplet, from δ_H = 3.93 to 4.95 ppm (Figure 3.5).

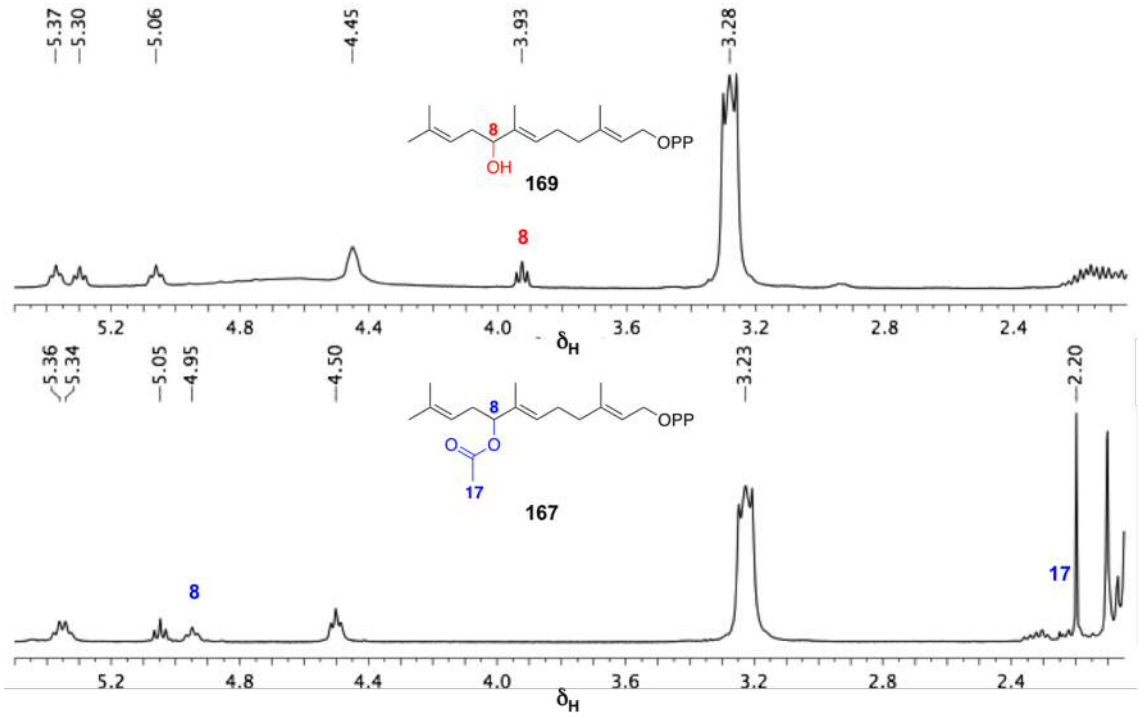

Figure 3.4 ^{1}H NMR (500 MHz, $CDCl_3$) spectrum of 8-hydroxy FDP 169 (top) and of 8-acetoxy FDP 167 (bottom). Expansion of the region from δ_H = 2.0 to 5.5 ppm.

3.4.4 8-Methoxy FDP (170) and 12-methoxy FDP (171)

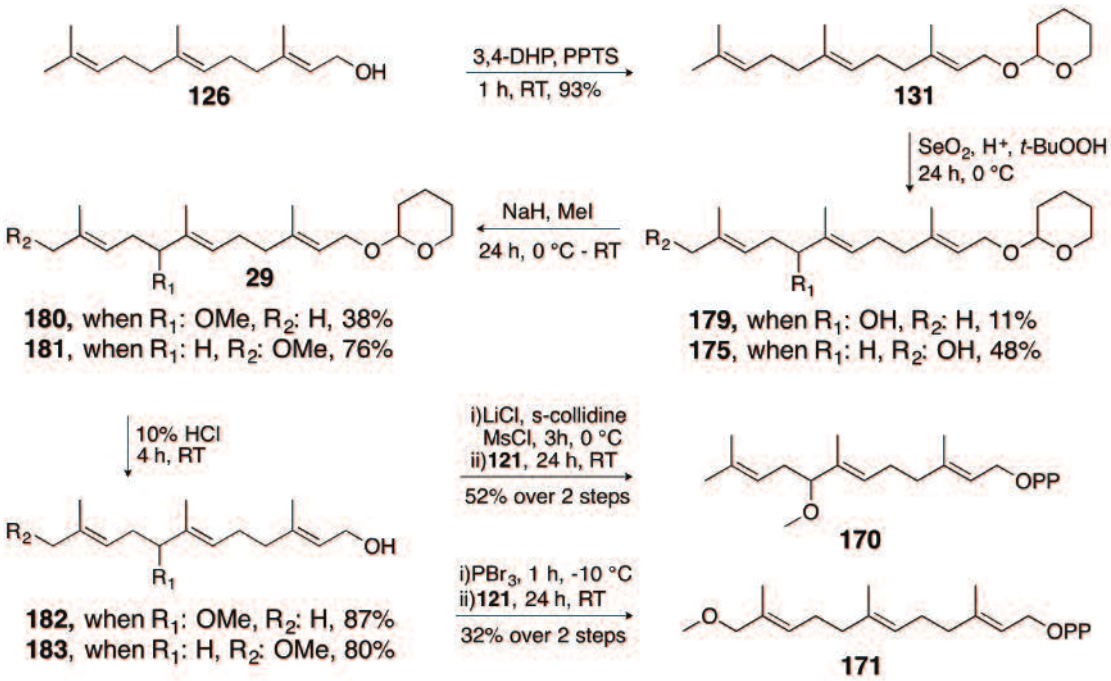

Scheme 3.11 Proposed synthesis of 8-methoxy FDP (170) and 12-methoxy FDP (171).

The addition of a methoxy functional group on FDP at C8 (8-methoxy FDP, **170**) and C12 (12-methoxy FDP, **171**) were carried out in the same manner (Scheme 3.11). Once both intermediates, **179** and **175,** were synthesised by allylic oxidation of **131**, they were treated with sodium hydride and methyl iodide to afford **180** and **181**, with a yield of 38% and 76%, respectively.[173,174,198] Both intermediates were deprotected to the corresponding farnesol derivatives, **182** and **183**, with 10% hydrochloric acid (87% and 80% yield, respectively), before being diphosphorylated to final compounds, 8-methoxy FDP (**170**) and 12-methoxy FDP (**171**).[169] Both FDP analogues were purified by flash chromatography on silica gel (6:2.5:0.5, isopropanol: water: 30% ammonium hydroxide) and used as the tris(tetrabutylammonium) salts (52% and 32% yield, respectively).[170]

3.5 Aza-FDP analogues

12-Acetamido FDP (**184**) and 12-amino FDP (**185**), both novel FDP analogues to our knowledge, were designed in attempts to create the corresponding aza derivatives of amorphadiene. There have been reports of novel artemisinin analogues containing nitrogen that possess antimalarial activities.[199,200] If ADS is capable of converting aza-FDP analogues to the bicyclic amorphadiene framework, there is a possibility of carrying that aza group through to the desired artemisinin structure, and this gives the possibility of creating new antimalarials. In addition to this, the additional functional group also provides a new platform to perform further reactions, once an amorphadiene analogue has been created.

3.5.112-Acetamido FDP (184)

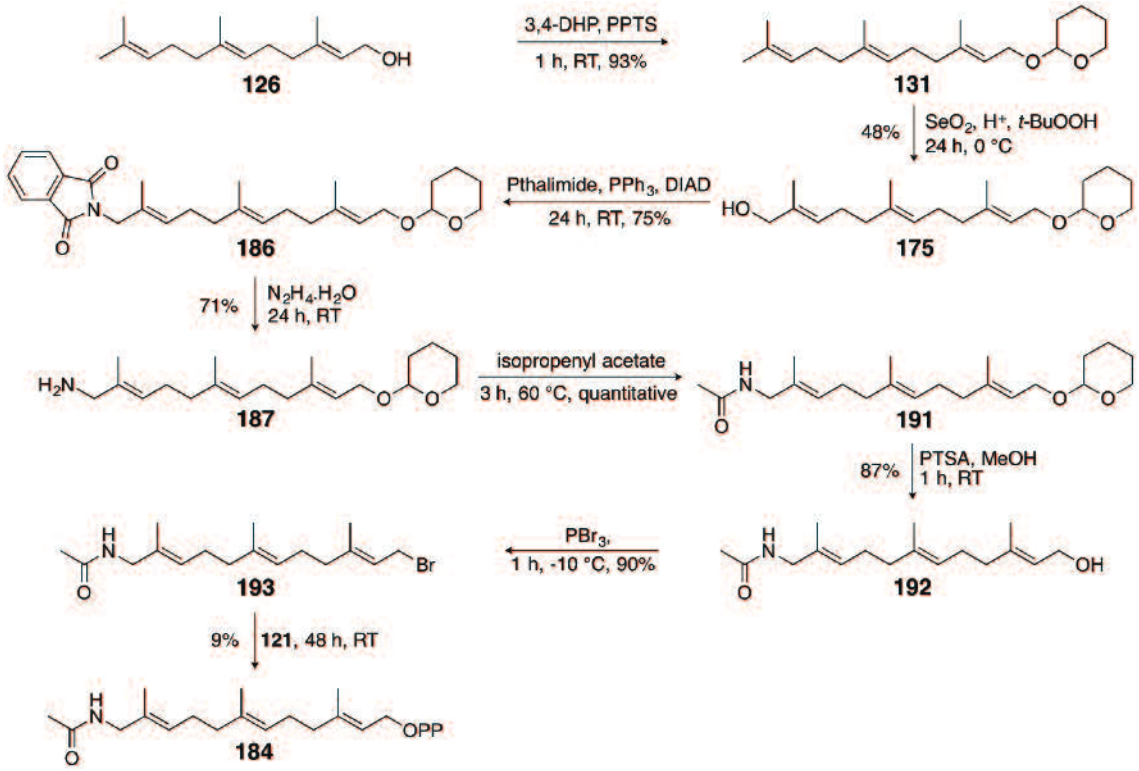

Scheme 3.12 Synthesis of 12-acetamido FDP (184).

12-Acetmido FDP (**184**) was synthesised in 8 steps (Scheme 3.12). Once the hydroxyl intermediate, **175** was formed, a Gabriel synthesis was carried out to convert the hydroxyl moiety to an amine. A Gabriel synthesis consisted of using potassium pthalimide, triphenylphosphine and diisopropyl azodicarboxylate (DIAD) to replace the alcohol with a pthalimide, forming **186** (75% yield), which was subsequently treated with hydrazine to give amine **187** (71% yield).[201–204] Acetylation of amine **187** was carried out with excess isopropenyl acetate (**188**) in the absence of a solvent and catalyst.[205] Isopropenyl acetate is an efficient source for adding an acetyl group to an amine moiety because the alcohol **189** produced as a side product tautomerises to acetone (**190**) and serves purpose as a solvent in addition to shifting the equilibrium to the product (Figure 3.6). The corresponding acetamide **191** was obtained in a quantitative yield that required no further purification.

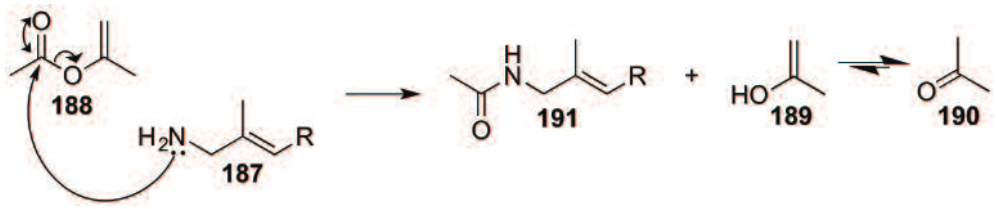

Figure 3.5 Acetylation of amine 187 with isopropenyl acetate (188).

The THP ether of **191** was deprotected with *p*-toluene sulfonic acid to yield 12-acetamido farnesol (**192**) in 87% yield.[168] The alcohol was brominated to **193** (90% yield) and diphosphorylation of the bromide led to the formation of 12-acetamido FDP (**184**).[169,177] The product was purified by flash chromatography on silica gel (6:2.5:0.5, isopropanol: water: 30% ammonium hydroxide) to provide a pure tris(tetrabutylammonium) salt, in 9% yield.

3.5.2 12-Amino FDP (185)

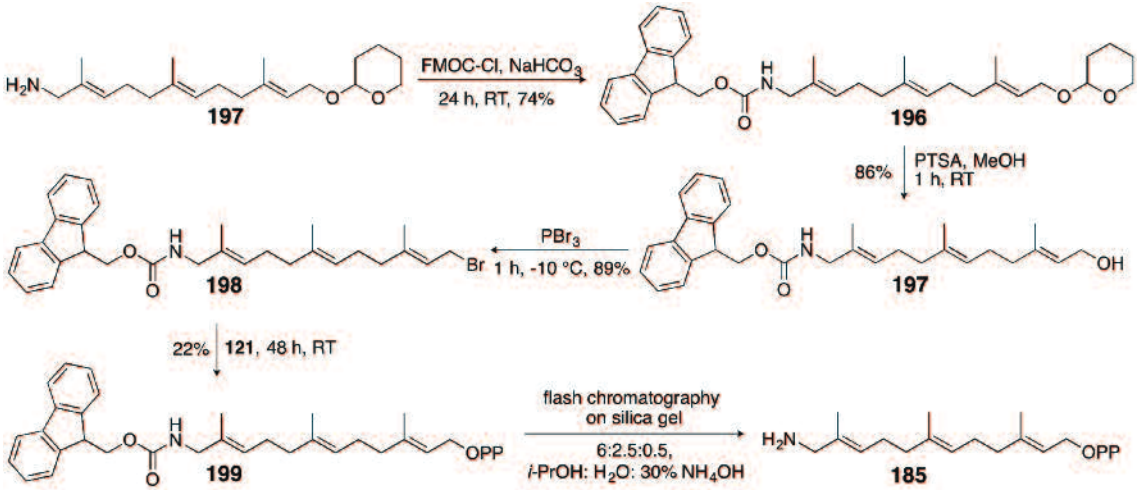

Scheme 3.13 Synthesis of 12-amino FDP (185).

The synthesis of 12-amino FDP (**185**, Scheme 3.13) also required the formation of intermediate **187**. It was not possible from this intermediate to deprotect the THP ether and diphosphorylate to 12-amino FDP (**185**), because of the nucleophilic property of the amine. The lone pair on the nitrogen will attack at C1 of a neighbouring molecule once the deprotected alcohol **194** is brominated (**195**) (Figure 3.7).

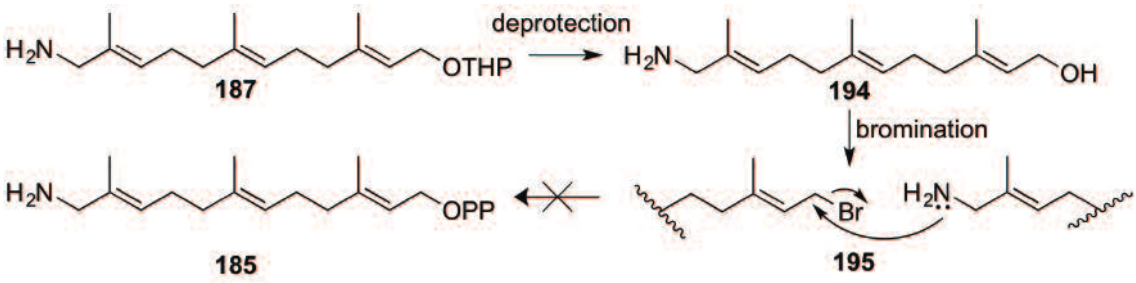

Figure 3.6 Intermolecular nucleophilic attack from the lone pair on the nitrogen preventing the diphosphorylation of 12-amino farnesyl bromide (195).

The amine group therefore had to be protected with fluorenylmethyloxycarbonyl chloride (Fmoc-Cl). Once **196** was formed with a 74% yield, the THP ether was deprotected to **197** (86% yield), brominated to **198** (89% yield) and finally diphosphorylated to **199**.[168,169,177] The crude product was purified by flash chromatography on silica gel (6:2.5:0.5, isopropanol: water: 30% ammonium hydroxide) to provide a pure tris(tetrabutylammonium) salt with a yield of 22%. In addition to purifying the FDP analogue, the purification also cleaved the FMOC group due to the basic solution used to elute the compound off the column to yield 12-amino FDP (**185**).

3.6 Summary

This chapter has covered the synthesis of a library of analogues that will be incubated with ADS to test for substrate activity. The library was designed to add various functional moieties in a range of locations on the FDP skeleton. Each FDP analogue, in turn, was tested with ADS and their enzymatic products, if any, are reported in Chapter 4.

Chapter 4. Characterisation of ADS generated products

4.1 Preface

FDP analogues were incubated with ADS in attempts to create novel amophadiene analogues. In addition to this goal, the incubations also gave insight into the extent of the enzymatic promiscuity by using a variety of functional groups, positioned in various locations on the FDP backbone. With this array of analogues, it was observed that ADS was capable of producing amophadiene analogues, as well as converting FDP analogues through different mechanisms to produce other cyclic and acyclic compounds. Incubations of ADS with FDP analogues were primarily analysed by GC-MS. The mass spectra of novel products formed in this report, catalysed by ADS, could not be definitively identified by the National Institute of Standards and Technology (NIST)[206] library due to the products being unnatural terpenes. However, their fragmentation patterns were compared to those of amorphadiene and other sesquiterpenes to see if there was any correlation that could help indicate the structure of the unknown products. Upon observing a maximum of two products, the incubation was repeated on a preparative scale to obtain enough material for NMR analysis. Preparative scale incubations were not carried out for incubations that produced more than two products because the enzymatic products proved difficult to separate. All incubations carried out with ADS and an FDP analogue were carried out in parallel to an incubation of the analogue with no ADS. This control was implemented so that any product observed by GC-MS was assured to be an enzymatic product.

4.2 Methylated FDP analogues

4.2.1 12-Methyl FDP (128)

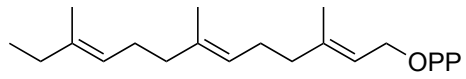

Figure 4.1 12-Methyl FDP (128)

Incubation of ADS with 12-methyl FDP (Figure 4.1) produced five pentane extractable products, when analysed by GC-MS (for the analysis of all enzymatic products, a temperature gradient of 80 °C (1 min hold) to 180 °C (4 °C min^{-1}, 2 min hold) was used, with an injector temperature of 100 °C) (Figure 4.2). All five compounds had a molecular ion with *m/z* = 218 corresponding to $C_{16}H_{26}$ or the expected mass for a methyl substituted sesquiterpenoid. Upon studying the mass spectra, it was clear that the compounds eluting at 16.82 and 17.66 min showed similar fragmentation patterns with base peaks at *m/z* = 189. The remaining three compounds, at 18.52, 19.21 and 24.68 min also showed similar fragmentation patterns, differing from the first pair, they

exhibited base peaks at *m/z* = 119. The mass spectra of the last three compounds were comparable with that of amorphadiene, which also has a base peak at *m/z* = 119 (Figure 4.2).

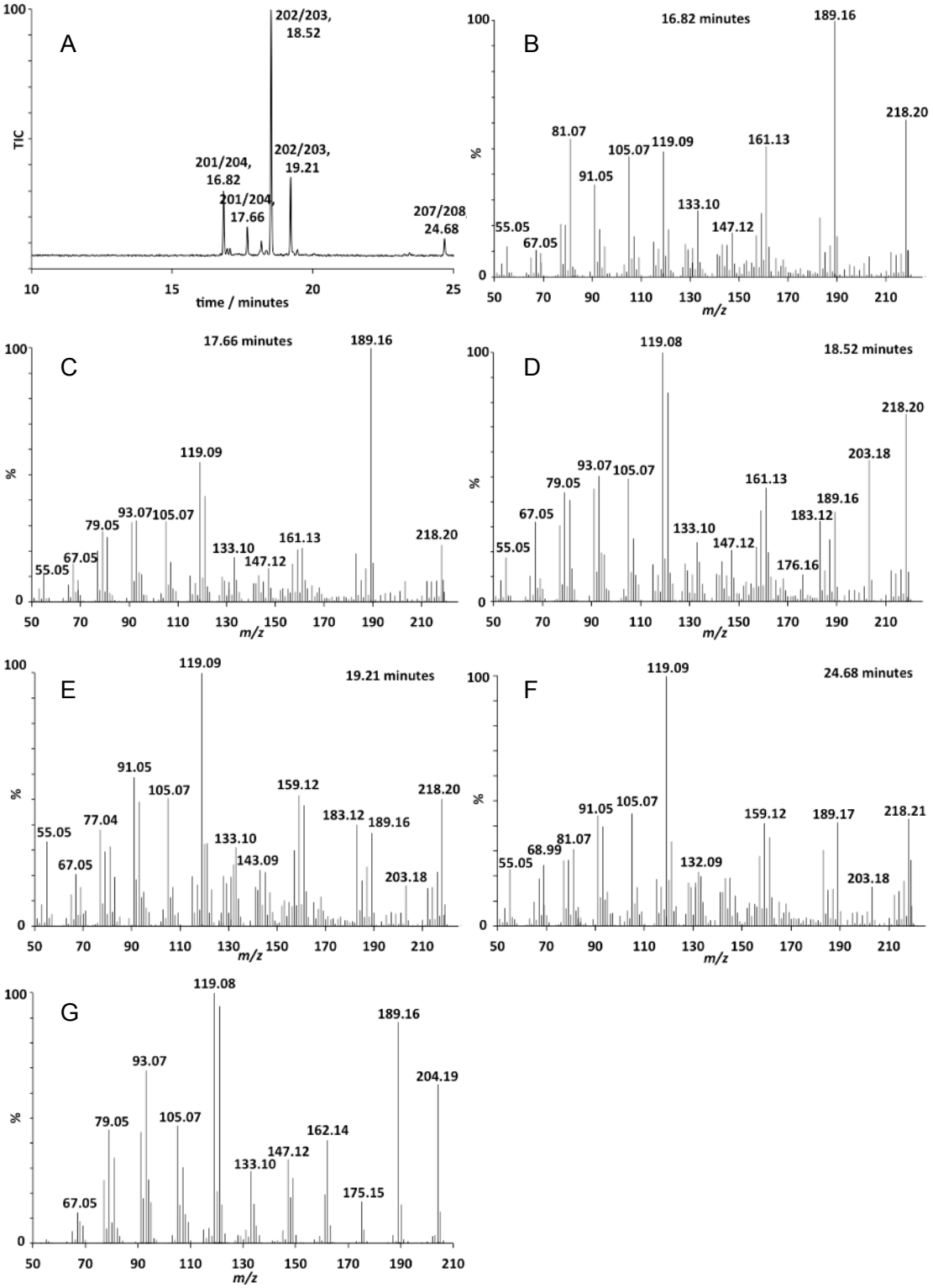

Figure 4.2 A: Total ion chromatogram of pentane extractable products from incubation of ADS and 12-methyl FDP (128). B-F: Mass spectra of the eluted compounds. G: Mass spectrum of amorphadiene (45).

The fragmentation patterns seen in mass spectra cannot give a definite identification of products, but can support predictions of products formed. Due to the incubation giving five products, it was not considered feasible to repeat this incubation on a preparative scale to analyse the products by NMR spectroscopy.

The identification of certain fragments in the mass spectra can aid in predicting possible products formed from an incubation of ADS with 12-methyl FDP. Brodelius and co-workers[128] report the use of single ([1-^{2}H]-FDP) and double ([1,1-$^2H_2$]-FDP) deuterated FDP at C1 to solve the identification of certain fragments observed in a mass spectrum of amorphadiene (Section 1.3.2, Figure 1.9). By combining the use of deuterated analogues with the knowledge of the catalytic mechanism of ADS, their group identified peaks at *m/z* = 189, 121, and 93 (Figure 4.3). The differences in *m/z* between the major fragment peaks in the mass spectra of amorphadiene arising from FDP, [1-^{2}H]-FDP and [1,1-$^2H_2$]-FDP led to assignment of cation **74** at *m/z* = 189, cation **75** at *m/z* = 121 and cation **76** at *m/z* = 93.

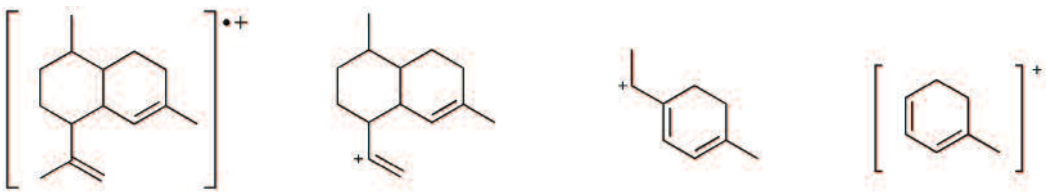

Figure 4.3 Proposed cations resulting from the fragmentation of amorphadiene (45) reported by Brodelius and co-workers.[128]

It was hypothesised that the additional methyl group on C12 would not interfere with the mechanism of ADS until the last cation, the '12-methyl amorphyl cation' (**200**, Scheme 4.1) was formed, because C12 is not directly involved in the catalytic cycle. The last step, a deprotonation to quench cation **200**, could then occur from three feasible locations. Deprotonation at C13 would result in an amorphadiene analogue, **201**. Alternatively, deprotonation at C12 would result in two isomers of another amorphadiene analogue, **202** and **203**. Lastly, a deprotonation at C10 could occur, and this would give rise to **204.** The formation of a fifth compound is not possible through an alternative deprotonation step to quench cation **200**. Instead it is postulated that either a 1,2 or 1,3-hydride shift, followed by a deprotonation of the subsequent cation, **205** or **206** respectively, could be plausible for the formation of the final compound yielding products such as **207** or **208** (Scheme 4.1).

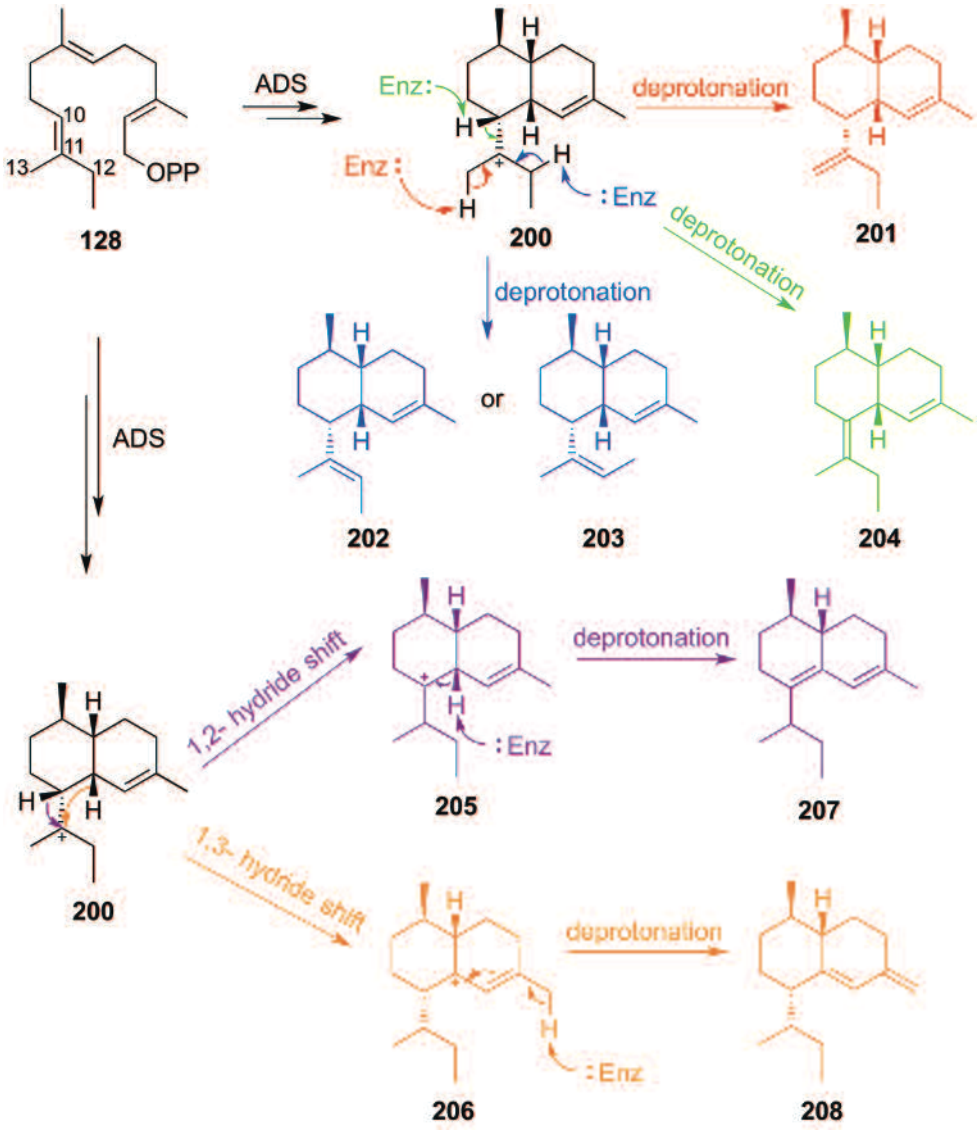

Scheme 4.1 Proposed products formed from incubation of ADS with 12-methyl FDP (128).

Furthermore to attempt identification of the products, plausible fragmentation routes for each proposed product were proposed. Hence it was postulated that compounds **201** and **204** would give mass spectra that had a base peak at *m/z* = 189 (16.82 and 17.66 min). This would indicate the loss of an ethyl group, giving cation **74** (Figure 4.3). The same peak at *m/z* = 189 is observed for amorphadiene, indicating a loss of a methyl group. Compounds **202** and **203** however do not have an ethyl group attached on C11 so the peak at *m/z* = 189 for these compounds will not represent the most stable cation formed. In fact in the mass spectra for the compounds at 18.52 and 19.21 min, the peak at *m/z* = 189 decreases to around 40%. In these mass spectra, the base peak is at *m/z* = 119, which represents cation **75**. This is a feasible base peak for compounds **202** and **203**. A base peak at *m/z* = 119 for products **207** and **208** is also feasible.

4.2.2 13-Methyl FDP (129)

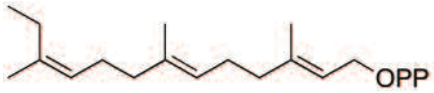

Figure 4.4 13-Methyl FDP (129)

Incubation of ADS with 13-methyl FDP (**129**, Figure 4.4) generated three pentane extractable products (Figure 4.5), which all had a molecular ion peak with *m/z* = 218. The fragmentation patterns observed in the mass spectra were found to be similar to those analysed for the analogue, 12-methyl FDP (**128**). Unfortunately these two substrates were tested with ADS in different periods of the research project and so they were not analysed using the same GC column. This precluded the possibility of comparing the enzymatic products by co-elution or by comparing their retention times. Nevertheless, it did not affect the fragmentation pattern in the mass spectra, and so these could still be used to compare the two sets of products.

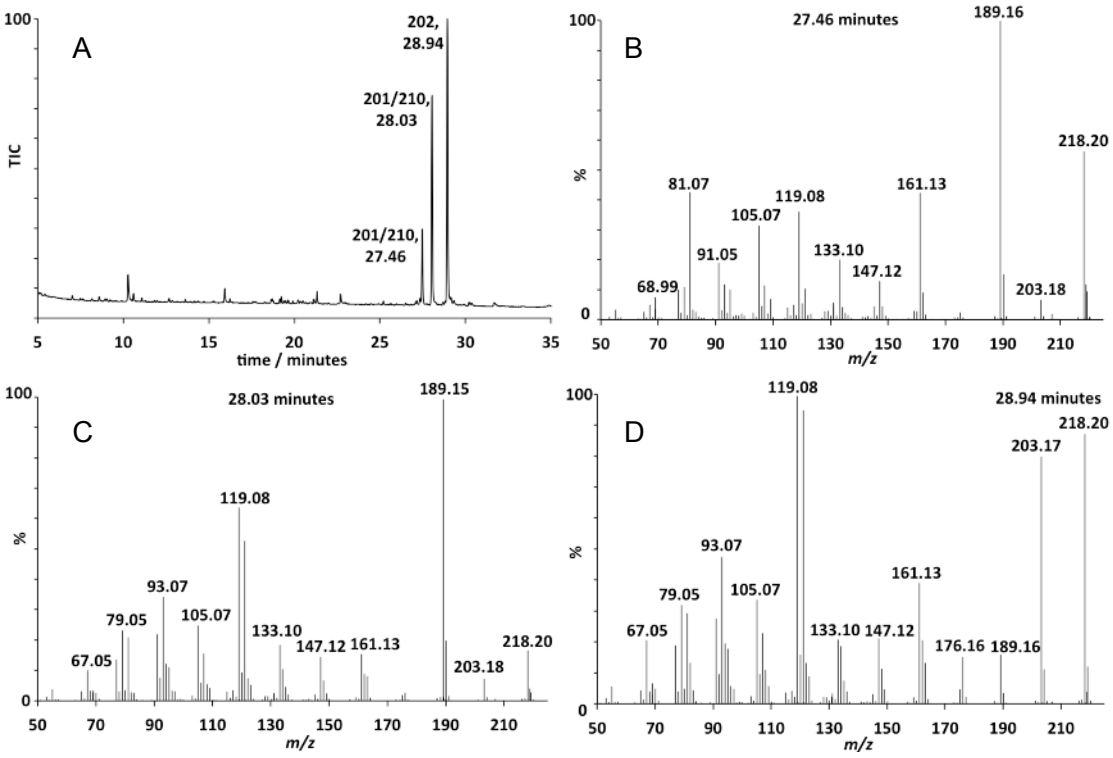

Figure 4.5 A: Total ion chromatogram of pentane extractable products from incubation of ADS and 13-methyl FDP (129). B-D: Mass spectra of the eluted compounds.

Similar to the mass spectra observed for 12-methyl FDP (**128**), the first two compounds observed in the GC, at 27.46 and 28.03 min, give a base peak at *m/z* = 189. Assuming ADS transforms 13-methyl FDP in the same manner to the natural substrate, FDP, until it forms the 13-methyl amorphyl cation **209**, structures such as **210** and **201** can be achieved with a deprotonation on C10 and C12 respectively, and seem fitting for the identification of the first two unknown compounds (Scheme 4.2). These assignments are based on the theory given behind the formation of compounds **201** and **204** discussed above (Section 4.2.1). The third compound at 28.94 min differs, with the base peak found at *m/z* = 119. The absence of a second compound with a base peak at *m/z* = 119 could imply that only the generation of **202** or **203** is possible (Scheme 4.1 and 4.2). The reduced number of products generated by 13-methyl FDP (**129**) and ADS, relative to 12-methyl FDP (**128**) and ADS, could suggest that the analogue is bound in an orientation in the active site that prevents the C10-C11 bond freely rotating when the corresponding 13-methyl amorphyl cation (**209**) is formed, and therefore the two analogues are not converted to the same products. If the conformations of 12-methyl FDP and 13-methyl FDP are different when bound in the enzymes active site, all of the viable locations to deprotonate and therefore quench the amorphyl cation **209** might not be accessible by basic residues. In addition to this, the C11-C13 bond may also not be capable of freely rotating (Scheme 4.2).

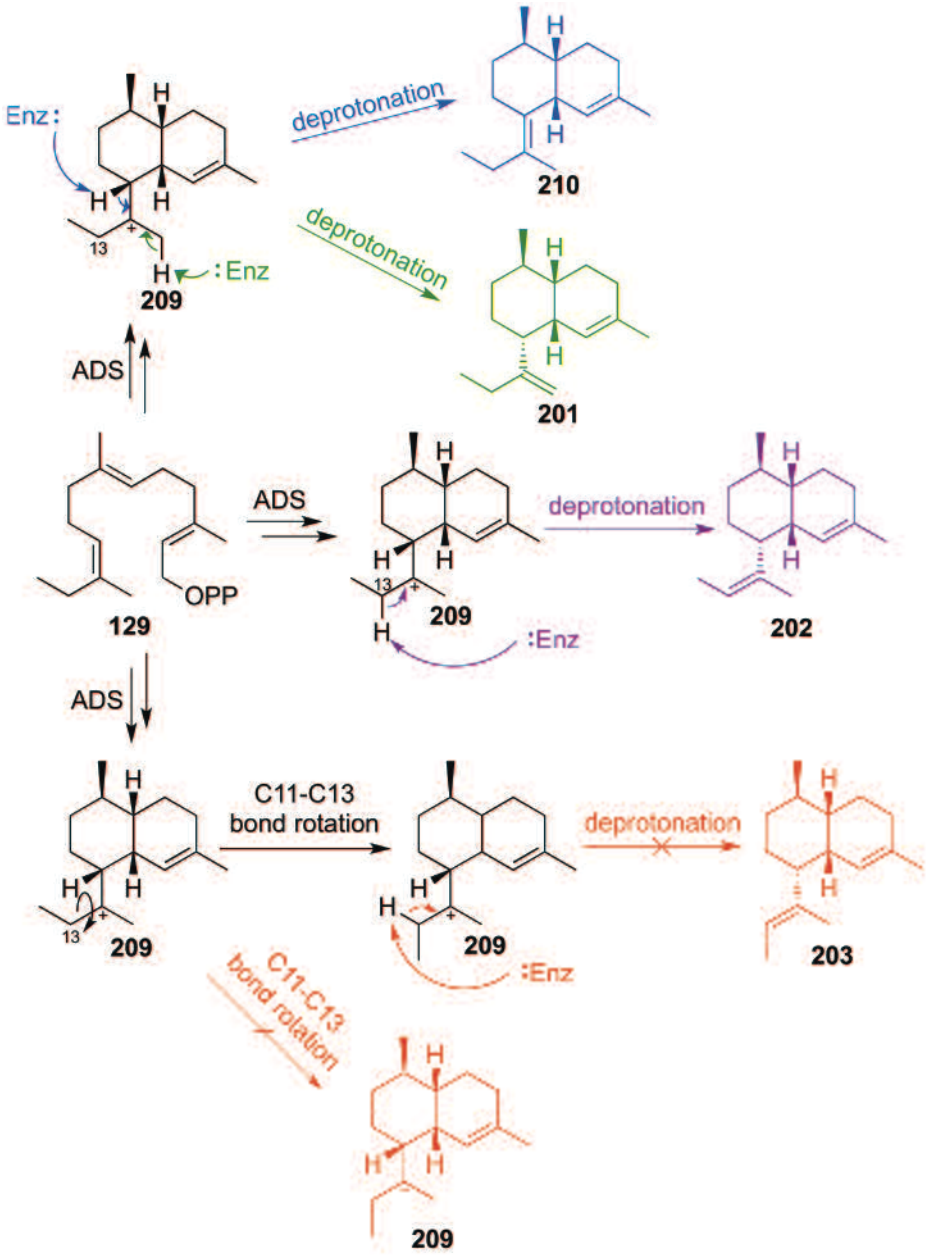

Scheme 4.2 Proposed products formed from incubation of ADS with 13-methyl FDP (129).

4.2.3 14-Methyl FDP (130)

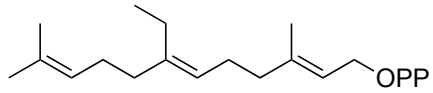

Figure 4.6 14-Methyl FDP (130)

Incubation of ADS with 14-methyl FDP (**130**, Figure 4.6) generated one pentane extractable product, when analysed by GC-MS. The single enzymatic product had the expected molecular ion peak with *m/z* = 218 (Figure 4.7).

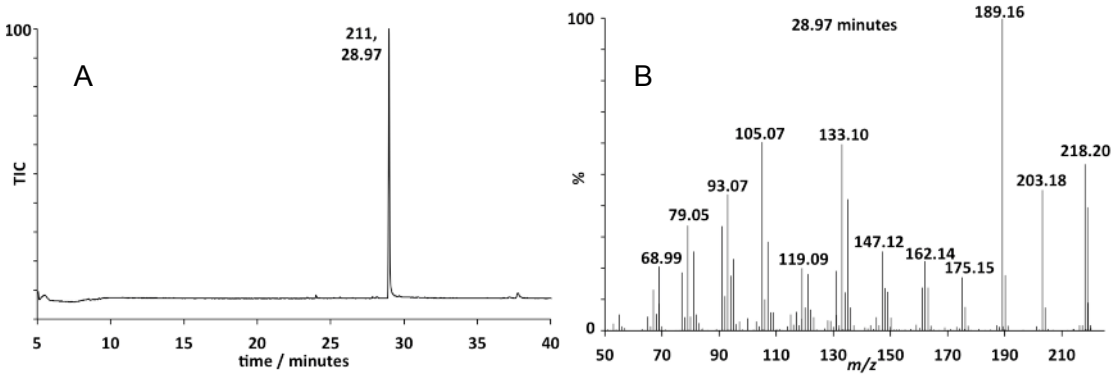

Figure 4.7 A: Total ion chromatogram of the pentane extractable product from incubation of ADS and 14-methyl FDP (130). B: Mass spectrum of the eluted compound.

It was hypothesised that if ADS carried out the same catalytic mechanism with 14-methyl FDP as it does with the natural substrate, FDP, it would form an amorphadiene analogue, 14-methyl amorphadiene (**211**, Scheme 4.3).

Since only one product was observed by GC-MS, this incubation was carried out on a preparative scale (Section 2.6.5) to generate enough material to analyse and characterise the enzymatic product by NMR spectroscopy. The ^{1}H NMR spectrum (Figure 4.8) of the enzymatic product supported the structure of an amorphadiene analogue. Due to the identical chemical shifts for the olefinic protons on C2 and C13, as well as the proton on C1, in both ^{1}H NMR spectra of amorphadiene (**45,** Section 2.6.5, Figure 2.13) and the proposed 14-methyl amorphadiene (**211,** Figure 4.8), it was confirmed that ADS had converted this compound via same mechanism as for the natural substrate, FDP. The region between δ_H = 2.0 and 0.5 ppm however was contaminated with impurities that were not successfully separated. Unfortunately this hindered the identification of the new alkyl peak for the additional methyl group on C14, as well as the possibility of observing the loss of the doublet around δ_H = 0.8 ppm for

the presence of the methyl group on C7 in the amorphadiene ^{1}H NMR spectrum. It was predicted that the position of the new methyl group on C14 would not affect the rest of the synthesis to achieve the corresponding artemisinin derivative, 14-methyl artemisinin (**212**, Scheme 4.3).

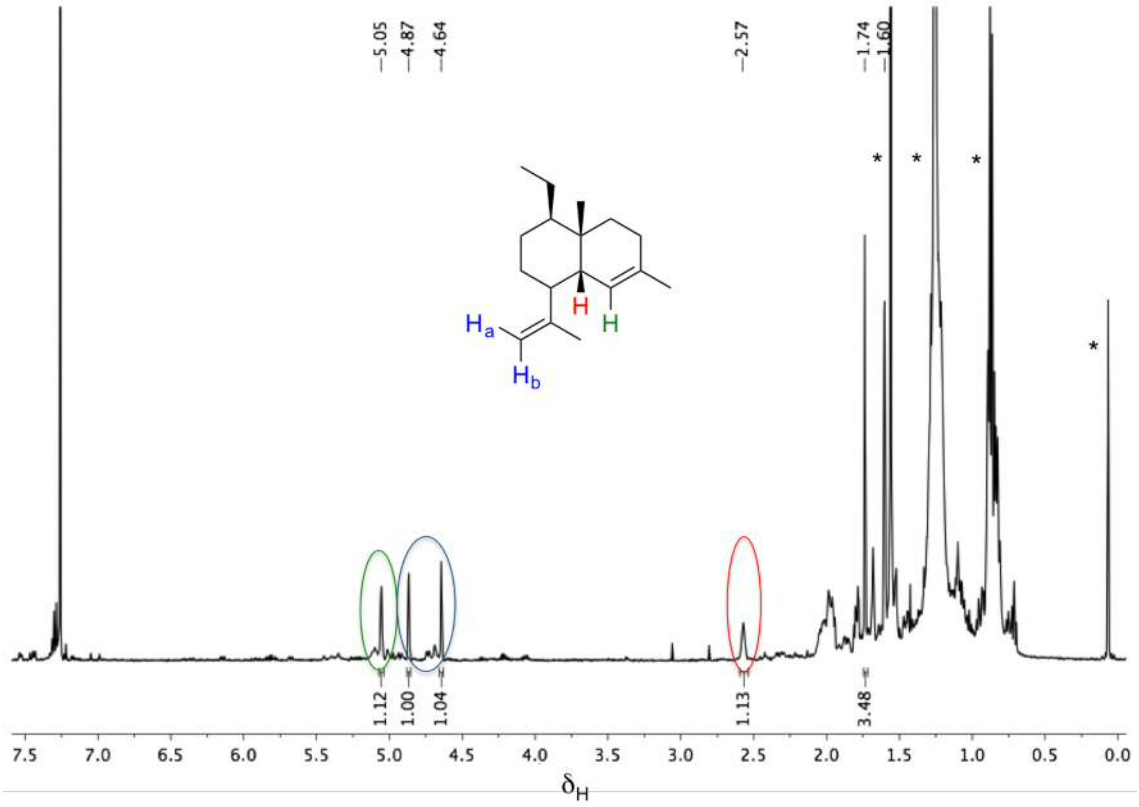

Figure 4.8 ^{1}H NMR spectrum (500 MHz, $CDCl_3$) of the pentane extractable product from a preparative scale incubation of ADS with 14-methyl FDP (130). '*' symbol indicates impurities.

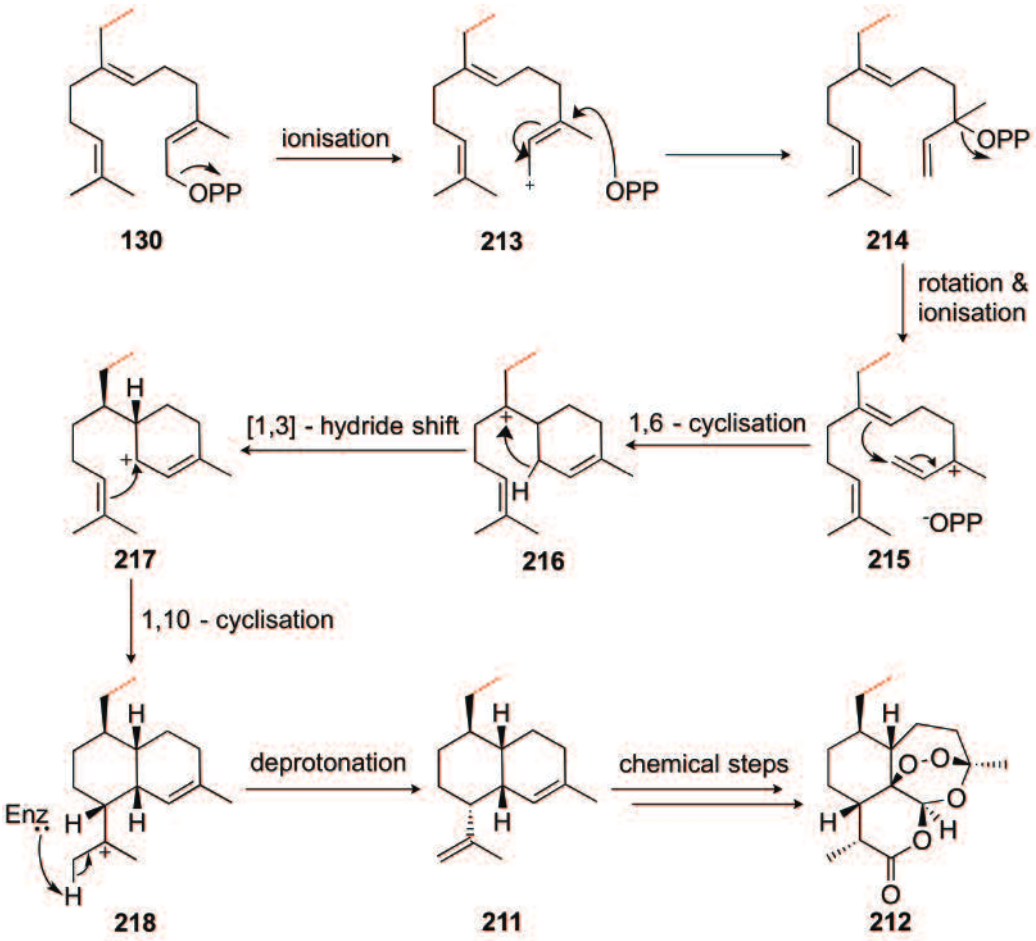

Scheme 4.3 Proposed mechanism of ADS catalysed turnover of 14-methyl FDP (130) and the corresponding artemisinin analogue (212).

4.2.4 15-Methyl FDP (219)

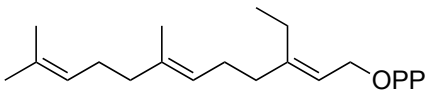

Figure 4.9 15-Methyl FDP (219)

15-Methyl FDP (**219**, Figure 4.9) was previously synthesised by Dr. Sabrina Touchet and was generously gifted to test with ADS on an analytical scale. Incubation of ADS with 15-methyl FDP produced one major pentane extractable product, when analysed by GC-MS. The mass spectrum of this product revealed a molecular ion peak with *m/z* = 218 (Figure 4.10).

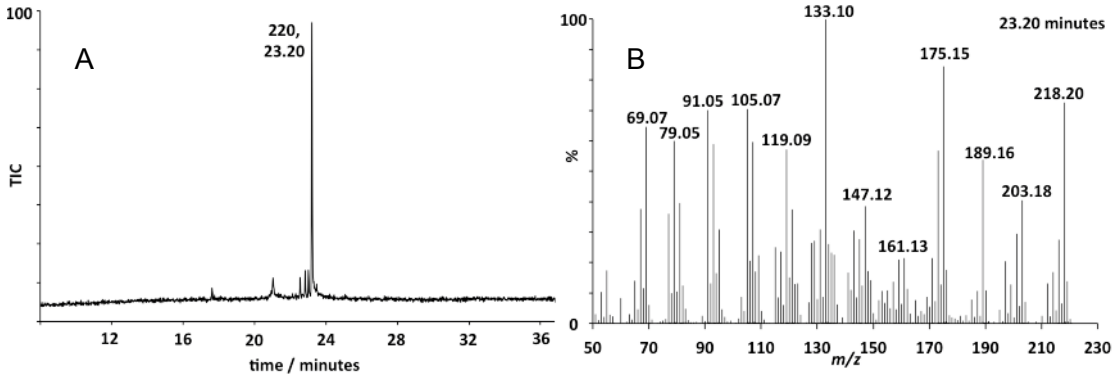

Figure 4.10 A: Total ion chromatogram of the pentane extractable product from incubation of ADS and 15-methyl FDP (219). B: Mass spectrum of the eluted compound.

It was predicted in this case that the additional methyl group on 15-methyl FDP, compared to the natural substrate, would not interfere with the usual reaction pathway demonstrated for FDP. A proposed mechanism (Scheme 4.4) conveys how it is plausible for ADS to convert 15-methyl FDP (**219**) into 15-methyl amorphadiene (**220**). In addition to not interfering with the mechanism of ADS, it was predicted that the position of the methyl group on C15 would not interfere with the formation of the corresponding artemisinin derivative, **221** (Scheme 4.4).

Fragments **228**-**231** were suggested as plausible cations resulting from the fragmentation of 15-methyl amorphadiene (Figure 4.11) and relate well with the fragmentation peaks observed in the mass spectrum (Figure 4.10). Cations **228**-**231** are also in agreement with cations **73**, **232**, **233** and **234** formed from the fragmentation of amophadiene. The base peak at *m/z* = 133, which represents cation **230,** correlates with the base peak observed for amorphadiene at *m/z* = 119, with an increase of *m/z* = 14 corresponding to the extra CH_2 group (Figure 4.11).

As this was a gift for an analytical scale incubation, there was not enough of the enzymatic product to analyse by NMR spectroscopy to confirm the formation of the proposed ‘15-methyl amorphadiene’.

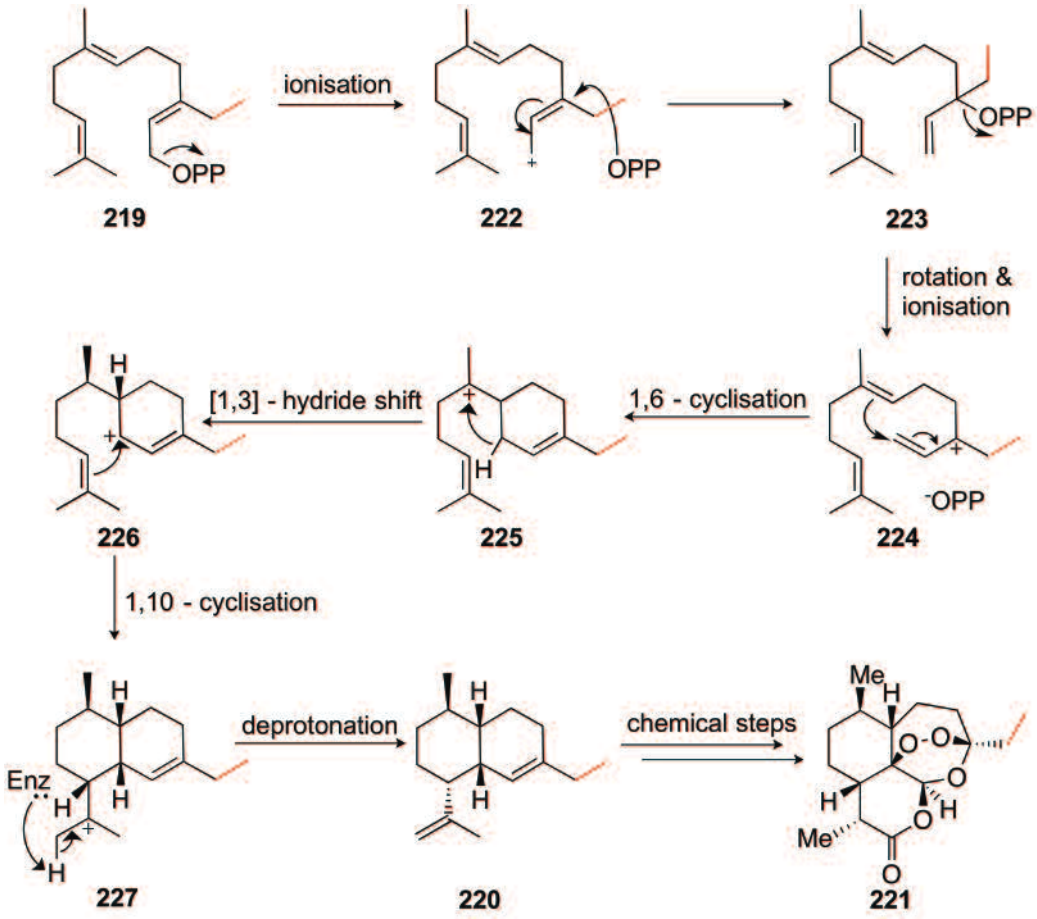

Scheme 4.4 Proposed mechanism of ADS catalysed turnover of 15-methyl FDP (219) and the corresponding artemisinin analogue (221).

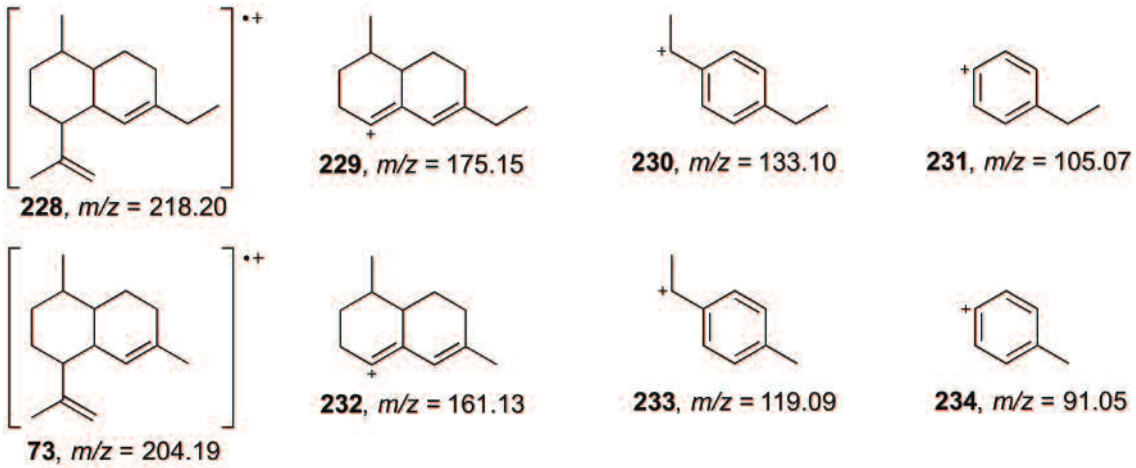

Figure 4.11 Plausible ions formed from the fragmentation of 15-methyl amorphadiene (top) and amorphadiene (bottom).

4.3 Oxygenated analogues

4.3.1 12-Hydroxy FDP (168)

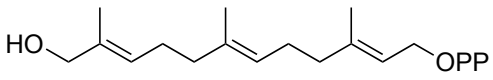

Figure 4.12 12-hydroxy FDP (168)

It is known that amorphadiene is oxidised at position C12 to create artemisinic alcohol (**46**) during the biosynthesis of artemisinin (Scheme 4.5). A plan was implemented to introduce an alcohol group on C12 of the FDP backbone, before the analogue was incubated with ADS, rendering the cytochrome P450 (CYP71AV1) reaction, which achieves this oxidation on amorphadiene *in-vivo*, unnecessary.[111,116] 12-Hydroxy FDP (**168**, Figure 4.12) was created on this basis, to incubate with ADS and attempt to create the corresponding compound, artemisinic alcohol directly and without the need for the subsequent oxidation reaction (**46**, Scheme 4.5).

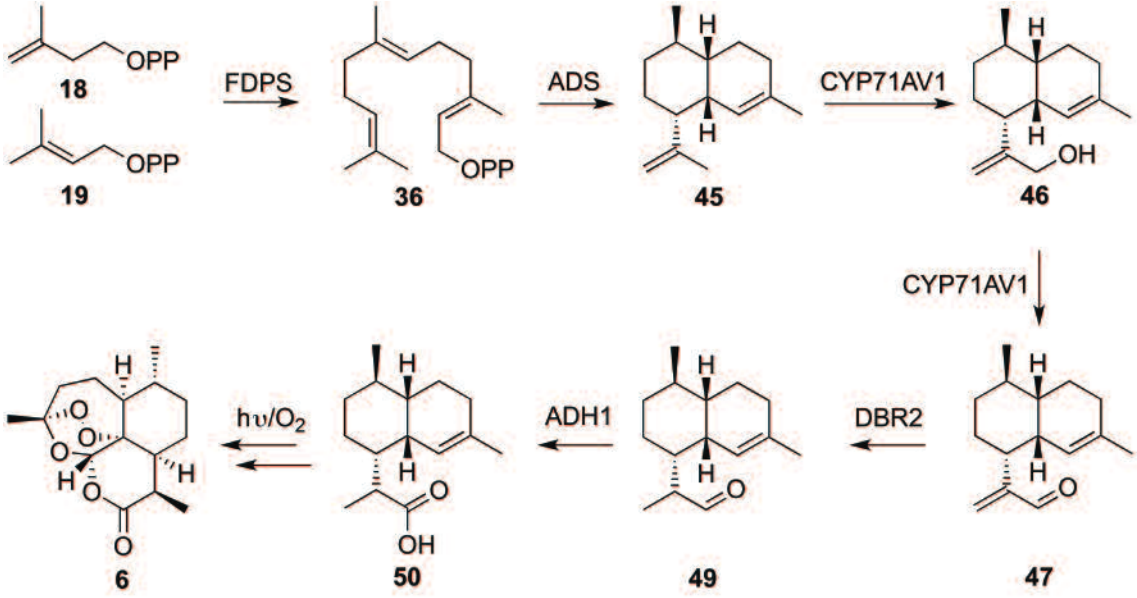

Scheme 4.5 Biosynthetic pathway to artemisinin (6) in *Artemisia annua*.

Incubation of ADS with 12-hydroxy FDP (**168**) generated three pentane extractable products, when analysed by GC-MS. All three compounds showed molecular ion peaks with *m/z* = 220 (Figure 4.13).

In order to identify the chemical structures of these compounds, preparative scale incubations were carried out to obtain enough material to characterise them by

NMR spectroscopy. Surprisingly, the ^{1}H NMR spectrum (Figure 4.14) of the enzymatic products showed that ADS did not convert 12-hydroxy FDP into artemisinic alcohol. The prominent pair of doublets found around δ_H = 9.6 ppm indicated the presence of two aldehydes. Furthermore, upon studying the ^{1}H NMR spectrum, it was confirmed that although artemisinic alcohol was not produced, as expected, the bicyclic hydrocarbon frame of amorphadiene was present in the unknown products. This was concluded from the presence of the olefinic protons at δ_H = 5.1 and 5.3 ppm and the protons at C1 observed at δ_H = 2.4 and 2.5 ppm, which are all representative of those protons found in amorphadiene (**45**, Section 2.6.5, Figure 2.13).

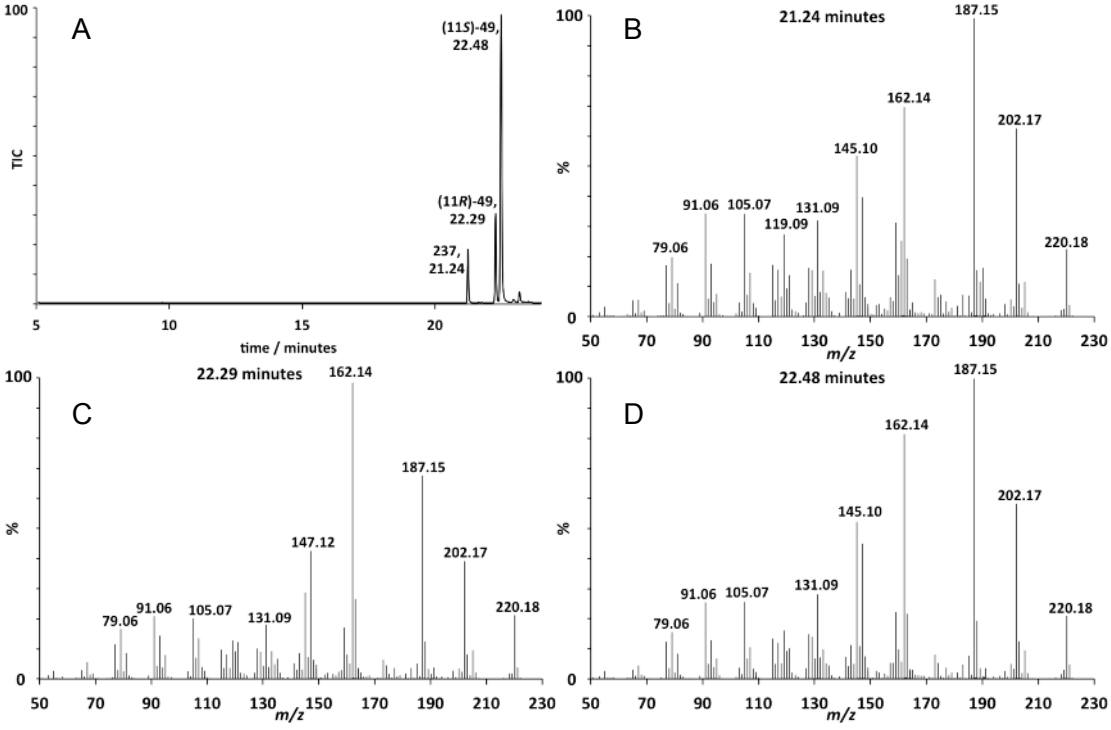

Figure 4.13 A: Total ion chromatogram of the pentane extractable products from incubation of ADS and 12-hydroxy FDP (168). B-D: Mass spectra of the eluted compounds.

It was evident instead that two aldehydes were present since the two sets of doublets around δ_H = 9.6 ppm are characteristic of CH=O protons. Artemisinic aldehyde (**47**) and dihydroartemisinic aldehyde (**49**) are both downstream intermediates in the biosynthesis of artemisinin. Artemisinic aldehyde, (**47**, Scheme 4.5) was eliminated as a possible product since the mass spectrum of this compound requires a molecular ion peak with *m/z* = 218, not 220 as observed.

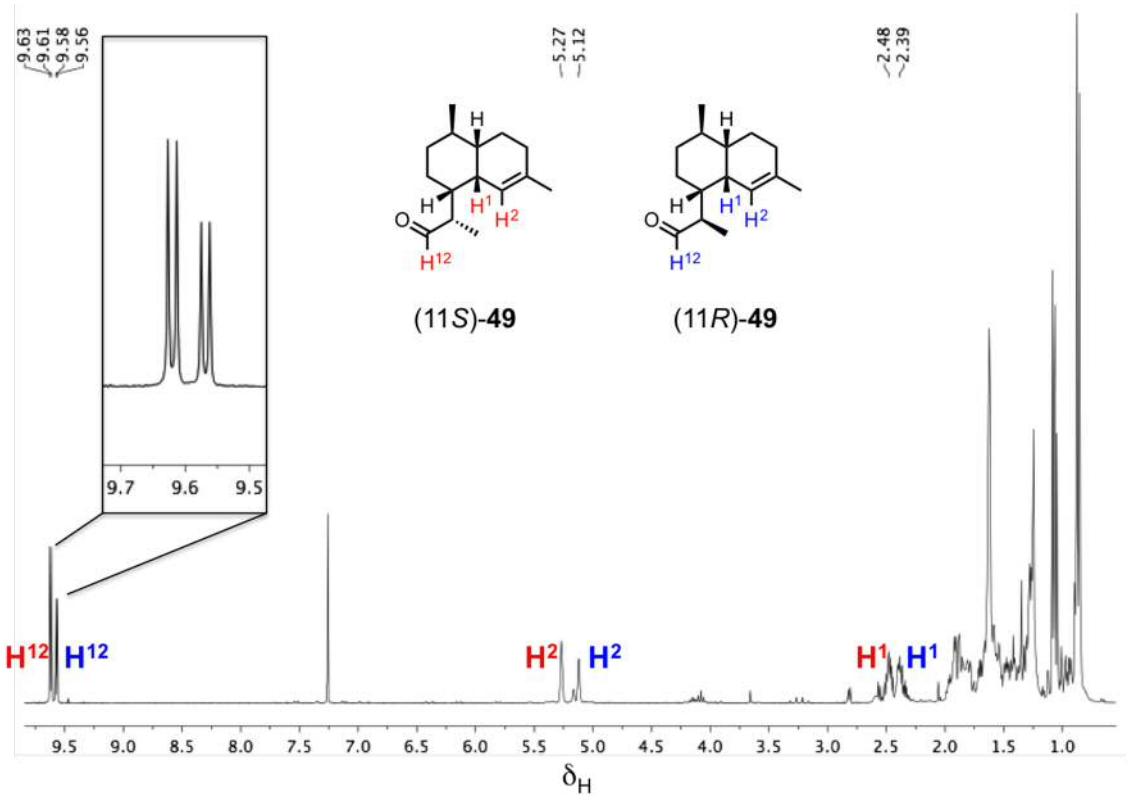

Figure 4.14 ^{1}H NMR spectrum (500 MHz, $CDCl_3$) of the enzymatic products generated from incubation of ADS with 12-hydroxy FDP (168).

By comparing the mass spectra and ^{1}H NMR spectrum of the enzymatic products, with those found in literature for dihydroartemisinic aldehyde, it was confirmed that the two epimers of dihydroartemisinic aldehyde (11*S*-**49** and 11*R*-**49**, Figure 4.14) were isolated from incubation of ADS and 12-hydroxy FDP.[105] The compounds observed in the GC at 22.29 and 22.48 min share similarities in the fragmentation patterns observed in the mass spectra, displaying peaks with identical *m/z* values, and only differing in their base peaks. The mass spectrum of 11*R*-**49** has a base peak at *m/z* = 162, whereas 11*S*-**49** displays a base peak at *m/z* = 187, and so it was proposed that these two peaks represented the two epimers generated in a 2:7 (*R*:*S*) ratio. Surprisingly, when the same sample was analysed by NMR spectroscopy, this ratio changed to 2:3 (*R*:*S*). The difference in ratios observed by GC-MS and NMR spectroscopy is still open for discussion, as a reasonable rationale has not been found yet. It has previously been stated that the (*R*)-epimer (11*R*-**49**) is the desired precursor to artemisinin with research groups managing to distinguish between the two epimers of dihydroartemisinic aldehyde by comparing their elution times with the elution time of an authentic sample of (11*R*)-dihydroartemisinic aldehyde.[114,162] By comparing the gas chromatogram with the gas chromatograms found in literature, the predominant compound produced from incubation of ADS and 12-hydroxy FDP (**168**) was found to

be (11*S*)-dihydroartemisinic aldehyde. In addition to this, (11*R*)-dihydroartemisinic aldehyde was synthesised from commercially available (11*R*)-dihydroartemisinic acid (**50**) *via* two steps to confirm this assignment, which will be further discussed in Section 5. The NMR spectroscopy and GCMS characterisation of the synthesised (11*R*)-dihydroartemisinic aldehyde was in agreement with the data found in literature.[105,162]

With a hydroxyl group added to C12 of FDP, it can be assumed that the enzyme will convert the analogue through the same mechanism as FDP until the '12-hydroxy amorphyl cation' (**235**) is formed. With the natural substrate, FDP (**36**), the enzyme completes the mechanism with a deprotonation at C12 or C13 to produce amorphadiene (**45**). Instead, with 12-hydroxy FDP, there are two plausible mechanisms to achieve dihydroartemisinic aldehyde. Firstly, a 1,2-hydride shift can take place on the α-carbon forming cation **236**, followed by a deprotonation of the alcohol group to afford the aldehyde. Alternatively, a deprotonation on the α-carbon can form an enol intermediate **237**. Tautomerism of the enol to the more stable aldehyde form, also affords dihydroartemisinic aldehyde (Scheme 4.6).

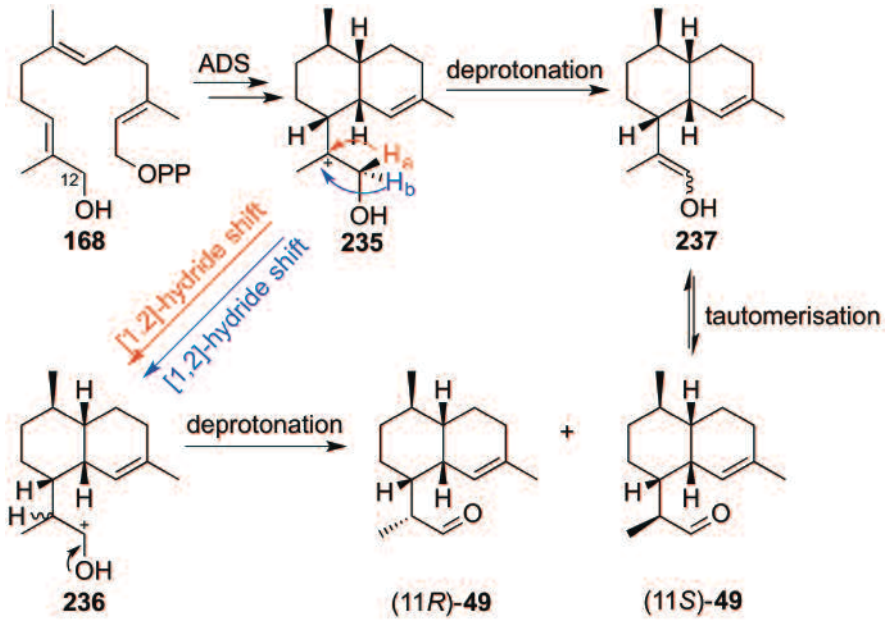

Scheme 4.6 Proposed mechanism for the formation of 49 from incubation of ADS and 12-hydroxy FDP (168).

In addition to the two epimers of dihydroartemisinic aldehyde, a third compound at 21.23 min was also observed in the gas chromatogram. The identity of this third compound is suggested to be the corresponding enol that tautomerizes with the aldehydes, but this has yet to be unambiguously demonstrated. To support this proposition and clarify whether the aldehydes tautomerise with an enol intermediate,

an incubation of ADS with 12-hydroxy FDP in a deuterated buffer was carried out. This experiment was intended to test whether an incorporation of a deuterium could be observed in the aldehydes, however this test would not be able to identify which mechanism achieves the products. The mass spectrum of the incubation products revealed that there was an incorporation of deuterium in (11*S*)-dihydroartemisinic aldehyde, shown by an increases of *m/z* = 1 in the molecular ion (Figure 4.15). This incorporation shows that it is viable for the enzyme to deprotonate the α-hydrogen, forming an enol (**237**), which effectively tautomerizes to the resulting aldehyde. Surprisingly, the deuterium incorporation was not observed in the mass spectrum for the (11*R*)-epimer. This suggests that only the (11*S*)-epimer is in equilibrium with enol **237**, whereas once the (11*R*)-epimer is formed, it remains as the stable conformer.

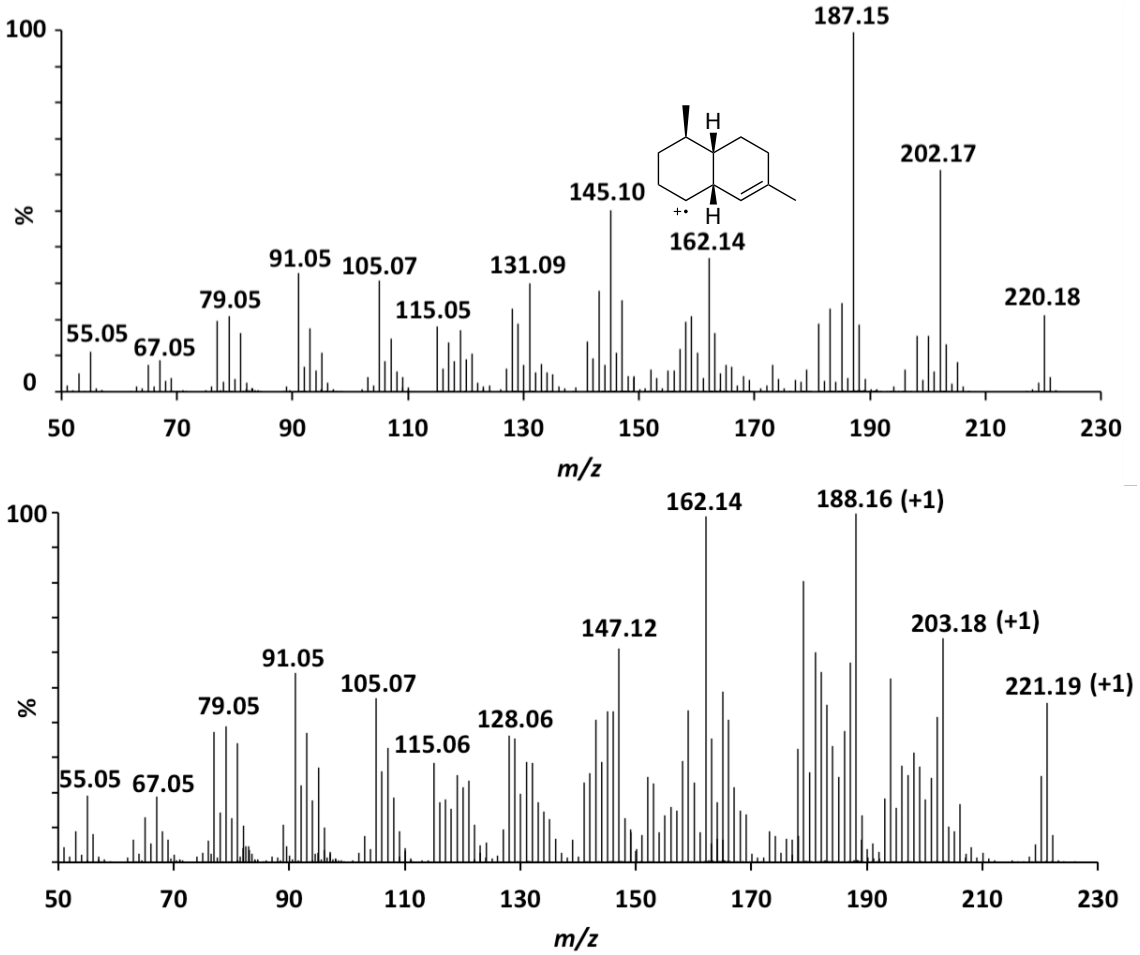

Figure 4.15 Mass spectra of (11-*S*)-[11-^{1}H]-dihydroartemisinic aldehyde (top) and (11-*S*)-[11-^{2}H]-dihydroartemisinic aldehyde (bottom). An increase of *m/z* = 1.01 can be observed prior to the fragmentation peak indicating a loss of the $CHOCHCH_3$ tail (*m/z* = 162.14). This observation further indicates that the incorporated deuterium is positioned on C11.

4.3.2 12-Acetoxy FDP (166)

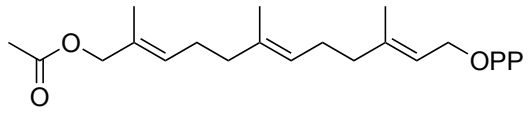

Figure 4.16 12-Acetoxy FDP (166)

12-Acetoxy FDP (**166**, Figure 4.16) was a synthetic precursor to the previously discussed analogue 12-hydroxy FDP (**168**) (Section 3.5.2, Scheme 3.9). The products generated when 12-acetoxy FDP was incubated with ADS were, surprisingly, identical to those generated from 12-hydroxy FDP (Figure 4.17).

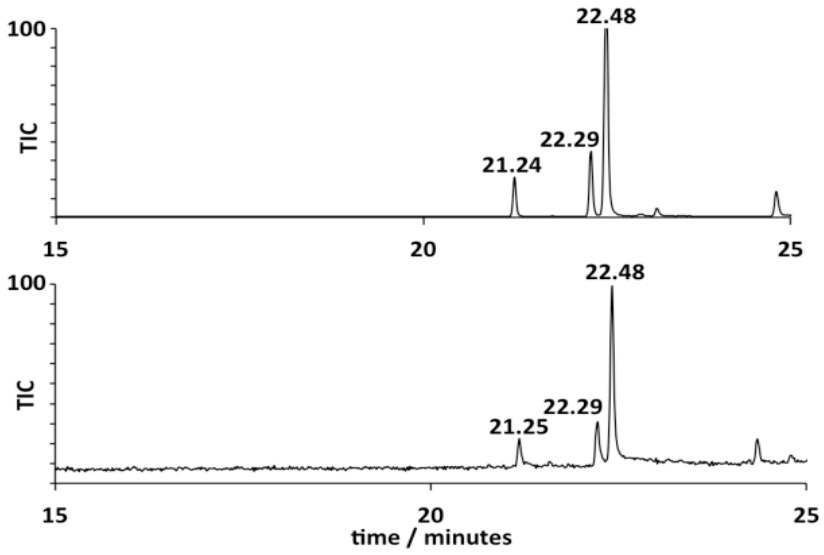

Figure 4.17 Total ion chromatogram of the pentane extractable products from incubation of ADS and 12-hydroxy FDP (168) (top) and 12-acetoxy FDP (166) (bottom).

There were three possibilities considered as to how 12-acetoxy FDP was converted to the same products as 12-hydroxy FDP. The first plausible solution was that the acetyl group is hydrolysed non-enzymatically in the buffer, forming 12-hydroxy FDP (**168**). This proposition however did not seem likely since the conditions required to de-protect the acetoxyl moiety to produce 12-hydroxy FDP (Section 3.5.2, Scheme 3.9) required a base, in this case 30% ammonium hydroxide, and the reaction was relatively slow, therefore it was not feasible for the analogue to de-acetylate in a buffer that has a pH value of 7.5. Additionally, a control incubation was set up with 12-acetoxy FDP in the incubation buffer without any enzyme. This was to verify whether it was the Mg^{2+}, present in the buffer, acting as a Lewis acid and cleaving the acetate group off. This

control experiment did not yield any 12-hydroxy FDP and therefore it was concluded that this was not the case.

The second possibility was that ADS de-acetylates 12-acetoxy FDP with the use of a nucleophilic residue, such as a cysteine or serine, to form 12-hydroxy FDP before the catalytic mechanism takes place. This de-acetylation could take place either outside or inside of the enzymes active site pocket. This possibility can also be argued against because the observation of a same product profile observed with analogues **168** and **166** is not observed with any other sesquiterpene synthases that are studied in the Allemann group. In fact 12-acetoxy FDP was not a substrate of any of the sesquiterpene synthases that are studied within the Allemann group, e.g. GAS, GDS and EBFS. On the other hand, 12-hydroxy FDP does generate enzymatic products when incubated with enzymes such as GDS (Section 1.4) and EBFS (Section 2.7).

The last possibility is that it is simply converted by the enzyme as a substrate (Scheme 4.8).

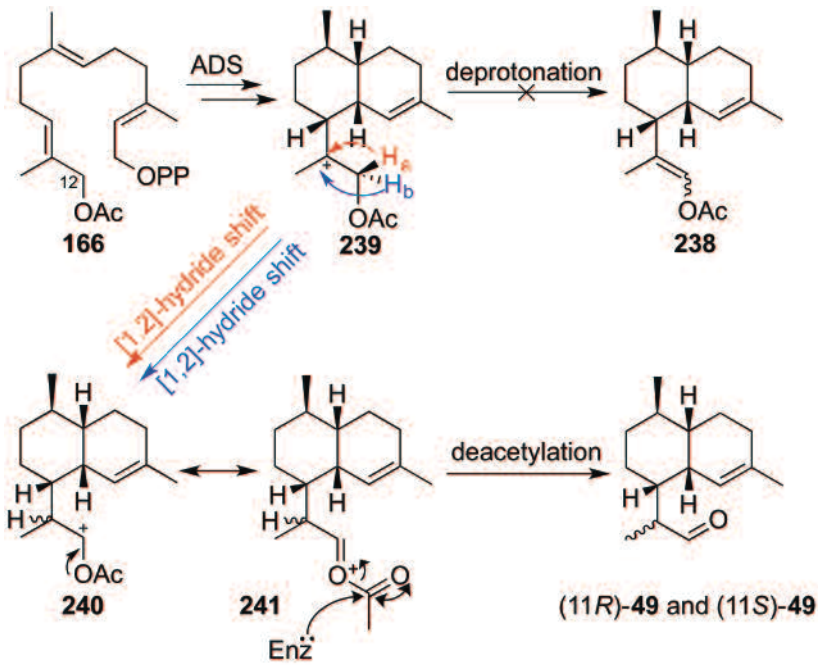

Scheme 4.7 Proposed mechanism for the formation of 49 from incubation of ADS and 12-acetoxy FDP (166).

The observation that no enol acetate **238** is produced from **166** *via* carbocation **239** (Scheme 4.7) implies that enol **237** (Scheme 4.6) is most likely not a product of ADS catalysis but forms exclusively from (11*S*)-**49** after its release from the enzymes active site.

4.3.3 13-Acetoxy FDP (165)

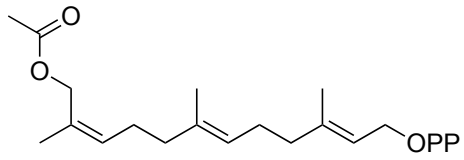

Figure 4.18 13-Acetoxy FDP (165)

13-Acetoxy FDP (**165**, Figure 4.18) was designed to determine whether the position of the hydroxyl/ acetoxyl group on C12 or C13 of FDP had an effect on the ratio of the epimers of dihydroartemisinic aldehyde generated. 12-Acetoxy FDP (**166**) and 12-hydroxy FDP (**168**) displayed 60-75% of the enzymatic product distribution to be (11*S*)-dihydroartemisinic aldehyde, however it is the (11*R*)-epimer that is required for the synthesis of artemisinin. By changing the position of the alcohol group to C13, there was a possibility of the ratio of epimers reversing, producing (11*R*)-dihydroartemisinic aldehyde as the dominant product. The synthesis of 13-acetoxy FDP is one step shorter than 13-hydroxy FDP (Section 3.5.1, Scheme 3.8), and for this reason, 13-acetoxy was tested first with ADS to prove or disprove the hypothesis made.

Incubation of ADS with 13-acetoxy FDP generated one pentane extractable product, when analysed by GC-MS, with a molecular ion of *m/z* = 220 (Figure 4.19). Surprisingly the compound was not (11*R*)-dihydroartemisinic aldehyde as expected, but the (11*S*)-epimer as determined by comparing the gas chromatogram with that of the material generated from 12-acetoxy FDP (Figure 4.19).

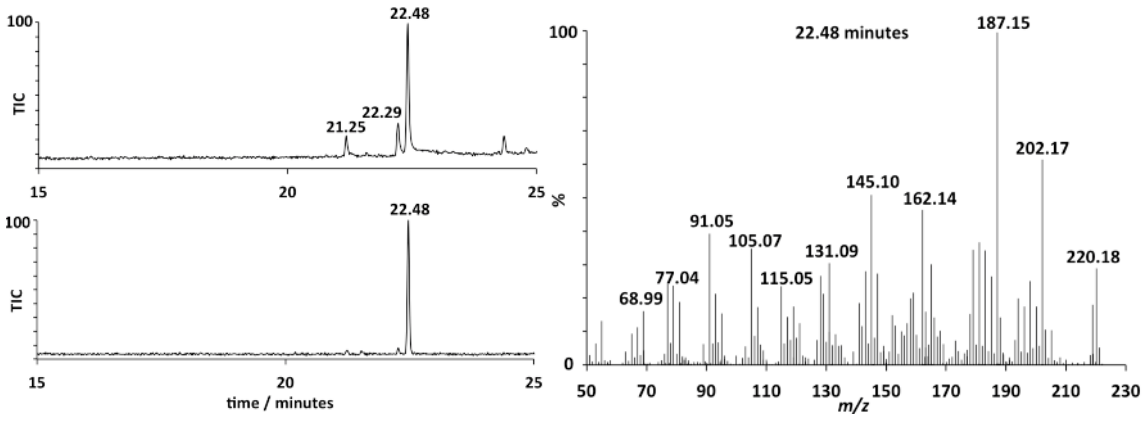

Figure 4.19 Left: Total ion chromatogram of the pentane extractable products from incubation of ADS and 12-acetoxy FDP (166) (top left) and 13-acetoxy FDP (165) (bottom left). Right: Mass spectrum of the eluted compound from incubation of ADS and 13-acetoxy FDP.

These results indicate that the dominant epimer generated is not a result of whether the hydroxyl/acetoxyl group is attached to C12 or C13 of FDP.

The absence of significant amounts of (11*R*)-dihydroartemisinic aldehyde could imply that enol **237** does not tautomerise to the (11*R*)-epimer under the reaction conditions used (*p*H ~7.5) (Scheme 4.6). These results suggest that only one pathway operates to yield the observered epimeric mixture of aldehydes **49**. The formation of both epimers of dihydroartemisinic aldehyde, from 12-hydroxy FDP (**168**) or 12-acetoxy FDP (**166**), most likely procedes through an oxygen-assisted non-stereopecific intramolecular 1,2-hydride shift at carbocation **235** and **239**, respectively, followed by a deprotonation on the alcohol group of the resulting carbocation **236** (or a deacetylation from **240**) (Scheme 4.6 and 4.7).

Since the stable enol acetate **242** is also not observed from incubation of ADS with 13-acetoxy FDP (**165**), a deprotonation at C13 of carbocation **243**, followed by subsequent tautomerisation of the resulting enol **242** to (11*S*)-**49** appears unlikely. Hence a stereospecific [1,2]-hydride shift of H_b on carbocation **243** followed by a deacetylation of the resulting carbocation **244** most likely accounts for the exclusive formation of (11*S*)-**49** (Scheme 4.8).

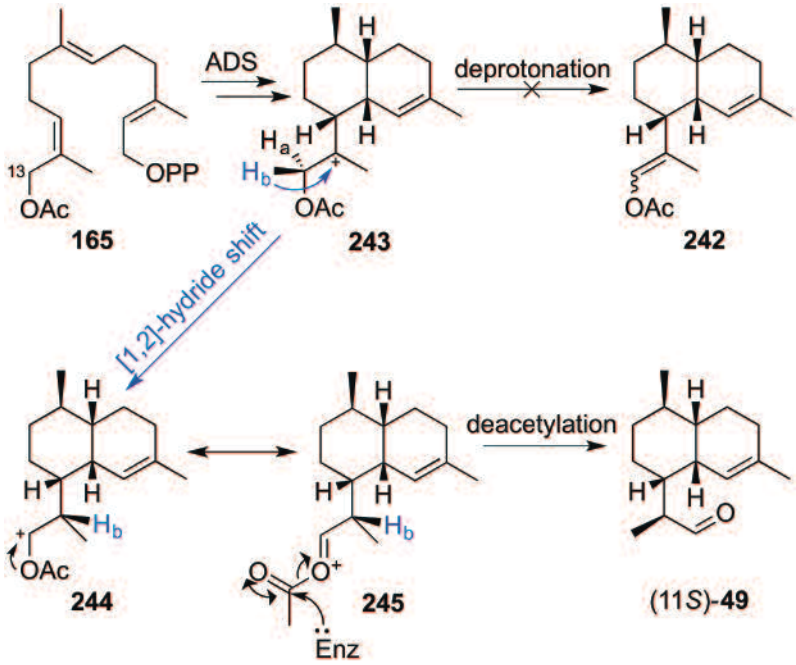

Scheme 4.8 Proposed mechanism for the formation of (11*S*)-49 from incubation of ADS and 13-acetoxy FDP (165).

4.3.4 8-Hydroxy FDP (169)

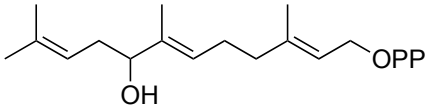

Figure 4.20 8-Hydroxy FDP (169)

During the biosynthetic conversion of amorphadiene to artemisinin, the groups corresponding to C8 and C9 on the FDP backbone are not transformed in any way (Scheme 4.9), hence an addition to FDP in either of those positions would potentially be a benign change to the substrate that may remain unchanged through subsequent steps and, ultimately, form an analogue of artemisinin. In addition to this, it was predicted that a functional group added on C8 would also not interfere with the formation of the endoperoxide bridge, which is crucial for the antimalarial activity.[41,45]

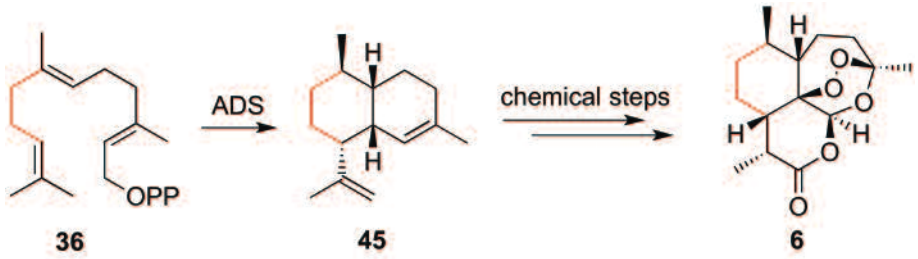

Scheme 4.9 FDP (36), Amorphadiene (45) and artemisinin (6) with C8 and C9 of the FDP skeleton highlighted in red.

Incubation of ADS with 8-hydroxy FDP (**169**, Figure 4.20) generated six pentane extractable products as judged by GC-MS analysis. The mass spectra for all six compounds revealed a molecular ion peak with *m/z* = 220 (Figure 4.21). The molecular weight of 220 indicated that the enzymatic product was consistent with a hydroxylated terpenoid.

Due to the large number of enzymatic products produced, this incubation was not repeated on a preparative scale to analyse the products by NMR spectroscopy, and therefore there is no definite conclusion as to what ADS produced when incubated with 8-hydroxy FDP.

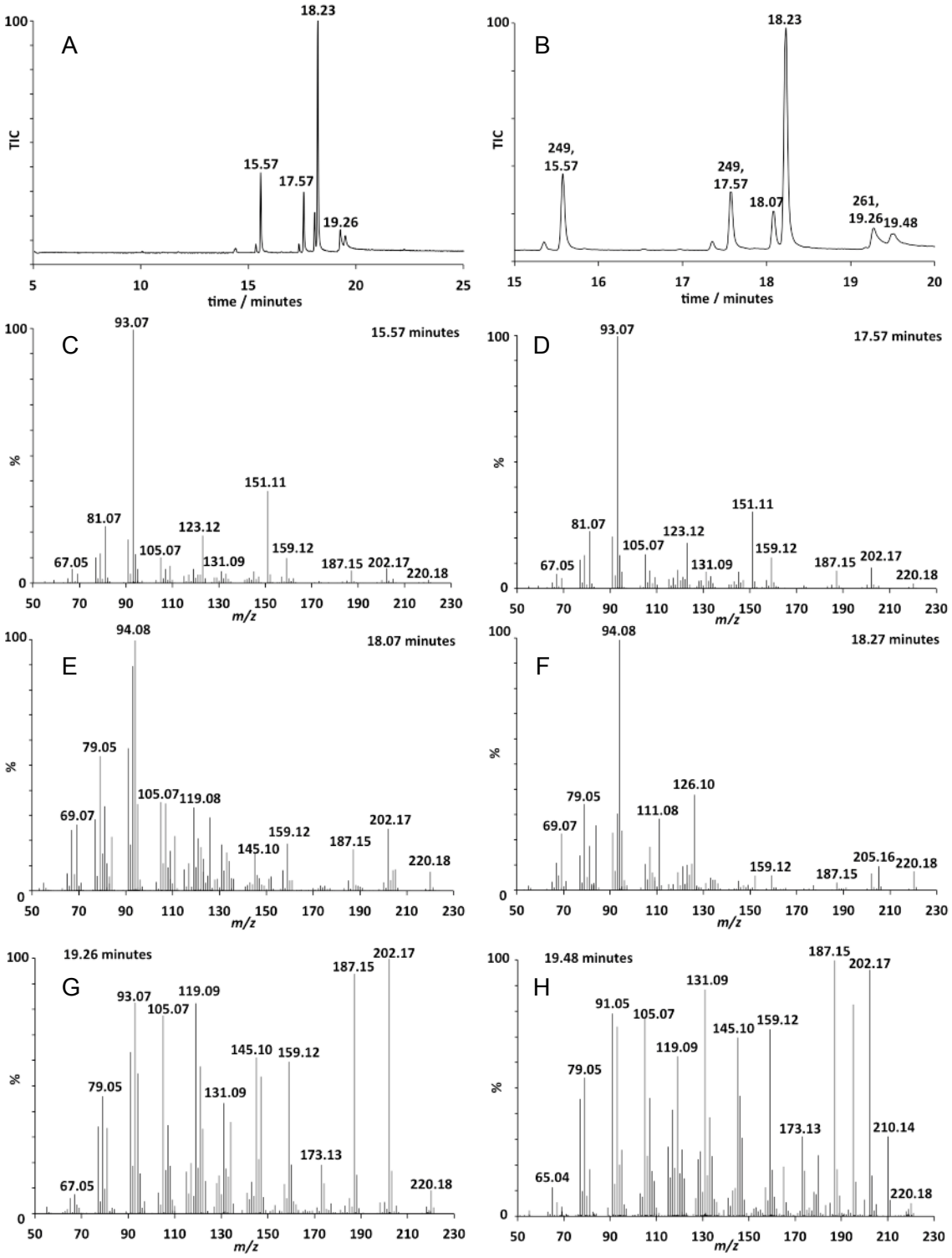

Figure 4.21 A: Total ion chromatogram of the pentane extractable product from incubation of ADS and 8-hydroxy FDP (169). B: Total ion chromatogram expanded between the region of 15 and 20 min. C-H: Mass spectra of the eluted compounds.

Examination of the mass spectra of all six compounds, revealed that the first two compounds observed in the GC, with retention times of 15.57 and 17.57 min, have very similar fragmentation patterns in their mass spectra, both with a base peak at *m/z*

= 93. It is proposed that these two products are two isomers of the same compound. This is understandable as 8-hydroxy FDP was prepared as a racemate, and therefore for each enzymatic product formed, there is a possibility of having the (*S*)- and (*R*)-isomer. The fragmentation pattern observed for the first two compounds is characteristic for the presence of a farnesene (Figure 4.22).[207,208] The base peak at *m/z* = 93 can be identified as fragment **246** (Scheme 4.10), which supports the formation of a farnesene. The peak at *m/z* = 151 indicates that the hydroxyl group has not migrated to another carbon to quench a cation. This is supported by the feasible fragmentation leading to cation **247** (Scheme 4.10). Cation **248**, with *m/z* = 202 is a prominent peak found in mass spectra of alcohols, it displays the loss of a water molecule. A plausible mechanism was predicted for the fragmentation leading to cations **246**, **247** and **248** starting with the molecular ion **249** (Scheme 4.10).

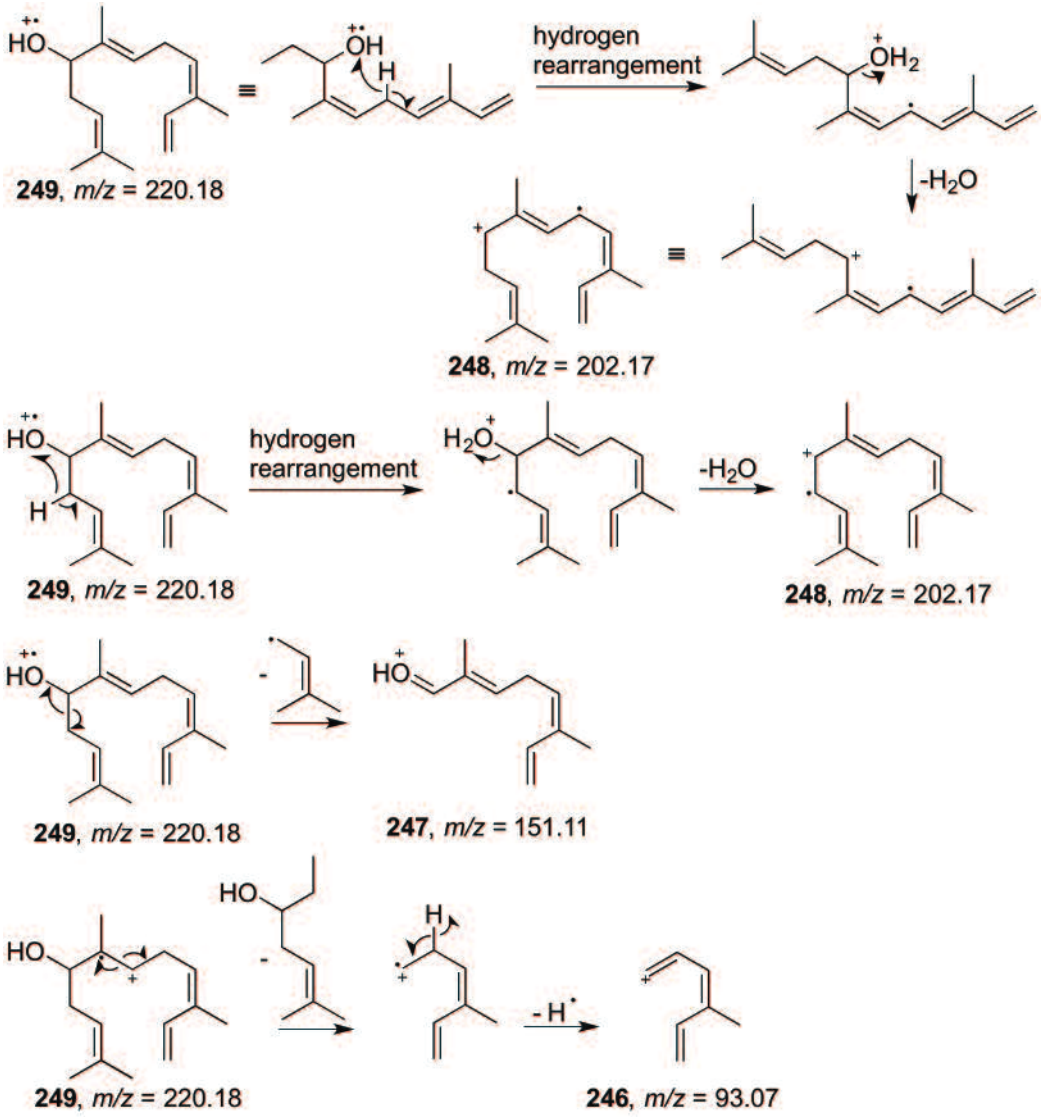

Scheme 4.10 Proposed mechanisms for the formation of the major fragments 246, 247 and 248.

8-Hydroxy FDP was incubated with *E*-β-farnesene synthase (EBFS), a sesquiterpene synthase also studied within the Allemann group. It was assumed that the enzymatic product produced from an incubation of EBFS and 8-hydroxy FDP was 8-hydroxy-*E*-β-farnesene (**250**, Figure 4.22). Based on this assumption, overlaid gas chromatograms of products formed from incubations with EBFS and ADS, each with 8-hydroxy FDP, suggested that none of the enzymatic products produced by ADS were 8-hydroxy-E-β-farnesene (**250**, Figure 4.22). This observation suggests that if the first two compounds observed in the GC are farnesenes, then they could either be the two isomers of 8-hydroxy-(*E*,*E*)-α-farnesene (**251**) or 8-hydroxy-(*Z*,*E*)-α-farnesene (**252**) (Figure 4.22).

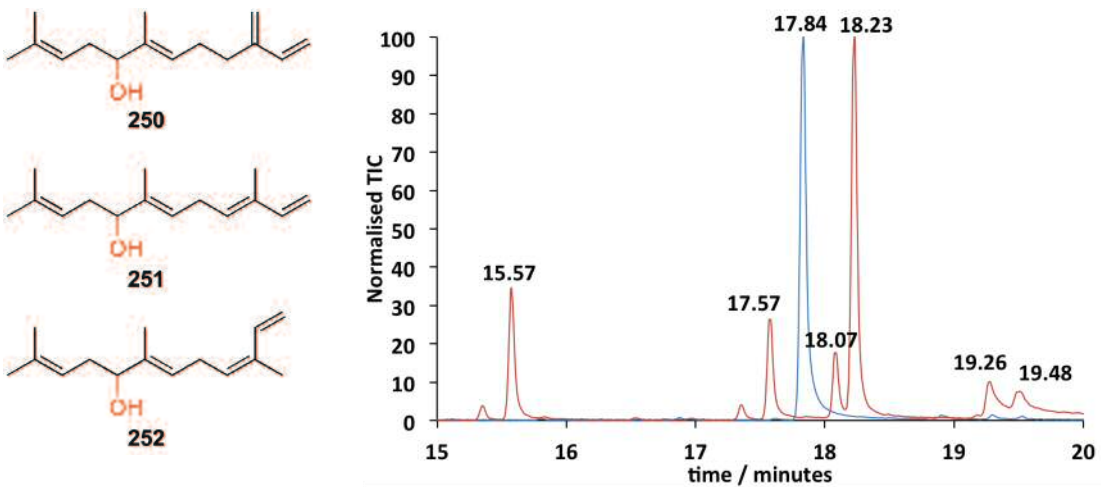

Figure 4.22 Left: 8-hydroxy-*E*-β-farnesene (250), 8-hydroxy-(*E*,*E*)-α-farnesene (251) and 8-hydroxy-(*Z*,*E*)-α-farnesene (252), Right: Overlaid gas chromatograms of pentane extractable products from incubation of EBFS with 8-hydroxy FDP (blue) and ADS with 8-hydroxy FDP (red).

It can also be argued that a base peak at *m/z* = 93 can also be identified as the 6 membered ring intermediate, **76** (Section 4.2.1, Figure 4.3), which is observed as the base peak for some 6-membered ring sesquiterpenes.[206,209] Once ADS has catalysed the isomerisation of 8-hydroxy FDP to the corresponding 8-hydroxy NDP (**253**), which is ionised to cation **254**, a 1,6-cyclisation follows to form **255**. The addition of an alcohol group on C8 might hinder the [1,3]-hydride shift that would occur next with the natural substrate FDP. Instead a deprotonation at C6 can yield compound **256**. Alternatively, a [1,3]-hydride shift can still take place, forming cation **257**, and then the addition of the alcohol group might hinder the following 1,10-cyclisation. In this case, deprotonation at C4, C6 or C15 will form compounds **258**, **259** and **260**, respectively (Scheme 4.11).

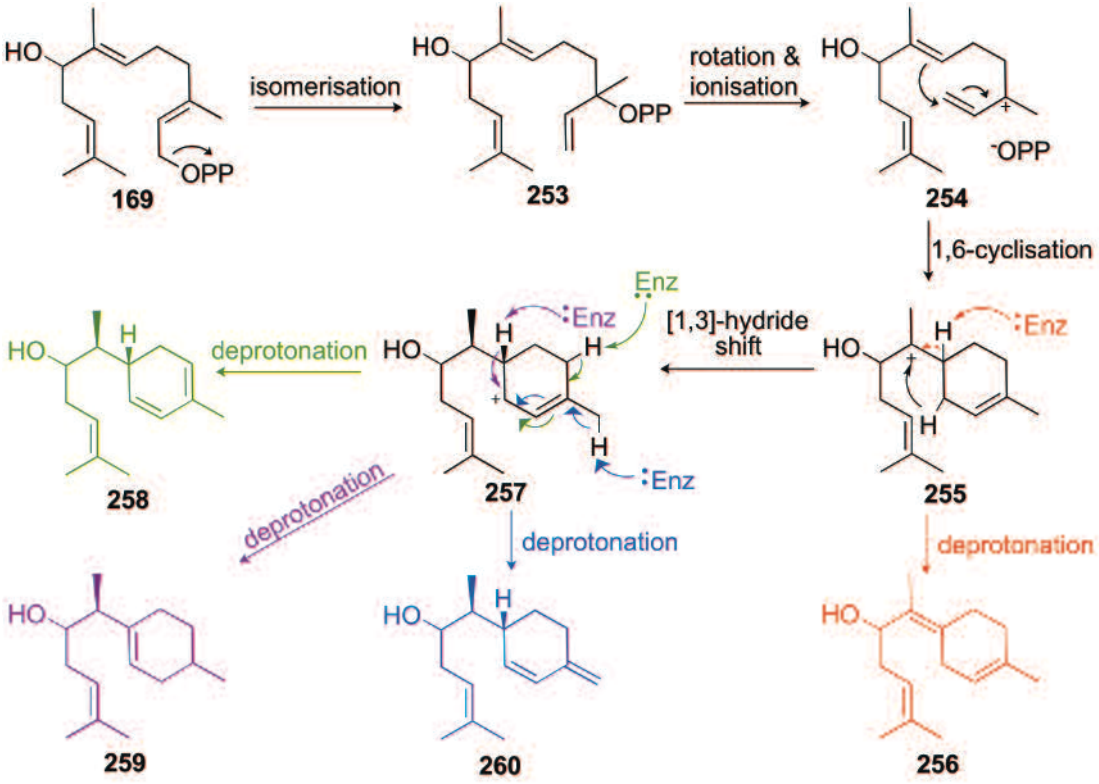

Scheme 4.11 Proposed mechanisms for the formation of 256, 258, 259 and 260 from incubation of ADS and 8-hydroxy FDP (169).

The fifth compound observed in the gas chromatogram, with a retention time of 19.26 min, again was not given a definite assignment but the mass spectrum was comparable to what was observed for the major product when ADS was incubated with analogue **170**, 8-methoxy FDP (Section 4.3.6). The structural assignment of the major product produced in Section 4.3.6 was made *via* NMR spectroscopic analysis and therefore when comparing the mass spectra, there was firm evidence to suggest the formation of 8-hydroxy-γ-humulene (**261**) (Figure 4.23).

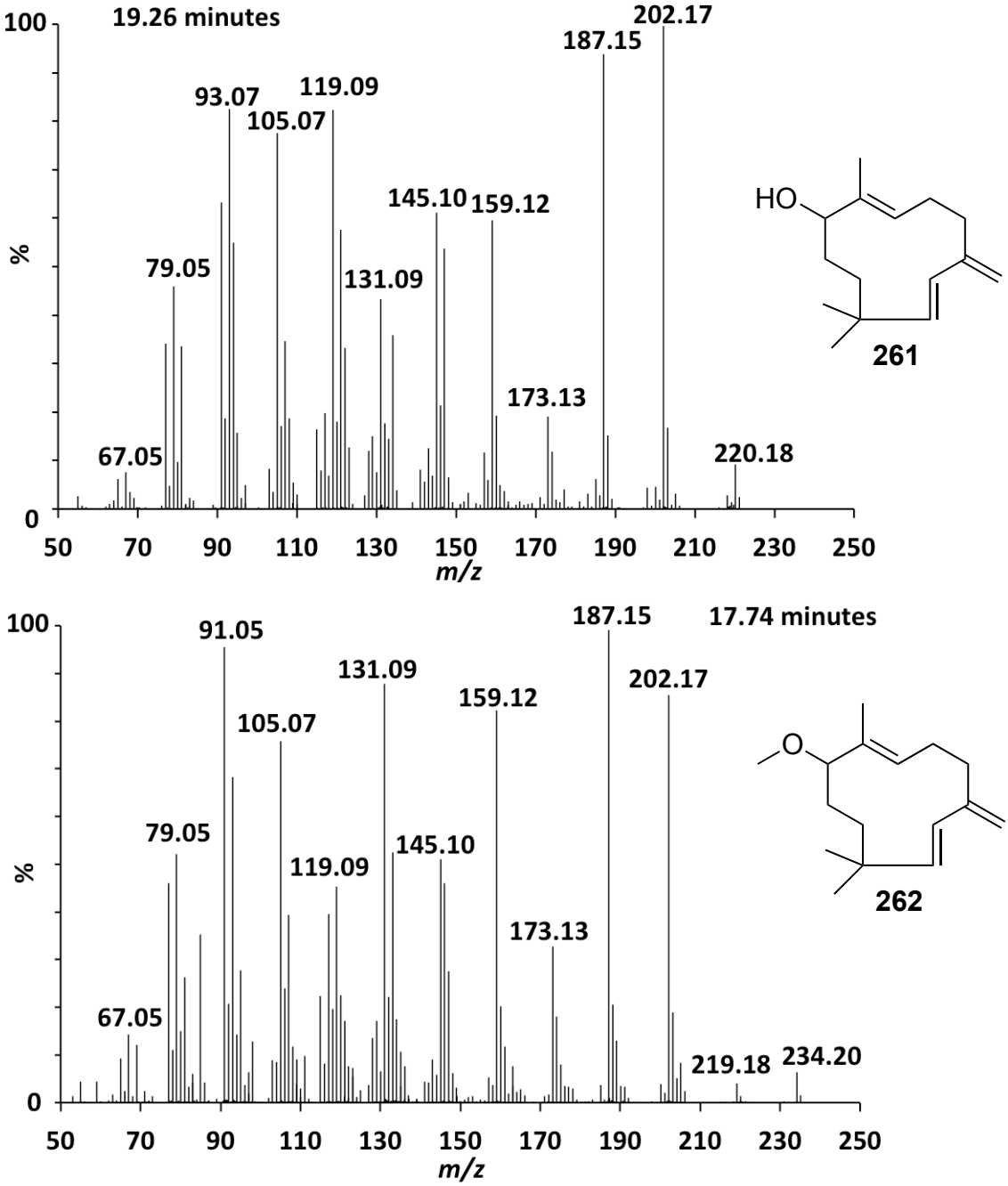

Figure 4.23 Mass spectra of proposed 8-hydroxy-γ-humulene (261) (top) and of identified 8-methoxy-γ-humulene (262) (bottom).

4.3.5 8-Acetoxy FDP (167)

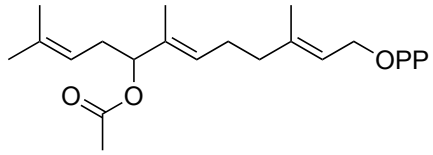

Figure 4.24 8-Acetoxy FDP (167)

8-Acetoxy FDP (**167**, Figure 4.24) was synthesised to test whether ADS would generate the same products with this analogue as it did with 8-hydroxy FDP (**169**, Section 4.3.4) by analogy with the fact that ADS created the same enzymatic products when incubated with 12-hydroxy FDP (**168**) and 12-acetoxy FDP (**166**) (4.3.1 and 4.3.2).

Incubation of ADS with 8-acetoxy FDP produced nine pentane extractable products (Figure 4.25). Six of those peaks correlated to the products generated from 8-hydroxy FDP (Section 4.3.4). There are three additional peaks observed in the GC that were not observed with 8-hydroxy FDP but these peaks were not further investigated.

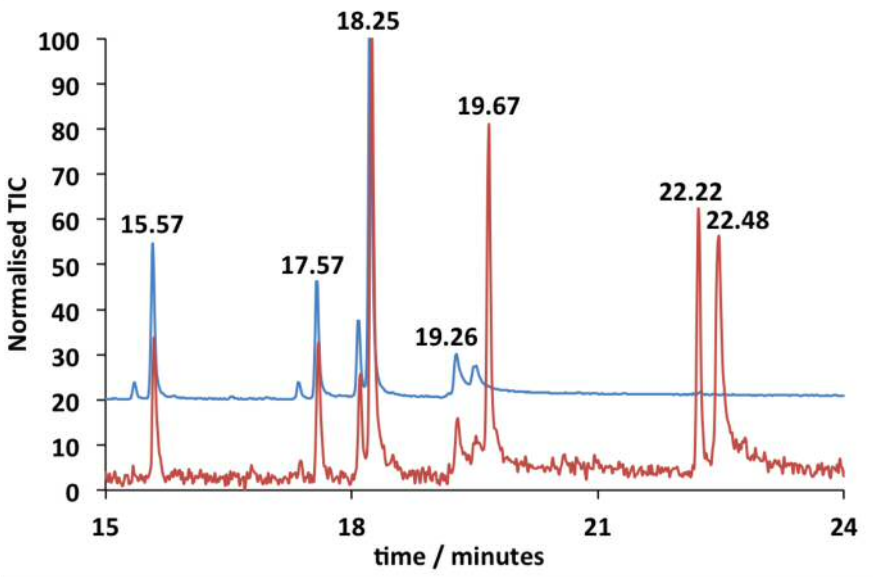

Figure 4.25 Overlaid gas chromatograms of the pentane extractable products from incubations of ADS with 8-hydroxy FDP (blue) and 8-acetoxy FDP (red).

Although additional products were generated, the gas chromatograms show that ADS produced the same products with substrates 8-acetoxy FDP and 8-hydroxy FDP (**169**). This observation implied that to achieve the same product profile, it did not matter

which carbon the hydroxyl and acetoxyl groups were placed on. This could also suggest that the same product profiles are due to the specific catalysis performed by the ADS enzyme, because other sesquiterpene synthases studied in the Allemann group did not generate the same compounds when tested with these two analogues.

4.3.6 8-Methoxy FDP (170)

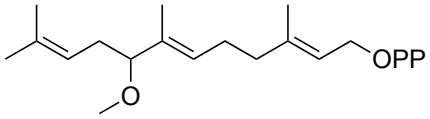

Figure 4.26 8-Methoxy FDP (170)

The methoxy group, positioned on C8, was based on the idea that in that position the additional group would hopefully not interfere with the synthesis of artemisinin, if the corresponding amorphadiene derivative was generated.

Incubation of ADS with 8-methoxy FDP (**170**, Figure 4.26) generated two pentane extractable products, when analysed by GC-MS, with mass spectra of each product revealing a molecular ion with *m/z* = 234 (Figure 4.27).

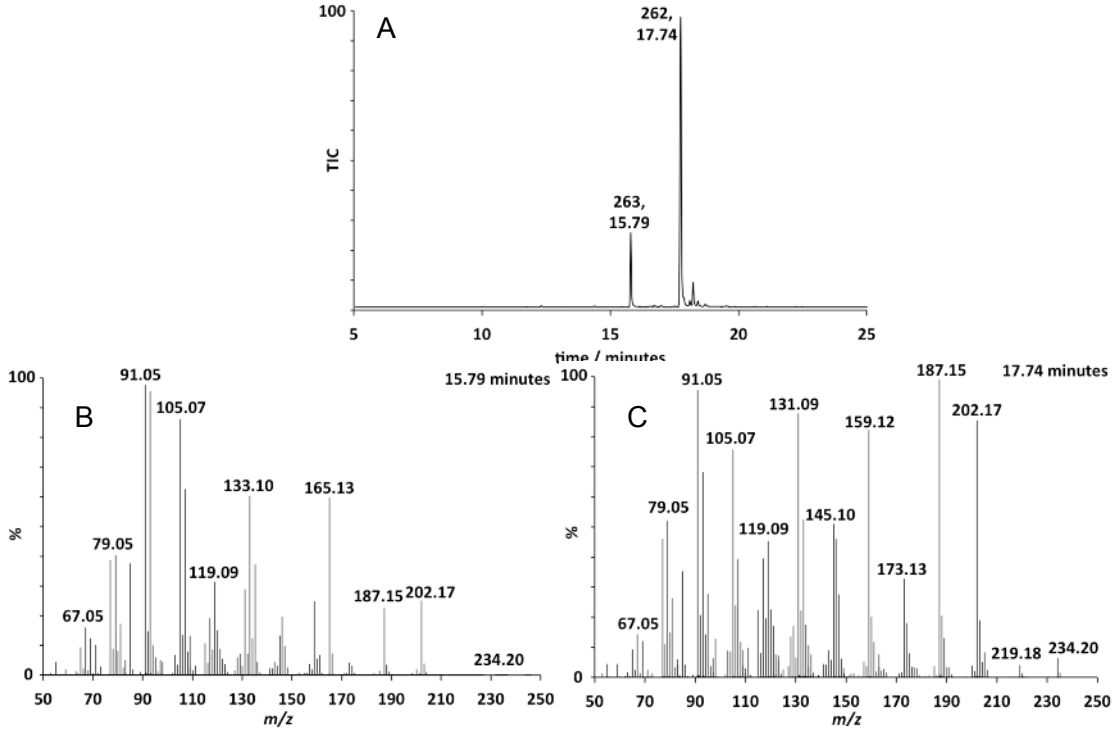

Figure 4.27 A: Total ion chromatogram of the pentane extractable products from incubation of ADS and 8-methoxy FDP (170). B-C: Mass spectra of the two major eluted compounds.

Since there were only two major enzymatic products, this incubation was carried out on a preparative scale for analysis by NMR spectroscopy.

^{1}H NMR spectroscopy (Figure 4.28) was carried out on the two compounds as a mixture and then they were separated using silica chromatography (95:5, hexane: ethyl acetate) and once separated, ^{1}H NMR spectroscopy was again carried out on the major product (Figure 4.29). Unfortunately, there was not enough of the minor product to give a useful 600 MHz ^{1}H NMR spectrum, however by subtracting the resonances belonging to the major product, from the spectrum with both compounds, the structure of the minor product was deciphered. After studying the ^{1}H, ^{13}C, HSQC and HMBC NMR spectra, it was concluded that the major product was 8-methoxy-γ-humulene (**262**) (Table 4.1). To our knowledge, there are no ^{1}H NMR spectra of γ-humulene reported in literature to compare these spectra with.

The identity of the minor product was established as 8-methoxy-*E*-β-farnesene (**263**). In addition to making this identification by studying the ^{1}H NMR spectroscopy, it was also confirmed by incubating 8-methoxy FDP with EBFS. Overlaid gas chromatograms of both incubations proved the presence of 8-methoxy-*E*-β-farnesene (**263**) (Figure 4.30). In addition to this, the mass spectra of farnesene **263**, generated by ADS and EBFS, are identical in their fragmentation patterns (Figure 4.31).

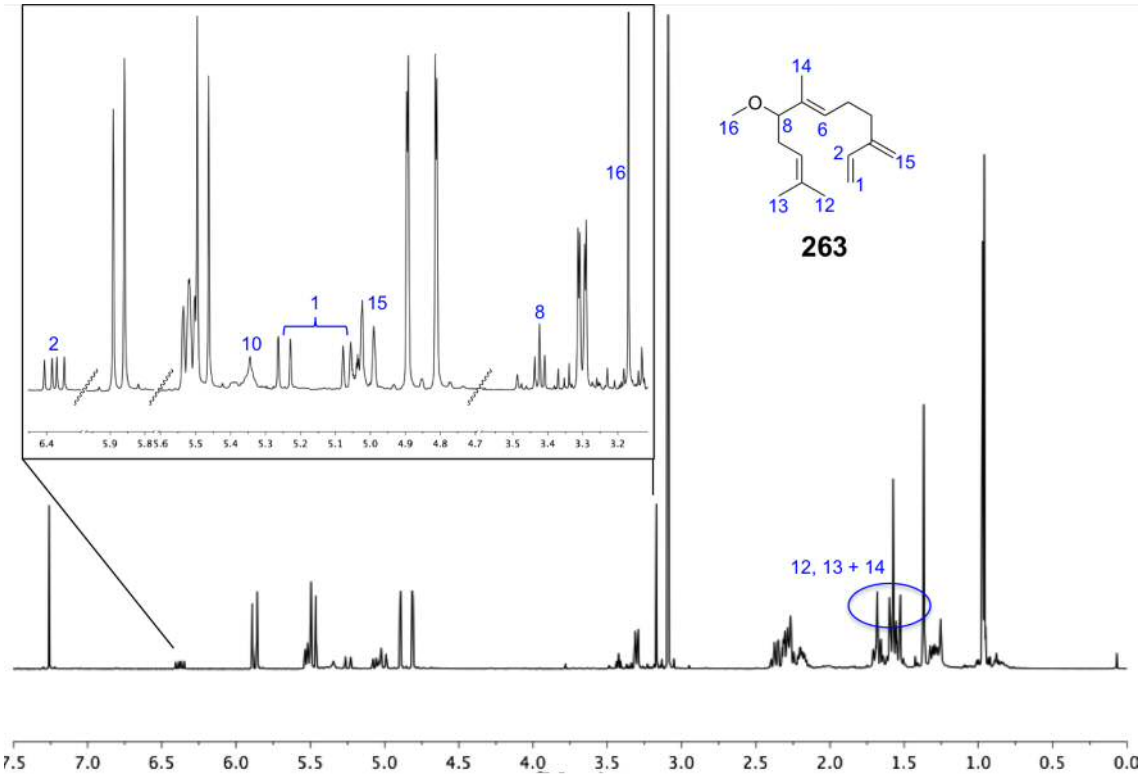

Figure 4.28. ^{1}H NMR spectrum (600 MHz, $CDCl_3$) of the enzymatic products generated from incubation of ADS with 8-methoxy FDP (170). The peaks belonging to the minor product, 8-methoxy-*E*-β-farnesene (263) are shown in blue.

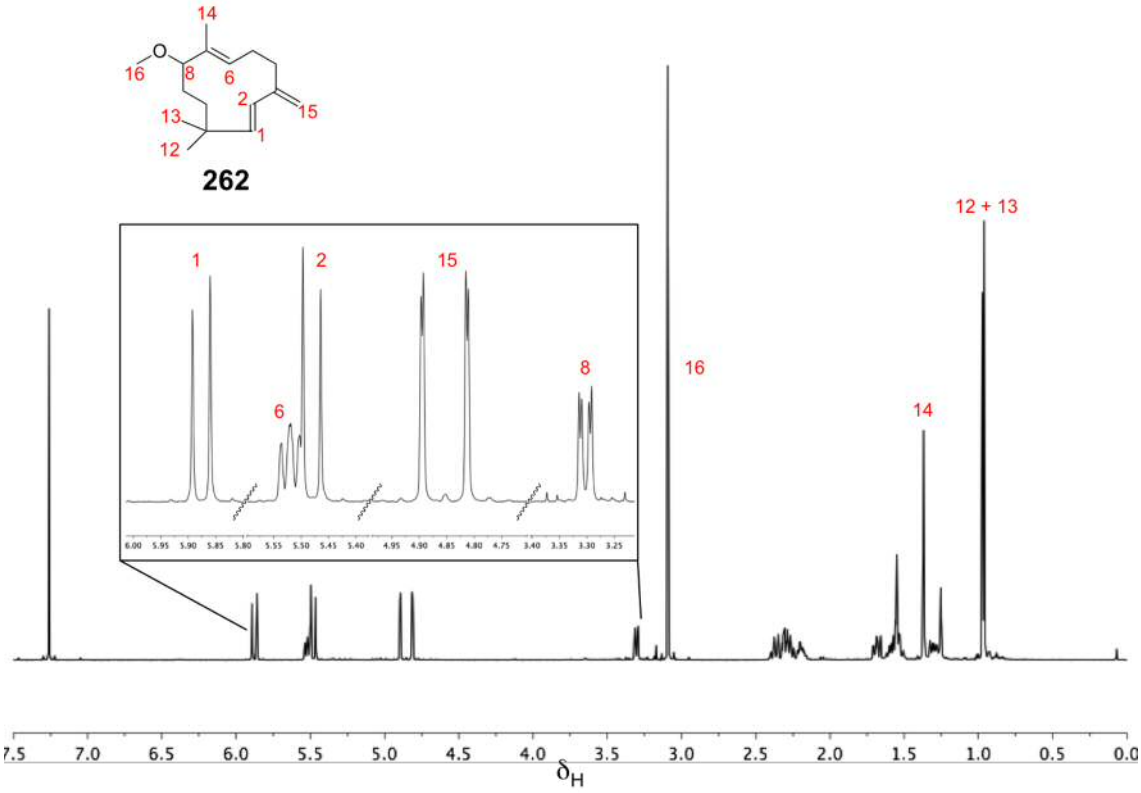

Figure 4.29. ^{1}H NMR spectrum (600 MHz, $CDCl_3$) of the major product, 8-methoxy-γ-humulene (262), generated from incubation of ADS with 8-methoxy FDP (170), with peak assignments in red.

Table 4.1 Complete assignment of 8-methoxy-γ-humulene (262). Chemical shifts are reported relative to TMS in ppm.

Carbon	^{1}H	^{13}C
1	5.48 (d, *J* = 6.0 Hz, 1 H)	129.4
2	5.88 (d, *J* = 6.0 Hz, 1 H)	125.5
3	-	148.8
4	1.25-1.71 (m, 2 H)	36.41
5	1.25-1.71 (m, 2 H)	28.33
6	5.52 (t, *J* = 8.0 Hz, 1 H)	135.9
7	-	143.0
8	3.30 (dd, *J* = 2.5 Hz, 9.0 Hz, 1 H)	90.28
9	1.25-1.71 (m, 2 H)	10.75
10	1.25-1.71 (m, 2 H)	32.78
11	-	41.36
12	0.96 (s, 3 H)	31.33
13	0.97 (s, 3 H)	30.29
14	1.37 (s, 3 H)	18.15
15	4.89 (d, *J* = 2.0 Hz, 1 H), 4.81 (d, *J* = 2.0 Hz, 1 H)	113.5
16	3.10 (s, 3 H)	55.65

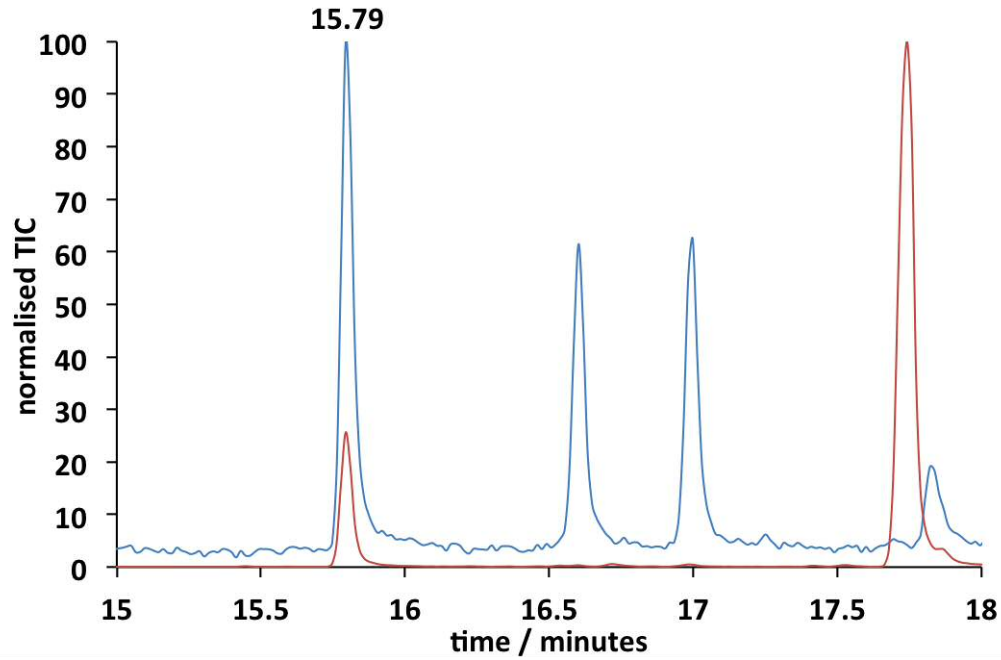

Figure 4.30 Overlaid gas chromatograms of pentane extractable products from an incubation of EBFS (blue) and ADS (red) with 8-methoxy FDP. Both chromatograms show the same compound eluting at 15.79 min.

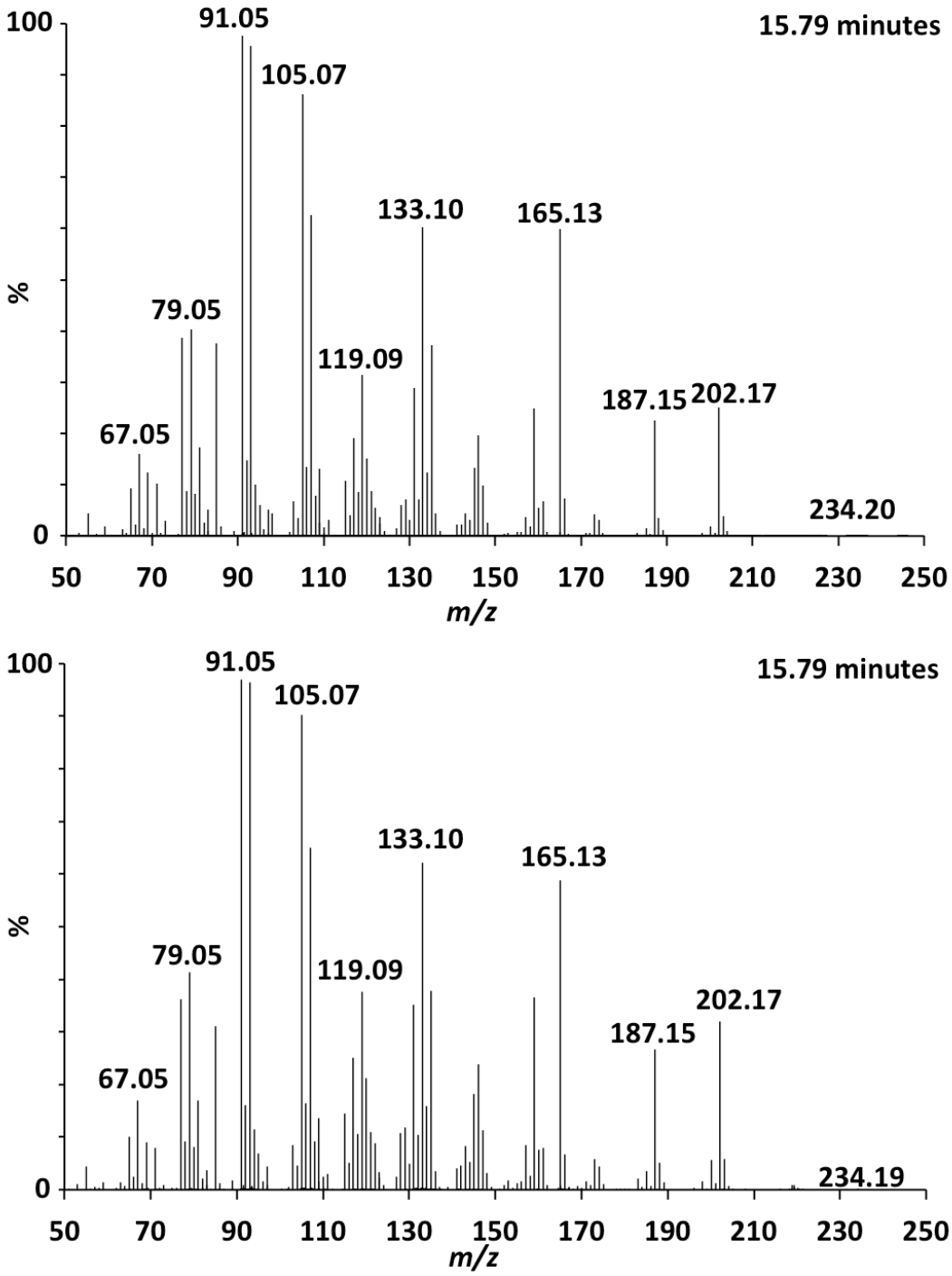

Figure 4.31 Mass spectra of the identified 8-methoxy-E-β-farnesene (263) generated from incubation of ADS (top) and EBFS (bottom) with 8-methoxy FDP.

The exact mechanism by which 8-methoxy-γ-humulene (**262**) and 8-methoxy-*E*-β-farnesene (**263**) are formed is unknown, however a mechanism can be proposed (Scheme 4.12). It is assumed that the nucleophilic oxygen attacks at C10 or C1 in a 1,11- or 1,8-cyclisation, respectively, at a faster rate than the formation of an NDP analogue, which facilitates the more usual 1,6-cyclisation. In the case of a 1,11-

cyclisation of cation **264**, the resulting cation **265** undergoes a [1,3]-hydride shift to form **266**, which is followed by a deprotonation at C15 to afford 8-methoxy-γ-humulene (**262**) (Scheme 4.12 A, blue pathway). For the minor product, once a 1,8-cyclisation takes place to form **267**, a deprotonation at C15 cleaves the 9-membered ring and forms the *E*-β-farnesene derivative, **263** (Scheme 4.12 B, blue pathway).

Alternatively the oxygen might not be involved in the catalysis at all and instead, after the diphosphate is eliminated, a subsequent deprotonation at C15 of **264** forms farnesene **263** (Scheme 4.12 B, red pathway). Similarly, for the formation of the humulene derivative **262**, 8-methoxy FDP might be bound in an orientation in the active site that facilitates the 1,11-cyclisation over the initial 1,6 cyclisation observed for FDP, which generates cation **268**. A [1,3]-hydride shift to cation **266**, followed by subsequent deprotonation at C15 again would allow for the formation of humulene **262** (Scheme 4.12 A, red pathway).

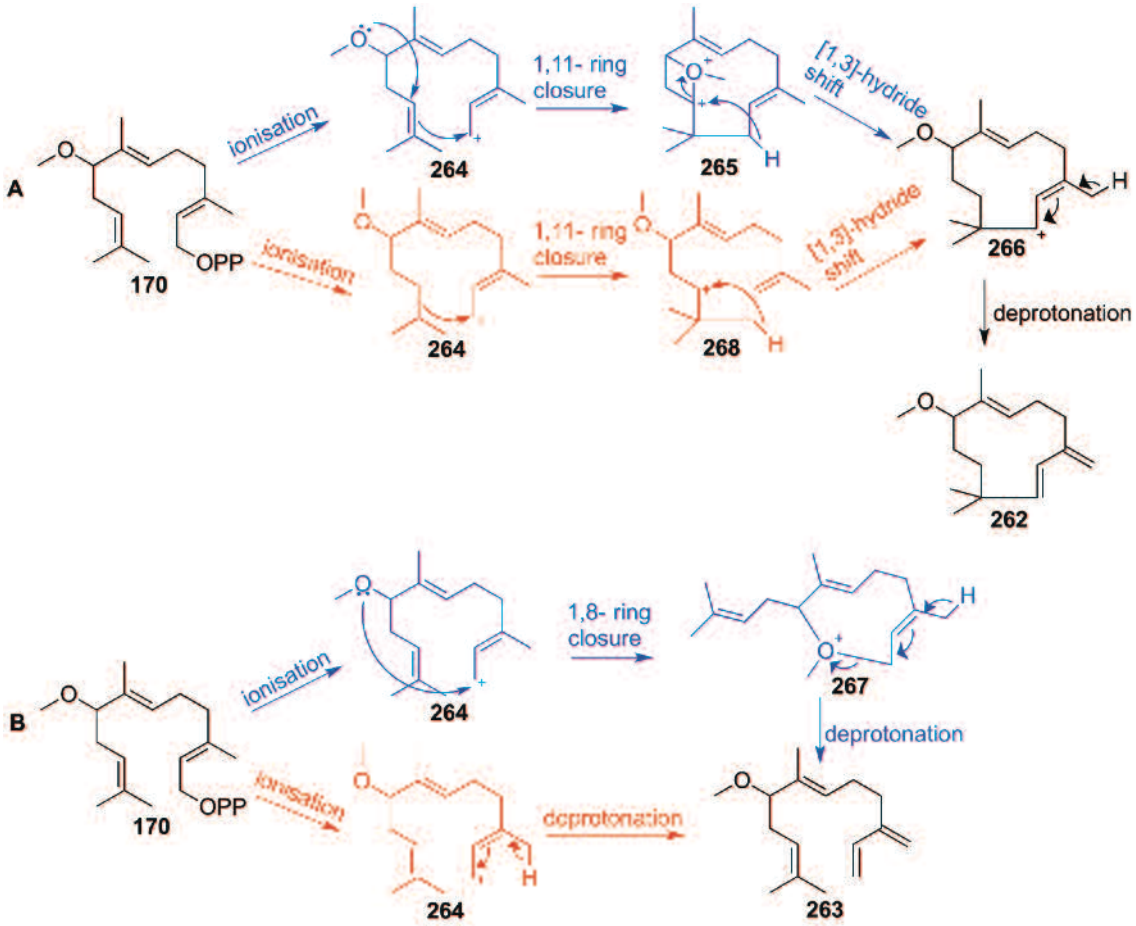

Scheme 4.12 Proposed mechanism for the formation of 8-methoxy-γ-humulene (262) and 8-methoxy-*E*-β-farnesene (263) from incubation of ADS and 8-methoxy FDP (170).

4.3.7 12-Methoxy FDP (171)

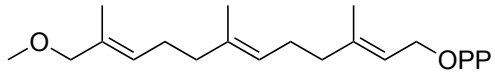

Figure 4.32 12-Methoxy FDP (171)

Incubation of ADS with 12-methoxy FDP (**171**, Figure 4.32) generated two pentane extractable products. Both products had a molecular weight with *m/z* = 234 (Figure 4.33).

The mass spectra for the two products both obtain base peaks at *m/z* = 118, with similar fragmentation patterns. This could imply that unlike 8-methoxy FDP (Section 4.3.6), 12-methoxy FDP is possibly converted into two sesquiterpenoids with the same terpenoid frame. This incubation was carried out on a preparative scale for analysis by NMR spectroscopy.

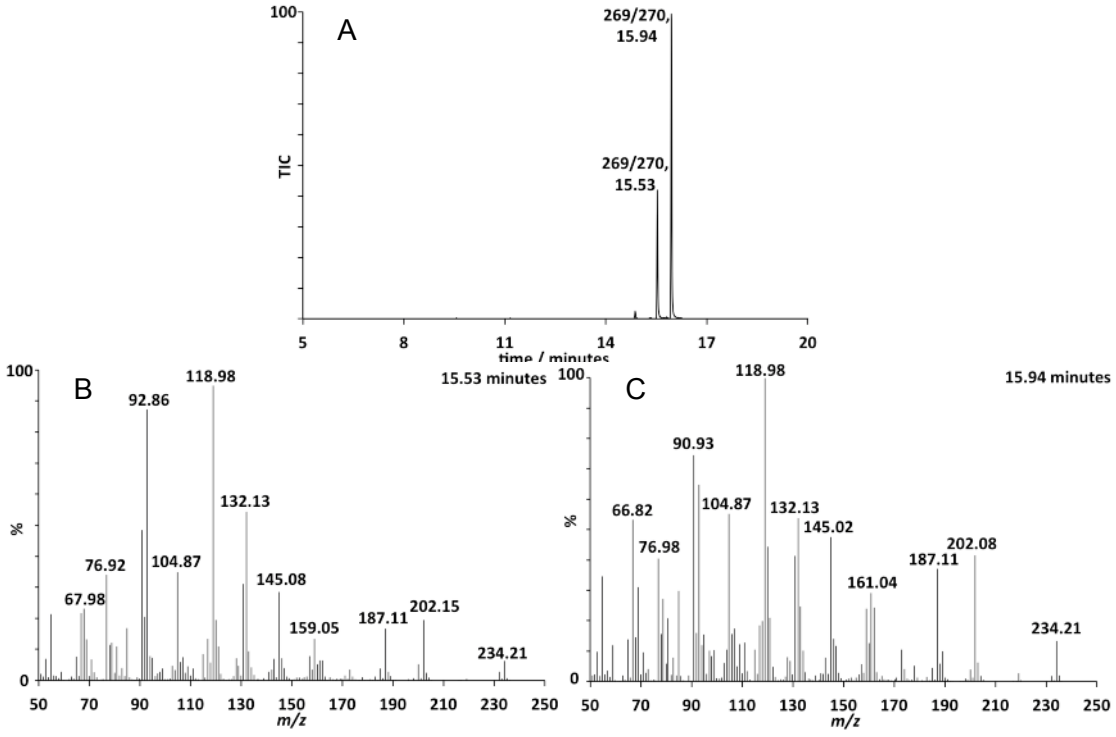

Figure 4.33 A: Total ion chromatogram of the pentane extractable products from incubation of ADS and 12-methoxy FDP (171). B-C: Mass spectra of the eluted compounds.

NMR spectroscopic analysis was carried out on the mixture of products because attempts at separation of the two compounds by chromatography were not successful.

The ^{1}H NMR spectrum (Figure 4.34) of the mixture instantly clarified that the two products produced were not analogues of amorphadiene. This was concluded from the presence of an excessive number of olefinic peaks observed in the region δ_H = 4.7 - 5.2 ppm. Although it was found that the bicyclic hydrocarbon frame had not been made, the pair of doublets found at 0.85 and 0.87 ppm suggested that ADS still carried out a 1,6-ring closure for both enzymatic products as these doublets corresponded to the methyl group at C14 of both compounds. The two singlets observed at δ_H = 3.27 and 3.78 ppm, with integrations of 3 and 2, respectively, have a similar chemical shift to that observed in the ^{1}H NMR spectrum of 12-methoxy FDP (Section 7). These singlets represent C12 and C16. This indicates that both products retain the methoxy group in the same position, and preclude the possibility of a methoxy group migration. The ^{13}C DEPT-135 (Figure 4.34) spectrum contained a negative peak at ~109 ppm, implying the presence of an olefinic CH_2. Through logical elimination of other possible locations, it was concluded that this CH_2 was positioned on C15 and this correlates with the two overlapped doublets observed at δ_H = 4.74 ppm. The integration of these singlets were measured as 2 protons and so that meant that this exocyclic alkene was present in only one of the products. Since one of the olefinic protons in the substrate, 8-methoxy FDP, was left intact in the products it was concluded that ADS catalysed a 1,6 ring closure of this substrate, but did not follow with the second 1,10 ring closure. The triplet found at δ_H = 5.39 ppm with an integration of 2 protons, representing a proton at C10 for each product, is consistent with this theory. By piecing together the assignments made for distinct peaks in both the ^{1}H NMR and ^{13}C NMR spectra, it was concluded that the enzymatic products were 12-methoxy-β-sesquiphellandrene (**269**) and 12-methoxy-zingiberene (**270**). The stereochemistry of the zingiberene is unknown and therefore it can either be a zingiberene or a 7-*epi*-zingiberene derivative. The predicted structures were in agreement with NMR spectra found in literature of β-sesquiphellandrene, zingiberene and 7-epizingiberene.[54,210–212] A proposed mechanism (Scheme 4.13) was predicted to explain the formation of each compound.

It is assumed that the catalysis of 12-methoxy FDP begins in the same manner as the natural substrate FDP. An isomerisation of the FDP analogue to the corresponding NDP analogue **271** allows for the rotation of the terminal alkene bond. Ionisation of this compound forms **272** which subsequently undergoes the initial 1,6 ring closure, seen with FDP, to generate **273**. A [1,3]-hydride shift affords cation **274**. With the natural substrate, FDP, a 1,10-ring closure would follow, however the identification of the monocyclic products proved that this second cyclisation does not follow in this case. There are two suggestions as to why a 1,10-ring cyclisation cannot follow. Either the nucleophilic oxygen attacks at C1 of cation **274** at a faster rate, forming intermediate **275**. Alternatively the methoxy group could just force an orientation of the distal alkyl

group that prevents the second ring closure. Accordingly, deprotonation at C15 (Scheme 4.13, blue pathway) and C4 (Scheme 4.13, red pathway) of either intermediate **274** or **275** allows the formation of 12-methoxy-β-sesquiphellandrene (**269**) and 12-methoxy-zingiberene (**270**).

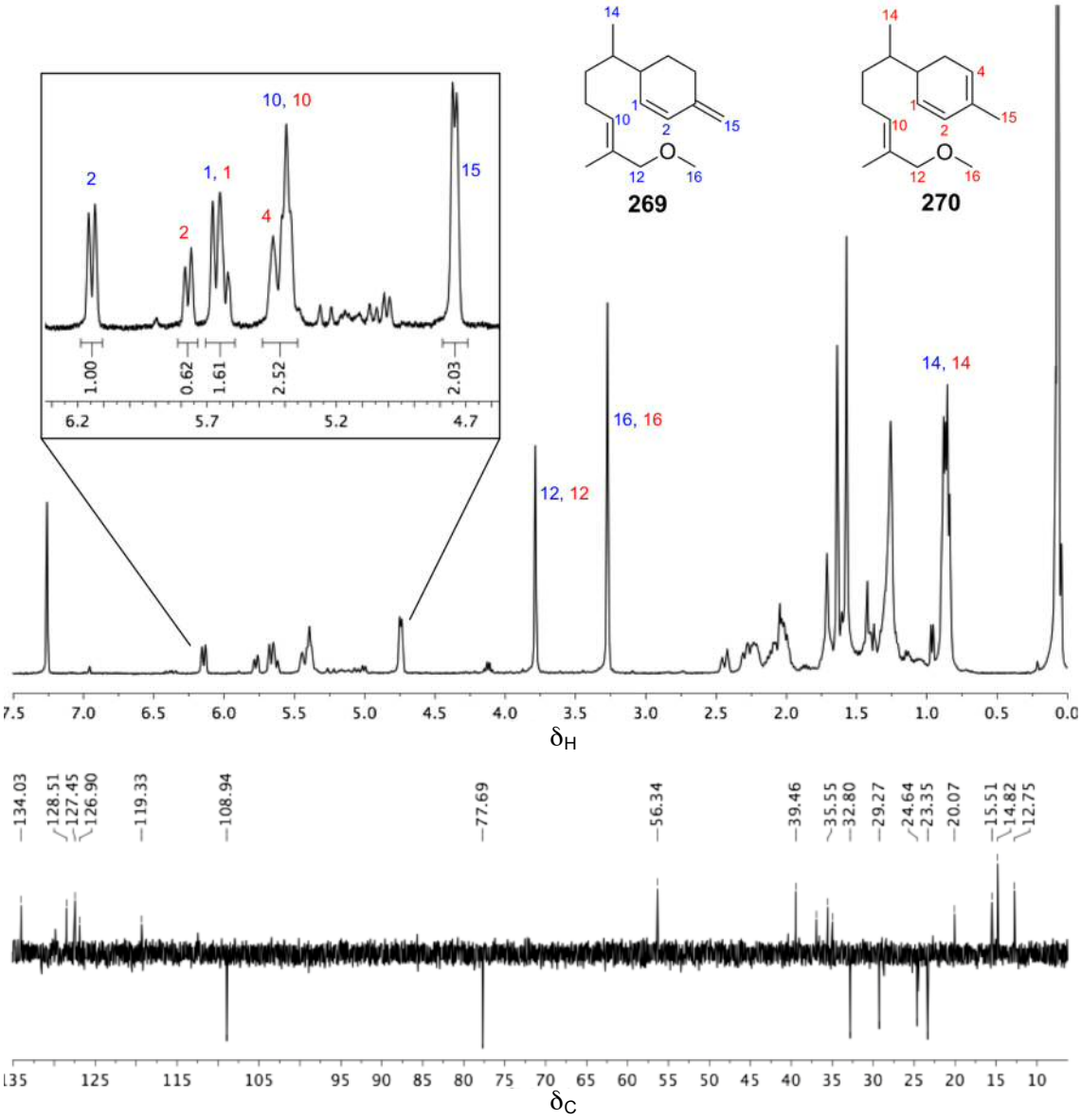

Figure 4.34 ^{1}H NMR (600 Hz, $CDCl_3$) (top) and ^{13}C DEPT-135 NMR (125 Hz, $CDCl_3$) (bottom) of the enzymatic products formed from incubation of ADS with 12-methoxy FDP (171).

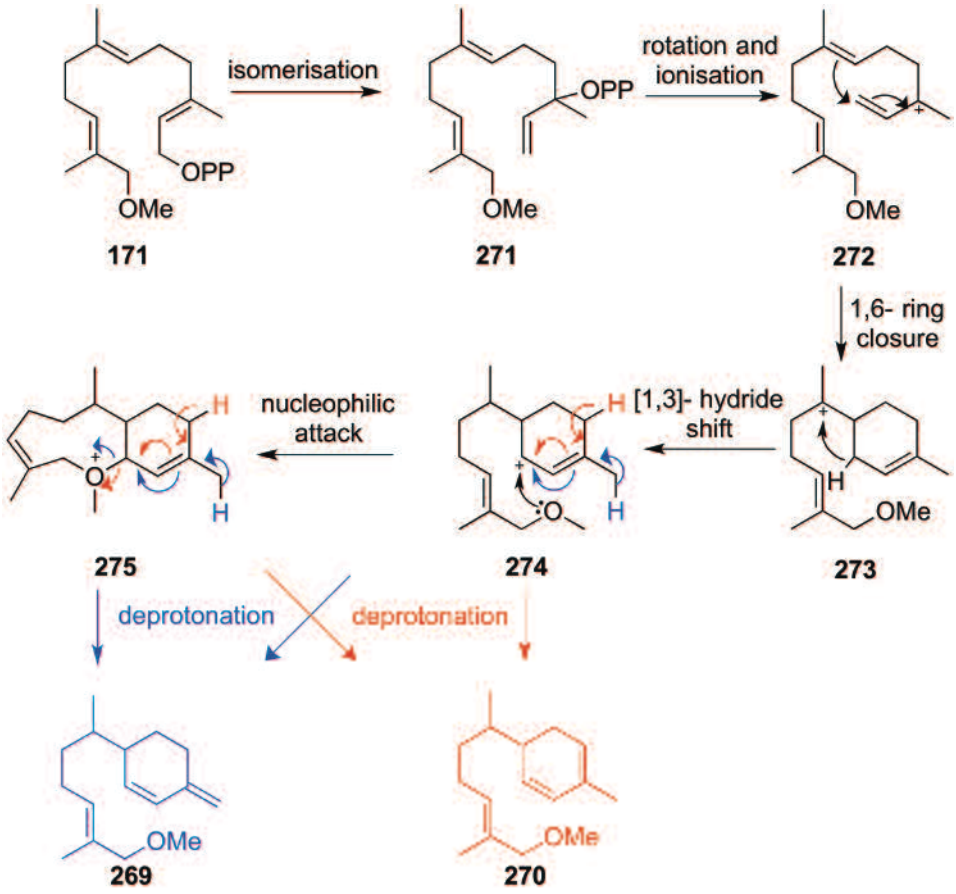

Scheme 4.13 Proposed mechanism for the formation of 12-methoxy-β-sesquiphellandrene (269) and 12-methoxy-zingiberene (270) from incubation of ADS and 12-methoxy FDP (171).

4.4 Nitrogen containing FDP analogues

4.4.1 12-Acetamido FDP (184)

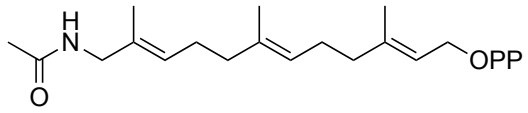

Figure 4.35 12-Acetamido FDP (184).

12-acetamido FDP (**184**, Figure 4.35) was designed in attempt to generate a nitrogen containing amorphadiene. With a similar structure to 12-acetoxy FDP it was thought that if the enzyme treated 12-acetamide FDP in a similar manner to 12-acetoxy FDP, it might convert the substrate into an aza-analogue of dihydroartemisinic aldehyde (**276**, Figure 4.36).

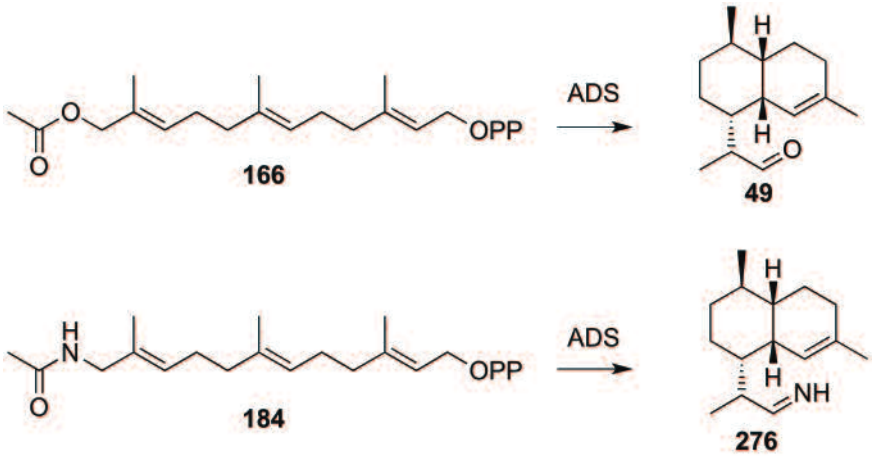

Figure 4.36 Top: Enzymatic conversion of 12-acetoxy FDP (166) with ADS. Bottom: Predicted enzymatic conversion of 12-acetamido FDP (184) with ADS.

Incubation of ADS with 12-acetamido FDP generated no pentane extractable products, with nothing visible by GC-MS analysis. It is proposed that due to the similar sizes of both 12-acetamide FDP and 12-acetoxy FDP, analogue **184** is still capable of entering the active site of ADS, but instead of acting as a substrate it behaves as an inhibitor. This could be demonstrated in future work by carrying out inhibition studies using 12-acetamide FDP with ADS and tritiated FDP.[207] Alternatively the analogue could be a suicide substrate. 12-acetamide FDP could enter the active site and form a covalent bond with a residue in the enzyme and block its activity.[213] This has been previously reported for aristolochene synthase, where a vinyl analogue of FDP was found to be an effective mechanism-based inactivator of the enzyme.[214] The last possibility would be that the analogue does not enter the active site at all, either because it does not fit, which would support the idea discussed earlier (Section 4.3.2) of 12-acetoxy FDP being de-acetylated before it enters the active site, or because the nitrogen reacts with an amino acid outside of the active site, preventing it from entering.

4.4.2 12-Amino FDP (185)

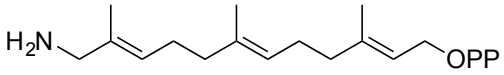

Figure 4.37 12-Amino FDP (185)

After observing an absence of products from an incubation of ADS with 12-acetamido FDP (**184**), 12-amino FDP (**185**, Figure 4.37) was synthesised. This compound was not

an ADS substrate either, with nothing visible in the pentane extractable products as judged by GC-MS. Initially it was thought that pH 8, which is the pH that the incubations were carried out in, was too low for this specific analogue. The pKa of a protonated amine is between 10 and 11 and therefore the substrate in the normal incubation buffer would exist in the protonated form. This could prevent the enzyme accepting it as a substrate due to the positive charge on the nitrogen and therefore the incubation was repeated at pH values of 9, 10, 11, and 12. Unfortunately no product was observed at any of those pH values either. The structure of the enzyme was studied by CD spectroscopy (Section 2.6.3) to examine whether the protein was still folded in the characteristic α-helical form when ADS was exposed to a high pH value. The stability profile for ADS was monitored over 20 minutes, measuring CD spectra every 10 minutes. It was clearly observed that the α-helical structure of ADS was unfolded at pH 12 due to the lack of minima at 208 and 220 nm (Figure 4.38).

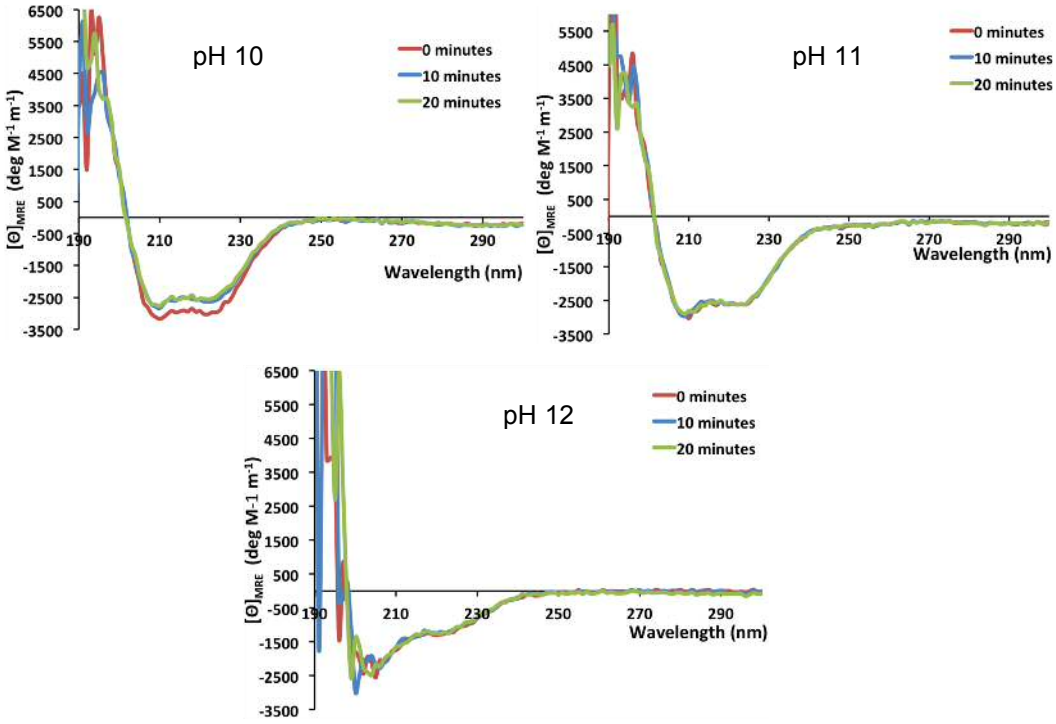

Figure 4.38 CD spectra of ADS at different pH values (pH 10-12). Spectra were recorded at 0, 10 and 20-minute intervals.

4.5 Summary

To conclude, ADS was incubated with a variety of FDP analogues to test the extent of the enzymes promiscuity. Each analogue incubated with ADS proved to be a substrate of the enzyme, except for the aza-FDP derivatives, 12-acetamido FDP (**184**) and 12-amino FDP (**185**). 14-Methyl FDP (**130**) was transformed into one enzymatic product

that gave sufficient evidence *via* NMR spectroscopic and GCMS analysis to be identified as an amorphadiene analogue. Interestingly, 12-acetoxy (**166**) and 12-hydroxy FDP (**168**) were converted by ADS into the same products, generating two epimers of dihydroartemisinic aldehyde (**49**). The methoxylated analogues, 8-methoxy FDP (**170**) and 12-methoxy FDP (**171**) were catalysed by ADS through a different mechanism to the natural substrate, FDP. These analogues, combined, generated derivatives of a farnesene, humulene, zingiberene and sesquiphellandrene. These results demonstrate that ADS can be defined as promiscuous and has the capability of accepting substrates with additional functional groups in various locations.

Chapter 5. Three-step formal chemoenzymatic total synthesis of dihydroartemisinic aldehyde

5.1 Preface

Artemisinin (**6**) and its derivatives in combination therapy are the world's number one treatment against malaria, but with resistance arising, methodology for producing novel and active analogues is a constant need. In addition to this, there is also a requirement to find an alternative method to source artemisinin, to combat the unreliable and fluctuating methods that are present today.[215] Here is presented a 3-step synthesis to dihydroartemisinic aldehyde (**49**), a precursor of artemisinin, starting from farnesyl chloride (**127**). Optimised conditions were developed for preparation of 12-hydroxy FDP (**168**), and for the conversion of this FDP analogue with ADS. The results demonstrate a highly efficient route to dihydroartemisinic aldehyde (**49**), bypassing several of the chemical steps previously required for artemisinin synthesis.

Previously, in Section 1, the various methods for sourcing artemisinin were discussed. To our knowledge, there are three main approaches to supplying artemisinin and its analogues; extracting the compound from the dry plant material,[129–132] total synthesis of the compound[135,136] and a combination of a biosynthetic and synthetic route that exploits the use of important biocatalysts to create the complex, chiral scaffold of the immediate precursor, dihydroartemisinic acid (**50**) (Section 1.3.3).[137–141] With the high demand for artemisinin, other routes to production remain active lines of research. Here it is reported how a biosynthetic approach can also be employed using a recombinant ADS *in vitro* to produce artemisinin precursors. In contrast to *in vivo* production using a full biosynthetic pathway, carrying out *in vitro* incubations gives the advantage of employing substrate analogues that may be converted by the enzyme to, ultimately, artemisinin analogues that may have improved efficacy over current treatments.

When using an *in vitro* biosynthetic approach, with the use of ADS, FDP is converted into amorphadiene, and then is further converted to artemisinin through a series of chemical steps (Scheme 5.1). The series of chemical steps, that have been previously reported by other research groups, begin with a selective hydroboration of the external double bond using 9-BBN or wilkinsons catalyst. The resulting dihydroartemisinic alcohol (**277**) can then be further oxidised to the corresponding dihydroartemisinic aldehyde (**49**) by using SO_3-pyridine complex. Finally, this is followed by treatment of the aldehyde with the oxidant $NaClO_2$ in DMSO to form dihydroartemisinic acid (**50**).[137] Once the acid is formed, the continuation of the pathway can involve the same procedures as described in Section 1.3.3 when the production of artemisinin *via* the biosynthetic method was discussed.[139] In brief, an esterification of the carboxylic acid moiety of **50** yields the methyl ester derivative, **74** and subsequent treatment with singlet oxygen generates the hydroperoxide moiety on

75. An acid catalysed Hock cleavage of **75** and rearrangement forms artemisinin (**6**) in the presence of triplet oxygen (Section 1.3.3, Scheme 1.11).[139,141]

Using the knowledge that sesquiterpene synthases are capable of accepting novel substrates,[143,148] 12-hydroxy FDP was synthesised (**168**, Scheme 5.1). 12-Hydroxy FDP was constructed with the alcohol group positioned on the ω-carbon, where the first chemical oxidation would take place following formation of amorphadiene in *A. annua*. This created the potential of forming a precursor further down the schematic pathway to the final compound, thus reducing the overall number of steps required to form artemisinin. 12-Hydroxy FDP proved to be a substrate of ADS and the enzymatic products formed were identified as two epimers of dihydroartemisinic aldehyde (11*R*-**49** and 11*S*-**49**, Section 4.3.1) – an advanced precursor in the chemical synthesis of artemisinin. By incubating ADS with 12-hydroxy FDP a reduction in the number of chemical steps required to produce artemisinin was demonstrated (Scheme 5.1).

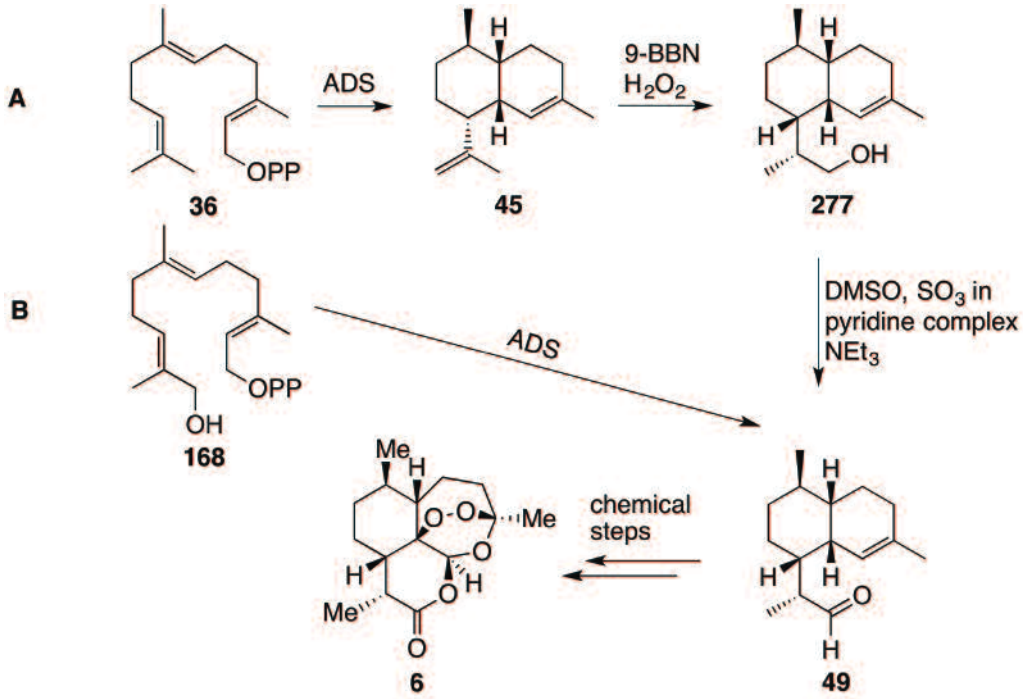

Scheme 5.1 Chemoenzymatic pathway to artemisinin starting with FDP (36, A) and the shortened pathway starting with 12-hydroxy FDP (168, B).

5.2 Optimisation of 12-hydroxy FDP synthesis

To ensure that this new *in vitro* approach to artemisinin production was efficient, every step to make dihydroartemisinic aldehyde (**49**) was optimised to give the shortest and highest yielding pathway. The initial methodology used to prepare 12-hydroxy FDP

consisted of a seven-step synthesis (Section 3.5.2, Scheme 3.9). A new pathway reducing the number of steps to just two was devised (Scheme 5.2).[216,217]

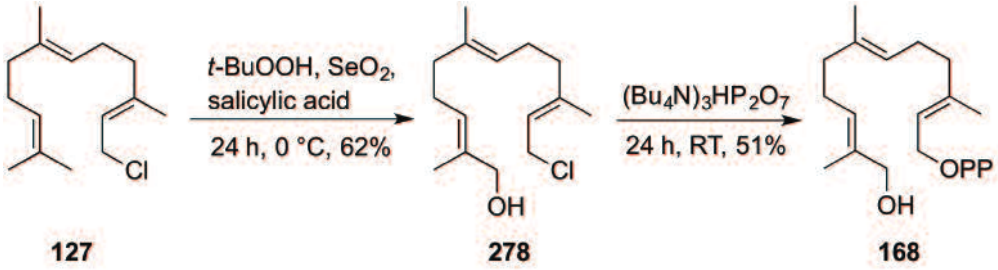

Scheme 5.2 Shortened optimised synthesis of 12-hydroxy FDP (168).

The first step, hydroxylation of the farnesyl chloride chain in the ω-position, was carried out with selenium dioxide and salicylic acid, and various reaction condition parameters were varied to obtain an optimal yield. Our results showed that controlling the molar equivalents of reagents used gave the biggest improvement in yields (Table 5.1). Using between 0.3 and 0.5 molar equivalents of both selenium dioxide and salicylic acid gave 12-hydroxy farnesyl chloride (**278**) in the best yield of 62%. Reducing the equivalents of oxidant gave insufficient turnover of the starting material farnesyl chloride (**127**, Scheme 5.2), whereas anything above 0.5 molar equivalents produced more of the corresponding over-oxidized aldehyde.

Table 5.1 Optimisation of conditions for the preparation of 12-hydroxy farnesyl chloride (278).

Entry	Molar equivalents			Yield (%)
	SeO_2	H^+	*t*-BuOOH	
1	0.1	0.1	5	47
2	0.2	0.2	5	53
3	0.3	0.3	5	62
4	0.5	0.5	5	57
5	1	1	5	8

The diphosphorylation of 12-hydroxy farnesyl chloride was carried out with tris(tetrabutylammonium) hydrogen diphosphate salt (TBDP, **121**) under anhydrous conditions (Table 5.2). Variables changed in this reaction step were molar equivalents of TBDP used and the reaction time. It was found that the use of 2 molar equivalents of TBDP and a reaction time of 48 h gave the best results. An average yield of 32% was obtained over the two steps.

Table 5.2 Optimisation of conditions for the preparation of 12-hydroxy FDP (168).

Entry	TBDP (molar equivalents)	Time (h)	Yield (%)
1	1.5	24	34
2	2	24	47
3	2	48	51

5.3 Optimisation for the catalytic conversion 12-hydroxy FDP to dihydroartemisinic aldehyde

Once the synthesis of the novel analogue, 12-hydroxy FDP was improved, the optimisation of the catalytic turnover of 12-hydroxy FDP to dihydroartemisinic aldehyde had to be accomplished. To obtain the optimal conditions for the catalytic turnover, analytical incubations of 12-hydroxy FDP with ADS at different substrate concentrations and with different organic solvents, overlaid for product extraction, were carried out (Table 5.3).

Table 5.3 Analytical incubations of 12-hydroxy FDP (168) with ADS.

Entry	**168** (μM)	Solvent overlay	Conversion (%)		Second extraction	
			calibration curve	internal standard	Solvent	Conversion (%)
1	100	Pentane	65.4	67.0	Pentane	4.3
2	200	Pentane	63.7	63.6	Pentane	1.9
3	300	Pentane	65.1	67.6	-	-
4	400	Pentane	62.0	59.3	-	-
5	200	Pentane	62.8	66.5	EtOAc	2.8
6	200	Pentane	71.9	73.3	DCM	4.6
7	200	EtOAc	15.1	17.9	-	-
8	200	DCM	10.1	10.3	-	-
9	200	No overlay	-		EtOAc	19.6
10	200	No overlay	-		DCM	21.6

The optimal enzyme concentration for substrate turnover was previosuly determined as 1 μM. This was determined by incubating ADS (between 1 to 20 μM) with FDP (400 μM). These incubations were overlaid with pentane and left for 24 h. Gas chromatography with flame ionisation detection (GC-FID) was used to measure the

product formation of amorphadiene in the solvent overlays and the enzymatic conversion was calculated by using an internal standard, commercially available α-humulene (Table 5.4 and Figure 5.1). It was assumed that the optimal enzyme concentration to give the maximum yield of amorphadiene would also apply when using novel FDP analogues. Therefore this parameter was not changed.

Table 5.4 Conversion (%) of FDP (36) to amorphadiene (45) with varying concentrations of ADS.

ADS (μM)	FDP (μM)	Conversion (%)
1	400	47.4
2	400	44.0
3	400	36.2
4	400	37.5
6	400	33.5
9	400	32.1
12	400	30.8
15	400	24.2
20	400	22.5

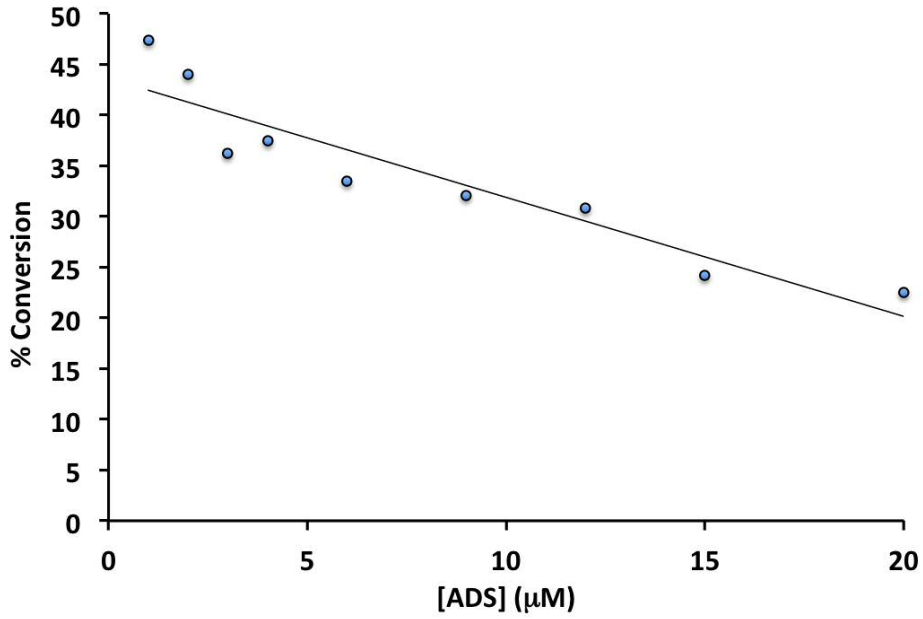

Figure 5.1 Conversion (%) of FDP (36) to amorphadiene (45) with varying concentrations of ADS.

The conversions of 12-hydroxy FDP to dihydroartemisinic aldehyde were also measured using GC-FID to analyse the solvent overlays. All incubations with ADS and

the novel analogue were carried out in parallel to identical incubations of ADS with the natural substrate, FDP, to compare the reaction efficiency.

All conversions were measured using calibration curves calculated with an analytical standard. Farnesal (**279**) was used as the standard for measuring the conversion of 12-hydroxy FDP to dihydroartemisinic aldehyde. FID response was recorded for concentrations of farnesal in the range 10 μM to 4 mM. Farnesal was synthesised from commercially available farnesol (**126**) with the use of manganese dioxide with a yield of 70% (Section 7.2.16). Farnesal was chosen as it has the same molecular weight and chemical formula as dihydroartemisinic aldehyde, hence likely to give a similar response in the flame ionization detector. The conversions of 12-hydroxy FDP to dihydroartemisinic aldehyde were measured using the calibration curve (Figure 5.2). For the analytical incubations, in addition to the calibration curve, farnesal was also used as an internal standard. The results using both internal and external standards were complementary, with a maximum discrepancy of ca. 4%. Similarily, to measure the conversions of the natural substrate FDP to amorphadiene, commercially available α-humulene was used as a standard, with concentrations also ranging from 10 μM to 4 mM (Figure 5.2). This was also used as an internal and external standard for the analytical incubations, also providing consistent results.

The results from analytical incubations showed that varying substrate concentration between 100 μM and 400 μM for both 12-hydroxy FDP and FDP showed no increase in the conversion rates. No tests were carried out using in excess of 400 μM substrate as concentrations higher than this have been observed previously to cause FDP precipitation.[171,218] The change in the solvent for the overlay of the incubations however was important. Pentane was found to be the most efficient at extracting the products (Table 5.3). The majority of the enzymatic products were extracted from the initial overlay, and less than 1% further material was present in the third extraction. The optimal incubation time was 24 h, with no improvement observed with extended incubations. Once the most favourable conditions on an analytical scale were found, they were repeated on larger scales consisting of 50 mg of substrate and 200 mg of substrate, to examine robustness and reproducibility.

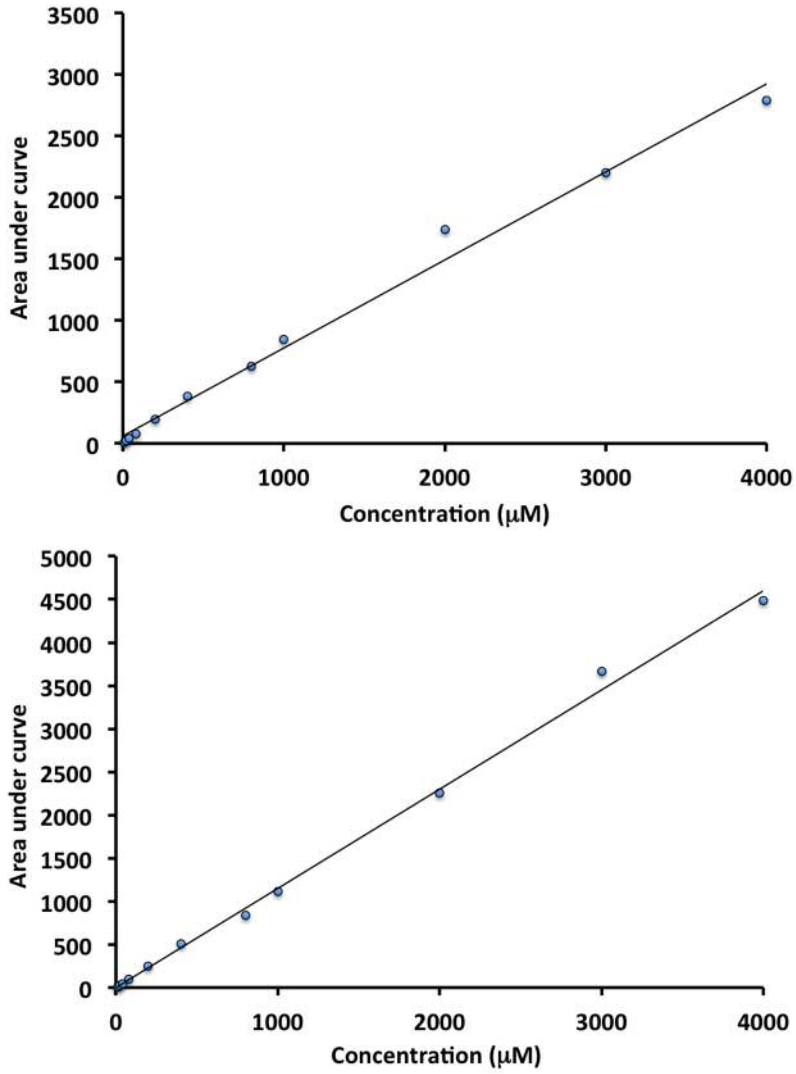

Figure 5.2 Calibration curves showing FID response for various concentrations of farnesal (top) and α-humulene (bottom).

The highest conversion rates obtained for 12-hydroxy FDP, when using the analytical incubations, were in the range 60 to 70%. When the same conditions were used for the incubation of the natural substrate, FDP, an average of 71% conversion was recorded. It was clear that the enzyme could convert, reproducibly, both the natural and unnatural substrate to a similar extent within a 24 h period. On a 50 mg scale, the conversion of 12-hydroxy FDP was still comparable to that of FDP, providing conversions of 77% and 79% respectively. Reproducing this yield on a 200 mg scale required an additional day of incubation. As the mass of substrate increased, so did the buffer volume, decreasing the ratio of extraction solvent overlay relative to the buffer. A typical 200 mg incubation contained 500 mL of buffer and was overlaid with only 20 mL of pentane. The method of extraction was less efficient, in contrast to the analytical 250 μL buffers overlaid with 1 mL of pentane. The increased relative quantity of buffer posed a problem as the

dihydroartemisinic aldehyde tautomerizes with the corresponding enol which is more soluble in the neutral aqueous buffer. To tackle this issue an additional night of incubation was performed with the pH adjusted to 10. In basic conditions, the equilibrium shifted to favour the aldehyde and therefore increased the percentage of product extracted by the pentane. There was a clear increase, where the conversion rate increased from 53 to 65% when pH was increased (Figure 5.3). The isolated yield for the mixture of epimers (11*R*-**49** and 11*S*-**49**) was recorded as 35% after purification was carried out by flash chromatography on silica gel (9:1, hexane: ethyl acetate).

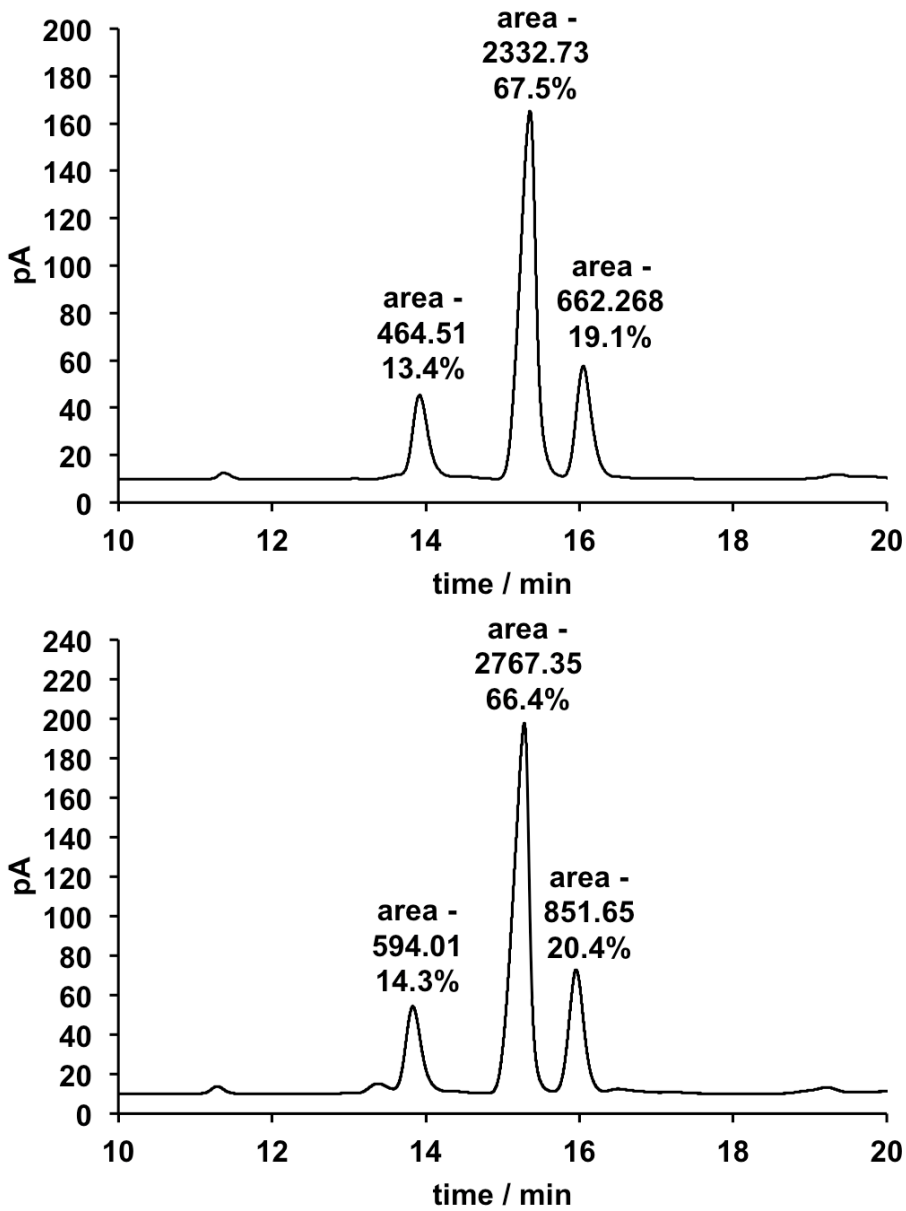

Figure 5.3 Gas chromatograms (FID) of pentane extractable products generated from incubations of ADS with 12-hydroxy FDP after 24 h at pH 7.5 (top) and after an additional 24 h at pH 10 (bottom).

5.4 Organic synthesis of (11*R*)-dihydroartemisinic aldehyde (49)

With the knowledge that only the (*R)*-epimer (11*R*-**49**) is the desired precursor to artemisinin,[114,162] a standard of (11*R*)-dihydroartemisinic aldehyde was synthesised to confirm which epimer was the dominant product from enzymatic incubations of ADS with 12-hydroxy FDP. (11*R*)-Dihydroartemisinic aldehyde was synthesised from commercially available (11*R*)-dihydroartemisinic acid (**50**) *via* two steps (Scheme 5.3). The first step was an esterification of the acid moiety of **50**.[139] This was carried out via an acyl chloride intermediate, which was treated with methanol to afford dihydroartemisinic methyl ester (**88**) with a yield of 78%. DIBAL reduction of the methyl ester **88** afforded the reduced products, dihydroartemisinic aldehyde (**49**) and dihydroartemisinic alcohol (**277**), both with yields of 31%.

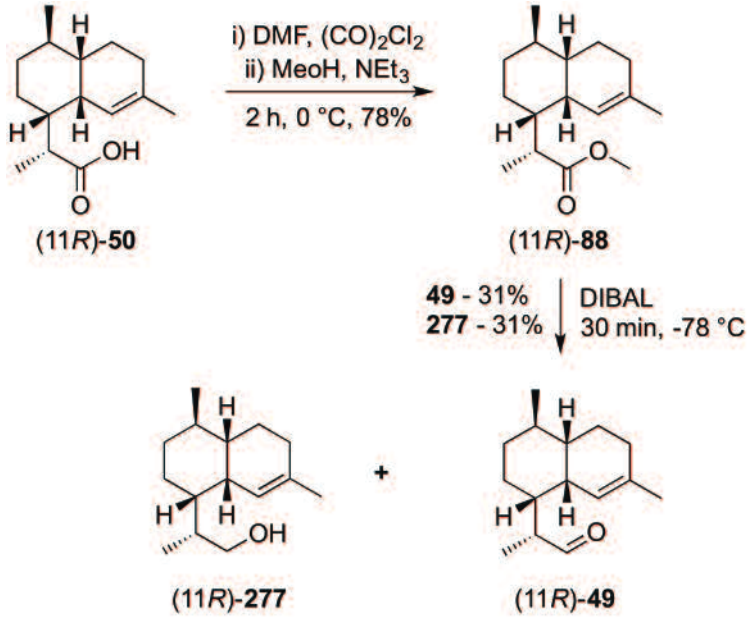

Scheme 5.3 Synthesis of (11*R*)-dihydroartemisinic aldehyde (49).

Overlaid gas chromatograms of the synthesised (11*R*)-dihydroartemisinic aldehyde and the pentane extractable products from an incubation of ADS with 12-hydroxy FDP clearly showed that the (11*R*)-epimer was the minor product (20%) formed by the enzymatic incubations (Figure 5.4). In addition to this observation, the ^{1}H NMR spectrum of the authentic sample of (11*R*)-dihydroartemisinic aldehyde displayed a doublet at δ_H = 9.57 ppm, showing that the minor epimer observed in the ^{1}H NMR spectrum of the mixture of epimers from the enzymatic incubation was (11*R*)-dihydroartemisinic aldehyde (Figure 5.5).

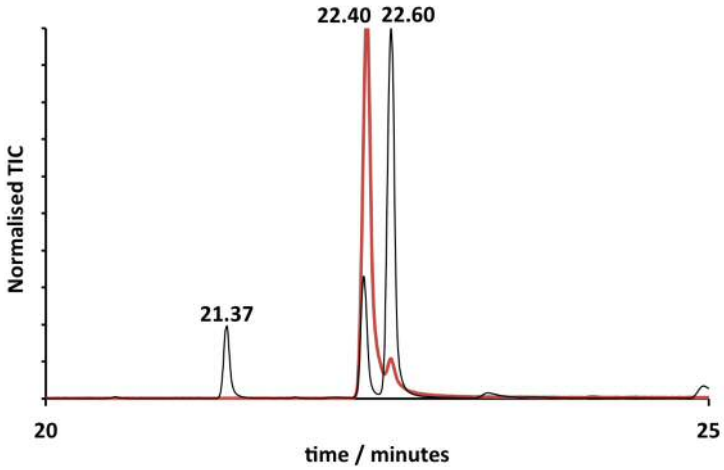

Figure 5.4 Overlaid gas chromatograms of chemically synthesised (11*R*)-dihydroartemisinic aldehyde (red) and pentane extractable products from an incubation of ADS with 12-hydroxy FDP (black).

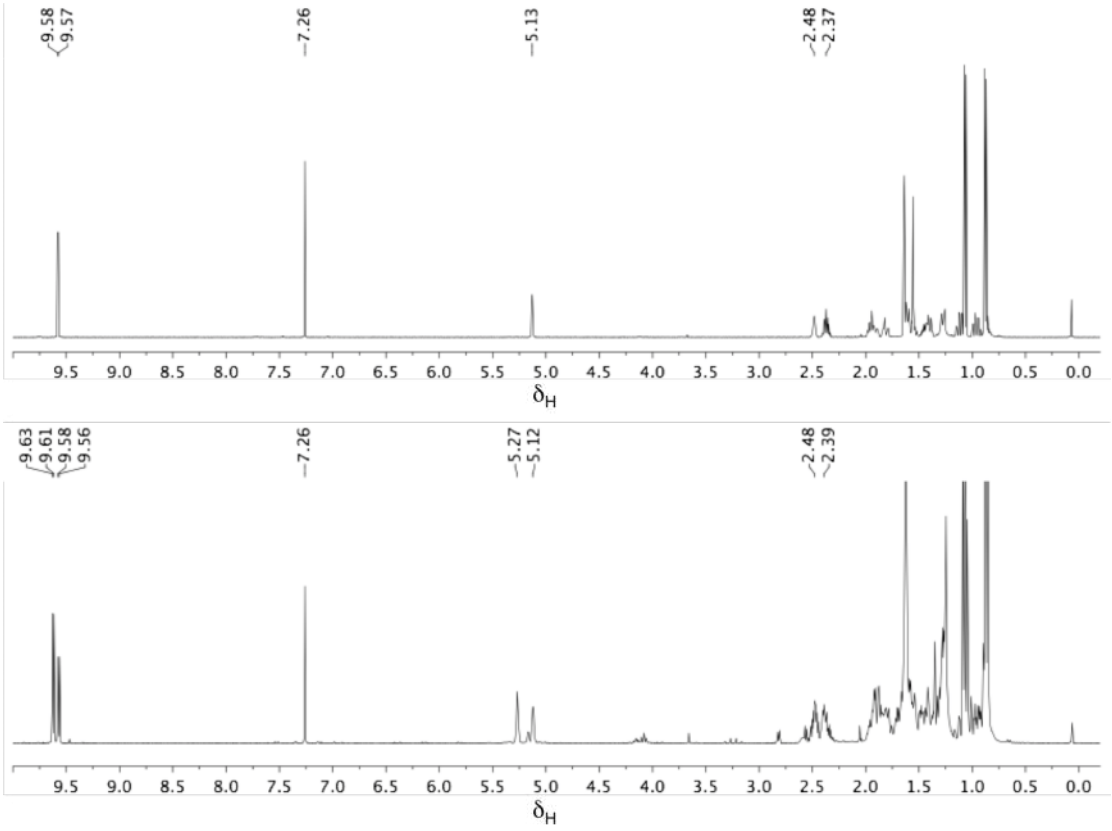

Figure 5.5 ^{1}H NMR spectra (500 MHz, $CDCl_3$) of authentic (11*R*)-dihydroartemisinic aldehyde (top) and the pentane extractable products from incubation of ADS with 12-hydroxy FDP (bottom).

5.5 Conclusions

Here is reported the efficient turnover of a novel FDP analogue, 12-hydroxy FDP, to a 3:2 mixture of dihydroartemisinic aldehydes using ADS. Also reported is a novel efficient synthesis for this substrate from farnesyl chloride. ADS proved to be partially promiscuous with this substrate giving two epimeric aldehydes as products but it is clear that sesquiterpene synthases which naturally produce only hydrocarbon products can be challenged with heteratom substituted substrates, including the nucleophilic (and potentially carbocation quenching) OH group to produce sesquiterpenoid analogues that may be useful for drug discovery or agrochemical purposes. Since a short series of chemical steps is required to convert dihydroartemisinic aldehyde to artemisinin, here is provided an efficient chemoenzymatic strategy for the synthesis of this valuable antimalarial. This strategy may prove useful for the production of further artemisinin analogues with functionality introduced at positions in its skeletal framework that are hard to achieve without extensive total synthesis.

Chapter 6. Conclusions and Future work

6.1 Overview

This project describes the investigation of the promiscuity of amorphadiene synthase. This was accomplished by testing the enzyme with novel FDP analogues. FDP analogues were designed with various functional groups in several positions on the FDP backbone to bring diversity to any resulting terpenoid structures. In addition to synthesising a selection of FDP analogues, and testing these with ADS, mutants of the enzyme were also designed and produced. Mutants of ADS were created to study the effect and contribution of the 'silent' N-terminal domain to the catalytic mechanism and structure of ADS.

ADS proved to be partially promiscuous with the library of analogues synthesised in this research but it is clear that sesquiterpene synthases which naturally produced only hydrocarbon products can be challenged with heteratom substituted substrates including the nucleophilic (and potentially carbocation quenching) OH group to produce potentially useful sesquiterpenoid analogues that may be useful for drug discovery or agrochemical purposes. The advantage of using this approach is that it is easier to decorate a linear isoprenyl diphosphate chain than the cyclic and stereoselective product produced once the diphosphate is incubated with a terpene synthase. This approach can be tested with other classes of terpenes and their respective synthases as it is not only specific to sesquiterpenes.

Since it is only a short set of chemical steps from dihydroartemisinic aldehyde to artemisinin, an efficient chemoenzymatic strategy for the synthesis of this valuable antimalaria is provided. This strategy may prove useful for the production of further artemisinin analogues with functionality introduced at positions in its skeletal framework that are hard to achieve without extensive total synthesis.

6.2 Synthesis of amorphadiene derivatives

Within the library of FDP analogues synthesised in this work, there is sufficient evidence, particularly from ^{1}H NMR spectroscopy, to confirm that 14-methyl FDP (**130**) is converted to the corresponding 14-methyl amorphadiene derivative (**211**) (Section 4.2.3). With the formation of 14-methyl amorphadiene (**211**), future work involves carrying out the remaining chemical steps, using procedures that are already published by Newman and co-workers,[139] and Paddon and co-workers,[137] to produce the corresponding artemisinin derivative, 14-methyl artemisinin (**212**) (Scheme 6.1).

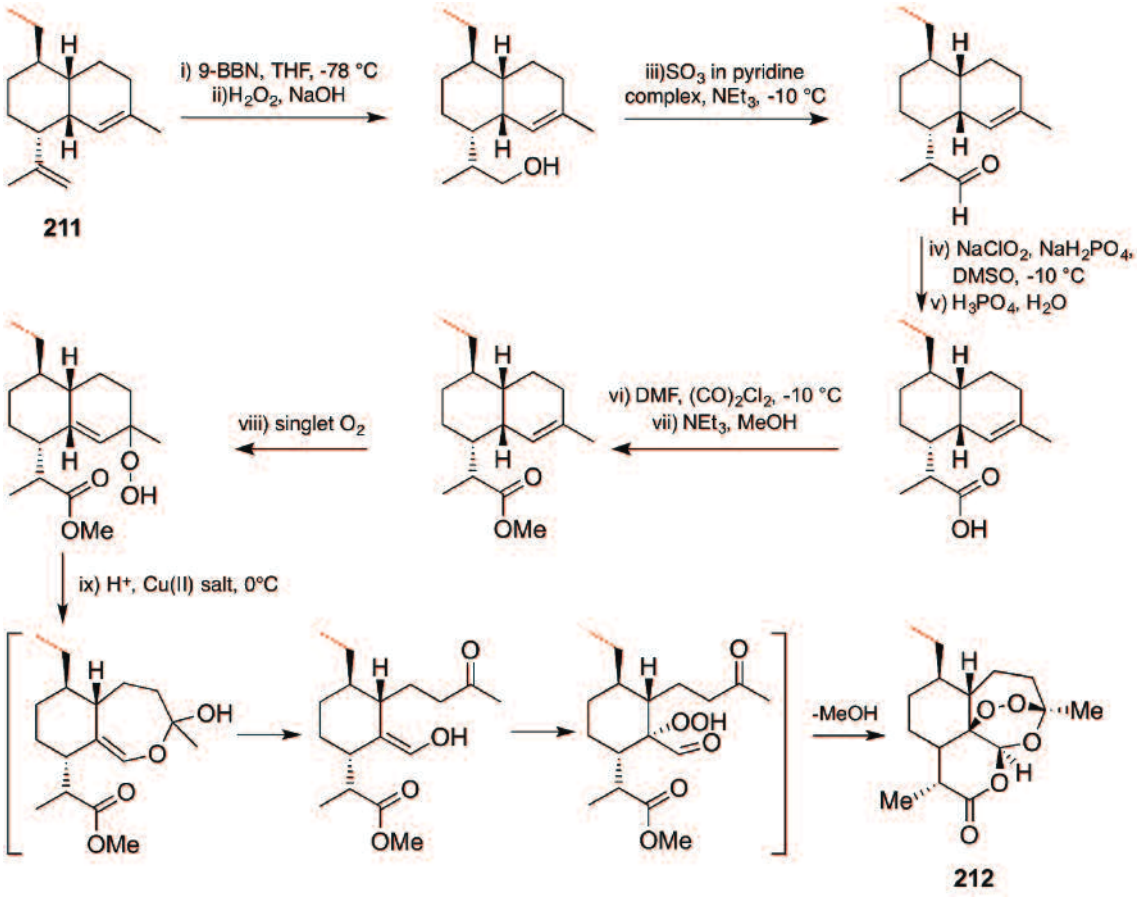

Scheme 6.1 Proposed synthetic pathway to form 14-methyl artemisinin (212) from 14-methyl amorphadiene (211).

In addition to successfully creating an analogue of amorphadiene, this project also included the formation of FDP analogues that proved to be substrates of ADS, forming sesquiterpenoids that do not possess the amorphadiene scaffold. 8-Methoxy FDP (**170**) was transformed into an acyclic sesquiterpenoid, 8-methoxy-*E*-β-farnesene (**263**), as well as an 11-membered monocyclic sesquiterpenoid, 8-methoxy-γ-humulene (**262**) (Section 4.3.6). 12-Methoxy FDP (**171**) was converted to two 6-membered monocyclic sesquiterpenoids, 12-methoxy-β-sesquiphellandrene (**269**) and 12-methoxy zingiberene (**270**) (Section 4.3.7). All four products were characterised by GC-MS and NMR spectroscopy (Figure 6.1). These findings demonstrate that ADS is capable of accepting heteroatom substituted FDP analogues, however due to the additional oxygenated groups, they are converted through different mechanisms, compared to the natural substrate FDP, to produce other novel sesquiterpenoids. The formation of these specific products by ADS was not surprising as Brodelius and co-workers[127] report the formation of γ-humulene (**58**), *E*-β-farnesene (**59**), β-sesquiphellandrene (**63**) and zingiberene (**115**) as minor products resulting from incubation of ADS and FDP. Although these minor products are not observed in this project, the identification of

them reported from another research group shows that the catalysis carried out by ADS is achievable.

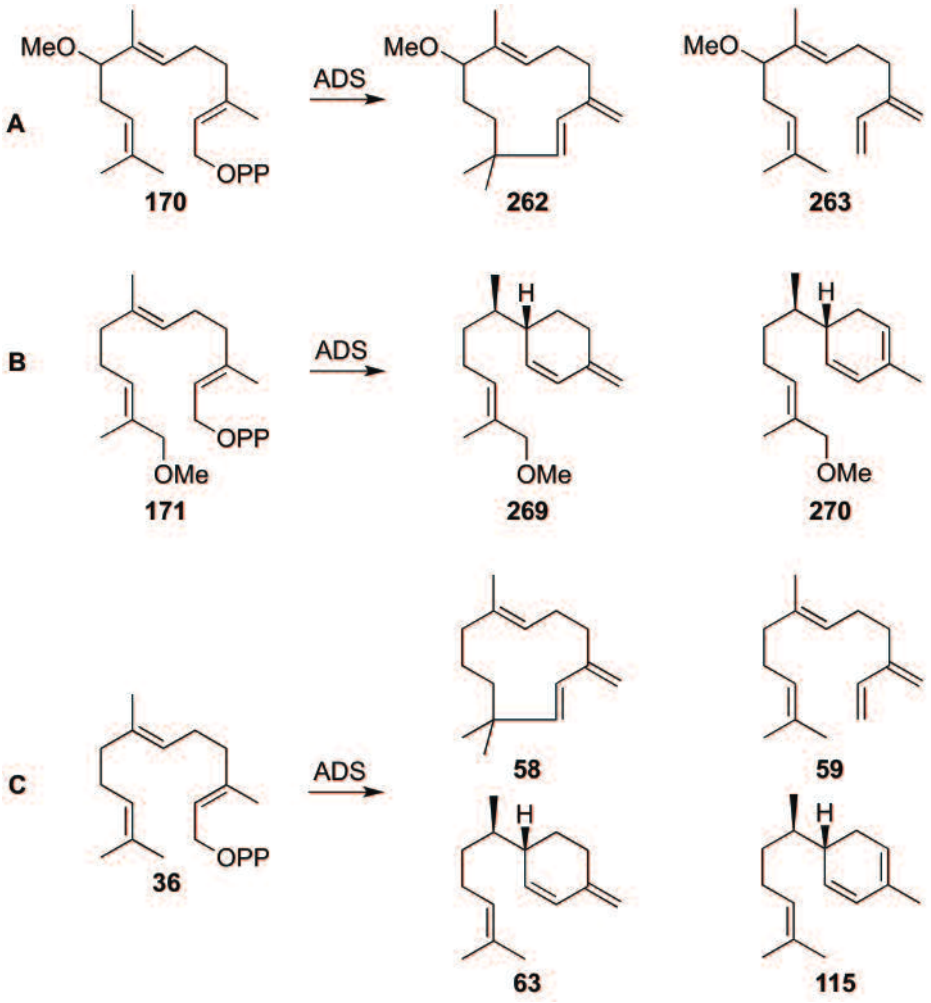

Figure 6.1 Enzymatic products produced from incubations of ADS and 8-methoxy FDP (170, A), 12-methoxy FDP (171, B) and FDP (36, C) reported by Brodelius and co-workers.

6.3 Synthesis of additional FDP analogues

Future work following the completion of this project could involve the synthesis of additional FDP analogues. ADS was capable of catalysing the conversion of 12-acetoxy FDP (**166**) and 12-hydroxy FDP (**168**), into dihydroartemisinic aldehyde (**49**), which was very valuable as it provides the shortest pathway to date for artemisinin (**6**) (Section 5, Scheme 5.1). The mechanism by which ADS converts 12-acetoxy FDP (**166**) and 12-hydroxy FDP (**168**) into the same product is still unclear. Two FDP analogues that could help better understand what happens to the acetoxyl moiety could be 12-formyl FDP (**280**) and [17-^{13}C]-12-acetoxy FDP (**281**) (Figure 6.2). By incubating 12-formyl FDP with ADS, it can be observed whether ADS can form the

same product as 12-acetoxy FDP and 12-hydroxy FDP by removing the formyl moiety. If de-formylation occurs, there will be greater evidence to suggest that the enzymatic catalysis is responsible for removing the acetoxyl/formyl moieties.

The use of ^{13}C labelling on the acetyl group (C17) of 12-acetoxy FDP enables the use of ^{13}C NMR spectroscopy to identify whether ADS de-acetylates the acetyl group before the enzymatic catalysis begins or whether an acyl-enzyme derivative is formed. In addition to the NMR spectroscopy technique, liquid chromatography-mass spectrometry (LCMS) can also be used to detect an increase in the molecular weight of the enzyme. If the enzyme gets acetylated during the formation of dihydroartemisinic aldehyde, then this increase can be observed by LCMS.

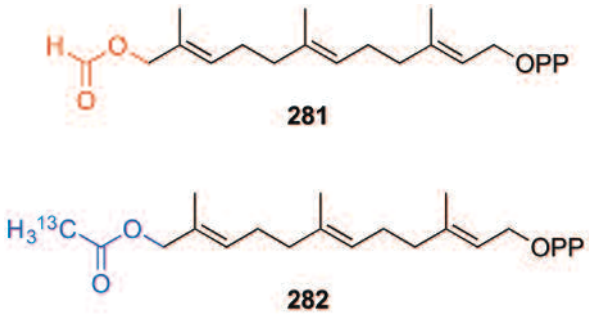

Figure 6.2 12-Formyl FDP (281) and ([17-^{13}C]-12-acetoxy FDP) (282)

To further exploit this promiscuity of ADS, the synthesis of a second-generation analogue, defined by the addition of two functional groups onto the FDP skeleton, is something to consider in additional work stemming from this project. The preferred second-generation analogue requires the hydroxyl group on C12, in addition to a second group, such as methyl, attached elsewhere. 14-Methyl FDP (Section 4.2) proved to transform into enzymatic products through the same mechanism as the natural substrate FDP, and therefore it was predicted that 'methylated' 12-hydroxy FDP analogues have the biggest probability of converting to derivatives of dihydroartemisinic aldehyde through ADS mediated catalysis. The synthesis of '8-methyl-12-hydroxy FDP' (**282**, Scheme 6.2) was attempted but was not completed by the end of this project. It is proposed that this analogue has the potential of being converted to '8-methyl' dihydroartemisinic aldehyde (**283**, Scheme 6.3). The formation of this analogue, coupled with published synthetic steps from (11*R*)-dihyroartemisinic aldehyde to artemisinin, combines the two objectives of this project; to successfully synthesise an artemisinin derivative and to find an efficient and alternative method to supply artemisinin.

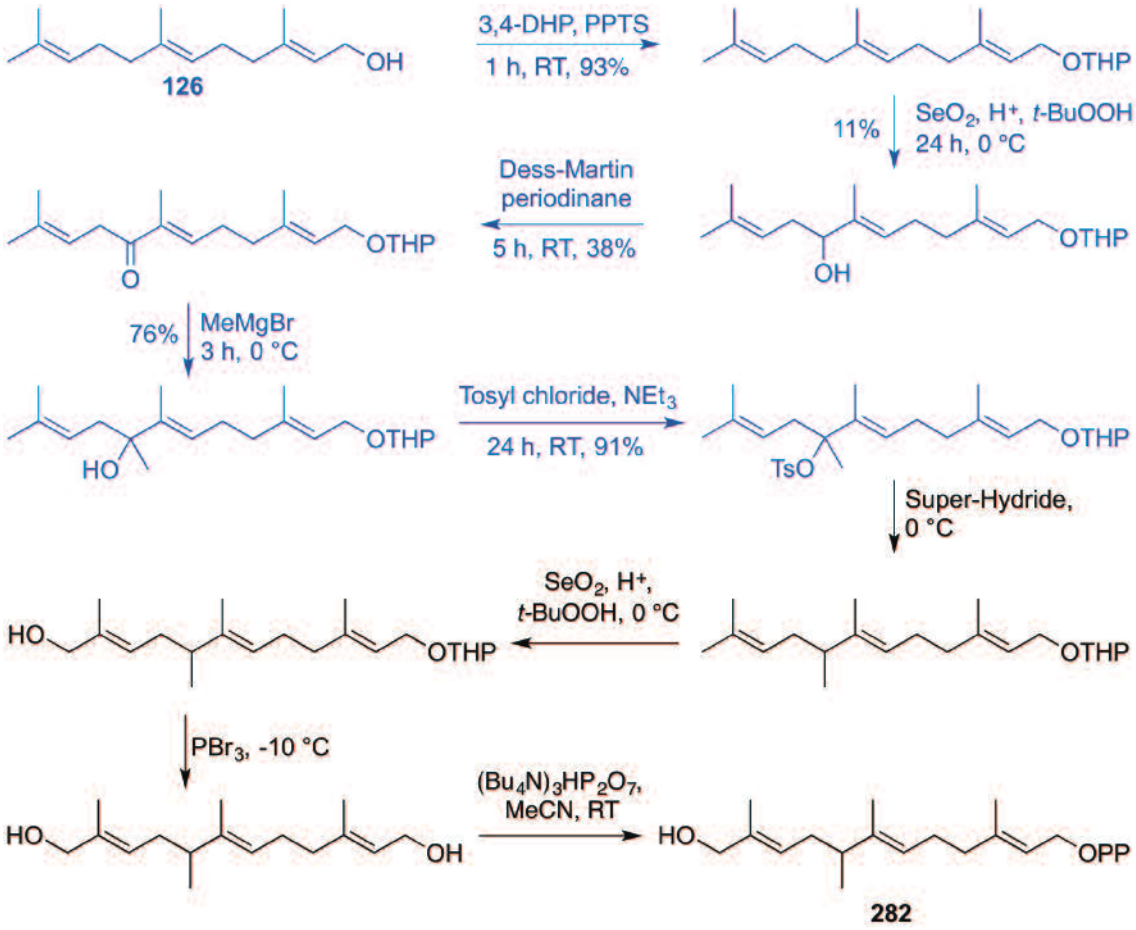

Scheme 6.2 Proposed synthesis of 8-methyl-12-hydroxy FDP (216). Intermediates in blue have been successfully prepared. Intermediates in black are the proposed remaining steps required to generate the product.

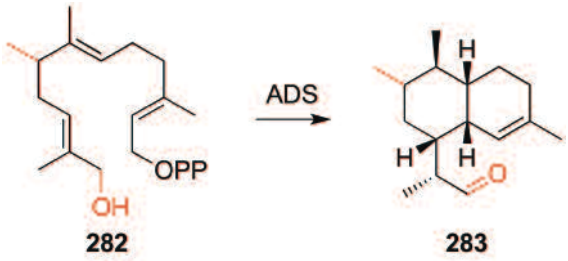

Scheme 6.3 Potential formation of 8-methyl dihydroartemisinic aldehyde (282) from incubation of ADS with 8-methyl-12-hydroxy FDP (283).

6.4 Inhibition studies

Analogues, 12-acetamido FDP (**184**) and 12-amino FDP (**185**), did not prove to be substrates of ADS as no pentane extractable products were observed by GC-MS after incubation (Section 4.4). Therefore further work could include carrying out inhibition

studies with these two analogues. If they are indeed shown to be inhibitors and hence, are accepted into the active site then mutagenesis of the protein may enable their conversion using ADS mutants as has been observed for conversion of 14,15-dimethyl FDP by a mutant of germacrene D synthase.[219]

6.5 The contribution of the N-terminal domain to the catalytic activity and structure of ADS

ADS mutants were designed in this project to study the effect(s) of the N-terminal domain on the catalysis and structure of ADS. Mutants ADS-M8 and ADS-F24A were created because of the results observed with analogous mutations on similar sesquiterpene synthases studied within the research group (Section 2.7).[96] ADS-M8, a mutant created by truncating the first 8 residues from the N-terminus, exhibited a K_M almost half the value and a k_{cat} 3.2 fold less, compared to the wild type (ADS-WT). This resulted in the catalytic efficiency of the enzyme, k_{cat}/K_M being almost half of that of ADS-WT. The reduced catalytic constant and catalytic efficiency of ADS-M8 led to the conclusion that the N-terminal domain, although previously considered as a 'silent' domain, plays a part in the structural contribution to the enzymes catalysis.[96]

Previous work also show that the single point mutations, F30A in EBFS and F36A in DCS have a substantial 4-fold increase in k_{cat} and a small reduction in K_M, compared to the wild type. When combined, these parameters gave a 7-fold enhancement of the catalytic efficiency for both enzymes (unpublished data).[96] This observation could imply that this phenylalanine residue is likely to be part of the structural determinant responsible for the product release, which is suggested to be the rate limiting step during the catalysis of sesquiterpene synthases.[166] The analogous mutant, ADS-F24A surprisingly did not follow the trend shown by EBFS and DCS but instead a k_{cat} that had decreased by more than 10-fold and a slightly larger K_M were found. This combination resulted in a 14-fold decrease in catalytic efficiency relative to wild type ADS.

6.6 Chemo-enzymatic approach to the production of dihydroartemisinic aldehyde allows for a possible one-pot synthesis of dihydroartemisinic acid.

Section 5 presented an efficient turnover of a novel FDP analogue, 12-OH FDP, to a mixture of dihydroartemisinic aldehydes using ADS. ADS proved to be promiscuous with this substrate endorsing the hypothesis that sesquiterpene synthases which naturally produce only hydrocarbon products can be challenged with heteratom substituted substrates to produce sesquiterpenoid analogues that may be useful for drug discovery or agrochemical purposes.

To exploit the chemoenzymatic approach for sourching the artemisinins, further work could be steered towards designing a one pot synthesis for dihydroartemisinic acid (**50**). This was attempted before the research for this thesis came to an end. Paddon and co-workers[137] report a succesful oxidation of dihydroartemisinic aldehyde to the corresponding acid with the use of sodium chlorite. The reported reaction was carried out in an aqueous buffer and therefore it was predicted that the same conditions could be adopted for the conversion of dihydroartemisinic aldehyde (**49**) to dihydroartemisinic acid (**50**) immediately after the 24 hour enzymatic incubation of ADS with 12-hydroxy FDP. An analytical incubation was set up with no organic overlay so the generated aldehyde would remain trapped in the aquoues buffer, then the synthetic procedure reported by Paddon and co-workers could be carried out with no requirement for a work up or purification of aldehyde **49**. Unfortunately the presence of dihydroartemisinic acid was not observed by the means of GC-MS.

Since the end of this project, Dr. Xiaoping Tang has repeated the sodium chlorite oxidation reaction with some modifications. The incubation containing ADS and 12-hydroxy FDP was set up with a toluene overlay. After 24 h of incubation, the toluene was removed and the sodium chlorite was added to the organic extract. This successfully saw the formation of dihydroartemisinic acid (**50**).

Another approach to creating a one pot synthesis of dihydroartemisinic acid is with the use of an additional enzyme.

Dr. Veronica Gonzalez is attempting to carry out the oxidation by using an aldehyde dehydrogenase (ALDH). ALDH is an NAD^+ dependent enzyme.[220] The catalytic mechanism begins with a nucleophilic attack on the adehyde moeity by a cysteine residue in the enzymes active site, in the form of a thiolate. This nucleophilic attack provides for a hydride transfer from the resulting hemithioacetal intermediate to the pyridine ring of NAD^+. Hydrolysis of the thioester intermediate, followed by a dissociation of the reduced cofactor affords acid **50** (Scheme 6.4). The use of a second enzyme is predicted to allow for a one pot synthesis of dihydroartemisinic acid as long as a buffer that enables both enzymes, ADS and ALDH, to function is used. If this one pot synthesis is successful, dihydroartemisinic acid will be efficiently produced in three steps starting from commercially available farnesyl chloride.

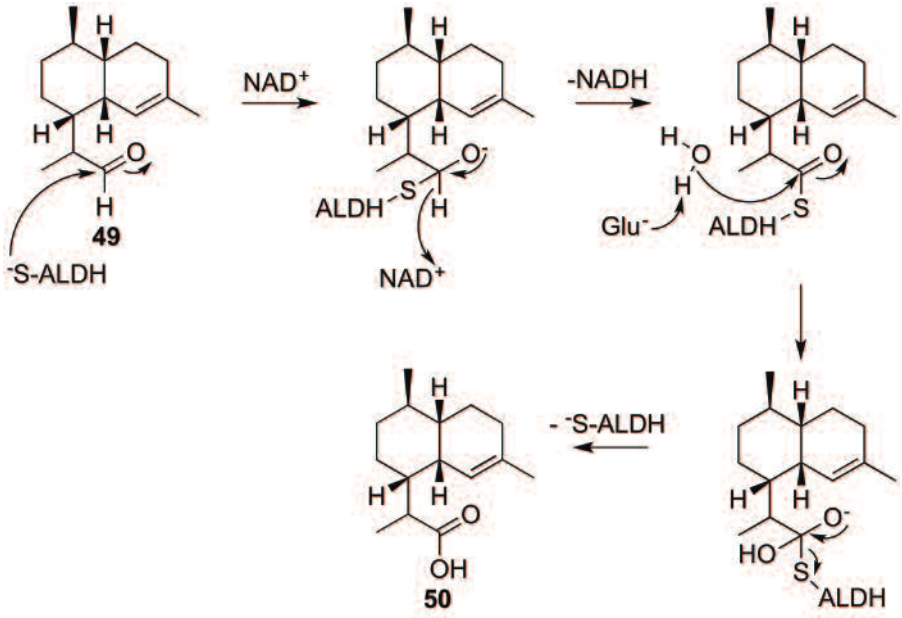

Scheme 6.4 Mechanism of NAD^+ dependant aldehyde dehydrogenase (ALDH) to catalyse the formation of dihydroartemisinic acid (50) from dihydroartemisinic aldehyde (49).

Chapter 7. Materials and Methods

7.1 Biological methods

7.1.1 General Materials and methods

The gene, codon optimised for expression in *E. coli*, encoding for amorphadiene synthase (ADS) from *Artemisia annua* was obtained from the GenBank (Acc. No. JF951730.1). The gene was supplied in a pTrc99a vector.

Restriction enzymes, Pfu DNA polymerase, unstained protein marker (14.4 kDa to 116.0 kDa) and amicon membranes were purchased from Fisher Scientific. The DNA ladder (high range) was purchased from Melford, the spin columns for DNA minipreps were purchased from Epoch and dialysis membrane was purchased from Medicell. Nickel beads used for nickel affinity chromatography were purchased from Expedion. The DNA sequencing service, to confirm successful SDM or PCR products, were carried out by Eurofins. Oligonucleotide primers and all other chemicals were purchased from Sigma Aldrich.

GC-MS analyses were measured on a Waters GCT Premier with a time of flight mass spectrometer detecting in the range *m/z* 50-800 in EI^+ mode. The column used was an Agilent J&W DB-35MS (30 m x 0.25 mm internal diameter). 10 μL samples were injected with a 5:1 split. Two methods were used for the elution of enzymatic products;

Method 1: Injector temperature was set to 100 °C and the initial oven temperature was 80 °C. A temperature gradient of 80 °C (1 min hold) to 180 °C (4 °C min^{-1}, 2 min hold) was used.

Method 2: Injector temperature was set to 100 °C and the initial oven temperature was 80 °C. A temperature gradient of 80 °C (1 min hold) to 180 °C (4 °C min^{-1}, 15 min hold) to 250 °C (20 °C min^{-1}, 4 min hold) was used.

DNA bands that were separated in agarose gel electrophoresis were visualized using a Syngene GeneFlash UV light box (Syngene, Cambridge, UK).

DNA concentration was measured using a nanodrop (Nanodrop 3300 Fluorospectrometer, Thermo scientific).

UV spectroscopy was measured using a Jasco V-660 spectrophotometer.

Size exclusion chromatography was carried out using a Superdex 75 10/300 GL pre-packed size exclusion column (24 mL) using an ÅKTA FPLC system.

CD experiments were carried out on an Applied PhotoPhysics Chirascan Spectrometer. CD spectra were measured in the range 190 nm to 300 nm in a 1 mm quartz cuvette. Spectra were recorded with a 50 nm/min scan speed, 0.5 nm data pitch, 1 nm bandwith and 0.5 s response time.

7.1.2 Bacterial strains

Two strains of *E*. coli were used in this project. The XL1-Blue cloning strain was used for the cloning of plasmid DNA and transformation of SDM products, whereas the BL21-(DE3)-Codon Plus RP (BL21-RP) expression strain was used for the expression of ADS and ADS mutants.[221]

7.1.3 Growth media

Luria-Bertani (LB) medium

Sodium chloride (10 g), tryptone (10 g) and yeast (5 g) were dissolved in deionised water (1 L). The solution was autoclaved (121 °C, 20 min) prior to use.[222]

LB agar plates

To LB medium (500 mL), agar (7.5 g) was added and the solution was autoclaved (121 °C, 20 min). The resulting mixture was stirred until the temperature cooled down to room temperature. Ampicillin (100 μg/mL) was added and the resulting mixture was poured (c.a. 50 mL for each) into sterile petri dishes. Once the agar had set, plates were stored at 4 °C.

7.1.4 Buffers

TAE buffer (50X): Tris-base (242 g, 2 M), glacial acetic acid (57.1 mL, 1 M) and EDTA (100 mL, 5 mM) was added to deionised water (900 mL). The pH was adjusted to 8 and the total volume was made up to 1 L with deionised water.

DNA Loading buffer: Glycerol (3 mL, 4 M) and 0.5% bromophenol blue solution (2 μL) were added to deionised water (7 mL).

NE Buffer 3.1: NaCl (0.58 g, 100 mM), Tris-HCl (0.8 g, 50 mM), $MgCl_2$ (96 mg, 10 mM), BSA (100 μg/ml) were dissolved in deionised water (100 mL). The pH was adjusted to 7.9.

QIAquick gel extraction buffers;

QG: Guanidine thiocyanate (65 g, 5.5 M) and Tris-HCl (32 mg, 2 mM) were dissolved in deionised water (100 mL). The pH was adjusted to 6.6.

PE: NaCl (117 mg, 20 mM) and Tris-HCl (32 mg, 2 mM) were added to a mixture of deionised water (20 mL) and ethanol (80 mL). The pH was adjusted to 7.5.

EB: Tris-HCl (0.3 g, 10 mM) was dissolved in deionised water (200 mL) and the pH was adjusted to 8.5.

QIAprep® spin miniprep buffers;

P1: Tris-HCl (3.94 g, 50 mM) and EDTA (1.86 g, 10 mM) was added to deionised water (450 mL). Once fully dissolved, the pH was adjusted to 8 and RNase A (25.0 mg, 1.82

μM) was added before the total volume was made up to 500 mL with deionised water. This buffer was stored at 4 °C.

P2: NaOH (0.8 g, 0.2 M) and SDS (1.00 g, 1% w/v, 34.7 mM) were dissolved in deionised water (100 mL).

N3: Guanidine hydrochloride (38.2 g, 4 M) and potassium acetate (4.90 g, 500 mM) were dissolved in deionised water (90 mL). The pH was adjusted to 4.2 and the total volume was made up to 100 mL with deionised water.

PB: Guanidine hydrochloride (47.8 g, 5 M) and Tris-HCl (300 mg, 20 mM) were added to deionised water (62 mL) and the pH was adjusted to 7.5. Ethanol (38 mL) was added last.

PE: NaCl (117 mg, 20 mM) and Tris-HCl (32.0 mg, 2.00 mM) were added to deionised water (20 mL) and the pH was adjusted to 7.5. Ethanol (80 mL) was added last.

EB: Tris-HCl (300 mg, 10 mM) was dissolved in deionised water (170 mL) and the pH was adjusted to 8.5. The total volume was then made up to 200 mL with additional deionised water.

Cell lysis buffer 1: Disodium hydrogenphosphate (30.5 mL, 20 mM), Monosodium dihydrogenphosphate (19.5 mL, 20 mM), NaCl (29.2 g, 50 mM), $MgCl_2$ (476 mg, 5.00 mM), glycerol (100 mL, 10% v/v), were all dissolved in deionised water (1 L) and the pH was adjusted to 7.

Cell lysis buffer 2: Tris-HCl (15.8 g, 100 mM), PMSF (174 mg, 1 mM), $MgCl_2$ (476 mg, 5 mM), glycerol (100 mL, 10% v/v), were all dissolved in deionised water (1 L) and the pH was adjusted to 8.

Cell lysis buffer 3: Tris-Base (6.06 g, 50 mM), NaCl (29.2 g, 50 mM), imidazole (340 mg, 5 mM), β-ME (1.40 mL, 20 mM), glycerol (100 mL, 10% v/v), were all dissolved in deionised water (1 L) and the pH was adjusted to 8.

Resolving buffer: Acrylamide/Bis-acrylamide, 30% solution (4 mL), 1.5 M tris buffer (2.5 mL, pH 8.8), and 10% SDS (100 μL) were dissolved in deionised water (3.4 mL).

Stacking buffer: Acrylamide/Bis-acrylamide, 30% solution (1.7 mL), 0.5 M tris buffer (2.5 mL, pH 6.8) and 10% SDS (100 μL) were dissolved in deionised water (5.7 mL).

10% APS (100 μL) and TEMED (20 μL) were added to both buffers as setting reagents when they were ready to be used. The resolving buffer was poured first into the templates and once this was set the stacking buffer was poured on top, followed immediately by a gel comb to create the wells. The comb was removed when the gel was set.

Electrode running buffer: Tris base (30.3 g, 250 mM) and glycine (150 g, 2 M) were dissolved in deionised water (600 mL). Once dissolved, SDS (10% w/v, 10 g) was added and left to stir to dissolve. Once fully dissolved, the final volume was brought up

to 1 L in deionised water. This buffer was diluted 10-fold with deionised water prior to use.

SDS sample buffer: 0.5 M Tris HCl (1.25 mL, pH 6.8), glycerol (2.5 mL), 0.6% (w/v) bromophenol blue (200 μL), 10% SDS (2 mL) and β-mercaptoethanol (500 μL) were dissolved in deionised water (3.55 mL).

SDS-PAGE stain buffer: Coomassie brilliant blue G-250 (0.25 g, 3 mM) was added to a mixture of ethanol and water (90 mL, 1:1). Glacial acetic acid (10 mL, 10% v/v) was added to the resulting mixture.

SDS-PAGE de-stain buffer: Ammonium sulphate (50 g, 0.76 mM) was added to a mixture of phosphoric acid (50 mL, 1.92 M) and deionised water (50 mL) and stirred. Once fully dissolved, Comassie brilliant blue G-250 (60 mg, 0.15 mM) was added and the solution was made up to 400 ml with deionised water before the addition of methanol (100 mL).

Dialysis buffer: HEPES (26.0 g, 25 mM), NaCl (23.4 g, 100 mM), and DTT (618 mg, 1 mM) were dissolved in deionised water (4 L) and the pH was adjusted to pH 7.5.

BSA (1 mg/ml): BSA (10 mg) was dissolved in deionised water (10 mL). 1 mL aliquots of this solution were stored at -20 °C until required.

Bradford reagent: Brilliant blue G250 (20 mg, 0.12 mM) was dissolved in ethanol (2 mL) and phosphoric acid (80%, 20 mL) was added. The final volume was brought up to 200 mL with deionised water and stored in the dark at 4 °C.

Size exclusion buffer: 0.2 M disodium hydrogenphosphate (76.3 mL, 50 mM), 0.2 M monosodium dihydrogenphosphate (48.8 mL, 50 mM) and β-mercaptoethanol (0.35 μL, 5 mM) were dissolved in deionised water (1L) and the pH was adjusted to 7.

CD spectroscopy buffers;

Sodium acetate-acetic acid buffer solutions (20 mM) for pH 4-5: 0.2M sodium acetate (1mL, 20 mM) and 0.2 M acetic acid (9 mL, 20 mM) were added to deionised water (1L) and the pH was adjusted to required value (pH 4-5).

Tris-HCl buffer solutions (20 mM) for pH 6-9: Tris-HCl (3.2 g, 20 mM) was dissolved in deionised water (1 L) and the pH was adjusted to the required value (pH 6-9).

Sodium phosphate buffer solutions (20 mM) for pH 10-12: Disodium hydrogenphosphate (30.5 mL, 20 mM) and monosodium dihydrogenphosphate (19.5 mL, 20 mM) were dissolved in deionised water (1 L) and the pH was adjusted to the required value (pH 10-12).

Incubation buffer: HEPES (20 mM), $MgCl_2$ (5 mM) and DTT (1 mM) were all dissolved in deionised water and the pH was adjusted to 7.5.

7.1.5 Cloning of ADS gene into pET21d vector

Restriction site digestion

Both pTrc99a-ADS and pET21d-GDS plasmids were, separately, double digested with *Nco*I and *BamH*I restriction endonucleases (1 μL of each enzyme, 5 μL of NEBuffer 3.1, 10 μL of plasmid) following the manufacturer's guidelines. The mixtures were left to incubate for 4 h at 37 °C.

Agarose gel electrophoresis

Agarose gels were prepared using TAE buffer (50 mL) with a 1% w/v ratio of agarose (0.5 g).[223] Electrophoresis was carried out in the same TAE buffer. DNA samples (10 μL) were mixed with DNA loading buffer (5 μL) and inserted into the gel wells. A DNA molecular weight ladder was also placed on the same gel to help identify the size of the fragments. Electrophoresis was carried out at a constant voltage of 80 mA for 80 min before being placed into a solution of ethidium bromide for 10 min. DNA fragments that corresponded to an open pET21d vector (5443 bp) and ADS gene (1634 bp), by comparison with the molecular weight ladder, were cut out of the gel and purified using a QIAquick gel extraction kit protocol.

Ligation of ADS gene into pET21d vector

The ADS gene and the open pET21d vector were ligated using T4 DNA ligase following the manufacturer's protocol (1:2 molar ratio of vector: insert, enzyme (1 μL), buffer (2 μL), sterile deionised water to make the total volume up to 20 μL). The resulting mixture was incubated using a PCR machine with the cycle as described in the Table 1. The cycle lasted for 50 min after which ligated plasmid was ready for effective transformation of competent *E. coli* XL1 Blue cells.

Table 7.1 PCR ligation cycle.

Temperature (°C)	Time (s)	Steps
4	20	4
22	20	
5	20	
21	20	
6	20	
20	20	
7	20	
19	20	
8	20	
18	20	
9	20	
17	20	
10	20	
16	20	
11	20	
15	20	
12	20	
13	20	
14	20	
4	20	1

Transformation of competent XL1-Blue cells

Super-competent *E. coli* XL1-Blue cells were used when cloning of DNA was required. Once the plasmid and cell had both gently thawed over ice, plasmid solution (5 μL) was added to the cell suspension (50 μL). The resulting mixture was stored on ice (30 min) before being heat shocked in a water bath (42 °C, 30-45 s) and placed back into ice (2 min). LB medium (1 mL) was added and the solution was incubated (60 min, 37 °C, 3300 *g*). The cells were harvested by centrifugation (1 min, 13000 *g*) and spread on an agar plate containing ampicillin (100 μg/mL) after re-suspending in a minimum amount of LB medium. Inverted plates were incubated overnight (37 °C).

QIAprep® Miniprep DNA extraction and purification.

A single colony from the agar plate harbouring the required transformed cells was used to inoculate LB medium (10 mL) containing ampicillin (100 μg/mL). The culture was shaken overnight (37 °C, 3300 *g*) and the following day centrifuged (3220 *g*, 10 min).

The pellet was purified using a QIAprep Spin Miniprep Kit (QIAprep Miniprep protocol). Confirmation of successful ligation was determined by DNA sequencing.

7.1.6 Site directed mutagenesis: Introduction of C-terminal hexa-histidine tag into the ADS gene

A single nucleotide deletion was required to bring the hexa-histidine coding sequence of pET21d in frame with the ADS coding sequence. A Quickchange site-directed mutagenesis kit was used to introduce the desired deletion according to the manufacturer's instructions (Table 2 and 3). The primers used for the deletion were:
5'- CGATGTCCATCTGTCCCGGGGATCC -3' and
5'- GGATCCCCGGGACAGATGGACATCG -3'.

Table 7.2 SDM reaction mixture.

Mixture component (stock concentration)	Volume
Parent plasmid	0.5 μL and 1 μL
Forward primer (10 μM)	2 μL
Reverse primer (10 μM)	2 μL
dNTP mix (10 mM)	1 μL
Pfu buffer with $MgSO_4$	5 μL
Pfu DNA polymerase	0.5 μL
Deionised water	38 μL

Table 7.3 SDM method:

Step	Temperature (°C)	Time	Number of cycles
Initial Denaturation	95	3	1
Denaturation	95	1	20
Annealing	55	2	
Extension	72	10	
Final extension	72	10	1

Once the SDM program was complete, samples were digested with *Dpn*I restriction enzyme (1 μL, 1 h, 37 °C).[151–153] Transformation, DNA extraction and measurement of the DNA concentration all followed the same procedures as stated above in Section 7.1.5. DNA sequencing was used to confirm successful SDM.

7.1.7 ADS mutants

Site directed mutagenesis

When site directed mutagenesis was carried out to create mutants of ADS, the same SDM reaction mixture and SDM method was used as in Section 7.1.6. The primers used for each mutant are as follows:

F24A

Forward 5'- CTATCTGGGGTGACCAGGCCCTGATCTACGAAAAG -3'

Reverse 5'- CTTTTCGTAGATCAGGGCCTGGTCACCCCAGATAG- 3'

I9M/R10G

Forward 5' GAAGAGAAACCCATGGGCCCGATCGCTAAC 3'

Reverse 5' GTTAGCGATCGGGCCCATGGGTTTCTCTTC 3'

I9M/G10R

Forward 5' CGAAGAGAAACCCATGCGTCCGATCGCTAACTTCC 3'

Reverse 5' GGAAGTTAGCGATCGGACGCATGGGTTTCTCTTCG 3'

M8-ADS G2R

Forward 5' GAGATATACCATGCGCCCGATCGCTAAC 3'

Reverse 5' GTTAGCGATCGGGCGCATGGTATATCTC 3'

Truncation of the first 8 amino acid residues of ADS (ADS-M8)

Once the production of mutant I9M/R10G was confirmed by sequencing, XL1 Blue cells were transformed to clone and increase the concentration of the variant. I9M/R10G (50 μL, 0.5 μg/mL) was diluted with fast digest buffer (10 μL) and to this was added *Nco*I (2 μL). The digestion was left at 37 °C for 4 h. The mixture was lyophilized to concentrate the sample, which was then separated on an agarose gel. It is worth noting that the length of the fragment cut from the plasmid is too small to witness a significant difference in the position of the band in the gel, from the wild type. Therefore the gel was not to confirm if the digestion was successful but to simply separate the plasmid from the isolated gene fragment. Purification of the open plasmid by gel extraction, and ligation of the open plasmid followed the same procedures as Section 7.1.5. To confirm if the ligation was successful and that the truncation of the enzyme was successful, transformation of XL1 blue cells, followed by DNA extraction by miniprep were carried out as described in Section 7.1.5. DNA sequencing proved that the truncation was a success.

7.1.8 Transformation and gene expression of ADS

Transformation of super-competent BL21 RP cells

E. coli BL21-RP cells were used for protein production. Once the plasmid and cell had both gently thawed over ice, plasmid solution (1 μL) was added to the cell suspension (50 μL). The resulting mixture was stored on ice (30 min) before being heat shocked in a water bath (42 °C, 30-45 s) and placed back into the ice (2 min). LB medium (1 mL) was added and the solution was incubated (1 h, 37 °C, 3300 *g*). The cells were harvested by centrifugation (3300 *g*, 1 min) and spread on an agar plate containing ampicillin (100 μg/mL) after re-suspending them in a minimum amount of LB medium. Inverted plates were incubated overnight (37 °C).

Test expression of ADS

To optimise the over-expression of ADS, the temperature and the length of expression were both varied (Table 4). Test incubations in 500 mL cultures were carried out. A single colony from the agar plate harbouring the required transformed cells was used to inoculate LB medium (100 mL) containing ampicillin (100 μg/mL). The culture was shaken overnight (37 °C, 3300 *g*) and the following day the resulting cell suspension was used to inoculate LB medium (3 x 500 mL, 10 mL of cell suspension in each flask) containing ampicillin (100 μg/mL).

Table 7.4 Optimisation of the over-expression of ADS.

Flask	Temperature of expression (°C)	Length of expression (h)
1	35	4
2	20	6
3	16	21

1 mL samples were removed at hourly intervals after induction, including one sample immediately prior to induction. The cells were harvested by centrifugation (3300 *g*, 1 min) and the pellets were re-suspended in SDS sample buffer and analysed by SDS-PAGE (Section 7.1.9.).

Expression of ADS

A single colony from the agar plate harbouring the required transformed cells was used to inoculate LB medium (100 mL) containing ampicillin (100 μg/mL). The culture was shaken overnight (37 °C, 3300 *g*) and the following day the resulting cell suspension was used to inoculate LB medium (6 x 500 mL, 10 mL of cell suspension in each flask) containing ampicillin (100 μg/mL). The cells were incubated (37 °C, 3300 *g*) until the

optical density at 600 nm (OD_{600}) reached 0.5. Isopropyl β-D-1-thiogalactopyranoside (IPTG) (48 mg, 0.40 mM) was added to each culture and shaking continued (20 °C, 3300 *g*, 6 h). The cells were harvested by centrifugation (4500 *g*, 10 min) and the resulting pellets were stored at -20 °C.

7.1.9 Purification of ADS

Cell lysis buffers

To optimize the extraction of protein process, from the cell pellets, three different protocols were followed (Table 5).[125,127,154] Each protocol used a cell lysis buffer with different compositions. It is worth noting that the protocol used for the extraction of the protein from the cell lysate was not varied so that the only factor being investigated was the composition of the buffers.

Table 7.5 Optimisation of protein extraction

Protocol	Buffer composition	Reducing agent	Detergent
Brodelius and co-workers[127] (Buffer 1)	20 mM sodium phosphate, 10% (v/v) glycerol, 0.5 M NaCl, 5 mM $MgCl_2$, pH 7	No	No
Kim and co-workers[125] (Buffer 2)	100 mM Tris-HCl, 10% (v/v) glycerol, 1 mM PMSF, 5 mM $MgCl_2$, pH 8	No	No
Noel and co-workers[154] (Buffer 3)	50 mM Tris-HCl, 10% (v/v) glycerol, 0.5 M NaCl, 5 mM $MgCl_2$, 5 mM imidazole, pH 8	20 mM β-ME	1% (v/v) Tween 20

Nickel affinity chromatography

Cell pellets were re-suspended in cell lysis buffer 3 (50 mL). Lysozyme (0.5 mg/mL) was added and the mixture was left to stir for 1 h at 5 °C. Cells were disrupted by sonication at 4 °C (38% amplitude for 3 min with 5 s on/10 s off cycles), the resulting suspension was centrifuged (17000 *g*, 30 min, 5 °C) and the resulting supernatant solution was loaded onto a Ni Sepharose™ 6 Fast Flow column (12 mL, under gravity controlled drip flow).[224] The flow through was eluted and the column was washed with cell lysis buffer 3 (10 CV) followed by a stepped gradient from 20 to 300 mM imidazole; buffer 3 with 20 mM imidazole (5 CV), 40 mM imidazole (5 CV), 100 mM imidazole (10 CV) and 300 mM imidazole (10 CV).

SDS-PAGE

Fractions eluted from the Ni^{2+} column were analysed by sodium dodecylsulfate-polyacrylamide gel electrophoresis (SDS-PAGE).[225] SDS polyacrylamide gels were prepared with a combination of stacking and resolving buffers. Electrophoresis was carried out in electrode running buffer (50 mL) using a Mini-PROTEAN system from Bio-Rad. Fraction samples (10 μL) were mixed with SDS sample buffer (10 μL) and inserted into the gel wells. A protein molecular weight ladder was also placed in the same gel to help identify the size of the bands. Electrophoresis was carried out (150 V, 60 min) before being stained in SDS gel stain (30 min). The gel was de-stained using gel de-stain buffer (30 min) until bands were visible. Protein bands that corresponded to a relative molecular mass of ~ 66 200 were pooled.

Dialysis and concentration of ADS

Purified protein was dialysed (MWCO 30000) overnight in dialysis buffer (4 L dialysis buffer: 100 mL protein) to remove the imidazole. The dialysed protein was then concentrated to a final volume of ~ 20 mL using an AMICON system (MWCO 30000). Concentrated solutions were stored at 4 °C.

Bradford assay

The concentration of ADS was determined using the Bradford assay.[155] A range of concentrations of bovine serum albumin protein (BSA) in water; 0.01 to 0.1 μg/mL were used as the calibration standard and the Bradford reagent (Coomassie Brilliant Blue dye) was used for the detection (Table 6).

Table 7.6 Preparation of the Bradford assay standards.

1 mg/mL stock of BSA (μL)	dH_20 (μL)	Bradford reagent (μL)	Concentration of Sample (μg/mL)
2	198	800	0.01
5	195	800	0.025
8	192	800	0.04
10	190	800	0.05
12	188	800	0.06
15	185	800	0.075
18	182	800	0.09
20	180	800	0.1

The absorbance shift of the dye was measured by UV spectrophotometry using a Jasco V-660 spectrophotometer. The ratio of absorbance at 590 nm and 450 nm was calculated and used to plot a standard curve.[156] The same procedure was carried out for samples of ADS. The concentration of ADS was calculated using the extrapolated calibration curve equation.

7.1.10 Size exclusion chromatography

Samples of various proteins were prepared by dissolving 1-2 mg of each protein in Na_XPO_4 buffer (pH 7.5, 1 mL). The resulting solution was injected (500 μl injection) and eluted through the column with 1.5 CV of size exclusion buffer at a rate of 0.8 mL/min. UV absorbance was monitored at 280 nm. [157]

7.1.11 Circular dichroism spectroscopy

Samples of ADS (10 μM) were prepared in buffers dependent on the pH under investigation.[86,100,158–160] For spectra measured at pH 4 and 5, NaOAc-AcOH buffer (20 mM) was used. For pH values of 6-9, Tris.HCl buffer (20 mM) was used. For pH values of 10-12, Na_xPO_4 buffer (20 mM) was used. The pH was adjusted with the addition of HCl (1M) and NaOH (1M). Each buffer (382 μL) was mixed with 77 μM ADS (52 μL) to give the concentration required. For each given pH, measurements were carried out at 0, 10 and 20 min to see if there was any change to the structure of the enzyme over time.

The spectra obtained from the CD spectrometer were converted to mean residue ellipticity (MRE) using the following equation:
Equation 1:

$$[\Theta]_{MRE} = \frac{[\Theta]}{10.\ n.\ c.\ l}$$

Where,
θ = molar ellipticity in millidegrees,
n = number of peptide bonds in the protein,
c = molar concentration of protein in the sample,
l = pathlength in cm

7.1.12 Steady state kinetics

Optimisation

The procedure for optimising incubation time involved the incubation of 6 samples of [1-^{3}H]-FDP (10 mM, specific activity 3.11 mCi/mmol) with ADS (100 nM) in incubation buffer. The reaction mixtures containing buffer, FDP and ADS were prepared on ice in a total volume of 250 μL and were overlaid with hexane (1 mL). Assays were initiated by the addition of enzyme (2 μL, 12.5 μM stock solution) to the assay mixture. The assay mixtures were incubated at 30 °C for varying times; 5, 10, 15, 20, 25, and 30 min. Each reaction was quenched with EDTA (200 μL, 100 mM), briefly vortexed and ice-cooled. The hexane overlay and 2 additional hexane extracts (2 x 750 μL) were passed through a short silica gel column in a Pasteur pipette (~1 g). The column was then eluted with additional hexane (2 x 750 μL). The pooled hexane extracts/eluents were emulsified with Ecoscint^{TM} O fluid (15 mL) and radioactivity was detected using a scintillation counter (Packard 2500 TR^{TM}) in ^{3}H mode for 4 min per sample.

After verifying that 10 min assays were optimal (section 2.6.4), in turn, enzyme concentration, magnesium ion concentration and pH values were all varied in order to maximise product concentration. Assays were carried out with 50, 100, 150, 200, 300 and 500 nM enzyme, 0, 2, 5, 10, 15 and 20 mM $MgCl_2$ and at pH values of 6.0, 6.5, 7.0, 7.5, 8.0, 8.5 and 9.0. Measurements were made in triplicate. The enzyme and Mg^{2+} concentrations that gave optimal rates were 100 nM and 5 mM, respectively, and the optimal pH was 7.5.

Michaelis-Menten kinetics

Steady state kinetic parameters for ADS were measured using the optimized assay conditions described above and variation of [1-^{3}H]-FDP concentration by fitting of the data to the Michaelis-Menten equation by nonlinear least squares regression in conjunction with the graphical procedures developed by Lineweaver-Burk using the commercial SigmaPlot package.[226–228] Assays (final volume 250 μL) were initiated with the addition of ADS (12.5 μM, 2 μL) to [1-^{3}H]-FDP (240000 dpm/nmol) with concentrations of FDP ranging from 0.2 to 12 μM. The buffer and protocol used was the same as what was used for the optimisation tests above.

The Michaelis Menten equation, Equation 2, was used to fit the raw data so that parameters k_{cat} and K_M could be deduced.

Equation 2:

$$V = \frac{V_{max}[S]}{K_M + [S]}$$

Using the calculated V_{max} from the equation above, k_{cat} was calculated with Equation 3:
Equation 3:

$$V_{max} = [E_{TOT}] \times k_{cat}$$

Where,
V_{max} = maximum rate of the enzyme catalysed reaction. At this point every active site is saturated.
$[E_{TOT}]$ = total concentration of enzyme.
k_{cat} = turnover number.
K_M = Michaelis constant.
[S] = substrate concentration.

7.1.13 Calculation of errors

Standard errors of the weighted mean

The estimate for the true value of K_M and k_{cat} was calculated as the weighted average. This is because each set of measurements for the same experiment was carried out separately and independently.

The weighted average mean (X_{wav}) was calculated using the following equation:
Equation 4

$$X_{wav} = \frac{\Sigma\, w_i x_i}{\Sigma\, w_i}$$

Where x_i is each value in the sample and w_i are the reciprocal squares of each measurements individual uncertainty, calculated with the following equation:
Equation 5

$$w_i = \frac{1}{\sigma_i^2}$$

The errors in this work are expressed as the standard error of the weighted mean (σ_{wav}) that is defined by the following equation:

Equation 6

$$\sigma_{wav} = \frac{1}{\sqrt{\Sigma w_i}}$$

Propagation of the errors

Propagation of errors was performed where appropriate using the following equations:

Equation 7

$$\text{If } Z = X/Y, \text{ then } \sqrt{\left(\frac{\Delta Z}{Z}\right)} = \left(\frac{\Delta X}{X}\right)^2 + \left(\frac{\Delta Y}{Y}\right)^2$$

Where X and Y are the experimentally measured values, ΔX and ΔY are their respective errors; Z is the calculated value and ΔZ the propagated error.

7.1.14 Normalisation

Where data has been normalised it has been performed using unity-based normalisation using the following equation:

Equation 8

$$X' = \frac{X - X_{min}}{X_{max} - X_{min}} \text{ x } 100$$

Where X' is the normalised value, X is the original value and X_{min} and X_{max} are the minimum and maximum values in the dataset, respectively.

7.2 Synthetic procedures

7.2.1 General methods and materials

^{1}H NMR, ^{13}C NMR, ^{31}P NMR and ^{19}F NMR spectra were measured on a Bruker Avance III 600, Bruker Avance 500, Bruker Avance III HD 400 and a Bruker Fourier 300 NMR spectrometer. The spectra are reported as chemical shifts in parts per million, downfield from tetramethylsilane (^{1}H and ^{13}C) and phosphoric acid (^{31}P), multiplicity (s

– singlet, d – doublet, t – triplet, q – quartet, m – multiplet, dd - doublet of doublet, dq - doublet of quartet), coupling (to the nearest 0.5 Hz) and assignment, respectively. Assignments are made to the limitations of COSY, DEPT 90/135, gradient HSQC, and gradient HMBC spectra.

Mass spectra were measured on a Waters GCT Premier time of flight mass spectrometer and a Waters LCT time of flight mass spectrometer. The methods used are the same as described in Section 7.1.1.

Thin layer chromatography (TLC) was performed on pre-coated aluminium plates of silica G/UV_{254}. TLC visualisations were performed with 4.2% ammonium molybdate and 0.2% ceric sulfate in 5% H_2SO_4 (Hanessian's stain) or UV light.
Ion-exchange chromatography was performed using ion-exchange resin (Amberlyst 131 wet, H^+ form) pre-equilibrated with ion-exchange buffer (25 mM NH_4HCO_3 containing 2% isopropanol, 2 CV).

Reverse phase HPLC was performed on a system comprising of a Dionex P680 pump and a Dionex UVD170U detector unit. The column used was a 150 x 21.2 mm Phenomenex Luna C-18 column. Crude diphosphates were eluted under isocratic conditions with 10% B for 20 min, a linear gradient to 60% B over 25 min, then a linear gradient to 100% B over 5 min and finally with 100% B for 10 min; solvent B: acetonitrile; solvent A: 25 mM ammonium bicarbonate in water, flow rate 5.0 cm^3 min^{-1}, detection at 220 nm.

All chemicals were purchased from Sigma-Aldrich, Alfa Aesar, or Fisher Scientific unless otherwise stated. Anhydrous tetrahydrofuran (THF), diethyl ether, toluene and acetonitrile were obtained from a MBraun SPS800 solvent purification system. Dichloromethane (DCM) and triethylamine were distilled from calcium hydride and potassium hydroxide under nitrogen respectively.

7.2.2 Index of synthetic compounds

	dodeca-2, 6, 10-trien-1-ol	
150	2-(((2E, 6E, 10Z)-12-Bromo-3, 7, 11-trimethyl dodeca-2, 6, 10-trien-1-yl) oxy) tetrahydro-2H-pyran	172
151	2-(((2E, 6E, 10Z)-3, 7, 11-Trimethyl trideca-2, 6, 10-trien-1-yl) oxy) tetrahydro-2H-pyran	172
152	(2E, 6E, 10Z)-3, 7, 11-Trimethyl trideca-2, 6, 10-trien-1-ol	173
155	Ethyl 7-methyl-3-oxooct-6-enoate	175
156	Ethyl (Z)-7-methyl-3-(((trifluoromethyl) sulfonyl) oxy) octa-2, 6-dienoate	175
157	Ethyl (E)-3-ethyl-7-methylocta-2, 6-dienoate	176
158	(E)-3-Ethyl-7-methylocta-2, 6-dien-1-ol	177
159	(E)-1-Bromo-3-ethyl-7-methylocta-2, 6-diene	177
160	Ethyl (E)-7-ethyl-11-methyl-3-oxododeca-6, 10-dienoate	178
161	Ethyl (2Z, 6E)-3-((diethoxyphosphoryl) oxy)-7-ethyl-11-methyl dodeca-2, 6, 10-trienoate	179
162	Ethyl (2E, 6E)-7-ethyl-3, 11-dimethyl dodeca-2, 6, 10-trienoate	180
163	(2E, 6E)-7-Ethyl-3, 11-dimethyl dodeca-2, 6, 10-trien-1-ol	181
164	(2E, 6E)-1-Bromo-7-ethyl-3, 11-dimethyl dodeca-2, 6, 10-triene	181
165	(2E, 6E, 10Z)-12-Acetoxy-3, 7, 11-trimethyl dodeca-2, 6, 10-trien-1-yl diphosphate	185
166	(2E, 6E, 10E)-12-Acetoxy-3, 7, 11-trimethyl dodeca-2, 6, 10-trien-1-yl diphosphate	188
167	(2E, 6E)-8-Acetoxy-3, 7, 11-trimethyl dodeca-2, 6, 10-trien-1-yl diphosphate	191
168	(2E, 6E, 10E)-12-Hydroxy-3, 7, 11-trimethyl dodeca-2, 6, 10-trien-1-yl diphosphate	189
169	(2E, 6E)-8-Acetoxy-3, 7, 11-trimethyl dodeca-2, 6, 10-trien-1-yl diphosphate	191
170	(2E, 6E)-8-Methoxy-3, 7, 11-trimethyl dodeca-2, 6, 10-trien-1-yl diphosphate	194
171	(2E, 6E, 10E)-12-Methoxy-3, 7, 11-trimethyl dodeca-2, 6, 10-trien-1-yl diphosphate	197
172	(2Z, 6E, 10E)-2, 6, 10-Trimethyl-12-((tetrahydro-2H-pyran-2-yl) oxy) dodeca-2, 6, 10-trien-1-yl acetate	183
173	(2Z, 6E, 10E)-12-Hydroxy-2, 6, 10-trimethyl dodeca-2, 6, 10-trien-1-yl acetate	183
174	(2Z, 6E, 10E)-12-Bromo-2, 6, 10-trimethyl dodeca-2, 6, 10-trien-1-yl acetate	184
175	(2E, 6E, 10E)-2, 6, 10-Trimethyl-12-((tetrahydro-2H-pyran-2-yl) oxy) dodeca-2, 6, 10-trien-1-ol	185

176	(2E, 6E, 10E)-2, 6, 10-Trimethyl-12-((tetrahydro-2H-pyran-2-yl) oxy) dodeca-2, 6, 10-trien-1-yl acetate	186
177	(2E, 6E, 10E)-12-Hydroxy-2, 6, 10-trimethyl dodeca-2, 6, 10-trien-1-yl acetate	187
178	(6E, 10E)-12-Chloro-2, 6, 10-trimethyl dodeca-2, 6, 10-trien-5-ol	190
179	(6E, 10E)-2, 6, 10-Trimethyl-12-((tetrahydro-2H-pyran-2-yl) oxy) dodeca-2, 6, 10-trien-5-ol	192
180	2-(((2E, 6E)-8-Methoxy-3, 7, 11-trimethyl dodeca-2, 6, 10-trien-1-yl) oxy) tetrahydro-2H-pyran	193
181	2-(((2E, 6E, 10E)-12-Methoxy-3, 7, 11-trimethyl dodeca-2, 6, 10-trien-1-yl) oxy) tetrahydro-2H-pyran	195
182	(2E, 6E)-8-Methoxy-3, 7, 11-trimethyl dodeca-2, 6, 10-trien-1-ol	194
183	(2E, 6E, 10E)-12-Methoxy-3, 7, 11-trimethyl dodeca-2, 6, 10-trien-1-ol	196
184	(2E, 6E, 10E)-12-Acetamido-3, 7, 11-trimethyl dodeca-2, 6, 10-trien-1-yl diphosphate	201
185	(2E, 6E, 10E)-12-Amino-3, 7, 11-trimethyl dodeca-2, 6, 10-trien-1-yl diphosphate	204
186	2-((2E, 6E, 10E)-2, 6, 10-Trimethyl-12-((tetrahydro-2H-pyran-2-yl) oxy) dodeca-2, 6, 10-trien-1-yl) isoindoline-1, 3-dione	198
187	(2E, 6E, 10E)-2, 6, 10-Trimethyl-12-((tetrahydro-2H-pyran-2-yl) oxy) dodeca-2, 6, 10-trien-1-amine	199
191	N-((2E, 6E, 10E)-2, 6, 10-Trimethyl-12-((tetrahydro-2H-pyran-2-yl) oxy) dodeca-2, 6, 10-trien-1-yl) acetamide	199
192	N-((2E, 6E, 10E)-12-Hydroxy-2, 6, 10-trimethyl dodeca-2, 6, 10-trien-1-yl) acetamide	200
193	N-((2E, 6E, 10E)-12-Bromo-2, 6, 10-trimethyldodeca-2, 6, 10-trien-1-yl) acetamide	201
196	(9H-Fluoren-9-yl) methyl ((2E, 6E, 10E)-2, 6, 10-trimethyl-12-((tetrahydro-2H-pyran-2-yl) oxy) dodeca-2, 6, 10-trien-1-yl) carbamate	202
197	(9H-Fluoren-9-yl) methyl ((2E, 6E, 10E)-12-hydroxy-2, 6, 10-trimethyl dodeca-2, 6, 10-trien-1-yl) carbamate	203
198	(9H-Fluoren-9-yl) methyl ((2E, 6E, 10E)-12-bromo-2, 6, 10-trimethyl dodeca-2, 6, 10-trien-1-yl) carbamate	204
211	14-Methyl amorphadiene	212
262	8-Methoxy-g-humulene	213
278	(2E, 6E, 10E)-12-Chloro-2, 6, 10-trimethyl dodeca-2, 6, 10-trien-1-ol	189
279	(2E, 6E)-3, 7, 11-trimethyldodeca-2, 6, 10-trienal	208
284	(2E, 6E, 10E)-12-Bromo-1-methoxy-2, 6, 10-trimethyl dodeca-2, 6, 10-triene	197

7.2.3Preparation of farnesyl diphosphate (FDP)

(2*E*, 6*E*)-1-Chloro-3, 7, 11-trimethyl dodeca-2, 6, 10-triene (127)[167]

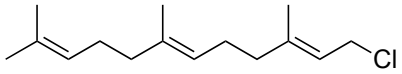

To a cold suspension (0 °C) of farnesol (500 mg, 2.25 mmol), lithium chloride (1.5 g, 35 mmol) and *s*-collidine (1.5 mL, 11 mmol) in dry dimethylformamide (DMF) (30 mL) was added methanesulfonyl chloride (0.80 mL, 9.6 mmol), via a syringe, under nitrogen. The mixture was stirred for 3 h and then poured into deionized water (100 mL). The biphasic layers were separated and the aqueous layer was extracted with hexane (4 x 20 mL). Combined organic extracts were washed with saturated copper sulfate solution (3 x 40 mL), deionized water (2 x 40 mL) and saturated sodium bicarbonate solution (2 x 40 mL) and dried over anhydrous magnesium sulfate. The resulting solution was filtered under gravity and concentrated under reduced pressure to give the title compound as light yellow oil (540 mg, 99%).

^{1}H NMR (500 MHz, $CDCl_3$): δ 5.48 (1 H, t, $J_{H,H}$ = 8.0, C=C<u>H</u>CH_2Cl), 5.11 (2 H, t, $J_{H,H}$ = 7.0, 2 x C=C<u>H</u>CH_2CH_2), 4.10 (2 H, d, $J_{H,H}$ = 8.0, C<u>H</u>$_2$Cl), 2.14-1.95 (8 H, m, 2 x C<u>H</u>$_2$C<u>H</u>$_2$), 1.73, 1.68 and 1.60 (2 x 3 H and 1 x 6 H, 3 x s, 4 x C<u>H</u>$_3$).

^{13}C NMR (125 MHz, $CDCl_3$): δ 143.0, 135.8 and 131.5 (3 x CH_3<u>C</u>$CHCH_2$), 124.5, 123.6 and 120.4 (3 x CH_3<u>C</u>$CHCH_2$), 41.39 (<u>C</u>H_2Cl), 39.86 and 39.62 (2 x $CCHCH_2$<u>C</u>H_2), 26.87 and 26.28 (2 x CCH<u>C</u>H_2CH_2), 25.91, 17.89, 16.31 and 16.23 (4 x <u>C</u>H_3).

Tris (tetrabutylammonium) hydrogendiphosphate (121)[169]

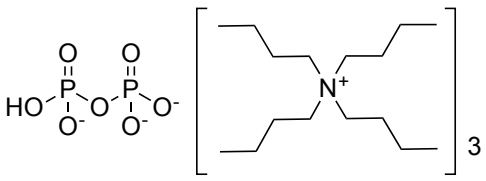

Disodium dihydrogen diphosphate (3.3 g, 15 mmol) in 10% (v/v) aqueous ammonium hydroxide (15 mL) was passed through a cation-exchange resin (H^+ form, amberlyst 131 wet, 10 g). Free acid was eluted with deionized water (110 mL) and the resulting solution was titrated to pH 7.3 by slow addition of tetrabutylammonium hydroxide (40% w/w in aqueous solution). The solution was lyophilized to attain the hygroscopic product.

The title compound was purified by recrystallization. The white solid was partially dried by treating with acetonitrile (75 mL) and by azeotropic removal of the water/solvent by reduced pressure to yield a tacky solid. The material was warmed to

40 °C in ethyl acetate (50 mL) before being filtered under vacuum to remove insoluble inorganic contaminants. The clear colourless filtrate was concentrated to half the volume and cooled to -20 °C to give the title compound as crystals (5 g, 38%).

^{1}H NMR (500 MHz, $CDCl_3$): δ 3.17-3.13 (24 H, m, 12 x $NCH_2CH_2CH_2CH_3$), 1.62-1.56 (24 H, m, 12 x $NCH_2CH_2CH_2CH_3$), 1.36-1.27 (24 H, m, 12 x $NCH_2CH_2CH_2CH_3$), 0.90 (36 H, t, $J_{H,H}$ = 7.5, 12 x $NCH_2CH_2CH_2CH_3$).

^{31}P NMR (121 MHz, D_2O): δ -7.93 (s).

HRMS (ES^-): calculated for $(C_{16}H_{39}NO_7P_2 - [H])^-$: 418.2124, found: 418.2134.

(2*E*, 6*E*)-3,7,11-Trimethyl dodeca-2,6,10-trien-1-yl diphosphate (36)[169]

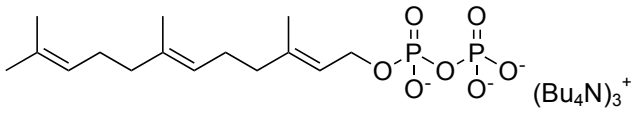

To a stirred solution of **121** (4.0 g, 4.5 mmol) in anhydrous acetonitrile (10 mL) under nitrogen was added a solution of crude **127** (540 mg, 2.25 mmol) in acetonitrile (3 mL) via a syringe. This was left to stir for 24 h. The solvent was removed and the resulting oil was dissolved in a minimum amount of ion-exchange buffer (25 mM ammonium bicarbonate solution containing 2% isopropanol).

The crude compound in buffer was eluted through the NH_4^+-form cation exchange column with additional ion exchange buffer. Fractions that contained the diphosphate as judged by comparison with an authentic FDP standard by TLC (6:3:1, isopropanol: water: ammonium hydroxide) were collected and lyophilized.

The resulting dry powder was re-dissolved in ion-exchange buffer and was purified by being passed through a reverse phase HPLC. Farnesyl diphosphate eluted at 35.7 min and fractions containing clean farnesyl diphosphate were pooled and lyophilized to give the title compound as a white powder (440 mg, 51%).

^{1}H NMR (500 MHz, D_2O): δ 5.41 (1 H, t, $J_{H,H}$ = 7.0, $CHCH_2O$), 5.18-5.10 (2 H, m, 2 x $C=CHCH_2CH_2$), 4.41 (2 H, t, $J_{H,H}$ = 6.5, $CHCH_2O$), 2.11-1.94 (8 H, m, 2 x $CHCH_2CH_2$), 1.67, 1.63 and 1.57 (2 x 3 H and 1 x 6 H, 3 x s, 4 x CH_3).

^{31}P NMR (121 MHz, D_2O): δ -6.49 (d, $J_{P,P}$ = 22), -10.25 (d, $J_{P,P}$ = 22).

LRMS (ES^-) *m/z*: 381.12 (100%, $[M - H]^-$), 301.17 (53).

HRMS (ES^-): calculated for $(C_{15}H_{28}O_7P_2 – [H])^-$: 381.1232, found: 381.1232.

7.2.4 Preparation of 12-methyl-farnesyl diphosphate (12-Methyl FDP, 128)[170,172–175]

2-(((2*E*, 6*E*)-3, 7, 11-Trimethyl dodeca-2, 6, 10-trien-1-yl) oxy) tetrahydro-2H-pyran (131)

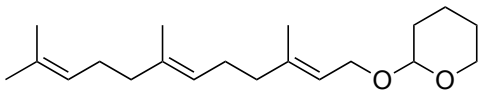

To a stirred solution of farnesol (5.00 g, 22.5 mmol) in DCM (25 mL) was added to 3,4-dihydropyran (8.10 mL, 88.8 mmol) and left to stir for 10 min. Pyridinium *p*-toluenesulfonate (0.6 g, 2.4 mmol) was added and the mixture was stirred for 1 h whereupon TLC analysis (8:2, hexane: ethyl acetate) showed full consumption of starting material. DCM was removed under reduced pressure and the residual crude product was dissolved in diethyl ether (50 mL). The organic solution was washed with saturated aqueous sodium bicarbonate solution (3 x 20 mL) and brine (20 mL), before being dried over anhydrous magnesium sulfate, filtered under gravity and concentrated under reduced pressure to give the title compound as a colourless oil (6.5 g, 93%). The product was judged by ^{1}H NMR spectroscopy to be sufficiently pure to carry forward without further purification.[172]

^{1}H NMR (300 MHz, $CDCl_3$): δ 5.36 (1 H, t, $J_{H,H}$ = 6.5, C$\underline{H}$CH_2O), 5.10-5.13 (2 H, m, 2 x CC$\underline{H}$CH_2CH_2), 4.63 (1 H, t, $J_{H,H}$ = 4.0, OC$\underline{H}$O), 4.24 (1 H, dd, $J_{H,H}$= 12.0 and 6.5, CCHC$\underline{H_A}$O), 4.06 (1 H, dd, $J_{H,H}$= 12.0 and 7.5, CCHC$\underline{H_B}$O), 3.93-3.47 (2 H, m, OC$\underline{H_2}$CH_2), 2.16-1.94 (8 H, m, 2 x CCHC$\underline{H_2}$C$\underline{H_2}$), 1.89-1.50 (6 H, m, OCHC$\underline{H_2}$C$\underline{H_2}$C$\underline{H_2}$), 1.68 and 1.60 (2 x 6 H, 2 x s, 4 x C$\underline{H_3}$).

^{13}C NMR (75 MHz, $CDCl_3$): δ 140.5, 135.4 and 131.5 (3 x $CH_3\underline{C}$CH), 124.5, 124.1 and 120.7 (3 x $CH_3C\underline{C}$H), 97.98 (O$\underline{C}$HO), 63.83 and 62.48 (2 x CHO$\underline{C}H_2$), 39.89 and 39.82 (2 x $CH_3C\underline{C}H_2$), 30.90 (OCH$\underline{C}H_2$), 26.90 and 26.47 (2 x CCH$\underline{C}H_2CH_2$), 25.90 (OC$H_2\underline{C}H_2$), 25.69 (O$CH_2CH_2\underline{C}H_2$), 19.82, 17.88, 16.62 and 16.20 (4 x $\underline{C}$H3).

LRMS (ES^+) *m/z*: 329.24 (100%, $[M + Na]^+$).

HRMS (ES^+): calculated for ($C_{20}H_{34}O_2$ + [Na])$^+$: 329.2457, found: 329.2463.

(2*E*, 6*E*, 10*E*)-2, 6, 10-Trimethyl-12-((tetrahydro-2*H*-pyran-2-yl) oxy) dodeca-2, 6, 10-trienal (132)

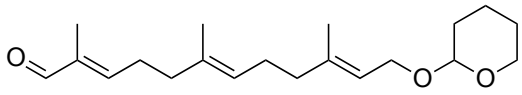

Selenium dioxide (593 mg, 5.39 mmol), salicylic acid (752 mg, 5.39 mmol) and *t*-butyl hydroperoxide (5.10 mL, 539 mmol) were stirred in DCM (100 mL) for 30 min. **131** (3.30 g, 10.9 mmol) was added and the reaction was left to stir for 6 h. DCM was removed under reduced pressure. *t*-Butyl hydroperoxide was removed by co-evaporation with toluene (2 x 20 mL) under reduced pressure. The crude residue was dissolved in diethyl ether (20 mL) and washed with saturated aqueous sodium bicarbonate solution (50 mL). The layers were separated and the aqueous layer was further extracted with diethyl ether (5 x 20 mL). The combined organic layers were washed with brine (20 mL) and dried over anhydrous magnesium sulfate before being filtered under gravity. The solvent was removed under reduced pressure and the crude oil was purified by flash chromatography on silica gel (9:1, hexane: ethyl acetate) to give the title compound as a colourless oil (0.8 g, 23%).[173,174]

^{1}H NMR (500 MHz, $CDCl_3$): δ 9.38 (1 H, s, C$\underline{H}$O), 6.46 (1 H, t, $J_{H,H}$ = 7.0, C$\underline{H}$C=CHO), 5.36 (1 H, t, $J_{H,H}$ = 6.5, CC$\underline{H}$CH$_2$O), 5.16 (1 H, t, $J_{H,H}$ = 7.0, CH$_2$CH$_2$C$\underline{H}$CCH$_2$), 4.62 (1 H, m, OC$\underline{H}$O), 4.24 (1 H, dd, $J_{H,H}$= 12.0 and 6.5, CCHC$\underline{H}_A$O), 4.02 (1 H, dd, $J_{H,H}$= 12.0 and 7.5, CCHC$\underline{H}_B$O), 3.91-3.50 (2 H, m, OC$\underline{H}_2$CH$_2$), 2.45 (2 H, m, CCHCH$_2$C$\underline{H}_2$), 2.17-2.11 (4 H, m, CCHC$\underline{H}_2$C$\underline{H}_2$), 2.06-2.03 (2 H, m, CCHC$\underline{H}_2$CH$_2$), 1.77-1.51 (6 H, m, OCHC$\underline{H}_2$C$\underline{H}_2$C$\underline{H}_2$), 1.74, 1.68 and 1.63 (9 H, 3 x s, 3 x C$\underline{H}_3$).

^{13}C NMR (125 MHz, $CDCl_3$): δ 195.5 (CH$_3$C$\underline{C}$HO), 154.7, 140.1 and 139.5 (3 x CH$_3$$\underline{C}$CH), 133.8, 125.5 and 121.0 (3 x CH$_3$C$\underline{C}$H), 98.07 (O$\underline{C}$HO), 63.85 and 62.51 (2 x CHO$\underline{C}$H$_2$), 39.64 and 38.15 (2 x CH$_3$C$\underline{C}$H$_2$), 30.90 (OCH$\underline{C}$H$_2$), 27.59 and 26.39 (2 x CCH$\underline{C}$H$_2$CH$_2$), 25.67 (OCH$_2$$\underline{C}H_2$), 19.82 (OCH$_2CH_2$$\underline{C}H_2$), 16.61, 16.11 and 9.42 (3 x $\underline{C}$H3).

LRMS (ES$^+$) *m/z*: 343.22 (100%, [M + Na]$^+$).

HRMS (ES$^+$): calculated for ($C_{20}H_{32}O_3$ + [Na])$^+$: 343.2249, found: 343.2232.

2-(((2*E*, 6*E*, 10*E*)-3, 7, 11-Trimethyl trideca-2, 6, 10, 12-tetraen-1-yl) oxy) tetrahydro-2H-pyran (133)

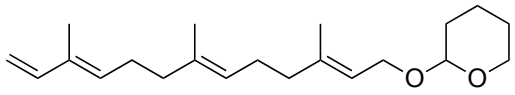

To a stirred solution of methyl triphenyl phosphonium bromide (2.0 g, 5.6 mmol) in anhydrous THF (20 mL) was added *n*-butyl lithium (2.5 M in hexanes, 2.3 mL, 5.6 mmol) at -10 °C. This solution was left to stir for 30 min before 13**2** (600 mg, 1.87 mmol) was added. The reaction was allowed to warm to room temperature and left to stir for 48 h. The reaction was quenched with the addition of saturated aqueous ammonium chloride solution (20 mL) and the organic layer was separated. The aqueous layer was extracted with diethyl ether (5 x 20 mL). The organic layers were combined and washed with saturated aqueous sodium bicarbonate solution (2 x 20 mL) and brine (20 mL). The organic solution was dried over anhydrous magnesium sulfate, filtered under gravity and concentrated under reduced pressure. The crude oil was purified by flash chromatography on silica gel (9:1, hexane: ethyl acetate) to give the title compound as a colourless oil (350 mg, 56%).[175]

^{1}H NMR (300 MHz, $CDCl_3$): δ 6.36 (1 H, dd, $J_{H,H}$ = 17.5 and 10.5, C$\underline{H}$CCHCH$_2$CH$_2$), 5.46 (1 H, t, $J_{H,H}$ = 7.0, CH$_3$CC$\underline{H}$), 5.36 (1 H, t, $J_{H,H}$ = 7.5, CH$_3$C=C$\underline{H}$), 5.13 (1 H, t, $J_{H,H}$ = 6.0, CH$_3$C=C$\underline{H}$), 5.07 (1 H, d, $J_{H,H}$ = 17.5, CH$_3$CCHC$\underline{H}_A$O), 4.92 (1 H, d, $J_{H,H}$ = 10.0, CH$_3$CCHC$\underline{H}_B$O), 4.63 (1 H, t, $J_{H,H}$ = 3.5, OC$\underline{H}$O), 4.24 (1 H, dd, $J_{H,H}$= 12.0 and 6.5, CCHC$\underline{H}_A$), 4.02 (1 H, dd, $J_{H,H}$= 12.0 and 6.5, CCHC$\underline{H}_B$), 3.93-3.47 (2 H, m, OC$\underline{H}_2$CH$_2$), 2.26-2.01 (8 H, m, 2 x CCHC$\underline{H}_2$C$\underline{H}_2$), 1.88-1.50 (6 H, m, OCHC$\underline{H}_2$C$\underline{H}_2$C$\underline{H}_2$), 1.73, 1.68 and 1.60 (9 H, 3 x s, 3 x C$\underline{H}_3$).

^{13}C NMR (75 MHz, $CDCl_3$): δ 141.8, 140.4 and 135.0 (3 x CH$_3$$\underline{C}$CH), 134.1, 133.1, 124.5 and 120.8 (4 x CH$_3$$\underline{C}$CH), 110.6 (CH$_3CCH\underline{C}H_2$), 97.99 (O$\underline{C}$HO), 63.84 and 62.48 (2 x CHO$\underline{C}$H$_2$), 39.76 and 39.39 (2 x CH$_3$$\underline{C}CH_2$), 30.89 (OCH$\underline{C}H_2$), 27.02 and 26.44 (2 x CCH$\underline{C}$H$_2$CH$_2$), 25.68 (OCH$_2$$\underline{C}H_2$), 19.81 (OCH$_2CH_2$$\underline{C}H_2$), 16.61, 16.18 and 11.86 (3 x $\underline{C}$H3).

LRMS (ES$^+$) *m/z*: 341.25 (100%, [M + Na]$^+$).

HRMS (ES$^+$): calculated for ($C_{21}H_{34}O_2$ + [Na])$^+$: 341.2457, found: 341.2469.

2-(((2*E*, 6*E*, 10*E*)-3, 7, 11-Trimethyl trideca-2, 6, 10-trien-1-yl) oxy) tetrahydro-2H-pyran (134)

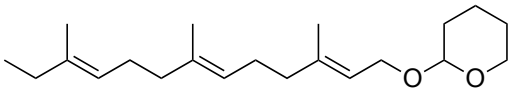

To a stirred solution of 13**3** (350 mg, 1.10 mmol) in toluene (10 mL) was added Wilkinson's catalyst (102 mg, 0.110 mmol). The air in the sealed round bottom flask was evacuated using a vacuum pump and replaced with hydrogen contained in a balloon. This procedure was repeated 5 times to ensure the atmosphere in the round bottom flask was solely made up of hydrogen. The reaction was left to stir for 5 h and quenched with saturated aqueous sodium bicarbonate solution (20 mL). The layers were separated and the aqueous layer was extracted with diethyl ether (5 x 10 mL). The organic layers were combined and washed with saturated aqueous sodium bicarbonate solution (10 mL) and brine (10 mL) before being dried over anhydrous magnesium sulfate and filtered under gravity. The solvent was removed using reduced pressure and the crude product was purified by flash chromatography on silica gel (9:1, hexane: ethyl acetate) to give the title compound as a colourless oil (250 mg, 71%).[176]

^{1}H NMR (300 MHz, $CDCl_3$): δ 5.36 (1 H, t, $J_{H,H}$ = 7.0, C$\underline{H}$C$\underline{H_2}$O), 5.12-5.05 (2 H, m, 2 x CC$\underline{H}$C$\underline{H_2}$C$\underline{H_2}$), 4.62 (1 H, t, $J_{H,H}$ = 3.5, OC$\underline{H}$O), 4.23 (1 H, dd, $J_{H,H}$= 12.0 and 6.5, CCHC$\underline{H_A}$O), 4.03 (1 H, dd, $J_{H,H}$ = 12.0 and 6.5, CCHC$\underline{H_B}$O), 3.92-3.49 (2 H, m, OC$\underline{H_2}$C$\underline{H_2}$), 2.14-1.90 (10 H, m, 2 x CCHC$\underline{H_2}$C$\underline{H_2}$ and CH_3CC$\underline{H_2}$C$\underline{H_3}$), 1.68 (3 H, s, CHCC$\underline{H_3}$), 1.62-1.51 (6 H, m, OCHC$\underline{H_2}$C$\underline{H_2}$C$\underline{H_2}$), 1.59 (6 H, s, 2 x CHCC$\underline{H_3}$) and 0.97 (3 H, t, $J_{H,H}$ = 7.5, CH_3C$\underline{H_2}$C$\underline{H_3}$).

^{13}C NMR (125 MHz, $CDCl_3$): δ 140.5, 137.0 and 135.5 (3 x $CH_3\underline{C}$CH), 124.1, 122.9 and 120.7 (3 x CH_3C$\underline{C}$H), 97.98 (O$\underline{C}$HO), 63.84 and 62.47 (2 x CHO$\underline{C}H_2$), 39.93, 39.84 and 32.52 (3 x $CH_3\underline{C}CH_2$), 30.91 (OCH$\underline{C}H_2$), 26.75 and 26.48 (2 x CCH$\underline{C}H_2CH_2$), 25.69 (OCH$_2\underline{C}H_2$), 19.82 (OCH$_2$CH$_2\underline{C}H_2$), 16.62, 16.21, 16.09 and 13.00 (4 x $\underline{C}H_3$).

LRMS (ES^+) *m/z*: 343.26 (100%, $[M + Na]^+$).

HRMS (ES^+): calculated for $(C_{21}H_{36}O_2 + [Na])^+$: 343.2613, found: 343.2602.

(2*E*, 6*E*, 10*E*)-3, 7, 11-Trimethyl trideca-2, 6, 10-trien-1-ol (135)

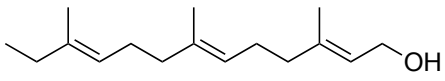

To a stirred solution of 13**4** (230 mg, 0.780 mmol) in methanol (5 mL) was added *p*-toluene sulfonic acid (13 mg, 0.078 mmol) and left to stir for 1 h. Once TLC analysis

(8:2, hexane: ethyl acetate) confirmed that all the starting material had been consumed, the methanol was removed under reduced pressure. The crude residual oil was dissolved in diethyl ether (10 mL) and washed with saturated aqueous sodium bicarbonate solution (20 mL). The separated aqueous layer was extracted with diethyl ether (5 x 10 mL). The organic layers were combined and washed with saturated aqueous sodium bicarbonate solution (20 mL) and brine (20 mL), before being dried over anhydrous magnesium sulfate and filtered under gravity. The solvent was removed under reduced pressure to give the title compound as a colourless oil (160 mg, 94%). The product was judged by ^{1}H NMR spectroscopy to be sufficiently pure to carry forward without further purification.[177]

^{1}H NMR (300 MHz, $CDCl_3$): δ 5.42 (1 H, t, $J_{H,H}$ = 7, C$\underline{H}$CH_2OH), 5.13-5.06 (2 H, m, 2 x C=C$\underline{H}$CH_2CH_2), 4.15 (2 H, d, $J_{H,H}$ = 7, C=CHC$\underline{H_2}$OH), 2.13-1.90 (10 H, m, 2 x C=CHC$\underline{H_2}$C$\underline{H_2}$ and C$\underline{H_2}$CH_3), 1.68 (3 H, s, C$\underline{H_3}$C=CH), 1.60 (6 H, s, 2 x C$\underline{H_3}$C=CH) and 0.97 (3 H, t, $J_{H,H}$ = 7.5, CH_3CCH_2C$\underline{H_3}$).

^{13}C NMR (125 MHz, $CDCl_3$): δ 140.1, 137.1 and 135.6 (3 x $CH_3\underline{C}$CH), 124.0, 123.5 and 122.9 (3 x CH_3C$\underline{C}$H), 59.61 (CHC$\underline{H_2}$OH), 39.91 and 39.74 and 32.52 (3 x $CH_3\underline{C}H_2$), 26.74 and 26.48 (2 x CCH$\underline{C}H_2CH_2$), 16.47, 16.21, 16.09, 12.99 (4 x $\underline{C}H_3$).

LRMS (EI^+) *m/z*: 218.20 (56%, $[M - H_2O]^+$), 189.17 (48), 161.13 (50), 119.09 (100), 93.07 (81).

HRMS (EI^+): calculated for $(C_{16}H_{28}O - [H_2O])^+$: 218.2041, found: 218.2035.

(2*E*, 6*E*, 10*E*)-1-Bromo-3, 7, 11-trimethyl trideca-2, 6, 10-triene (136)

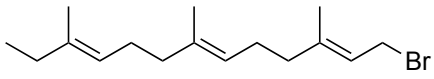

To a stirred solution of 13**5** (160 mg, 0.677 mmol) in anhydrous THF (5 mL) was added phosphorous tribromide (31.8 μL, 335 μmol). The reaction was left to stir for 30 min under argon. Once TLC analysis (8:2, hexane: ethyl acetate) confirmed full consumption of the starting material, THF and phosphorous tribromide were removed under reduced pressure. The residual oil was dissolved in diethyl ether (20 mL) and the organic solution was washed with saturated aqueous sodium bicarbonate solution (20 mL). The layers were separated and the aqueous layer was extracted with additional diethyl ether (3 x 10 mL). The combined organic layers were washed with brine (20 mL), dried over anhydrous magnesium sulfate and filtered under gravity. The solvent was removed under reduced pressure to give the title compound as a yellow oil (180 mg, 89%). The product was judged by ^{1}H NMR spectroscopy to be sufficiently pure to carry forward without further purification.[168]

^{1}H NMR (300 MHz, $CDCl_3$): δ 5.53 (1 H, t, $J_{H,H}$ = 8.5, C<u>H</u>CH_2Br), 5.13-5.03 (2 H, m, 2 x C=C<u>H</u>CH_2CH_2), 4.02 (2 H, d, $J_{H,H}$ = 8.5, C<u>H$_2$</u>Br), 2.18-1.87 (10 H, m, 2 x C=CHC<u>H$_2$</u>C<u>H$_2$</u> and C<u>H$_2$</u>CH_3), 1.73 (3 H, s, C<u>H$_3$C=CH</u>), 1.60 (6 H, s, 2 x C<u>H$_3$C=CH</u>) and 0.98 (3 H, t, $J_{H,H}$ = 7.5, CH_2C<u>H$_3$</u>).

(2*E*, 6*E*, 10*E*)-3, 7, 11-Trimethyl trideca-2, 6, 10-trien-1-yl diphosphate (128)

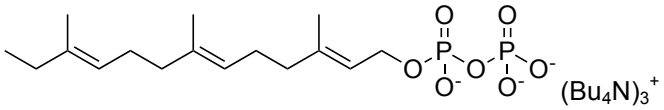

A stirred solution of **136** (180 mg, 0.604 mmol) in anhydrous acetonitrile (10 mL) was treated with **121** (1.1 g, 1.2 mmol). The reaction was left for 48 h to stir under nitrogen. The solvent was removed under reduced pressure and the resulting crude oil was purified by flash chromatography on silica gel (6:2.5:0.5, isopropanol: water: ammonium hydroxide). Fractions that contained the diphosphate as judged by comparison with an authentic FDP standard by TLC (6:3:1, isopropanol: water: ammonium hydroxide) were collected. The isopropanol was removed under reduced pressure and the remaining solution was lyophilized to give the title compound as colourless oil (0.12 g, 51%).[169]

^{1}H NMR (500 MHz, $CDCl_3$): δ 5.46 (1 H, t, $J_{H,H}$ = 6.5, C<u>H</u>CH_2O), 5.25-5.16 (2 H, m, 2 x CC<u>H</u>CH_2CH_2), 4.48 (2 H, t, $J_{H,H}$ = 6.5, CHC<u>H$_2$</u>O), 3.22-3.18 (24 H, m, 12 x NC<u>H$_2$</u>$CH_2CH_2CH_3$), 2.21-1.91 (10 H, m, 2 x CCHC<u>H$_2$</u>C<u>H$_2$</u> and CH_3CC<u>H$_2$</u>CH_3), 1.73-1.63 (33 H, m, 12 x NCH_2C<u>H$_2$</u>CH_2CH_3 and 3 x CHCC<u>H$_3$</u>), 1.41-1.32 (24 H, m, 12 x NCH_2CH_2C<u>H$_2$</u>CH_3), 0.99-0.93 (39 H, m, 12 x $NCH_2CH_2CH_2$C<u>H$_3$</u> and CH_3CCH_2C<u>H$_3$</u>).

^{31}P NMR (121 MHz, D_2O): δ -9.59 (d, $J_{P,P}$ = 18), -10.82 (d, $J_{P,P}$ = 18).

HRMS (ES^-): calculated for $(C_{16}H_{30}O_7P_2 – [H])^-$: 395.1389, found: 395.1371.

7.2.5 Preparation of 13-methyl farnesyl diphosphate (13-Methyl FDP, 129)

(6*E*, 10*E*)-2-Bromo-2, 6, 10-trimethyl-12-((tetrahydro-2*H*-pyran-2-yl) oxy) dodeca-6,10-dien-3-ol (137)[179]

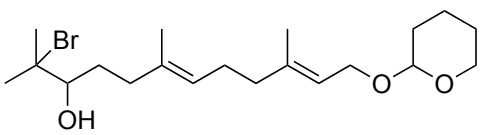

N-bromosuccinimide (1.90 g, 10.7 mmol) was added in small portions to a stirred solution of **131** (3.0 g, 9.8 mmol) in a mixture of THF (100 mL) and water (40 mL) at 5

°C. Additional water was added drop-wise when needed to retain the cloudiness of the solution. Once TLC analysis (8:2, hexane: ethyl actetate) confirmed that there was no starting material left, the reaction was quenched with brine (50 mL). The layers were separated and the aqueous layer was extracted with diethyl ether (5 x 20 mL). Pooled diethyl ether extracts were washed with saturated aqueous sodium bicarbonate solution (20 mL), brine (30 mL), dried over anhydrous magnesium sulfate, filtered under gravity and concentrated under reduced pressure. The crude oil was purified by flash chromatography on silica gel (4:1, hexane: ethyl acetate) to give the title compound as a colourless oil (2.3 g, 67%).[178]

^{1}H NMR (400 MHz, $CDCl_3$): δ 5.36 (1 H, t, $J_{H,H}$ = 6.5, C<u>H</u>CH_2O), 5.20 (1 H, t, $J_{H,H}$ = 6.5, CH_3CC<u>H</u>CH_2CH_2), 4.63 (1 H, t, $J_{H,H}$ = 3.5, OC<u>H</u>O), 4.24 (1 H, dd, $J_{H,H}$ = 12 and 6.5, CCHC<u>H$_A$</u>O), 4.03 (1 H, dd, $J_{H,H}$ = 12 and 7.5, CCHC<u>H$_B$</u>O), 3.97 (1 H, dt, $J_{H,H}$ = 11.5 and 1.5, OHC<u>H</u>CH_2), 3.92-3.49 (2 H, m, OC<u>H$_2$</u>CH_2), 2.35-2.04 (8 H, m, 2 x CCHC<u>H$_2$</u>C<u>H$_2$</u>), 1.86-1.51 (6 H, m, OCHC<u>H$_2$</u>C<u>H$_2$</u>C<u>H$_2$</u>), 1.68, 1.59, 1.34, 1.33 (4 x 3 H, 4 x s, 4 x C<u>H$_3$</u>).

^{13}C NMR (125 MHz, $CDCl_3$): δ 139.4 and 133.5 (2 x CH_3<u>C</u>=CH), 125.9 and 120.9 (2 x CH_3C=<u>C</u>H), 97.98 (O<u>C</u>HO), 94.85 (<u>C</u>HOH), 63.87 and 62.52 (2 x CHO<u>C</u>H_2), 39.65 (CH_3<u>C</u>Br), 38.31 and 32.23 (2 x CH_3<u>C</u>CH_2), 30.88 (OCH<u>C</u>H_2), 26.72 and 26.39 (2 x C=CH<u>C</u>H_2CH_2), 26.03 and 25.66 (2 x OHCHC<u>C</u>H_3), 25.41 (OCH_2<u>C</u>H_2), 19.80 (OCH_2CH_2<u>C</u>H_2), 16.63 and 16.03 (2 x CH_2<u>C</u>CH_3).

LRMS (ES^+) *m/z*: 425.17 (100%, $[C_{20}H_{35}O_3{}^{79}Br + Na]^+$), 427.17 (91, $[C_{20}H_{35}O_3{}^{81}Br + Na]^+$).

HRMS (ES^+): calculated for $(C_{20}H_{35}O_3{}^{79}Br + [Na])^+$: 425.1667, found: 425.1660.

2-(((2*E*, 6*E*)-9-(3, 3-Dimethyl oxiran-2-yl)-3, 7-dimethyl nona-2, 6-dien-1-yl) oxy) tetrahydro-2*H*-pyran (138)[179]

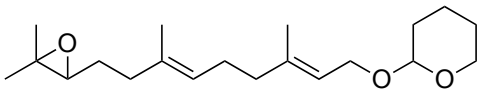

To a stirred solution of potassium carbonate (2.40 g, 17.4 mmol) in methanol (50 mL) was added **137** (3.5 g, 8.7 mmol). The mixture was stirred for 1 h at room temperature. The methanol was removed and the residual oil was dissolved in diethyl ether (20 mL). A solution of saturated aqueous sodium bicarbonate solution (80 mL) was added to dilute the solution. The layers were separated and the aqueous layer was washed with additional diethyl ether (5 x 20 mL). Combined ether extracts were washed with brine (20 mL), dried over anhydrous magnesium sulfate, filtered under gravity and concentrated under reduced pressure. The crude oil was purified by flash

chromatography on silica gel (4:1, hexane: ethyl acetate) to give the title compound as a colourless oil (2.3 g, 81%).[178]

^{1}H NMR (300 MHz, $CDCl_3$): δ 5.36 (1 H, t, $J_{H,H}$ = 7.0, C$\underline{H}$CH_2O), 5.15 (1 H, t, $J_{H,H}$ = 6.5, CH_3CC$\underline{H}$CH_2CH_2), 4.62 (1 H, t, $J_{H,H}$ = 3.5, OC$\underline{H}$O), 4.24 (1 H, dd, $J_{H,H}$ = 12.0 and 6.5, CCHC$\underline{H_A}$O), 4.01 (1 H, dd, $J_{H,H}$ = 12.0 and 7.5, CCHC$\underline{H_B}$O), 3.92-3.47 (2 H, m, OC$\underline{H_2}$CH_2), 2.70 (1 H, t, $J_{H,H}$ = 6.0, COC$\underline{H}$), 2.15-1.80 (8 H, m, 2 x CCHC$\underline{H_2}$C$\underline{H_2}$), 1.72 - 1.49 (6 H, m, OCHC$\underline{H_2}$C$\underline{H_2}$C$\underline{H_2}$), 1.67, 1.61, 1.29 and 1.25 (4 x 3 H, 4 x s, 4 x C$\underline{H_3}$).

^{13}C NMR (125 MHz, $CDCl_3$): δ 140.3 and 134.5 (2 x $CH_3\underline{C}$CH), 124.7 and 120.8 (2 x CH_3C$\underline{C}$H), 98.02 (O$\underline{C}$HO), 64.37, 63.83, 62.48 and 58.52 (2 x O$\underline{C}$H and 2 x O$\underline{C}H_2$), 39.72 and 36.48 (2 x $CH_3\underline{C}CH_2$), 30.89 (OCH$\underline{C}H_2$), 27.61 and 26.45 (2 x CCH$\underline{C}H_2$CH_2), 25.67 (OC$H_2\underline{C}H_2$), 25.08 (O$\underline{C}CH_3$), 19.81 (OCH_2C$H_2\underline{C}H_2$), 18.93 (O$\underline{C}CH_3$), 16.61 and 16.19 (2 x $CH_2\underline{C}CH_3$).

LRMS (ES^+) *m/z*: 345.24 (100%, $[M + Na]^+$), 309.17 (25), 250.14 (7).

HRMS (ES^+): calculated for $(C_{20}H_{34}O_3 + [Na])^+$: 345.2406, found: 345.2393.

(4*E*, 8*E*)-4, 8-Dimethyl-10-((tetrahydro-2*H*-pyran-2-yl) oxy) deca-4, 8-dienal (139)

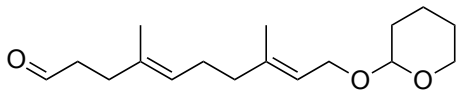

A stirred solution of **138** (330 mg, 1.02 mmol) in a mixture of THF (10 mL) and water (1 mL) at 0 °C was treated sequentially with sodium periodate (130 mg, 0.610 mmol) and periodic acid (260 mg, 1.14 mmol). The resulting biphasic solution was stirred at 0 °C for 10 min and was then allowed to warm to room temperature. After 1 h at room temperature, the reaction was quenched with saturated aqueous sodium bicarbonate solution (25 mL) and poured into brine (25 mL). The layers were separated and the aqueous layer was extracted with diethyl ether (5 x 20 mL). Combined organic layers were washed with brine (20 mL), dried over anhydrous magnesium sulfate, filtered under gravity and concentrated under reduced pressure. The resulting oil was purified by flash chromatography on silica gel (4:1, hexane: ethyl acetate) to give the title compound as a colourless oil (250 mg, 87%).[179]

^{1}H NMR (300 MHz, $CDCl_3$): δ 9.75 (1 H, t, $J_{H,H}$ = 2.0, $CCH_2CH_2C\underline{H}O$), 5.34 (1 H, t, $J_{H,H}$ = 6.5, C$\underline{H}$CH_2O), 5.13 (1 H, t, $J_{H,H}$ = 6.5, CC$\underline{H}$CH_2CH_2), 4.62 (1 H, t, $J_{H,H}$ = 4.0, OC$\underline{H}$O), 4.24 (1 H, dd, $J_{H,H}$ = 12.0 and 6.5, CCHC$\underline{H_A}$O), 4.01 (1 H, dd, $J_{H,H}$ = 12.0 and 7.5, CCHC$\underline{H_B}$O), 3.93-3.47 (2 H, m, OC$\underline{H_2}$CH_2), 2.54-2.48 (2 H, m, OCHC$\underline{H_2}$CH_2C), 2.31 (2 H, t, $J_{H,H}$ = 7.5, OCHCH_2C$\underline{H_2}$C), 2.13-2.03 (4 H, m, CCHC$\underline{H_2}$C$\underline{H_2}$), 1.75-1.50 (6 H, m, OCHC$\underline{H_2}$C$\underline{H_2}$C$\underline{H_2}$), 1.67 and 1.61 (2 x 3 H, 2 x s, 2 x C$\underline{H_3}$).

^{13}C NMR (125 MHz, $CDCl_3$): δ 202.9 ($CCH_2CH_2\underline{C}HO$), 140.1 and 133.4 (2 x $CH_3\underline{C}CH$), 125.2 and 121.0 (2 x $CH_3C\underline{C}H$), 98.05 ($O\underline{C}HO$), 63.83 and 62.50 (2 x $CHO\underline{C}H_2$), 42.33 ($CCH_2\underline{C}H_2CHO$), 39.57 and 31.99 (2 x $CH_3C\underline{C}H_2$), 30.90 ($OCH\underline{C}H_2$), 26.34 ($CCH\underline{C}H_2CH_2$), 25.67 ($OCH_2\underline{C}H_2$), 19.81 ($OCH_2CH_2\underline{C}H_2$), 16.58 and 16.29 (2 x $\underline{C}H_3$).
LRMS (ES^+) *m/z*: 303.19 (100%, $[M + Na]^+$), 227.13 (10).
HRMS (ES^+): calculated for $(C_{17}H_{28}O_3 + [Na])^+$: 303.1936, found: 303.1943.

(2*Z*, 6*E*, 10*E*)-Ethyl-2, 6, 10-trimethyl-12-((tetrahydro-2*H*-pyran-2-yl) oxy) dodeca-2, 6, 10-trienoate (140)

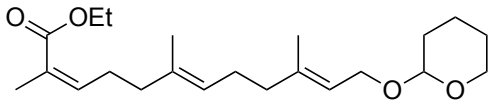

To a stirred solution of **141** (123 mg, 0.355 mmol) in anhydrous THF (5 mL) was added 18-crown-6 (400 μL, 1.88 mmol) and the solution was cooled to -78 °C. Potassium bis(trimethylsilyl)amide (KHMDS) (1 M in THF, 360 μL, 0.360 mmol) was added drop-wise over 5 min and then was left to stir for 15 min. **139** (100 mg, 0.357 mmol) was dissolved in a minimal amount of anhydrous THF (5 mL) and added slowly over 5 min to the reaction. The reaction was stirred for 1 h before being quenched with saturated aqueous ammonium chloride solution (20 mL). The layers were separated and the aqueous layer was extracted with diethyl ether (3 x 20 mL). Combined ether extracts were washed with brine (10 mL), dried over magnesium sulfate, filtered under gravity and concentrated under reduced pressure. The crude product was purified by flash chromatography on silica gel (9:1, hexane: ethyl acetate) to give the title compound as a colourless oil (36 mg, 41%).
^{1}H NMR (300 MHz, $CDCl_3$): δ 5.90 (1 H, t, $J_{H,H}$ = 7.5, $EtO_2CC=C\underline{H}$), 5.36 (1 H, t, $J_{H,H}$ = 6.5, $C\underline{H}CH_2O$), 5.13 (1 H, t, $J_{H,H}$ = 6.5, $CC\underline{H}CH_2CH_2$), 4.62 (1 H, t, $J_{H,H}$ = 4.0, $OC\underline{H}O$), 4.27-4.16 (3 H, m, $CCHC\underline{H}_AO$ and $COC\underline{H}_2CH_3$), 4.19 (2 H, q, $J_{H,H}$ = 7.0, $COC\underline{H}_2CH_3$), 4.02 (1 H, dd, $J_{H,H}$ = 12.0 and 7.5, $CCHC\underline{H}_BO$), 3.93-3.47 (2 H, m, $OC\underline{H}_2CH_2$), 2.59-2.51 (2 H, m, 2 x $C=CHC\underline{H}_2CH_2$), 2.16-2.03 (6 H, m, $C=CHC\underline{H}_2C\underline{H}_2$ and 2 x $C=CHCH_2C\underline{H}_2$), 1.88 and 1.68 (2 x 3 H, 2 x s, 2 x $C\underline{H}_3$), 1.64-1.49 (6 H, m, $OCHC\underline{H}_2C\underline{H}_2C\underline{H}_2$), 1.59 (3 H, s, $C\underline{H}_3$), 1.30 (3 H, t, $J_{H,H}$ = 7.0, $CH_2C\underline{H}_3$).
^{13}C NMR (75 MHz, $CDCl_3$): δ 168.4 ($\underline{C}OCH_2CH_3$), 142.8, 140.4 and 134.7 (3 x $CH_3\underline{C}CH$), 127.3, 124.7 and 120.8 (3 x $CH_3C\underline{C}H$), 98.01($O\underline{C}HO$), 63.84 and 62.48 (2 x $CHO\underline{C}H_2$), 60.23 ($CO\underline{C}H_2CH_3$), 39.78 and 39.30 (2 x $CH_3C\underline{C}H_2$), 30.90 ($OCH\underline{C}H_2$), 28.14 and 26.46 (2 x $CCH\underline{C}H_2CH_2$), 25.68 ($OCH_2\underline{C}H_2$), 20.84 ($OCC\underline{C}H_3$), 19.81 ($OCH_2CH_2\underline{C}H_2$), 16.62 and 16.05 (2 x $CH_2C\underline{C}H_3$), 14.49 ($COCH_2\underline{C}H_3$).

LRMS (AP^+) *m/z*: 387.25 (100%, $[M + Na]^+$), 347.26 (21, $[M\text{-}OH]^+$).

HRMS (AP^+): calculated for ($C_{22}H_{36}O_4$ + $[Na]$)$^+$: 387.2511, found: 387.2514.

(2*Z*, 6*E*, 10*E*)-2, 6, 10-Trimethyl-12-((tetrahydro-2H-pyran-2-yl) oxy) dodeca-2, 6, 10-trien-1-ol (149)

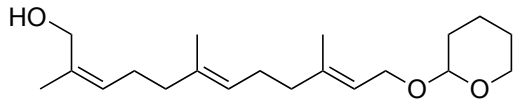

To a stirred solution of **140** (0.20 g, 0.55 mmol) in anhydrous THF (5 mL) at 78 °C was added, drop-wise, DIBAL-H (1 M in toluene, 1.7 mL, 1.7 mmol) and the reaction was left to stir until TLC analysis (8:2, hexane: ethyl acetate) showed full consumption of starting material (ca. 1 h). The reaction was quenched with saturated aqueous sodium bicarbonate solution (30 mL) and left to stir for 1 h. The layers were separated and the aqueous layer was washed with diethyl ether (3 x 10 mL), brine (10 mL) and dried over anhydrous magnesium sulfate before being filtered under gravity and concentrated under reduced pressure. The crude oil was purified by flash chromatography on silica gel (4:1, hexane: ethyl acetate) to give the title compound as a colourless oil (110 mg, 62%).[145]

^{1}H NMR (300 MHz, $CDCl_3$): δ 5.36 (1 H, t, $J_{H,H}$ = 7.0, C$\underline{H}$CH_2O), 5.28 (1 H, t, $J_{H,H}$ = 7.0, OHCH_2CC$\underline{H}$), 5.10 (1 H, t, $J_{H,H}$ = 6.5, CC$\underline{H}$CH_2CH_2), 4.63 (1 H, t, $J_{H,H}$ = 4.0, OC$\underline{H}$O), 4.24 (1 H, dd, $J_{H,H}$= 12.0 and 6.5, CCHC$\underline{H}_A$O), 4.11 (2 H, s, OHC$\underline{H}_2$), 4.03 (1 H, dd, $J_{H,H}$= 12.0 and 7.5, CCHC$\underline{H}_B$O), 3.93-3.48 (2 H, m, OC$\underline{H}_2$CH_2), 2.18-1.96 (8 H, m, 2 x CCHC$\underline{H}_2$C$\underline{H}_2$), 1.79 and 1.68 (2 x 3 H, 2 x s, 2 x C$\underline{H}_3$), 1.61-1.48 (6 H, m, OCHC$\underline{H}_2$C$\underline{H}_2$C$\underline{H}_2$), 1.59 (3 H, s, C$\underline{H}_3$).

^{13}C NMR (75 MHz, $CDCl_3$): δ 140.3, 135.0 and 134.6 (3 x $CH_3\underline{C}$CH), 128.4, 124.7 and 120.8 (3 x $CH_3\underline{C}\underline{C}$H), 98.00 (O$\underline{C}$HO), 63.84 and 62.49 (2 x CHO$\underline{C}H_2$), 61.79 (OH$\underline{C}H_2$), 39.99 and 39.75 (2 x $CH_3\underline{C}CH_2$), 30.89 (OCH$\underline{C}H_2$), 26.39 and 25.67 (2 x CCH$\underline{C}H_2$CH_2), 21.47 (OC$H_2\underline{C}H_2$), 19.80 (OCH_2C$H_2\underline{C}H_2$), 16.60, 16.23 and 14.32 (3 x CH_3).

LRMS (ES^+) *m/z*: 345.24 (100%, $[M + Na]^+$).

HRMS (ES^+): calculated for ($C_{20}H_{34}O_3$ + $[Na]$)$^+$: 345.2406, found: 345.2390.

2-(((2*E*, 6*E*, 10*Z*)-12-Bromo-3, 7, 11-trimethyl dodeca-2, 6, 10-trien-1-yl) oxy) tetrahydro-2*H*-pyran (150)

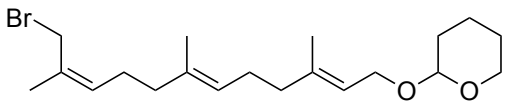

To a stirred solution of **149** (400 mg, 1.24 mmol) in anhydrous THF (12 mL) at -45 °C was added anhydrous triethylamine (0.50 mL, 3.5 mmol) followed by methanesulfonyl chloride (140 μL, 1.81 mmol) and the reaction was left to stir for 15 min. Lithium bromide (121 mg, 1.40 mmol) was added and the solution was warmed to room temperature. The reaction was left to stir until TLC analysis (8:2, hexane: ethyl acetate) showed full consumption of starting material (ca. 2 h). The reaction was quenched with saturated brine (10 mL) and the biphasic layers were separated. The aqueous layer was washed with diethyl ether (3 x 10 mL), 1 M hydrochloric acid (2 x 10 mL) and brine (10 mL). The resulting solution was dried over anhydrous magnesium sulfate, filtered under gravity, and concentrated under reduced pressure to give the title compound as an orange oil (450 mg, 97%). The product was judged by ^{1}H NMR spectroscopy to be sufficiently pure to carry forward without further purification.

^{1}H NMR (300 MHz, $CDCl_3$): δ 5.36 (2 H, t, $J_{H,H}$ = 7.0, C$\underline{H}$C$\underline{H_2}$O and C$\underline{H}$C$\underline{H_2}$Br), 5.12 (1 H, t, $J_{H,H}$ = 7.0, CC$\underline{H}$C$\underline{H_2}$C$\underline{H_2}$), 4.63 (1 H, t, $J_{H,H}$ = 4.0, OC$\underline{H}$O), 4.24 (1 H, dd, $J_{H,H}$= 12.0 and 6.5, CCHC$\underline{H_A}$O), 4.03 (1 H, dd, $J_{H,H}$= 12.0 and 7.5, CCHC$\underline{H_B}$O), 3.98 (2 H, s, C$\underline{H_2}$Br), 3.93-3.48 (2 H, m, OC$\underline{H_2}$CH$_2$), 2.17-2.01 (8 H, m, 2 x CCHC$\underline{H_2}$C$\underline{H_2}$), 1.82 and 1.68 (2 x 3 H, 2 x s, 2 x C$\underline{H_3}$), 1.63-1.52 (6 H, m, OCHC$\underline{H_2}$C$\underline{H_2}$C$\underline{H_2}$), 1.61 (3 H, s, C$\underline{H_3}$).

2-(((2*E*, 6*E*, 10*Z*)-3, 7, 11-Trimethyl trideca-2, 6, 10-trien-1-yl) oxy) tetrahydro-2*H*-pyran (151)

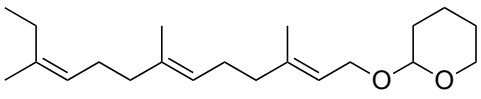

Copper iodide (475 mg, 2.49 mmol) and methyl lithium (1.6 M in diethyl ether, 3.5 mL, 5.0 mmol) were mixed together at 0 °C for 30 min. An initial yellow precipitate formed which turned into a colourless solution (presence of lithium dimethylcuprate). **150** (480 mg, 1.25 mmol) in minimal anhydrous diethyl ether (5 mL) was added and the temperature was reduced to -78 °C. Once TLC analysis (8:2, hexane: ethyl acetate) showed full consumption of starting material, ammonia (10 mL) was added to quench the reaction and the solution was left stirring overnight for the phases to separate. The biphasic layers were separated and the aqueous layer was washed with diethyl ether

(4 x 10 mL). Combined organic layers were washed with brine (10 mL), dried over anhydrous magnesium sulfate, filtered under gravity and concentrated under reduced pressure. The crude product was purified by flash chromatography on silica gel (4:1, hexane: ethyl acetate) to give the title compound as a colourless oil (240 mg, 60%).

^{1}H NMR (400 MHz, $CDCl_3$): δ 5.36 (1 H, t, $J_{H,H}$ = 6.5, C<u>H</u>CH_2O), 5.13-5.04 (2 H, m, 2 x CC<u>H</u>CH_2CH_2), 4.62 (1 H, t, $J_{H,H}$ = 4.0, OC<u>H</u>O), 4.24 (1 H, dd, $J_{H,H}$= 12.0 and 6.5, CCHC<u>H</u>$_A$O), 4.03 (1 H, dd, $J_{H,H}$= 12.0 and 7.5, CCHC<u>H</u>$_B$O), 3.92-3.49 (2 H, m, OC<u>H</u>$_2$$CH_2$), 2.14-1.79 (10 H, m, 2 x CCHC<u>H</u>$_2$C<u>H</u>$_2$ and CH_3C<u>H</u>$_2$C), 1.68 (3 H, s, CC<u>H</u>$_3$), 1.61-1.50 (6 H, m, OCHC<u>H</u>$_2$C<u>H</u>$_2$C<u>H</u>$_2$), 1.59 (6 H, s, 2 x CC<u>H</u>$_3$), 0.96 (3 H, t, $J_{H,H}$ = 7.5, CH_2C<u>H</u>$_3$).

^{13}C NMR (100 MHz, $CDCl_3$): δ 140.4, 134.6 and 131.6 (3 x CH_3<u>C</u>CH), 131.6, 124.8 and 120.8 (3 x CH_3C<u>C</u>H), 98.02 (O<u>C</u>HO), 63.86 and 62.49 (2 x CHO<u>C</u>H_2), 39.76, 39.21 and 32.69 (3 x CH_3<u>C</u>CH_2), 30.91 (OCH<u>C</u>H_2), 26.78 and 26.46 (2 x CCH<u>C</u>H_2CH_2), 25.69 (OCH_2<u>C</u>H_2), 22.06 (CH_3CH_2<u>C</u>CH_3), 19.83 (OCH_2CH_2<u>C</u>H_2), 16.63, 16.20 and 14.32 (<u>C</u>H_3).

HRMS (EI^+): calculated for $C_{21}H_{36}O_2^+$: 320.2715, found: 320.2732.

(2*E*, 6*E*, 10*Z*)-3, 7, 11-Trimethyl trideca-2, 6, 10-trien-1-ol (152)

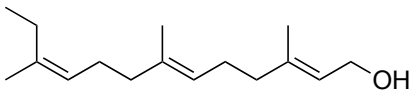

To a stirred solution of **151** (110 mg, 340 μmol) was added pyridinium p-toluenesulfonate (8.0 mg, 30 μmol) in methanol (25 mL) and stirred at room temperature overnight. The reaction mixture was heated to 50 °C for 1 h before being quenched with triethylamine (10 mL). The solvent was removed under reduced pressure and the residual oil was dissolved with diethyl ether (20 mL) and washed with saturated sodium bicarbonate solution (2 x 10 mL) and brine (10 mL). The resulting solution was dried over anhydrous magnesium sulfate, filtered under gravity and concentrated under reduced pressure to give the title compound as a colourless oil (40 mg, 49%). The product was judged by ^{1}H NMR spectroscopy to be sufficiently pure to carry forward without further purification.[177]

^{1}H NMR (300 MHz, $CDCl_3$): δ 5.42 (1 H, t, $J_{H,H}$ = 7.0, C<u>H</u>CH_2O), 5.12-5.04 (2 H, m, 2 x CC<u>H</u>CH_2CH_2), 4.15 (2 H, d, $J_{H,H}$ = 7.0, C<u>H</u>$_2$OH), 2.15-1.87 (10 H, m, 2 x CCHC<u>H</u>$_2$C<u>H</u>$_2$ and CH_3C<u>H</u>$_2$C), 1.68 (6 H, s, 2 x C<u>H</u>$_3$), 1.60 (3 H, s, C<u>H</u>$_3$), 1.01-0.93 (3 H, m, CH_2C<u>H</u>$_3$).

^{13}C NMR (75 MHz, $CDCl_3$): δ 140.0, 137.3 and 135.5 (3 x CH_3<u>C</u>CH), 124.1, 124.0 and 123.5 (3 x CH_3C<u>C</u>H), 59.57 (<u>C</u>H_2OH), 40.18, 39.72 and 39.54 (CH_3<u>C</u>CH_2), 26.47 and

26.45 (2 x CCH$\underline{C}$H$_2$CH$_2$), 23.04 (CH$_3$CH$_2$C$\underline{C}$H$_3$), 16.46 and 16.20 (2 x C$\underline{C}$H$_3$), 13.00 (CH$_2\underline{C}$H$_3$).

HRMS (EI$^+$): calculated for $C_{16}H_{28}O^+$: 236.2140, found: 236.2150.

(2*E*, 6*E*, 10*Z*)-3, 7, 11-Trimethyl trideca-2, 6, 10-trien-1-yl diphosphate (129)

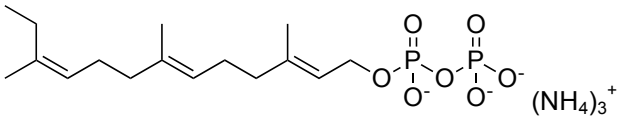

To a cold suspension (0 °C) of **152** (40 mg, 0.17 mmol), lithium chloride (115 mg, 2.71 mmol) and *s*-collidine (134 μL, 1.03 mmol) in anhydrous DMF (10 mL) was added methanesulfonyl chloride (26.2 μL, 340 μmol), under nitrogen. The mixture was stirred for 3 h. The solution was poured into ice-cold water (30 mL) and extracted with diethyl ether (4 x 15 mL). Combined organic extracts were washed with saturated aqueous copper sulfate solution (3 x 20 mL), water (2 x 20 mL) and saturated aqueous ammonium bicarbonate solution (2 x 20 mL), dried over anhydrous magnesium sulfate, filtered under gravity and concentrated under reduced pressure to give the crude chloride intermediate.

To a stirred solution of **121** (46 mg, 0.52 mmol) in anhydrous acetonitrile (5 mL) under N_2 was added the crude chloride in acetonitrile (3 mL). This was left for 24 h at room temperature. The solvent was removed under reduced pressure and the resulting oil was dissolved in a minimum amount of ion-exchange buffer (25 mM ammonium bicarbonate solution containing 2% isopropanol).

The crude compound in buffer was then eluted through the NH_4^+-form cation exchange column with additional ion exchange buffer. Fractions that contained the diphosphate as judged by comparison with an authentic FDP standard by TLC (6:3:1 isopropanol: water: ammonium hydroxide) were collected and lyophilized. The resulting dry powder was purified by methanol precipitation to give the title compound as a colourless oil (27 mg, 36%).

^{1}H NMR (500 MHz, D_2O): δ 5.44 (1 H, t, $J_{H,H}$ = 6.5, CH$_3$CC$\underline{H}$CH$_2$O), 5.20 (1 H, t, $J_{H,H}$ = 6.5, CH$_3$CC$\underline{H}$), 5.14 (1 H, t, $J_{H,H}$ = 6.5, CH$_3$CC$\underline{H}$), 4.46 (2 H, m, CHC$\underline{H}_2$O), 2.16-1.91 (10 H, m, 2 x CCHC$\underline{H}_2$C$\underline{H}_2$ and CH$_3$C$\underline{H}_2$C), 1.70, 1.67 and 1.60 (3 x 3 H, 3 x s, 3 x CC$\underline{H}_3$), 0.93 (3 H, t, $J_{H,H}$ = 7.5, CH$_2$C$\underline{H}_3$).

^{31}P NMR (121 MHz, D_2O): δ -10.64 (m).

HRMS (ES$^-$): calculated for $(C_{16}H_{30}O_7P_2 - [H])^-$: 395.1389, found: 395.1401.

7.2.6 Preparation of 14-methyl farnesyl diphosphate (14-Methyl FDP, 130)

Ethyl 7-methyl-3-oxooct-6-enoate (155)

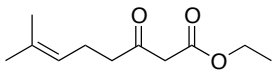

To a stirred suspension of sodium hydride (3.2 g, 60% in mineral oil, 80 mmol) in anhydrous THF (50 mL) at 0 °C, was added ethyl acetoacetate (5.2 g, 40 mmol) and then *n*-butyllithium solution (2.2 M in hexane, 20 mL, 49 mmol). The solution was left to stir for 30 min. A cooled solution of 3,3-dimethylallyl bromide (2.0 g, 15.4 mmol) in anhydrous THF (10 mL) was added via syringe drop-wise. After 3 h the solution was quenched with saturated aqueous ammonium chloride solution (50 mL) and the biphasic layers were separated. The aqueous layer was washed with additional diethyl ether (3 x 50 mL). Combined organic layers were washed with water (10 mL), brine (10 mL), dried over anhydrous magnesium sulfate, filtered under gravity and concentrated under reduced pressure. The crude oil was purified by flash chromatography on silica gel (4:1, hexane: ethyl acetate) to give the title compound as a colourless oil (1.7 g, 64%).

^{1}H NMR (300 MHz, $CDCl_3$): δ 5.05 (1 H, t, $J_{H,H}$ = 7.0, CC<u>H</u>CH_2), 4.19 (2 H, q, $J_{H,H}$ = 7.0, OC<u>H</u>$_2$$CH_3$), 3.43 (2 H, s, C<u>H</u>$_2$CO), 2.56 (2 H, t, $J_{H,H}$ = 7.5, $CCHCH_2C$<u>H</u>$_2$), 2.31-2.20 (2 H, m, $CCHC$<u>H</u>$_2$$CH_2$), 1.67 (3 H, s, CC<u>H</u>$_3$), 1.61 (3 H, s, CC<u>H</u>$_3$), 1.28 (3 H, t, $J_{H,H}$ = 7, CH_2C<u>H</u>$_3$).

^{13}C NMR (75 MHz, $CDCl_3$): δ 202.9 (O<u>C</u>O), 167.4 (O<u>C</u>CH_2), 133.3 (CH_3<u>C</u>CH), 122.4 (CH_3C<u>C</u>H), 61.54 (O<u>C</u>H_2CH_3), 49.58 (OC<u>C</u>H_2CO), 43.22 (OC<u>C</u>H_2CH_2), 25.86 ($OCCH_2$<u>C</u>H_2), 22.37 and 17.84 (2 x CHC<u>C</u>H_3), 14.28 (CH_2<u>C</u>H_3).

LRMS (EI+): 198.13 (16, M+), 180.11 (43), 152.08 (37), 130.06 (44), 82.08 (100), 67.05 (55).

HRMS (EI^+): calculated for $C_{11}H_{18}O_3^+$: 198.1256, found: 198.1257.

Ethyl (*Z*)-7-methyl-3-(((trifluoromethyl) sulfonyl) oxy) octa-2, 6-dienoate (156)

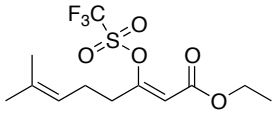

To a stirred solution of **155** (2.0 g, 10 mmol) in anhydrous DCM (150 mL) at 0 °C was added lithium trifluoromethane sulfonate (1.9 g, 12 mmol) and freshly distilled triethylamine (2.0 mL, 13 mmol). After 1 h, trifluoromethane sulfonic anhydride (2.0 mL, 12 mmol) was added and the resulting orange solution was left for an additional 2 h.

The reaction was quenched with saturated aqueous ammonium chloride solution (100 mL). The biphasic layers were separated and the aqueous layer was washed with additional DCM (3 x 50 mL). The combined organic layers were washed with saturated aqueous sodium bicarbonate solution (3 x 40 mL), brine (50 mL), dried over anhydrous magnesium sulfate, filtered under gravity and concentrated under reduced pressure. The crude oil was purified by flash chromatography on silica gel (9.7:0.3, hexane: ethyl acetate) to give the title compound as a colourless oil (2.7 g, 80%).

^{1}H NMR (300 MHz, $CDCl_3$): δ 5.74 (1 H, s, OCC<u>H</u>), 5.04 (1 H, t, $J_{H,H}$ = 7.0, $CH_3CC\underline{H}$), 4.24 (2 H, q, $J_{H,H}$ = 7.0, $OC\underline{H}_2CH_3$), 2.42-2.22 (4 H, m, $CHC\underline{H}_2C\underline{H}_2$), 1.70 (3 H, s, $CC\underline{H}_3$), 1.61 (3 H, s, $CC\underline{H}_3$), 1.30 (3 H, t, $J_{H,H}$ = 7.0, $OCH_2C\underline{H}_3$).

^{13}C NMR (75 MHz, $CDCl_3$): δ 189.3 (O<u>C</u>CH), 162.7 (O<u>C</u>O), 158.7 (CF_3), 134.7 ($CH_3\underline{C}CH$), 120.9 ($CH_3C\underline{C}H$), 112.2 (OC<u>C</u>H), 61.43 ($O\underline{C}H_2CH_3$), 34.76 ($\underline{C}H_2CH_2$), 25.84 ($C\underline{C}H_3$), 24.66 ($\underline{C}H_2CH_2$), 17.86 ($C\underline{C}H_3$), 14.21 ($OCH_2\underline{C}H_3$).

HRMS (EI^+): calculated for $C_{12}H_{17}O_5F_3S^+$: 330.0749, found: 330.0700.

Ethyl (*E*)-3-ethyl-7-methylocta-2, 6-dienoate (157)

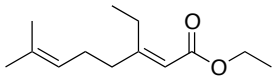

To a stirred suspension of copper iodide (3.4 g, 18 mmol) in anhydrous THF (60 mL) at 0 °C was added ethyl magnesium bromide (6.7 mL, 18 mmol) and the resulting black solution was left to stir for 30 min. The solution was cooled to -78 °C and a solution of **156** (1.0 g, 3.0 mmol) in anhydrous THF (10 mL) was added via syringe. This was left to stir for 1 h before being quenched with saturated aqueous ammonium chloride solution (50 mL). 35% ammonium hydroxide (20 mL) was added and left to stir for 1 h to allow the copper salts, formed during the quenching, to dissolve. The biphasic layers were separated and the blue aqueous layer was washed with diethyl ether (3 x 40 mL). The combined organic layers were washed with 10% ammonium hydroxide (2 x 20 mL), water (2 x 20 mL), and brine (50 mL). The resulting solution was dried over anhydrous magnesium sulfate, filtered under gravity and concentrated under reduced pressure. The crude oil was purified by flash chromatography on silica gel (9:1, hexane: ethyl acetate) to give the title compound as a colourless oil (510 mg, 80%).

^{1}H NMR (300 MHz, $CDCl_3$): δ 5.61 (1 H, s, OCC<u>H</u>), 5.09 (1 H, m, $CH_3CC\underline{H}$), 4.14 (2 H, q, $J_{H,H}$ = 7, $OC\underline{H}_2CH_3$), 2.61 (2 H, q, $J_{H,H}$ = 7.5, $CH_3C\underline{H}_2C$), 2.16 (4 H, m, $CHC\underline{H}_2C\underline{H}_2$), 1.69 (3 H, s, $CC\underline{H}_3$), 1.60 (3 H, s, $CC\underline{H}_3$), 1.28 (3 H, t, $J_{H,H}$ = 7, $OCH_2C\underline{H}_3$), 1.07 (3 H, t, $J_{H,H}$ = 7.5, $CCH_2C\underline{H}_3$).

^{13}C NMR (75 MHz, $CDCl_3$): δ 166.7 (O<u>C</u>O), 165.8 (CH_3CH_3<u>C</u>), 132.6 (CH_3<u>C</u>CH), 123.3 (CH_3C<u>C</u>H), 115.0 (C<u>C</u>HC), 59.65 (O<u>C</u>H_2CH_3), 38.13 (C<u>C</u>H_2CH_2), 26.41 (CCH$_2$<u>C</u>H$_2$), 25.87 (C<u>C</u>H_2CH_3), 25.52 and 17.90 (2 x C<u>C</u>H_3), 14.50 (OCH$_2$<u>C</u>H$_3$), 13.17 (CCH$_2$<u>C</u>H$_3$).
HRMS (EI^+): calculated for $C_{13}H_{22}O_2^+$: 210.1620, found: 210.1590.

(*E*)-3-Ethyl-7-methylocta-2, 6-dien-1-ol (158)

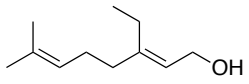

To a stirred solution of **157** (0.75 g, 3.6 mmol) in anhydrous toluene (30 mL) at -78 °C, was added diisobutylaluminium hydride (DIBAL-H) (1 M in THF, 7.1 mL, 7.1 mmol) drop-wise and the resulting solution was left to stir for 1 h whereupon TLC analysis (8:2, hexane: ethyl acetate) showed full consumption of the starting material. Methanol (10 mL) was added drop-wise and stirred whilst the reaction warmed to room temperature. Saturated aqueous ammonium chloride solution and hydrochloric acid (1 M) (80 mL; 1: 1) was added and stirred for 30 min. The biphasic layers were separated and the aqueous layer was extracted with diethyl ether (3 x 20 mL). The combined organic layers were washed with water (2 x 20 mL), brine (25 mL), dried over anhydrous magnesium sulfate, filtered under gravity and concentrated under reduced pressure to give the title compound as a colourless oil (528 mg, 88%). The product was judged by ^{1}H NMR spectroscopy to be sufficiently pure to carry forward without further purification.
^{1}H NMR (300 MHz, $CDCl_3$): δ 5.37 (1 H, t, $J_{H,H}$ = 7.0, C<u>H</u>CH$_2$OH), 5.13-5.08 (1 H, m, C<u>H</u>CH$_2$CH$_2$), 4.16 (2 H, d, $J_{H,H}$ = 7.0, CHC<u>H$_2$</u>OH), 2.13-2.05 (6 H, m, CHC<u>H$_2$</u>C<u>H$_2$</u> and CC<u>H$_2$</u>CH$_3$), 1.68 (3 H, s, CC<u>H$_3$</u>), 1.61 (3 H, s, CC<u>H$_3$</u>), 0.99 (3 H, t, $J_{H,H}$ = 7.5, CH$_2$C<u>H$_3$</u>).
^{13}C NMR (75 MHz, $CDCl_3$): δ 145.9 (CH_3CH_2<u>C</u>), 131.9 (CH_3<u>C</u>CH), 124.2 (<u>C</u>HCH$_2$OH), 122.9 (<u>C</u>HCH$_2$CH$_2$), 59.30 (CH<u>C</u>H$_2$OH), 36.56 (C<u>C</u>H$_2$CH$_2$), 26.77 (CCH$_2$<u>C</u>H$_2$), 25.88 (C<u>C</u>H$_2$CH$_3$), 23.69 and 17.90 (2 x C<u>C</u>H$_3$), 13.89 (CCH$_2$<u>C</u>H$_3$).
HRMS (EI^+): calculated for $C_{11}H_{20}O^+$: 168.1514, found: 168.1527.

(*E*)-1-Bromo-3-ethyl-7-methylocta-2, 6-diene (159)

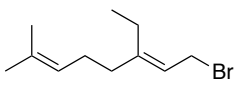

To a stirred solution of **158** (0.45 g, 2.7 mmol) in anhydrous THF (15 mL) at -45 °C was added freshly distilled triethylamine (1.1 mL, 7.9 mmol) and methanesulfonyl chloride

(0.4 mL, 5.3 mmol). After 45 min, lithium bromide (1.0 g, 10.7 mmol) was added and the solution was warmed to 0 °C and left for 2 h whereupon TLC analysis (8:2, hexane: ethyl acetate) showed full consumption of the starting material.

The solution was diluted with hexane and quenched with saturated ammonium chloride solution (20 mL). The biphasic layers were separated and the aqueous layer was washed with hexane (4 x 20 mL). Combined organic layers were washed with saturated sodium bicarbonate solution (20 mL), water (20 mL) and brine (20 mL). The solution was dried over anhydrous magnesium sulfate, filtered under gravity and concentrated with reduced pressure to give the title compound as a colourless oil (610 mg, 99%). The product was judged by ^{1}H NMR spectroscopy to be sufficiently pure to carry forward without further purification.

^{1}H NMR (300 MHz, $CDCl_3$): δ 5.49 (1 H, t, $J_{H,H}$ = 8.5, C<u>H</u>CH_2Br), 5.08 (1 H, m, C<u>H</u>CH_2CH_2), 4.04 (2 H, d, $J_{H,H}$ = 8.5, CHC<u>H$_2$</u>Br), 2.19-2.07 (6H, m, CHC<u>H$_2$</u>C<u>H$_2$</u> and CC<u>H$_2$</u>CH_3), 1.68 (3H, s, CC<u>H$_3$</u>), 1.60 (3H, s, CC<u>H$_3$</u>), 1.03 (3H, t, $J_{H,H}$ = 7.5, CH_2C<u>H$_3$</u>).

^{13}C NMR (75 MHz, $CDCl_3$): δ 149.3 (CH_3CH_2<u>C</u>), 132.2 (CH_3<u>C</u>CH), 123.8 (<u>C</u>HCH_2OH), 120.2 (<u>C</u>HCH_2CH_2), 36.59 (CH<u>C</u>H$_2$Br), 29.55 (C<u>C</u>H$_2$$CH_2$), 26.56 (CC<u>H$_2$</u>C<u>H$_2$</u>), 25.88 (C<u>C</u>H$_2$$CH_3$), 23.37 and 17.92 (2 x C<u>C</u>H$_3$), 13.13 (C<u>C</u>H$_2$C<u>H$_3$</u>).

Ethyl (*E*)-7-ethyl-11-methyl-3-oxododeca-6, 10-dienoate (160)

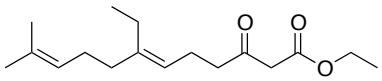

To a stirred suspension of sodium hydride (1.2 g, 30.6 mmol) in anhydrous THF (50 mL) at 0 °C, was added ethyl acetoacetate (19.7 mL, 15.3 mmol) and then *n*-butyllithium (2.5 M in hexane, 7.2 mL, 17.9 mmol). The solution was stirred for 30 min. A cooled solution of **159** (1.2 g, 5.1 mmol) in dry THF (10 mL) was added and left to stir until TLC analysis (8:2, hexane: ethyl acetate) showed complete consumption of the starting material. The reaction was quenched with saturated aqueous ammonium chloride solution (20 mL) and the biphasic layers were separated. The aqueous layer was washed with hexane (4 x 20 mL). Combined organic layers were washed with water (2 x 10 mL) and brine (10 mL) and then dried over anhydrous magnesium sulfate. The resulting solution was filtered under gravity and concentrated under reduced pressure. The crude oil was purified by flash chromatography on silica gel (8:2, hexane: ethyl acetate) to give the title compound as a colourless oil (800 mg, 56%).

^{1}H NMR (300 MHz, $CDCl_3$): δ 5.12-4.98 (2 H, m, 2 x CC<u>H</u>), 4.19 (2 H, q, $J_{H,H}$ = 7,0, OC<u>H$_2$</u>CH_3), 3.43 (2 H, s, OCC<u>H$_2$</u>CO), 2.57 (2 H, t, $J_{H,H}$ = 7.5, C<u>H$_2$</u>CH_2), 2.34-2.26 (2 H,

m, C$\underline{H}_2$CH$_2$), 2.07-1.97 (6 H, m, CH$_3$C$\underline{H}_2$ and C$\underline{H}_2$C$\underline{H}_2$), 1.68 (3 H, s, CC$\underline{H}_3$), 1.59 (3 H, s, C$\underline{H}_3$), 1.28 (3 H, t, $J_{H,H}$ = 7.0, OCH$_2$C$\underline{H}_3$), 0.95 (3 H, t, $J_{H,H}$ = 7.5, CCH$_2$C$\underline{H}_3$).

^{13}C NMR (125 MHz, $CDCl_3$): δ 202.8 (O$\underline{C}$O), 167.4 (O$\underline{C}$CH$_2$CH$_2$), 142.9 ($\underline{C}$CHCH$_2$), 131.6 ($\underline{C}$CHCH$_2$), 124.5 (C$\underline{C}$HCH$_2$), 121.8 (C$\underline{C}$HCH$_2$), 61.54 (O$\underline{C}$H$_2$CH$_3$), 49.62 (OC$\underline{C}$H$_2$CO), 43.57 (OC$\underline{C}$H$_2$CH$_2$), 36.64 ($\underline{C}$H$_2$), 27.02 ($\underline{C}$H$_2$), 25.87 (OCCH$_2$$\underline{C}H_2$), 23.32 ($\underline{C}H_2$), 22.00 and 17.88 (2 x C$\underline{C}$H$_3$), 14.29 (OCH$_2$C$\underline{H}_3$), 13.37 (CCH$_2$C$\underline{H}_3$).

LRMS (ES$^+$) *m/z*: 303.19 (100%, [M + Na]$^+$), 242.28 (31).

HRMS (ES$^+$): calculated for $C_{17}H_{28}O_3$[Na]$^+$: 303.1936, found: 303.1932.

Ethyl (2*Z*, 6*E*)-3-((diethoxyphosphoryl) oxy)-7-ethyl-11-methyl dodeca-2, 6, 10-trienoate (161)

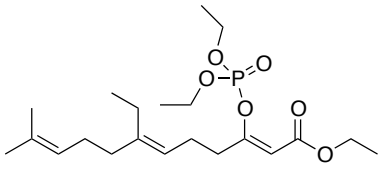

To a stirred suspension of sodium hydride (200 mg, 8.33 mmol) at 0 °C in anhydrous diethyl ether (10 mL) was added **160** (412 mg, 1.47 mmol) and the resulting solution was stirred for 30 min. Diethyl chlorophosphate (434 μL, 3.00 mmol) was added and after TLC analysis (8:2, hexane: ethyl acetate) showed complete consumption of starting material the reaction was quenched with saturated aqueous ammonium chloride solution (10 mL). The product was extracted with diethyl ether (3 x 10 mL) and the combined organic layers were washed with saturated aqueous ammonium bicarbonate solution (2 x 10 mL) and brine (10 mL). The resulting solution was dried over anhydrous magnesium sulfate, filtered under gravity and concentrated under reduced pressure. The crude oil was purified by flash chromatography on silica gel (gradient from 8:2, hexane: ethyl acetate; to 100% ethyl acetate) to give the title compound as a colourless oil (368 mg, 62%)

^{1}H NMR (300 MHz, $CDCl_3$): δ 5.35 (1 H, s, OCC$\underline{H}$), 5.11-5.02 (2 H, m, 2 x CC$\underline{H}$CH$_2$), 4.28 (2 H, q, $J_{H,H}$ = 7.0, POC$\underline{H}_2$CH$_3$), 4.25 (2 H, q, $J_{H,H}$ = 7.0, POC$\underline{H}_2$CH$_3$), 4.14 (2 H, q, $J_{H,H}$ = 7.0, COC$\underline{H}_2$CH$_3$), 2.46 (2 H, t, $J_{H,H}$ = 7.5, CC$\underline{H}_2$CH$_2$), 2.28 (2 H, m, CCH$_2$C$\underline{H}_2$), 2.09-1.95 (6 H, m, C$\underline{H}_2$ and C$\underline{H}_2$C$\underline{H}_2$), 1.67 (3 H, s, CC$\underline{H}_3$), 1.59 (3 H, s, CC$\underline{H}_3$), 1.36 (3 H, t, $J_{H,H}$ = 7.0, POCH$_2$C$\underline{H}_3$), 1.36 (3 H, t, $J_{H,H}$ = 7.0, POCH$_2$C$\underline{H}_3$), 1.27 (3 H, t, $J_{H,H}$ = 7.0, COCH$_2$C$\underline{H}_3$), 0.95 (3 H, t, $J_{H,H}$ = 7.5, CCH$_2$C$\underline{H}_3$).

^{13}C NMR (125 MHz, $CDCl_3$): δ 164.0 (O$\underline{C}$CH), 161.2 (O$\underline{C}$O), 143.1 ($\underline{C}$CHCH$_2$), 131.6 ($\underline{C}$CHCH$_2$), 124.5 (C$\underline{C}$HCH$_2$), 121.5 (C$\underline{C}$HCH$_2$), 105.5 (OC$\underline{C}$H), 66.05 (PO$\underline{C}$H$_2$CH$_3$), 66.00 (PO$\underline{C}$H$_2$CH$_3$), 60.04 (CO$\underline{C}$H$_2$CH$_3$), 36.59 (C$\underline{C}$H$_2$CH$_2$), 35.72 (CCH$_2$$\underline{C}H_2$), 27.02

($\underline{C}H_2$), 25.84 ($\underline{C}H_2$), 24.74 ($\underline{C}H_2$), 23.36 and 17.86 ($C\underline{C}H_3$), 15.93 ($POCH_2\underline{C}H_3$), 15.87 ($POCH_2\underline{C}H_3$), 14.41 ($COCH_2\underline{C}H_3$), 13.29 ($CCH_2\underline{C}H_3$).

^{31}P NMR (121 MHz, D_2O): δ -8.76 (s).

LRMS (AP^+) *m/z*: 417.24 (100%, $[M + H]^+$), 155.45 (36), 120.02 (37).

HRMS (AP^+): calculated for $(C_{21}H_{37}O_6P + [H])^+$: 417.2406, found: 417.2387.

Ethyl (2*E*, 6*E*)-7-ethyl-3, 11-dimethyl dodeca-2, 6, 10-trienoate (162)

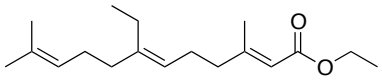

To a stirred solution of copper iodide (0.29 g, 1.5 mmol) in anhydrous diethyl ether (5 mL), was added methyl lithium (1.6 M in diethyl ether, 2.0 mL, 3.0 mmol) and the reaction was left to stir for 20 min at 0 °C under argon. The reaction was cooled to -78 °C before **161** (0.32 g, 0.76 mmol) in anhydrous diethyl ether (5 mL) was added drop-wise. After 2 h the reaction was warmed to -45 °C and methyl iodide (0.27 g, 1.9 mmol) was added. The reaction was left to stir for an additional 45 min. The reaction was quenched with saturated aqueous ammonium chloride solution (10 mL). Stirring the reaction overnight with the addition of ammonium hydroxide (20 mL) dissolved the copper salts formed. The biphasic layers were separated and the aqueous layer was washed with diethyl ether (4 x 10 mL). The combined organic layers were washed with 10% ammonium hydroxide (3 x 10 mL), water (2 x 10 mL) and brine (10 mL). The resulting solution was dried over anhydrous magnesium sulfate, filtered under gravity and concentrated under reduced pressure. The crude oil was purified by flash chromatography on silica gel (9:1, hexane: ethyl acetate) to give the title compound as a colourless oil (100 mg, 47%).

^{1}H NMR (300 MHz, $CDCl_3$): δ 5.67 (1 H, s, $CC\underline{H}C$), 5.12-5.02 (2 H, m, 2 x $CC\underline{H}CH_2$), 4.14 (2 H, q, $J_{H,H}$ = 7.0, $OC\underline{H}_2CH_3$), 2.16-1.95 (13 H, 2 x m, $CC\underline{H}_3$, $CC\underline{H}_2CH_3$ and 2 x $CHC\underline{H}_2C\underline{H}_2$), 1.60 (3 H, s, $CC\underline{H}_3$), 1.55 (3 H, s, $CC\underline{H}_3$), 1.25 (3 H, t, $J_{H,H}$ = 7.0, $OCH_2C\underline{H}_3$), 0.95 (3 H, t, $J_{H,H}$ = 7.5, $CCH_2C\underline{H}_3$).

^{13}C NMR (125 MHz, $CDCl_3$): δ 167.1 ($O\underline{C}O$), 160.1 ($CH_3\underline{C}CH_2$), 142.2 ($CH_3CH_2\underline{C}$), 131.6 ($CH_3\underline{C}CHCH_2$), 124.5 ($CC\underline{H}CH_2$), 122.6 ($CC\underline{H}CH_2$), 115.8 ($CC\underline{H}C$), 59.65 ($CO\underline{C}H_2CH_3$), 41.49 ($CH_3C\underline{C}H_2$), 36.63 ($CH_3C\underline{C}H_2$), 27.03 and 25.89 ($CCH\underline{C}H_2CH_2$), 25.79 ($C\underline{C}H_2CH_3$), 23.32, 19.04 and 17.89 (3 x $C\underline{C}H_3$), 14.52 ($COCH_2\underline{C}H_3$), 13.40 ($CCH_2\underline{C}H_3$).

HRMS (EI^+): calculated for $C_{18}H_{30}O_2^+$: 278.2246, found: 278.2238.

(2*E*, 6*E*)-7-Ethyl-3, 11-dimethyl dodeca-2, 6, 10-trien-1-ol (163)

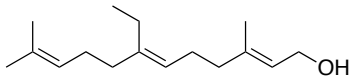

To a stirred solution of **162** (0.1 g, 0.4 mmol) in anhydrous toluene (5 mL) at -78 °C was added DIBAL-H (1 M in toluene, 0.72 mL, 0.72 mmol) drop-wise and the reaction was left to stir for 1 h. After TLC analysis (8:2, hexane: ethyl acetate) confirmed complete consumption of starting material, methanol (5 mL) was added drop-wise while the reaction was allowed to warm to room temperature. Saturated aqueous ammonium chloride solution and hydrochloric acid (1 M) (1:1; 10 mL) was added and stirred for 30 min. The biphasic layers were separated and the aqueous layer was washed with diethyl ether (4 x 10 mL). The combined organic layers were washed with water (10 mL) and brine (10 mL). The resulting solution was dried over anhydrous magnesium sulfate, filtered under gravity and concentrated under reduced pressure to give the title compound as a colourless oil (73 mg, 86%).

^{1}H NMR (300 MHz, $CDCl_3$): δ 5.42 (1 H, t, $J_{H,H}$ = 7, C<u>H</u>CH_2OH), 5.12-5.05 (2 H, m, 2 x C<u>H</u>CH_2CH_2), 4.15 (2 H, d, $J_{H,H}$ = 7, CHC<u>H$_2$</u>OH), 2.16-1.99 (10 H, m, C<u>H$_2$</u>CH_3 and 2 x C<u>H$_2$</u>C<u>H$_2$</u>), 1.68 (6 H, s, 2 x CC<u>H$_3$</u>), 1.60 (3 H, s, CC<u>H$_3$</u>), 0.95 (3 H, t, $J_{H,H}$ = 7.5, CH_2C<u>H$_3$</u>).

^{13}C NMR (125 MHz, $CDCl_3$): δ 141.49, 140.09 and 138.11 (3 x <u>C</u>CH), 129.28, 124.62 and 123.48 (3 x C<u>C</u>H), 59.62 (<u>C</u>H_2OH), 40.09 and 36.68 (2 x C<u>C</u>H_2), 27.11, 26.14 and 25.90, 23.35 (2 x CCH_2<u>C</u>H_2 and C<u>C</u>H_2CH_3), 17.91 and 16.52 (2 x C<u>C</u>H_3), 13.44 (CH_2<u>C</u>H_3).

HRMS (EI^+): calculated for $(C_{16}H_{28}O - [H_2O])^+$: 218.2035, found: 218.2038.

(2*E*, 6*E*)-1-Bromo-7-ethyl-3, 11-dimethyl dodeca-2, 6, 10-triene (164)

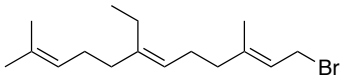

To a stirred solution of **163** (0.1 g, 0.4 mmol) in anhydrous THF (5 mL) at -10 °C, was added phosphorous tribromide (20 μL, 0.2 mmol), and this was left to stir for 1 h. When TLC analysis (8:2, hexane: ethyl acetate) confirmed complete consumption of starting material, the phosphorous tribromide and THF were removed under reduced pressure. The residual product was diluted in diethyl ether (10 mL) and washed with saturated aqueous ammonium bicarbonate solution (3 x 20 mL) and brine (10 mL). The resulting solution was dried over anhydrous magnesium sulfate, filtered under gravity and

concentrated under reduced pressure to give the title compound as a colourless oil (118 mg, 94%).[168]

^{1}H NMR (300 MHz, $CDCl_3$): δ 5.34 (1 H, t, $J_{H,H}$ = 8.5, C<u>H</u>CH_2Br), 5.12-5.02 (2 H, m, 2 x C<u>H</u>CH_2CH_2), 4.03 (2 H, d, $J_{H,H}$ = 8.5, CHC<u>H$_2$</u>Br), 2.15-1.98 (10 H, m, 2 x C<u>H$_2$</u>C<u>H$_2$</u> and C<u>H$_2$</u>CH_3), 1.73 (3 H, s, CC<u>H$_3$</u>), 1.68 (3 H, s, CC<u>H$_3$</u>), 1.60 (3 H, s, CC<u>H$_3$</u>), 0.95 (3 H, t, $J_{H,H}$ = 7.5, CH_2C<u>H$_3$</u>).

(2*E*, 6*E*)-7-Ethyl-3, 11-dimethyl dodeca-2, 6, 10-trien-1-yl diphosphate (130)

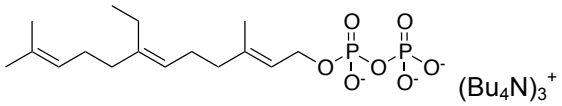

To a stirred solution of **164** (60 mg, 0.20 mmol) in anhydrous acetonitrile (10 mL) was added **121** (0.37 g, 0.40 mmol). The reaction was left for 48 h to stir under nitrogen. After 48 h, the solvent was removed under reduced pressure and the resulting crude oil was purified by flash chromatography on silica gel (6:2.5:0.5, isopropanol: water: ammonium hydroxide). Fractions that contained the diphosphate as judged by comparison with an authentic FDP standard by TLC (6:3:1, isopropanol: water: ammonium hydroxide) were collected. The isopropanol was removed under reduced pressure and the remaining solution was lyophilized to give the title compound as colourless oil (100 mg, 44%).[169,170]

^{1}H NMR (500 MHz, D_2O): δ 5.46 (1 H, m, C<u>H</u>CH_2O), 5.20-5.16 (2 H, m, 2 x C<u>H</u>CH_2CH_2), 4.48 (2 H, m, CHC<u>H$_2$</u>O), 3.20-3.17 (24 H, m, 12 x NC<u>H$_2$</u>$CH_2CH_2CH_3$), 2.18-2.04 (10 H, m, 2 x CCHC<u>H$_2$</u>C<u>H$_2$</u> and CC<u>H$_2$</u>CH_3), 1.72-1.62 (33 H, m, 12 x NCH_2C<u>H$_2$</u>CH_2CH_3 and 3 x CHCC<u>H$_3$</u>), 1.37-1.33 (24 H, m, 12 x NCH_2CH_2C<u>H$_2$</u>CH_3), 0.94 (39 H, m, 12 x $NCH_2CH_2CH_2$C<u>H$_3$</u> and CH_2C<u>H$_3$</u>).

^{31}P NMR (121 MHz, D_2O): δ -10.38 (d, $J_{P,P}$ = 17.5), -6.51 (d, $J_{P,P}$ = 17.5).

LRMS (ES^-) *m/z*: 395.14 (100%, $[M - H]^-$), 315.20 (24).

HRMS (ES^-): calculated for $(C_{16}H_{30}O_7P_2 – [H])^-$: 395.1389, found: 395.1406.

7.2.7 Preparation of 13-acetoxy farnesyl diphosphate (13-Acetoxy FDP, 165)

(2*Z*, 6*E*, 10*E*)-2, 6, 10-Trimethyl-12-((tetrahydro-2H-pyran-2-yl) oxy) dodeca-2, 6, 10-trien-1-yl acetate (172)

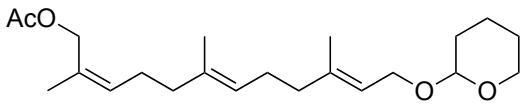

To a stirred solution of **149** (0.11 g, 0.34 mmol) in DCM (5 mL), was added acetic anhydride (0.13 mL, 1.4 mmol) and pyridine (0.11 mL, 1.4 mmol). The reaction was left to stir at room temperature for 24 h and quenched with saturated aqueous sodium bicarbonate solution (10 mL). The biphasic layers were separated and the aqueous layer was washed with diethyl ether (4 x 10 mL). The combined organic layers were washed with brine (5 x 10 mL) and dried over anhydrous magnesium sulfate before being filtered under gravity. The solvent was removed under reduced pressure and the crude oil was purified by flash chromatography on silica gel (8:1, hexane: ethyl acetate) to give the title compound as a colourless oil (119 mg, 96%).

^{1}H NMR (300 MHz, $CDCl_3$): δ 5.40-5.34 (2 H, m, 2 x C$\underline{H}$C$\underline{H_2}$O and OC$\underline{H_2}$C$\underline{C}$H), 5.11 (1 H, t, $J_{H,H}$ = 6.5, CC$\underline{H}$C$\underline{H_2}$C$\underline{H_2}$), 4.62 (1 H, t, $J_{H,H}$ = 4.0, OC$\underline{H}$O), 4.57 (2 H, s, OC$\underline{H_2}$CH), 4.24 (1 H, dd, $J_{H,H}$ = 12.0 and 6.5, CCHC$\underline{H_A}$O), 4.02 (1 H, dd, $J_{H,H}$ = 12.0 and 7.5, CCHC$\underline{H_B}$O), 3.93-3.47 (2 H, m, OC$\underline{H_2}$C$\underline{H_2}$), 2.19-1.96 (8 H, m, 2 x CCHC$\underline{H_2}$C$\underline{H_2}$), 2.07 (3 H, s, OCC$\underline{H_3}$), 1.75-1.49 (6 H, m, CHC$\underline{H_2}$C$\underline{H_2}$C$\underline{H_2}$), 1.74, 1.68 and 1.58 (3 x 3 H, 3 x s, 3 x CHCC$\underline{H_3}$).

^{13}C NMR (75 MHz, $CDCl_3$): δ 171.4 (O$\underline{C}$O), 140.4, 134.7 and 130.7 (3 x $\underline{C}$CHCH$_2$), 129.9, 124.6 and 120.7 (3 x C$\underline{C}$HCH$_2$), 98.00 (O$\underline{C}$HO), 63.83 (C$\underline{C}$H$_2$O), 63.42 and 62.47 (2 x CHO$\underline{C}$H$_2$), 39.76 and 30.88 (2 x CCHCH$_2$$\underline{C}H_2$), 26.45 and 25.67 (2 x CCH$\underline{C}$H$_2$CH$_2$), 24.72 (OCH$_2$$\underline{C}H_2CH_2$), 21.61 (OCH$_2CH_2$$\underline{C}H_2$), 21.18, 19.81, 16.62, 16.14 (4 x C$\underline{C}$H$_3$).

LRMS (ES$^+$) *m/z*: 387.25 (100%, [M + Na]$^+$).

HRMS (ES$^+$): calculated for ($C_{22}H_{36}O_4$ + [Na])$^+$: 387.2511, found: 387.2506.

(2*Z*, 6*E*, 10*E*)-12-Hydroxy-2, 6, 10-trimethyl dodeca-2, 6, 10-trien-1-yl acetate (173)

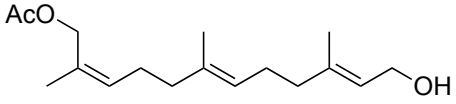

To a stirred solution of **172** (0.11 g, 0.30 mmol) in methanol (5 mL) was added *p*-toluenesulfonic acid (6 mg, 0.03 mmol) and stirred at room temperature for 1 h until TLC analysis (8:2, hexane: ethyl acetate) confirmed complete consumption of starting

material. The solvent was removed under reduced pressure and the residual oil was dissolved with diethyl ether (10 mL) and washed with saturated aqueous sodium bicarbonate solution (3 x 10 mL) and brine (10 mL). The resulting solution was dried over anhydrous magnesium sulfate, filtered under gravity and concentrated under reduced pressure to give the title compound as a colourless oil (84 mg, 99%). The product was judged by ^{1}H NMR spectroscopy to be sufficiently pure to carry forward without further purification.

^{1}H NMR (300 MHz, $CDCl_3$): δ 5.41 (1 H, t, $J_{H,H}$ = 7.0, $OCH_2CC\underline{H}$), 5.38 (1 H, t, $J_{H,H}$ = 7.5, $CC\underline{H}$), 5.11 (1 H, t, $J_{H,H}$ = 6.5, $CC\underline{H}CH_2$), 4.57 (2 H, s, $OC\underline{H_2}C$), 4.15 (2 H, d, $J_{H,H}$ = 7.0, $CHC\underline{H_2}O$), 2.18-1.98 (8 H, m, 2 x $CCHC\underline{H_2}C\underline{H_2}$), 2.07 (3 H, s, $OCC\underline{H_3}$), 1.74, 1.68 and 1.59 (3 x 3 H, 3 x s, 3 x $CH_2CC\underline{H_3}$).

^{13}C NMR (75 MHz, $CDCl_3$): δ 171.5 ($O\underline{C}O$), 139.8, 134.9 and 130.7 (3 x $\underline{C}CHCH_2$), 129.9, 124.4 and 123.7 (3 x $C\underline{C}HCH_2$), 63.43 ($\underline{C}H_2OC$), 59.59 ($\underline{C}H_2OH$), 39.75 and 39.64 (2 x $CCHCH_2\underline{C}H_2$), 26.55 and 26.35 (2 x $CCH\underline{C}H_2CH_2$), 21.61, 21.18, 16.44 and 16.19 (4 x $C\underline{C}H_3$).

LRMS (ES^+) *m/z*: 303.19 (100%, $[M + Na]^+$), 261.19 (12), 210.03 (8).

HRMS (ES^+): calculated for $(C_{17}H_{28}O_3 + [Na])^+$: 303.1936, found: 303.1930.

(2*Z*, 6*E*, 10*E*)-12-Bromo-2, 6, 10-trimethyl dodeca-2, 6, 10-trien-1-yl acetate (174)

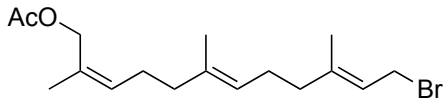

To a stirred solution of **173** (90 mg, 0.30 mmol) in anhydrous THF (5 mL) at -10 °C, was added phosphorous tribromide (15 μL, 0.20 mmol), and the reaction was left to stir for 1 h. When TLC analysis (8:2, hexane: ethyl acetate) confirmed complete consumption of starting material, the phosphorous tribromide and THF were removed under reduced pressure. The residual product was diluted in diethyl ether (10 mL) and washed with saturated aqueous ammonium bicarbonate solution (3 x 20 mL) and brine (10 mL). The resulting solution was dried over anhydrous magnesium sulfate, filtered under gravity and concentrated under reduced pressure to give the title compound as a colourless oil (40 mg, 36%).[168]

^{1}H NMR (300 MHz, $CDCl_3$): δ 5.52 (1 H, t, $J_{H,H}$ = 8.5, $CC\underline{H}$), 5.37 (1 H, t, $J_{H,H}$ = 7.0, $CC\underline{H}$), 5.08 (1 H, t, $J_{H,H}$ = 8.0, $CC\underline{H}CH_2$), 4.57 (2 H, s, $OC\underline{H_2}C$), 4.02 (2 H, d, $J_{H,H}$ = 8.5, $CHC\underline{H_2}Br$), 2.19-1.96 (8 H, m, 2 x $CCHC\underline{H_2}C\underline{H_2}$), 2.07 (3 H, s, $OCC\underline{H_3}$), 1.74, 1.72 and 1.58 (3 x 3 H, 3 x s, 3 x $CHCCH_3$).

(2*E*, 6*E*, 10*Z*)-12-Acetoxy-3, 7, 11-trimethyl dodeca-2, 6, 10-trien-1-yl diphosphate (165)

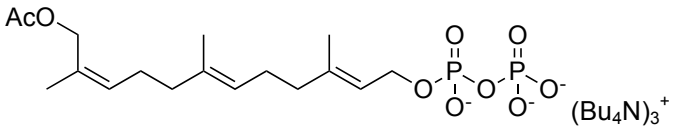

To a stirred solution of **164** (40 mg, 0.10 mmol) in anhydrous acetonitrile (5 mL) was added **121** (0.21 g, 0.20 mmol). The reaction was left for 48 h to stir under nitrogen. The solvent was removed under reduced pressure and the resulting crude oil was purified by flash chromatography on silica gel (6:2.5:0.5, isopropanol: water: ammonium hydroxide). Fractions that contained the diphosphate as judged by comparison with an authentic FDP standard by TLC (6:3:1, isopropanol: water: ammonium hydroxide) were collected. The isopropanol was removed under reduced pressure and the remaining solution was lyophilized to give the title compound as colourless oil (30 mg, 20%).

^{1}H NMR (500 MHz, D_2O): δ 5.49 (1 H, t, $J_{H,H}$ = 7.5, CC<u>H</u>), 5.45 (1 H, t, $J_{H,H}$ = 7.0, CC<u>H</u>), 5.20 (1 H, t, $J_{H,H}$ = 6.5, CC<u>H</u>CH_2), 4.62 (2 H, s, OC<u>H$_2$</u>C), 4.48 (2 H, t, $J_{H,H}$ = 7.0, CHC<u>H$_2$</u>O), 3.21-3.17 (24 H, m, 12 x NC<u>H$_2$</u>$CH_2CH_2CH_3$), 2.22-2.03 (11 H, m, 2 x CCHC<u>H$_2$</u>C<u>H$_2$</u> and OCC<u>H$_3$</u>), 2.03 (3 H, s, OCC<u>H$_3$</u>), 1.73-1.61 (33 H, m, 12 x NCH_2C<u>H$_2$</u>CH_2CH_3 and 3 x CH_2CC<u>H$_3$</u>), 1.39-1.32 (24 H, m, 12 x NCH_2CH_2C<u>H$_2$</u>CH_3), 0.94 (36 H, t, $J_{H,H}$ = 7, 12 x $NCH_2CH_2CH_2$C<u>H$_3$</u>).

^{31}P NMR (121 MHz, D_2O): δ -10.21 (m), -10.73 (m).

LRMS (ES^-) *m/z*: 439.13 (100%, $[M - H]^-$), 397.11 (33), 359.16 (41).

HRMS (ES^-): calculated for $(C_{17}H_{30}O_9P_2 – [H])^-$: 439.1287, found: 439.1286.

7.2.8 Preparation of 12-acetoxy farnesyl diphosphate (12-Acetoxy FDP,166)

(2*E*, 6*E*, 10*E*)-2, 6, 10-Trimethyl-12-((tetrahydro-2H-pyran-2-yl) oxy) dodeca-2, 6, 10-trien-1-ol (175)

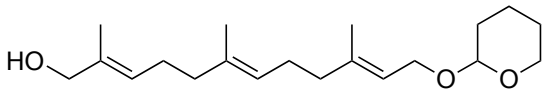

Selenium dioxide (0.11 g, 1.0 mmol), salicylic acid (0.14 g, 1.0 mmol), and tert-butyl hydroperoxide (1.6 mL, 16.3 mmol) were stirred in DCM (20 mL) for 30 min at room temperature. The temperature was reduced to 0 °C before the addition of **131** (1.0 g, 3.3 mmol). The reaction was left to stir for 24 h whilst remaining between 0 – 4 °C. DCM was removed using reduced pressure and *t*-Butyl hydroperoxide was removed by

co-evaporation with toluene (2 x 20 mL) under reduced pressure. The crude residue was dissolved in diethyl ether (20 mL) and washed with saturated aqueous sodium bicarbonate solution (50 mL). The biphasic layers were separated and the aqueous layer was extracted with diethyl ether (5 x 20 mL). The combined organic layers were washed with brine (20 mL) and dried over anhydrous magnesium sulfate before being filtered under gravity. The solvent was removed under reduced pressure and the crude oil was purified by flash chromatography on silica gel (9:1, hexane: ethyl acetate) to give the title compound as a colourless oil (0.5 g, 48%).[173,174]

^{1}H NMR (300 MHz, $CDCl_3$): δ 5.41-5.33 (2 H, m, 2 x CC<u>H</u>CH_2), 5.11 (1 H, t, $J_{H,H}$ = 6.5, CC<u>H</u>CH_2), 4.63 (1 H, t, $J_{H,H}$ = 4, OC<u>H</u>O), 4.23 (1 H, dd, $J_{H,H}$ = 12 and 6.5, CCHC<u>H$_A$</u>O), 4.01 (1 H, dd, $J_{H,H}$ = 12 and 7.5, CCHC<u>H$_B$</u>O), 3.99 (2 H, s, OHC<u>H_2</u>), 3.93-3.48 (2 H, m, OC<u>H_2</u>CH_2), 2.20-1.99 (8 H, m, 2 x CCHC<u>H_2</u>C<u>H_2</u>), 1.75-1.50 (6 H, m, CHC<u>H_2</u>C<u>H_2</u>C<u>H_2</u>), 1.68, 1.66 and 1.60 (3 x 3 H, 3 x s, 3 x C<u>H_3</u>).

^{13}C NMR (75 MHz, $CDCl_3$): δ 140.2, 135.0 and 135.0 (3 x CH_3<u>C</u>CH), 126.1, 124.5 and 121.0 (3 x CH_3<u>C</u>CH), 97.96 (O<u>C</u>HO), 69.15 (OH<u>C</u>H_2), 63.85 and 62.48 (2 x CHO<u>C</u>H_2), 39.77 and 39.45 (2 x C<u>C</u>H_2CH_2), 30.92 (OC<u>C</u>H_2), 26.42 and 26.32 (2 x CCH_2<u>C</u>H_2), 25.72 (OCH_2<u>C</u>H_2CH_2), 19.81 (OCH_2CH_2<u>C</u>H_2), 16.59, 16.18 and 13.87 (<u>C</u>CH_3).

LRMS (ES^+) *m/z*: 345.24 (100%, $[M + Na]^+$).

HRMS (ES^+): calculated for ($C_{20}H_{34}O_3$ + [Na])$^+$: 345.2406, found: 345.2415.

(2*E*, 6*E*, 10*E*)-2, 6, 10-Trimethyl-12-((tetrahydro-2H-pyran-2-yl) oxy) dodeca-2, 6, 10-trien-1-yl acetate (176)

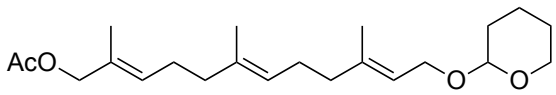

To a stirred solution of **175** (1.3 g, 4.1 mmol) in DCM (20 mL), was added acetic anhydride (1.5 mL, 16.1 mmol) and pyridine (1.3 mL, 16.1 mmol). The reaction was left to stir at room temperature for 24 h and was quenched with saturated aqueous sodium bicarbonate solution (20 mL). The biphasic layers were separated and the aqueous layer was washed with diethyl ether (4 x 20 mL). The combined organic layers were washed with brine (5 x 20 mL) and dried over anhydrous magnesium sulfate before being filtered under gravity. The solvent was removed under reduced pressure and the crude oil was purified by flash chromatography on silica gel (8:1, hexane: ethyl acetate) to give the title compound as a colourless oil (1.4 g, 95%).

^{1}H NMR (300 MHz, $CDCl_3$): δ 5.44 (1 H, t, $J_{H,H}$ = 6.5, CC<u>H</u>CH_2), 5.36 (1 H, t, $J_{H,H}$ = 7.0, CC<u>H</u>CH_2), 5.11 (1 H, t, $J_{H,H}$ = 7.0, CC<u>H</u>CH_2), 4.62 (1 H, t, $J_{H,H}$ = 4.0, OC<u>H</u>O), 4.44 (2 H, s, CC<u>H_2</u>O), 4.24 (1 H, dd, $J_{H,H}$ = 12.0 and 6.5, CCHC<u>H$_A$</u>O), 4.02 (1 H, dd, $J_{H,H}$ = 12.0

and 7.5, CCHC$\underline{H}_B$O), 3.93-3.47 (2 H, m, OC$\underline{H}_2$CH$_2$), 2.20-1.98 (8 H, m, 2 x CCHC$\underline{H}_2$C$\underline{H}_2$), 2.07 (3 H, s, OCC$\underline{H}_3$), 1.75-1.49 (6 H, m, CHC$\underline{H}_2$C$\underline{H}_2$C$\underline{H}_2$), 1.68, 1.65 and 1.60 (3 x 3 H, 3 x s, 3 x CC$\underline{H}_3$).

^{13}C NMR (75 MHz, $CDCl_3$): δ 171.1 ($CH_3\underline{C}O$), 140.2, 134.7 and 130.0 (3 x $CH_3\underline{C}CH$), 129.6, 124.3 and 120.6 (3 x $CH_3C\underline{C}H$), 97.83 (O$\underline{C}$HO), 70.54 (C$\underline{C}H_2O$), 63.82 and 62.48 (2 x CHO$\underline{C}H_2$), 39.76 and 39.21 (2 x C$\underline{C}H_2CH_2$), 30.89 (OC$\underline{C}H_3$), 26.54 and 26.45 (2 x CCH$_2\underline{C}$H$_2$), 25.67 (OCH$_2\underline{C}$H$_2$CH$_2$), 19.81 (OCH$_2$CH$_2\underline{C}$H$_2$), 16.62, 16.17 and 14.15 (3 x C$\underline{C}H_3$).

LRMS (AP$^+$) *m/z*: 387.25 (100%, [M + Na]$^+$).

HRMS (AP$^+$): calculated for ($C_{22}H_{36}O_4$ + [Na])$^+$: 387.2511, found: 387.2501.

(2*E*, 6*E*, 10*E*)-12-Hydroxy-2, 6, 10-trimethyl dodeca-2, 6, 10-trien-1-yl acetate (177)

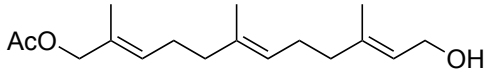

To a stirred solution of **176** (0.93 g, 2.5 mmol) in methanol (20 mL) was added *p*-toluenesulfonic acid (47 mg, 0.25 mmol) and stirred at room temperature for 1 h until TLC analysis (8:2, hexane: ethyl acetate) confirmed complete consumption of starting material (ca. 1 h). The solvent was removed under reduced pressure and the residual oil was dissolved with diethyl ether (20 mL) and washed with saturated aqueous sodium bicarbonate solution (3 x 10 mL) and brine (10 mL). The resulting solution was dried over anhydrous magnesium sulfate, filtered under gravity and concentrated under reduced pressure to give the title compound as a colourless oil (690 mg, 97%). The product was judged by ^{1}H NMR spectroscopy to be sufficiently pure to carry forward without further purification.

^{1}H NMR (300 MHz, $CDCl_3$): δ 5.46-5.39 (2 H, m, 2 x CC$\underline{H}$), 5.11 (1 H, t, $J_{H,H}$ = 6.5, CC$\underline{H}$CH$_2$), 4.44 (2 H, s, OC$\underline{H}_2$C), 4.15 (2 H, d, $J_{H,H}$ = 7.0, C$\underline{H}_2$OH), 2.14-2.00 (8 H, m, 2 x CCHC$\underline{H}_2$C$\underline{H}_2$), 2.07 (3 H, s, OCC$\underline{H}_3$), 1.68, 1.65 and 1.60 (3 x 3 H, 3 x s, 3 x CHCC$\underline{H}_3$).

^{13}C NMR (75 MHz, $CDCl_3$): δ 171.3 ($CH_3\underline{C}O$), 139.8, 135.0 and 130.1 (3 x $CH_3\underline{C}CH$), 129.8, 124.4 and 123.6 (3 x $CH_3C\underline{C}H$), 70.56 (C$\underline{C}H_2O$), 59.56 ($\underline{C}H_2OH$), 39.66 and 39.18 (2 x C$\underline{C}H_2CH_2$), 26.46 and 26.41 (2 x CCH$_2\underline{C}$H$_2$), 21.23 (OC$\underline{C}H_3$), 16.46, 16.15 and 14.17 (3 x CHCC$\underline{H}_3$).

LRMS (ES$^+$) *m/z*: 303.19 (100%, [M + Na]$^+$), 291.17 (74), 242.25 (44), 203.16 (47), 89.05 (44).

HRMS (ES$^+$): calculated for ($C_{17}H_{28}O_3$ + [Na])$^+$: 303.1936, found: 303.1945.

(2*E*, 6*E*, 10*E*)-12-Acetoxy-3, 7, 11-trimethyl dodeca-2, 6, 10-trien-1-yl diphosphate (166)

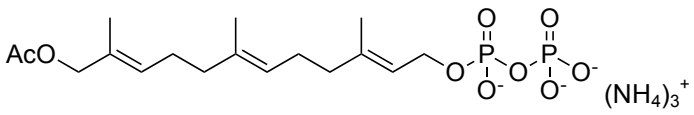

To a stirred, cold suspension (0 °C) of **177** (900 mg, 3.20 mmol), lithium chloride (545 mg, 12.9 mmol) and *s*-collidine (2.5 mL, 19.3 mmol) in anhydrous DMF (10 mL) was added methanesulfonyl chloride (0.5 mL, 6.4 mmol), under nitrogen. The solution was stirred for 3 h. The solution was poured into cold water (50 mL) and extracted with diethyl ether (4 x 20 mL). Combined organic extracts were washed with saturated aqueous copper sulfate solution (3 x 20 mL), water (2 x 20 mL) and saturated aqueous ammonium bicarbonate solution (2 x 20 mL), dried over anhydrous magnesium sulfate, filtered under gravity and concentrated under reduced pressure to give the crude chloride intermediate.

To a stirred solution of **121** (5.8 g, 6.4 mmol) in anhydrous acetonitrile (10 mL) under N_2 was added the solution of the crude chloride in acetonitrile (5 mL). This was left for 24 h at room temperature. The solvent was removed under reduced pressure and the resulting oil was dissolved in a minimum amount of ion-exchange buffer (25 mM ammonium bicarbonate solution containing 2% isopropanol).

The crude compound in buffer was then eluted through the NH_4^+-form cation exchange column with additional ion exchange buffer. Fractions that contained the diphosphate and therefore gave a spot with TLC (6:3:1 isopropanol: water: ammonium hydroxide) were collected and lyophilized. The resulting dry powder was purified by HPLC to give the title compound as a colourless oil (0.6 g, 35%).

^{1}H NMR (500 MHz, D_2O): δ 5.51-5.46 (2 H, m, 2 x CC<u>H</u>), 5.22 (1 H, t, $J_{H,H}$ = 6.5, CC<u>H</u>), 4.50 (2 H, s, CC<u>H$_2$</u>O), 4.48 (2 H, t, $J_{H,H}$ = 6.5, CHC<u>H$_2$</u>O), 2.25-2.03 (8 H, m, 2 x CCHC<u>H$_2$</u>C<u>H$_2$</u>), 2.10 (3 H, s, OCC<u>H$_3$</u>), 1.73, 1.65 and 1.63 (3 x 3 H, 3 x s, 3 x CHCC<u>H$_3$</u>).

^{31}P NMR (121 MHz, D_2O): δ -10.33 (d, $J_{P,P}$ = 21.5), -6.57 (d, $J_{P,P}$ = 21.5)

LRMS (AP^+) *m/z*: 439.13 (70%, $[M - H]^-$), 359.17 (100).

HRMS (ES^-): calculated for $(C_{17}H_{30}O_9P_2 - [H])^-$: 439.1287, found: 439.1290.

7.2.9 Preparation of 12-hydroxy farnesyl diphosphate (12-Hydroxy FDP, 168)

(2*E*, 6*E*, 10*E*)-12-Hydroxy-3, 7, 11-trimethyl dodeca-2, 6, 10-trien-1-yl diphosphate (168)

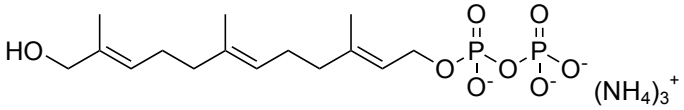

To a stirred solution of **166** (0.3 g, 0.6 mmol) in deuterated water (10 mL) was added ammonium hydroxide (2 mL) and left to stir for 24 h. The following day ^{1}H NMR analysis continued to show the presence of the acetate group. Additional ammonium hydroxide (2 mL) was added and left for another 24 h. The following day the deuterated water and ammonium hydroxide was lyophilized to give the title compound as a colourless oil (290 mg, 97%).

^{1}H NMR (500 MHz, D_2O): δ 5.41-5.33 (2 H, m, 2 x CC<u>H</u>), 5.15 (1 H, t, $J_{H,H}$ = 6.5, CC<u>H</u>), 4.40 (2 H, t, $J_{H,H}$ = 6.5, CHC<u>H$_2$</u>O), 3.88 (2 H, s, C<u>H$_2$</u>OH), 2.16-1.96 (8 H, m, 2 x CCHC<u>H$_2$</u>C<u>H$_2$</u>), 1.65, 1.57 and 1.56 (3 x 3 H, 3 x s, 3 x C<u>H$_3$</u>).

^{31}P NMR (121 MHz, D_2O): δ -7.93 (d, $J_{P,P}$ = 17), -7.53 (m).

HRMS (ES^-): calculated for $(C_{15}H_{28}O_8P_2 - 2[H] + [Na])^-$: 419.1001, found: 419.0983.

(2*E*, 6*E*, 10*E*)-12-Chloro-2, 6, 10-trimethyl dodeca-2, 6, 10-trien-1-ol (278)

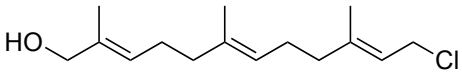

Selenium dioxide (33 mg, 0.3 mmol), salicylic acid (41 mg, 0.3 mmol) and 90% *t*-butyl hydroperoxide (0.48 mL, 5 mmol) were dissolved in DCM (10 mL) and left to stir for 30 min at room temperature. The solution was cooled to 0 ºC after which farnesyl chloride (220 mg, 1.0 mmol) in DCM (5 mL) was added and left to stir for 24 h at 0 ºC. The reaction was quenched with saturated aqueous sodium bicarbonate solution (20 mL). Hexane (20 mL) was added and DCM was removed under reduced pressure. *t*-Butyl hydroperoxide was removed by co-evaporation with toluene (2 x 20 mL) under reduced pressure. The crude oil was dissolved in diethyl ether (20 mL). The biphasic layers were separated and the aqueous layer was washed with additional diethyl ether (3 x 20 mL). The organic extracts were combined, washed with brine (10 mL), dried over anhydrous sodium sulfate and filtered under gravity. The solvent was removed under reduced pressure. The crude oil was purified by flash chromatography on silica gel (9.5:0.5, hexane: ethyl acetate) to give the title compound as a yellow oil (145 mg, 62%).

^{1}H NMR (300 MHz, $CDCl_3$): δ (ppm) 5.47-5.36 (2 H, m, 2 x C=CH), 5.10 (1 H, t, $J_{H,H}$ = 6.0, C=CH), 4.10 (2 H, d, J = 6.0, CH_2Cl), 3.99 (2 H, s, CH_2OH), 2.16-1.99 (8 H, m, CH_2CH_2), 1.73, 1.66 and 1.60 (3 x 3 H, 3 x s, 3 x CH_3).

^{13}C NMR (75 MHz, $CDCl_3$): δ 142.7, 135.3, 134.7, 126.0, 123.7, 120.3, 69.02, 41.21, 39.41, 39.26, 26.18, 26.06, 16.14, 16.05, 13.72.

HRMS (ES^+): calculated for $(C_{15}H_{25}O^{35}Cl + [Na])^+$: 279.1483, found: 279.1492.

7.2.10 Preparation of 8-hydroxy farnesyl diphosphate (8-Hydroxy FDP, 169)

(6*E*, 10*E*)-12-Chloro-2, 6, 10-trimethyl dodeca-2, 6, 10-trien-5-ol (178)

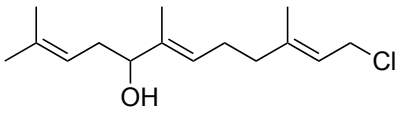

Selenium dioxide (33 mg, 0.30 mmol), salicylic acid (41 mg, 0.30 mmol) and 90 % *t*-butyl hydroperoxide (0.48 mL, 5.0 mmol) were dissolved in DCM (10 mL) and left to stir for 30 min at room temperature. The reaction mixture was cooled to 0 ºC after which farnesyl chloride (0.22 g, 1.0 mmol) in DCM (5 mL) was added and left to stir for 24 h at 0 °C. The reaction was quenched with saturated aqueous sodium bicarbonate solution (20 mL). Hexane (20 mL) was added and DCM was removed under reduced pressure. *t*-Butyl hydroperoxide was removed by co-evaporation with toluene (2 x 20 mL) under reduced pressure. The crude oil was dissolved in diethyl ether (20 mL). The biphasic layers were separated and the aqueous layer was washed with additional diethyl ether (3 x 20 mL). The organic extracts were combined, washed with brine (10 mL) and dried over anhydrous sodium sulfate. The solvent was removed under reduced pressure. The crude oil was purified by flash chromatography on silica gel (9.5:0.5, hexane: ethyl acetate) to give the title compound as a yellow oil (42 mg, 21%).

^{1}H NMR (300 MHz, $CDCl_3$): δ (ppm) 5.44 (1 H, t, $J_{H,H}$ = 8.0, C$\underline{H}CH_2Cl$), 5.36 (1 H, t, $J_{H,H}$ = 7.0, C$\underline{H}CH_2CH_2$), 5.08 (1 H, t, $J_{H,H}$ = 8.0, C$\underline{H}CH_2CHOH$), 4.10 (2 H, d, $J_{H,H}$ = 8.0, C$\underline{H}_2Cl$), 3.98 (1 H, t, $J_{H,H}$ = 8.0, $CCHCH_2C\underline{H}OH$), 2.33-2.05 (6 H, m, C$\underline{H}_2$CHOH and C$\underline{H}_2C\underline{H}_2$), 1.73 (6 H, s, 2 x C$\underline{H}_3$), 1.64 and 1.62 (2 x 3 H,2 x s,2 x C$\underline{H}_3$).

^{13}C NMR (75 MHz, $CDCl_3$): δ 142.5, 138.2 and 137.4 (3 x $CH_3\underline{C}CH$), 125.2, 120.5 and 120.2 (3 x $CH_3\underline{C}CH$), 52.80 ($\underline{C}HOH$), 45.94 ($\underline{C}H_2Cl$), 39.05 ($CH_3C\underline{C}H_2$), 34.20 ($OHCH\underline{C}H_2$), 25.99 ($CH_3CCH_2\underline{C}H_2$), 25.64, 25.03, 8.76 and 8.14 (4 x $\underline{C}H_3$).

(2*E*, 6*E*)-8-Hydroxy-3, 7, 11-trimethyl dodeca-2, 6, 10-trien-1-yl diphosphate (169)

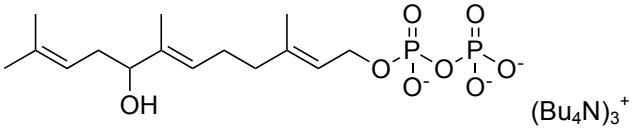

To a stirred solution of **178** (40 mg, 0.20 mmol) in anhydrous acetonitrile (5 mL) was added **121** (0.28 g, 0.30 mmol). The reaction was left for 48 h to stir under nitrogen. The solvent was removed under reduced pressure and the resulting crude oil was purified by flash chromatography on silica gel (6:2.5:0.5, isopropanol: water: ammonium hydroxide). Fractions that contained the diphosphate as judged by comparison with an authentic FDP standard by TLC (6:3:1, isopropanol: water: ammonium hydroxide) were collected. The isopropanol was removed under reduced pressure and the remaining solution was lyophilized to give the title compound as colourless oil (100 mg, 57%).

^{1}H NMR (500 MHz, $CDCl_3$): δ 5.37 (1 H, t, $J_{H,H}$ = 6.0, C<u>H</u>CH_2O), 5.30 (1 H, t, $J_{H,H}$ = 7.0, $CHCH_2CH_2$), 5.06 (1 H, t, $J_{H,H}$ = 7.0, C<u>H</u>CH_2CHOH), 4.45 (2 H, m, $CHC\underline{H_2}O$), 3.93 (1 H, t, $J_{H,H}$ = 6.5, $CHCH_2C\underline{H}OH$), 3.30-3.26 (24 H, m, 12 x $NC\underline{H_2}CH_2CH_2CH_3$), 2.25 -1.98 (6 H, m, $C\underline{H_2}CH$ and $C\underline{H_2}C\underline{H_2}$), 1.67-1.56 (36 H, m, 12 x $NCH_2C\underline{H_2}CH_2CH_3$and 4 x $CC\underline{H_3}$), 1.45-1.40 (24 H, m, 12 x $NCH_2CH_2C\underline{H_2}CH_3$), 0.96 (36 H, t, $J_{H,H}$ = 7.0, 12 x $NCH_2CH_2CH_2C\underline{H_3}$).

^{31}P NMR (121 MHz, D_2O): δ -7.53 (m), -7.93 (d, $J_{P,P}$ = 16.5).

LRMS (ES^-) *m/z*: 397.12 (100%, $[M - H]^-$), 379.10 (3, $M\text{-}H_2O$).

HRMS (ES^-): calculated for $(C_{15}H_{28}O_8P_2 - [H])^-$: 397.1181, found: 397.1190.

7.2.11 Preparation of 8-acetoxy farnesyl diphosphate (8-Acetoxy FDP, 167)

(2*E*, 6*E*)-8-Acetoxy-3, 7, 11-trimethyl dodeca-2, 6, 10-trien-1-yl diphosphate (167)

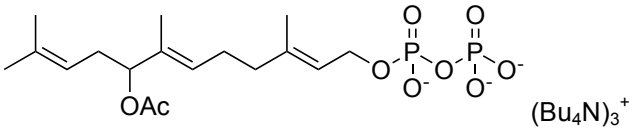

To a stirred solution of **169** (50 mg, 0.045 mmol) in deuterated chloroform (2 mL), was added acetic anhydride (0.017 mL, 0.18 mmol) and pyridine (0.014 mL, 0.18 mmol). The reaction was left to stir at room temperature over 48 h and was quenched with saturated aqueous sodium bicarbonate solution (10 mL). The biphasic layers were separated and the chloroform layer was washed with brine (5 x 5 mL) to remove the pyridine. The resulting organic layer was washed dried over anhydrous magnesium

sulfate before being filtered under gravity. The solvent was removed under reduced pressure to give the title compound as a colourless oil (35 mg, 67%).

^{1}H NMR (500 MHz, D_2O): δ 5.38-5.33 (2 H, m, 2 x CC<u>H</u>), 5.05 (1 H, t, $J_{H,H}$ = 7.0, CC<u>H</u>), 4.95 (1 H, t, $J_{H,H}$ = 7.0, $CH_2C\underline{H}OH$), 4.50 (2 H, t, $J_{H,H}$ = 6.0, $CHCH_2O$), 3.25-3.21 (24 H, m, 12 x $NC\underline{H}_2CH_2CH_2CH_3$), 2.36-2.14 (6 H, m, $C\underline{H}_2CHOH$ and 2 x $CHC\underline{H}_2C\underline{H}_2$), 2.20 (3 H, s, $OCC\underline{H}_3$), 1.64-1.57 (36 H, m, 12 x $NCH_2C\underline{H}_2CH_2CH_3$ and 4 x $CHCC\underline{H}_3$), 1.42-1.36 (24 H, m, 12 x $NCH_2CH_2C\underline{H}_2CH_3$), 0.95 (36 H, t, $J_{H,H}$ = 7.0, 12 x $NCH_2CH_2CH_2C\underline{H}_3$).

^{31}P NMR (121 MHz, D_2O): δ -10.06 (m), -10.69 (m).

LRMS (AP^+) *m/z*: 439.13 (100%, $[M - H]^-$), 359.16 (37).

HRMS (ES^-): calculated for $C_{17}H_{30}O_9P_2$ - $[H]^-$: 439.1287, found: 439.1287.

7.2.12 Preparation of 8-methoxy farnesyl diphosphate (8-Methoxy FDP, 170)

(6*E*, 10*E*)-2, 6, 10-Trimethyl-12-((tetrahydro-2H-pyran-2-yl) oxy) dodeca-2, 6, 10-trien-5-ol (179)

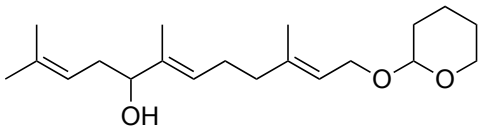

Selenium dioxide (0.11 g, 1.0 mmol), salicylic acid (0.14 g, 1.0 mmol), and *t*-butyl hydroperoxide (1.6 mL, 16.3 mmol) were stirred in DCM (20 mL) for 30 min at room temperature. The temperature was reduced to 0 °C before the addition of **131** (1.0 g, 3.3 mmol). The reaction was left to stir for 24 h whilst remaining between 0 – 4 °C. DCM was removed using reduced pressure. *t*-Butyl hydroperoxide was removed by co-evaporation with toluene (2 x 20 mL) under reduced pressure. The crude residue was dissolved in diethyl ether (20 mL) and washed with saturated aqueous sodium bicarbonate solution (50 mL). The layers were separated and the aqueous layer was extracted with diethyl ether (5 x 20 mL). The combined organic layers were washed with brine (20 mL) and dried over anhydrous magnesium sulfate before being filtered under gravity. The solvent was removed under reduced pressure and the crude oil was purified by flash chromatography on silica gel (9:1, hexane: ethyl acetate) to give the title compound as a colourless oil (116 mg, 11%).[173,174]

^{1}H NMR (300 MHz, $CDCl_3$): δ 5.39-5.34 (2 H, m, 2 x CC<u>H</u>CH_2), 5.08 (1 H, t, $J_{H,H}$ = 7.0, CC<u>H</u>CH_2), 4.63 (1 H, m, OCHO), 4.25 (1 H, dd, $J_{H,H}$ = 12.0 and 6.5, $CCHC\underline{H}_AO$), 4.05-3.95 (2 H, m, $CCHC\underline{H}_BO$ and C<u>H</u>OH), 3.98 (1 H, t, $J_{H,H}$ = 7.5, C<u>H</u>OH), 3.92-3.48 (2 H, m, $OC\underline{H}_2CH_2$), 2.34-2.04 (6 H, m, $CHC\underline{H}_2CH$ and $CHC\underline{H}_2C\underline{H}_2$), 1.88-1.50 (6 H, m, $CHC\underline{H}_2C\underline{H}_2C\underline{H}_2$), 1.72, 1.68, 1.63 and 1.61 (4 x 3 H, 4 x s, 4 x $C\underline{H}_3$).

^{13}C NMR (125 MHz, $CDCl_3$): δ 140.0, 137.3 and 134.8 (3 x $CH_3\underline{C}CH$), 125.9, 121.1 and 120.4 (3 x $CH_3C\underline{C}H$), 98.12 ($O\underline{C}HO$), 63.90 ($\underline{C}HOH$), 63.85 and 62.46 (2 x $\underline{C}H_2O$), 39.39 ($CH_3C\underline{C}H_2$), 34.34 ($\underline{C}H_2CHOH$), 30.86 ($CH_2OCH\underline{C}H_2$), 26.10 ($OCH_2\underline{C}H_2CH_2$), 25.67 ($OCH_2CH_2\underline{C}H_2$), 19.77, 18.19, 16.57 and 11.85 ($\underline{C}H_3$)

LRMS (ES^+) *m/z*: 345.24 (100%, $[M + Na]^+$).

HRMS (ES^+): calculated for $(C_{20}H_{34}O_3 + [Na])^+$: 345.2406, found: 345.2418.

2-(((2*E*, 6*E*)-8-Methoxy-3, 7, 11-trimethyl dodeca-2, 6, 10-trien-1-yl) oxy) tetrahydro-2H-pyran (180)

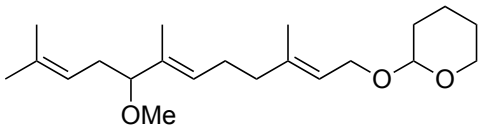

To a stirred suspension of sodium hydride (0.40 g, 60% in mineral oil, 9.3 mmol) in anhydrous THF (30 mL), was added a solution of **179** (0.50 g, 1.6 mmol) in anhydrous THF (20 mL) followed by the addition of methyl iodide (1.5 mL, 23 mmol) 15 min later. The reaction was left to stir under argon for 24 h whereupon TLC analysis (8:2, hexane: ethyl acetate) showed full consumption of starting material. The reaction was quenched with 10% hydrochloric acid (50 mL) and the layers were separated. The aqueous layer was washed with diethyl ether (4 x 20 mL) and the pooled extracts were washed with 5% sodium hydroxide (3 x 10 mL) and dried over anhydrous magnesium sulfate. The solvent was removed under reduced pressure. The crude oil was purified by flash chromatography on silica gel (4:1, hexane: ethyl acetate) to give the title compound as a colourless oil (0.2 g, 38%).

^{1}H NMR (300 MHz, $CDCl_3$): δ 5.37 (1 H, t, $J_{H,H}$ = 6.5, $CC\underline{H}CH_2$), 5.30 (1 H, t, $J_{H,H}$ = 6.5, $CC\underline{H}CH_2$), 5.03 (1 H, t, $J_{H,H}$ = 7.0, $CC\underline{H}CH_2$), 4.62 (2 H, t, $J_{H,H}$ = 4.0, $OC\underline{H}O$), 4.27-3.98 (2 H, m, $CCHC\underline{H}_2O$), 3.92-3.48 (2 H, m, $OC\underline{H}_2CH_2$), 3.41 (1 H, t, $J_{H,H}$ = 7.0, $C\underline{H}OCH_3$), 3.16 (3 H, s, OCH_3), 2.34-2.04 (6 H, m, $CCHC\underline{H}_2CH$ and $CCHC\underline{H}_2C\underline{H}_2$), 1.75-1.52 (6 H, m, $OC\underline{H}_2C\underline{H}_2C\underline{H}_2$), 1.68, 1.59, and 1.52 (2 x 3 H and 1 x 6 H, 3 x s, 4 x $CHCC\underline{H}_3$).

^{13}C NMR (125 MHz, $CDCl_3$): δ 139.9, 134.5 and 132.9 (3 x $CH_3\underline{C}CH$), 128.5, 121.2 and 120.9 (3 x $CH_3C\underline{C}H$), 98.11 ($O\underline{C}HO$), 87.64 ($\underline{C}HOCH_3$), 63.87 and 62.46 ($O\underline{C}H_2$), 55.90 ($O\underline{C}H_3$), 39.52 ($CH_3C\underline{C}H_2$), 32.74 ($CCH\underline{C}H_2CH$), 30.92 ($CH_2OCH\underline{C}H_2CH_2$), 26.05 ($CH_3CCH_2\underline{C}H_2$), 25.94 ($CHC\underline{C}H_3$), 25.71 ($OCH_2\underline{C}H_2CH_2$), 19.80 ($OCH_2CH_2\underline{C}H_2$), 18.12, 16.55 and 10.69 (3 x $CHC\underline{C}H_3$).

LRMS (ES^+) *m/z*: 359.26 (100%, $[M + Na]^+$).

HRMS (ES^+): calculated for $(C_{21}H_{36}O_3 + [Na])^+$: 359.2562, found: 359.2554.

(2*E*, 6*E*)-8-Methoxy-3, 7, 11-trimethyl dodeca-2, 6, 10-trien-1-ol (182)

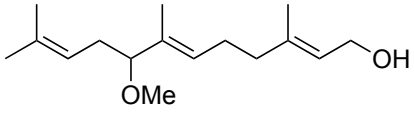

To a solution of **180** (0.20 g, 1.6 mmol) in anhydrous THF (10 mL) was added a solution of 10% hydrochloric acid (7 mL) and was left to stir for 4 h. The reaction was quenched with saturated sodium bicarbonate solution (10 mL) and the biphasic layers were separated. The aqueous layer was washed with diethyl ether (4 x 10 mL) and the pooled extracts were washed with brine (10 mL) before being dried over anhydrous magnesium sulfate, filtered under gravity and concentrated under reduced pressure. The crude oil was purified by flash chromatography on silica gel (4:1, hexane: ethyl acetate) to give the title compound as colourless oil (130 mg, 87%).

^{1}H NMR (300 MHz, $CDCl_3$): δ 5.42 (1 H, t, $J_{H,H}$ = 7.0, CC<u>H</u>CH_2), 5.30 (1 H, t, $J_{H,H}$ = 7.0, CC<u>H</u>CH_2), 5.02 (1 H, t, $J_{H,H}$ = 7.0, CC<u>H</u>CH_2), 4.15 (2 H, d, $J_{H,H}$ = 7.0, C<u>H$_2$</u>OH), 3.41 (1 H, t, $J_{H,H}$ = 7.0, C<u>H</u>OCH_3), 3.16 (3 H, s, OC<u>H$_3$</u>), 2.34-2.04 (6 H, m, CHC<u>H$_2$</u>CHO and CHC<u>H$_2$</u>C<u>H$_2$</u>), 1.68 (6 H, s, 2 x CC<u>H$_3$</u>), 1.59 and 1.52 (2 x 3 H,2 x s, 2 x CC<u>H$_3$</u>).

^{13}C NMR (125 MHz, $CDCl_3$): δ 139.6, 134.5 and 133.0 (3 x <u>C</u>$CHCH_2$), 128.4, 123.8 and 120.8 (3 x <u>C</u>$CHCH_2$), 87.57 (<u>C</u>$HOCH_3$), 59.57 (<u>C</u>H_2OH), 55.92 (O<u>C</u>H_3), 39.42 (CH_3<u>C</u>CH_2), 32.65 (CCH<u>C</u>H_2CH), 26.01 (CH_3CCH_2<u>C</u>H_2), 25.97, 18.14, 16.41 and 10.70 (4 x CHC<u>C</u>H_3).

LRMS (ES^+) *m/z*: 275.20 (100%, $[M + Na]^+$), 262.22 (20), 221.19 (32), 203.18 (56), 109.10 (25).

HRMS (ES^+): calculated for $(C_{16}H_{28}O_2 + [Na])^+$: 275.1987, found: 275.1978.

(2*E*, 6*E*)-8-Methoxy-3, 7, 11-trimethyl dodeca-2, 6, 10-trien-1-yl diphosphate (170)

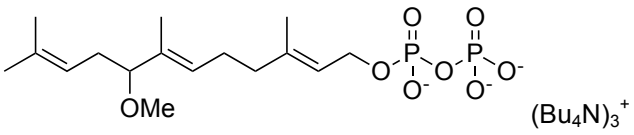

To a cold, stirred suspension (0 °C) of **182** (0.13 g, 0.50 mmol), lithium chloride (87 mg, 2.0 mmol) and *s*-collidine (0.40 mL, 3.0 mmol) in anhydrous DMF (10 mL) was added methanesulfonyl chloride (0.026 mL, 0.34 mmol), under nitrogen. The solution was stirred for 3 h. The solution was poured into cold water (30 mL) and extracted with diethyl ether (4 x 10 mL). Combined organic extracts were washed with saturated aqueous copper sulfate solution (3 x 20 mL), water (2 x 20 mL) and saturated aqueous ammonium bicarbonate solution (2 x 20 mL). The resulting solution was dried over

anhydrous magnesium sulfate, filtered under gravity and concentrated under reduced pressure to give the crude chloride intermediate. To a stirred solution of **121** (0.9 g, 1.0 mmol) in anhydrous acetonitrile (5 mL) under N_2 was added the solution of the crude chloride in acetonitrile (3 mL). This was left to stir for 48 h at room temperature. The solvent was removed under reduced pressure and the resulting crude oil was purified by flash chromatography on silica gel (6:2.5:0.5, isopropanol: water: ammonium hydroxide). Fractions that contained the diphosphate as judged by comparison with an authentic FDP standard by TLC (6:3:1, isopropanol: water: ammonium hydroxide) were collected. The isopropanol was removed under reduced pressure and the remaining solution was lyophilized to give the title compound as colourless oil (306 mg, 52%).

^{1}H NMR (300 MHz, $CDCl_3$): δ 5.40 (2 H, m, 2 x CC<u>H</u>CH_2), 5.05 (1 H, t, $J_{H,H}$ = 7.5, CC<u>H</u>CH_2), 4.46 (2 H, m, C<u>H$_2$</u>O), 3.61 (1 H, t, $J_{H,H}$ = 7.0, C<u>H</u>OCH_3), 3.19-3.14 (27 H, m, 12 x NC<u>H$_2$</u>$CH_2CH_2CH_3$ and CHOC<u>H$_3$</u>), 2.35-2.06 (6 H, m, CHC<u>H$_2$</u>CH and CHC<u>H$_2$</u>C<u>H$_2$</u>), 1.69-1.51 (36 H, m, 12 x NCH_2C<u>H$_2$</u>CH_2CH_3 and 4 x CH_3), 1.36-1.29 (24 H, m, 12 x NCH_2CH_2C<u>H$_2$</u>CH_3), 0.92 (36 H, t, $J_{H,H}$ = 7.5, 12 x $NCH_2CH_2CH_2$C<u>H$_3$</u>).

^{31}P NMR (121 MHz, D_2O): δ -10.69 (m).

LRMS (ES^-) *m/z*: 411.13 (100%, $[M - H]^-$), 395.14 (19), 331.17 (20).

HRMS (ES^-): calculated for $(C_{16}H_{30}O_8P_2 - [H])^-$: 411.1338, found: 411.1342.

7.2.13 Preparation of 12-methoxy farnesyl diphosphate (12-Methoxy FDP, 171)

2-(((2*E*, 6*E*, 10*E*)-12-Methoxy-3, 7, 11-trimethyl dodeca-2, 6, 10-trien-1-yl) oxy) tetrahydro-2H-pyran (181)

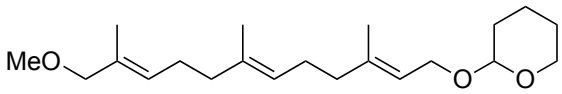

To a stirred suspension of sodium hydride (0.14 g, 60% in mineral oil, 3.7 mmol) in anhydrous THF (5 mL), was added a solution of **175** (0.2 g, 0.6 mmol) in anhydrous THF (5 mL) followed by the addition of methyl iodide (1.5 mL, 23 mmol) after 15 min. The reaction was left to stir under argon for 24 h whereupon TLC analysis (8:2, hexane: ethyl acetate) showed full consumption of starting material. The reaction was quenched with 10% hydrochloric acid (10 mL) and the layers were separated. The aqueous layer was washed with diethyl ether (4 x 10 mL) and the pooled extracts were washed with 5% sodium hydroxide (3 x 10 mL) and dried over anhydrous magnesium sulfate. The solvent was removed under reduced pressure and the crude oil was purified by flash chromatography on silica gel (4:1, hexane: ethyl acetate) to give the title compound as a colourless oil (158 mg, 76%).

^{1}H NMR (300 MHz, $CDCl_3$): δ 5.40-5.33 (2 H, m, 2 x CC<u>H</u>CH_2), 5.11 (1 H, t, $J_{H,H}$ = 7.0, CC<u>H</u>CH_2), 4.62 (2 H, t, $J_{H,H}$ = 4.0, OC<u>H</u>O), 4.24 (1 H, dd, $J_{H,H}$ = 12.0 and 6.5, CCHC<u>H</u>$_A$O), 4.02 (1 H, dd, $J_{H,H}$ = 12.0 and 7.5, CCHC<u>H</u>$_B$O), 3.93-3.47 (2 H, m, OC<u>H</u>$_2$C<u>H</u>$_2$), 3.77 (2 H, s, C<u>H</u>$_2$OC<u>H</u>$_3$), 3.26 (3 H, s, OC<u>H</u>$_3$), 2.15-1.99 (8 H, m, 2 x CHC<u>H</u>$_2$C<u>H</u>$_2$), 1.71-1.54 (6 H, m, OC<u>H</u>$_2$C<u>H</u>$_2$C<u>H</u>$_2$), 1.68, 1.63, and 1.60 (3 x 3 H, 3 x s, 3 x CC<u>H</u>$_3$).

^{13}C NMR (125 MHz, $CDCl_3$): δ 140.4, 135.1 and 132.1 (3 x <u>C</u>CHCH_2), 128.4, 124.3 and 120.8 (3 x <u>C</u>CHCH_2), 98.01 (O<u>C</u>HO), 78.90 (<u>C</u>H_2OCH3), 63.84 and 62.49 (2 x CHO<u>C</u>H_2), 51.69 (CH_2O<u>C</u>H3), 39.79 and 39.47 (2 x CH_3<u>C</u>CH_2), 30.90 (OCH<u>C</u>H_2), 26.47 and 26.42 (2 x CCH<u>C</u>H_2CH_2), 25.68 (OCH_2<u>C</u>H_2CH_2), 19.82 (OCH_2CH_2<u>C</u>H_2), 16.62, 16.16 and 13.97 (3 x C<u>C</u>H_3).

LRMS (AP^+) *m/z*: 359.26 (100%, $[M + Na]^+$).

HRMS (AP^+): calculated for ($C_{21}H_{36}O_3$ + [Na])$^+$: 359.2549, found: 359.2562.

(2*E*, 6*E*, 10*E*)-12-Methoxy-3, 7, 11-trimethyl dodeca-2, 6, 10-trien-1-ol (183)

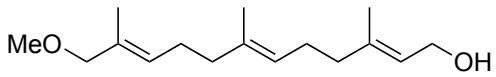

To a stirred solution of **181** (0.15 g, 0.45 mmol) in methanol (5 mL) was added *p*-toluenesulfonic acid (9.0 mg, 45 μmol) and stirred at room temperature for 1 h until TLC analysis (8:2, hexane: ethyl acetate) confirmed complete consumption of starting material. The solvent was removed under reduced pressure and the residual oil was dissolved with diethyl ether (10 mL) and washed with saturated aqueous sodium bicarbonate solution (3 x 10 mL) and brine (10 mL). The resulting solution was dried over anhydrous magnesium sulfate, filtered under gravity and concentrated under reduced pressure to give the title compound as a colourless oil (91 mg, 80%). The product was judged by ^{1}H NMR spectroscopy to be sufficiently pure to carry forward without further purification.

^{1}H NMR (400 MHz, $CDCl_3$): δ 5.43-5.36 (2 H, m, 2 x CC<u>H</u>CH_2), 5.11 (1 H, t, $J_{H,H}$ = 7.0, CC<u>H</u>CH_2), 4.15 (2 H, d, $J_{H,H}$ = 7.0, C<u>H</u>$_2$OH), 3.78 (2 H, s, C<u>H</u>$_2$OCH_3), 3.27 (3 H, s, CH_2OC<u>H</u>$_3$), 2.14-2.00 (8 H, m, 2 x CHC<u>H</u>$_2$C<u>H</u>$_2$), 1.68, 1.63, and 1.60 (3 x 3 H, 3 x s, 3 x CC<u>H</u>$_3$).

^{13}C NMR (125 MHz, $CDCl_3$): δ 139.8, 135.2 and 132.1 (3 x <u>C</u>CHCH_2), 128.2, 124.2 and 123.6 (3 x C<u>C</u>HCH_2), 78.85 (<u>C</u>H_2OCH3), 59.59 (<u>C</u>H_2OH), 57.52 (CH_2O<u>C</u>H3), 39.67 and 39.43 (2 x CH_3C<u>C</u>H_2), 26.42 and 26.40 (CCH<u>C</u>H_2CH_2), 16.47, 16.16 and 13.99 (C<u>C</u>H_3).

LRMS (ES^+) *m/z*: 275.20 (100%, $[M + Na]^+$), 251.20 (6, $[M]^+$), 235.21 (16), 203.18 (45).

HRMS (ES^+): calculated for ($C_{16}H_{28}O_2$ + [Na])$^+$: 275.1987, found: 275.1982.

(2*E*, 6*E*, 10*E*)-12-Bromo-1-methoxy-2, 6, 10-trimethyl dodeca-2, 6, 10-triene (284)

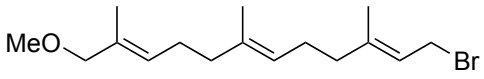

To a stirred solution of **183** (0.66 g, 2.6 mmol) in anhydrous THF (10 mL) at -10 °C, was added phosphorous tribromide (0.12 mL, 1.3 mmol), and this was left to stir for 1 h. When TLC analysis (8:2, hexane: ethyl acetate) confirmed complete consumption of starting material, the phosphorous tribromide and THF were removed under reduced pressure. The residual product was diluted with diethyl ether (10 mL) and washed with saturated aqueous ammonium bicarbonate solution (3 x 20 mL) and brine (10 mL). The resulting solution was dried over anhydrous magnesium sulfate, filtered under gravity and concentrated under reduced pressure to give the title compound as a colourless oil (820 mg, 100%). The product was judged by ^{1}H NMR spectroscopy to be sufficiently pure to carry forward without further purification.[168]

^{1}H NMR (300 MHz, $CDCl_3$): δ 5.53 (1 H, t, $J_{H,H}$ = 8.5, C$\underline{H}$C$\underline{H}_2$Br), 5.38 (1 H, t, $J_{H,H}$ = 7.0, CC$\underline{H}$C$\underline{H}_2$), 5.09 (1 H, m, CC$\underline{H}$C$\underline{H}_2$), 4.02 (2 H, d, $J_{H,H}$ = 8.5, C$\underline{H}_2$Br), 3.78 (2 H, s, C$\underline{H}_2$OC$\underline{H}_3$), 3.27 (3 H, s, CH$_2$OC$\underline{H}_3$), 2.18-2.00 (8 H, m, 2 x CHC$\underline{H}_2$C$\underline{H}_2$), 1.73, 1.64, and 1.60 (3 x 3 H, 3 x s, 3 x CC$\underline{H}_3$).

(2*E*, 6*E*, 10*E*)-12-Methoxy-3, 7, 11-trimethyl dodeca-2, 6, 10-trien-1-yl diphosphate (171)

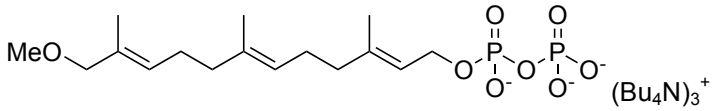

To a stirred solution of **284** (0.82 g, 2.6 mmol) in anhydrous acetonitrile (10 mL) was was added **121** (4.7 g, 5.2 mmol). The reaction was left for 48 h to stir under nitrogen. The solvent was removed under reduced pressure and the resulting crude oil was purified by flash chromatography on silica gel (6:2.5:0.5, isopropanol: water: ammonium hydroxide). Fractions that contained the diphosphate as judged by comparison with an authentic FDP standard by TLC (6:3:1, isopropanol: water: ammonium hydroxide) were collected. The isopropanol was removed under reduced pressure and the remaining solution was lyophilized to give the title compound as colourless oil (900 mg, 32%).

^{1}H NMR (500 MHz, $CDCl_3$): δ 5.36-5.32 (2 H, m, 2 x CC$\underline{H}$C$\underline{H}_2$), 5.07 (1 H, t, $J_{H,H}$ = 6.5, CC$\underline{H}$C$\underline{H}_2$), 4.45 (2 H, t, $J_{H,H}$ = 5.5, CHC$\underline{H}_2$O), 3.74 (2 H, s, C$\underline{H}_2$OCH$_3$), 3.31-3.28 (24 H, m, 12 x NC$\underline{H}_2$CH$_2$CH$_2$CH$_3$), 3.21 (3 H, s, CH$_2$OC$\underline{H}_3$), 2.10-1.90 (8 H, m, 2 x

$CHC\underline{H_2}C\underline{H_2}$), 1.61-1.54 (33 H, m, 12 x $NCH_2C\underline{H_2}CH_2CH_3$ and 3 x $CC\underline{H_3}$), 1.45-1.38 (24 H, m, 12 x $NCH_2CH_2C\underline{H_2}CH_3$), 0.94 (36 H, t, $J_{H,H}$ = 7.5, 12 x $NCH_2CH_2CH_2C\underline{H_3}$).

^{31}P NMR (121 MHz, $CDCl_3$): δ -7.40 (d, $J_{P,P}$ = 17), -7.73(d, $J_{P,P}$ = 17).

LRMS (ES^-) *m/z*: 411.13 (87%, $[M - H]^-$), 397.13 (19), 379.12 (8), 347.18 (5), 331.17 (100).

HRMS (ES^-): calculated for $(C_{16}H_{30}O_8P_2 - [H])^-$: 411.1338, found: 411.1336.

7.2.14 Preparation of 12-acetamido farnesyl diphosphate (12-Acetamido FDP, 184)

2-((2*E*, 6*E*, 10*E*)-2, 6, 10-Trimethyl-12-((tetrahydro-2H-pyran-2-yl) oxy) dodeca-2, 6, 10-trien-1-yl) isoindoline-1, 3-dione (186)

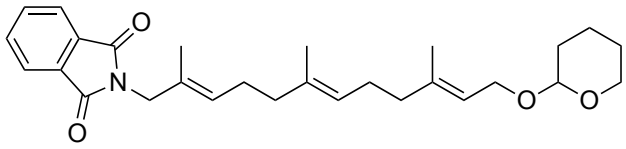

To a stirred solution of pthalimide (0.28 g, 1.9 mmol), triphenylphosphine (0.49 g, 1.9 mmol), and **175** (0.55 g, 1.7 mmol) in anhydrous THF was added diisopropyl azodicarboxylate (0.37 mL, 1.9 mmol) and the reaction was left to stir for 24 h. The THF was removed under reduced pressure and the crude residual oil was dissolved in ether (2 ml) and purified by flash chromatography on silica gel (6:1, hexane: ethyl acetate) to give the title compound as a colourless oil (575 mg, 75%).

^{1}H NMR (500 MHz, $CDCl_3$): δ 7.85 (2 H, dd, $J_{H,H}$ = 5.5 and 3.0, 2 x NCCC$\underline{H}$CH), 7.71 (2 H, dd, $J_{H,H}$ = 5.5 and 3.0, 2 x NCCCHC$\underline{H}$), 5.33 (2 H, t, $J_{H,H}$ = 7.0, 2 x $CC\underline{H}CH_2$), 5.06 (1 H, t, $J_{H,H}$ = 6.5, $CC\underline{H}CH_2$), 4.62 (1 H, t, $J_{H,H}$ = 4.0, $OC\underline{H}O$), 4.26-4.18 (3 H, m, $CC\underline{H_2}N$ and $CCHC\underline{H_A}O$), 4.01 (1 H, dd, $J_{H,H}$ = 12.0 and 7.5, $CCHC\underline{H_B}O$), 3.93-3.46 (2 H, m, $OC\underline{H_2}CH_2$), 2.17-1.94 (8 H, m, 2 x $CHC\underline{H_2}C\underline{H_2}$), 1.71-1.46 (6 H, m, $OC\underline{H_2}C\underline{H_2}C\underline{H_2}$), 1.65, 1.63 and 1.56 (3 x 3 H, 3 x s, 3 x $C\underline{H_3}$).

^{13}C NMR (125 MHz, $CDCl_3$): δ 168.4 (2 x $N\underline{C}O$), 140.4 and 134.9 (2 x $CH_3\underline{C}CH$), 134.1 (2 x NCCCH$\underline{C}$H), 132.3 ($CH_3\underline{C}CH$), 129.3 (2 x NC$\underline{C}$CHCH), 127.6 and 124.4 (2 x $CH_3C\underline{C}H$), 123.4 (2 x NCC$\underline{C}$HCH), 120.7 ($CH_3C\underline{C}H$), 97.96 ($O\underline{C}HO$), 63.82 and 62.46 (2 x $O\underline{C}H_2$), 45.12 ($\underline{C}H_2N$), 39.75 and 39.31 ($CHCH_2\underline{C}H_2$), 30.89 ($OCH\underline{C}H_2$), 26.59 and 26.45 ($CH\underline{C}H_2CH_2$), 25.67 ($OCH_2\underline{C}H_2CH_2$), 19.81 ($OCH_2CH_2\underline{C}H_2$), 16.60, 16.16 and 14.82 ($\underline{C}H_3$).

LRMS (AP^+) *m/z*: 474.26 (100%, $[M + Na]^+$).

HRMS (AP^+): calculated for $(C_{28}H_{37}O_3N + [Na])^+$: 474.2620, found: 474.2610.

(2*E*, 6*E*, 10*E*)-2, 6, 10-Trimethyl-12-((tetrahydro-2H-pyran-2-yl) oxy) dodeca-2, 6, 10-trien-1-amine (187)

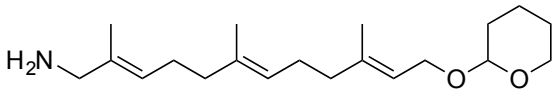

To a stirred solution of **186** (0.12 g, 0.30 mmol) in anhydrous ethanol (10 mL) was added hydrazine monohydrate (56 μL, 1.2 mmol). The reaction was left to stir for 24 h under argon. The ethanol was removed under reduced pressure and the residual oil was dissolved in ether (2 mL) and purified by flash chromatography on silica gel (99:1, ethyl acetate: triethylamine) to give the title compound as a colourless oil (60 mg, 71%).

^{1}H NMR (500 MHz, $CDCl_3$): δ 5.36 (1 H, t, $J_{H,H}$ = 6.5, CC<u>H</u>CH_2), 5.27 (1 H, t, $J_{H,H}$ = 7.0, CC<u>H</u>CH_2), 5.11 (1 H, t, $J_{H,H}$ = 6.5, CC<u>H</u>CH_2), 4.62 (1 H, t, $J_{H,H}$ = 4.0, OC<u>H</u>O), 4.24 (1 H, dd, $J_{H,H}$ = 12.0 and 6.5, CCHC<u>H</u>$_A$O), 4.03 (1 H, dd, $J_{H,H}$ = 12.0 and 7.5, CCHC<u>H</u>$_B$O), 3.93-3.46 (2 H, m, OC<u>H</u>$_2$$CH_2$), 3.17 (2 H, s, C<u>H</u>$_2$$NH_2$), 2.17-1.96 (8 H, m, 2 x CHC<u>H</u>$_2$C<u>H</u>$_2$), 1.72-1.49 (6 H, m, OC<u>H</u>$_2$C<u>H</u>$_2$C<u>H</u>$_2$), 1.68, 1.64 and 1.60 (3 x 3 H, 3 x s, 3 x C<u>H</u>$_3$).

^{13}C NMR (125 MHz, $CDCl_3$): δ 140.3, 135.2 and 135.1 (3 x <u>C</u>CHCH_2), 125.7, 124.4 and 120.9 (3 x C<u>C</u>HCH_2), 98.03 (O<u>C</u>HO), 63.87 and 62.49 (2 x O<u>C</u>H_2), 49.46 (<u>C</u>H_2NH2), 39.80 and 39.55 (CHCH_2<u>C</u>H_2), 30.94 (OCH<u>C</u>H_2), 26.61 and 26.51 (CH<u>C</u>$H_2$$CH_2$), 25.72 (OC$H_2$<u>C</u>$H_2$$CH_2$), 19.84 (OC$H_2$$CH_2$<u>C</u>$H_2$), 16.62, 16.20 and 14.74 (3 x C<u>C</u>H_3).

LRMS (AP^+) *m/z*: 322.27 (100%, $[M + H]^+$), 242.28 (5), 177.11 (12), 118.13 (17).

HRMS (AP^+): calculated for $(C_{20}H_{35}O_2N + [H])^+$: 322.2746, found: 322.2732.

N-((2*E*, 6*E*, 10*E*)-2, 6, 10-Trimethyl-12-((tetrahydro-2H-pyran-2-yl) oxy) dodeca-2, 6, 10-trien-1-yl) acetamide (191)

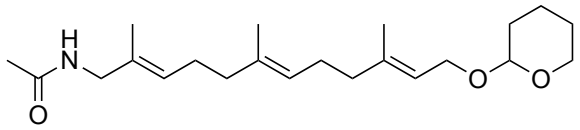

A stirred solution of **187** (0.14 g, 0.40 mmol) dissolved in isopropenyl acetate (0.22 mL, 2.2 mmol) was heated to 60 °C and left to stir for 3 h. The excess isopropenyl acetate and side product, acetone, was removed under reduced pressure to give the title compound as a colourless oil (156 mg, 99%). The product was judged by ^{1}H NMR spectroscopy to be sufficiently pure to carry forward without further purification.

^{1}H NMR (500 MHz, $CDCl_3$): δ 5.49 (1 H, m, NH), 5.35 (1 H, t, $J_{H,H}$ = 6.0, CCHCH$_2$), 5.26 (1 H, t, $J_{H,H}$ = 7.0, CCHCH$_2$), 5.11 (1 H, t, $J_{H,H}$ = 6.0, CCHCH$_2$), 4.62 (1 H, t, $J_{H,H}$ = 4.0, CH), 4.22 (1 H, dd, $J_{H,H}$ = 12.0 and 6.5, CCHCH$_A$O), 4.02 (1 H, dd, $J_{H,H}$ = 12.0 and 7.5, CCHCH$_B$O), 3.92-3.48 (2 H, m, OCH$_2$CH$_2$), 3.76 (2 H, d, $J_{H,H}$ = 6.0, NHCH$_2$), 2.17-1.94 (11 H, m, 2 x CCHCH$_2$CH$_2$ and NHCCH$_3$), 1.72-1.52 (6 H, m, OCH$_2$CH$_2$CH$_2$), 1.67, 1.60 and 1.59 (3 x 3 H, 3 x s, 3 x CH$_2$CCH$_3$).

^{13}C NMR (125 MHz, $CDCl_3$): δ 170.1 (NHCO), 140.2, 135.0 and 131.9 (3 x CH$_3$CCH), 126.9, 124.5 and 121.0 (3 x CH$_3$CCH), 98.02 (OCHO), 63.85 and 62.52 (2 x OCH$_2$), 47.25 (NHCH$_2$), 39.79 and 39.45 (CCHCH$_2$CH$_2$), 30.93 (OCHCH$_2$), 26.53 and 26.46 (CCHCH$_2$CH$_2$), 25.71 (OCH$_2$CH$_2$CH$_2$), 23.49 (NHCCH$_3$), 19.85 (OCH$_2$CH$_2$CH$_2$), 16.61, 16.18 and 14.67 (3 x CH$_2$CCH$_3$).

LRMS (AP$^+$) *m/z*: 386.27 (100%, [M + Na]$^+$), 364.29 (2, [M + H]$^+$), 177.11 (11).

HRMS (AP$^+$): calculated for (C$_{22}$H$_{37}$O$_3$N + [Na])$^+$: 386.2671, found: 386.2670.

N-((2*E*, 6*E*, 10*E*)-12-Hydroxy-2, 6, 10-trimethyl dodeca-2, 6, 10-trien-1-yl) acetamide (192)

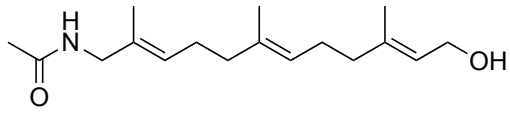

To a stirred solution of **191** (0.13 g, 0.40 mmol) in methanol (5 mL) was added *p*-toluenesulfonic acid (9 mg, 0.04 mmol) and stirred at room temperature for 1 h. The solvent was removed under reduced pressure and the residual oil was dissolved with diethyl ether (10 mL) and washed with saturated aqueous sodium bicarbonate solution (3 x 10 mL) and brine (10 mL). The resulting solution was dried over anhydrous magnesium sulfate, filtered under gravity and concentrated under reduced pressure to give the title compound as a colourless oil (90 mg, 87%). The product was judged by ^{1}H NMR spectroscopy to be sufficiently pure to carry forward without further purification.

^{1}H NMR (500 MHz, $CDCl_3$): δ 5.40 (1 H, t, $J_{H,H}$ = 7.0, CCHCH$_2$), 5.27 (1 H, t, $J_{H,H}$ = 7.0, CCHCH$_2$), 5.10 (1 H, t, $J_{H,H}$ = 7.0, CCHCH$_2$), 4.14 (2 H, d, $J_{H,H}$ = 7.0, CH$_2$OH), 3.75 (2 H, d, $J_{H,H}$ = 6.0, NHCH$_2$), 2.15-1.97 (8 H, m, 2 x CCHCH$_2$CH$_2$), 1.99 (3 H, s, NCCH$_3$), 1.67, 1.60 and 1.59 (3 x 3 H, 3 x s, 3 x CH$_2$CCH$_3$).

^{13}C NMR (125 MHz, $CDCl_3$): δ 170.1 (NHCO), 139.5, 135.0 and 131.8 (3 x CH$_3$CCH), 126.8, 124.3 and 123.8 (3 x CH$_3$CCH), 59.56 (CH$_2$OH), 47.20 (NHCH$_2$), 39.63 and 39.38 (2 x CCHCH$_2$CH$_2$), 26.39 and 26.33 (2 x CCHCH$_2$CH$_2$), 23.48 (NHCCH$_3$), 16.44, 16.16 and 14.68 (3 x CH$_2$CCH$_3$).

LRMS (AP^+) *m/z*: 302.21 (100%, $[M + Na]^+$), 262. 21 (4, $[M - H_2O]^+$), 242.28 (9), 177.11 (20).

HRMS (AP^+): calculated for $(C_{17}H_{29}O_2N + [Na])^+$: 302.2096, found: 302.2096.

N-((2*E*, 6*E*, 10*E*)-12-Bromo-2, 6, 10-trimethyldodeca-2, 6, 10-trien-1-yl) acetamide (193)

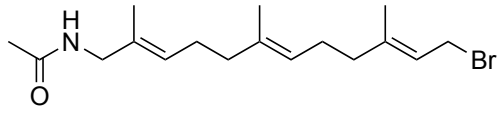

To a stirred solution of **192** (90 mg, 0.30 mmol) in anhydrous THF (5 mL) at -10 °C, was added phosphorous tribromide (15 μL, 0.20 mmol), and this was left to stir for 1 h. The phosphorous tribromide and THF were removed under reduced pressure. The residual product was diluted in diethyl ether (10 mL) and washed with saturated aqueous ammonium bicarbonate solution (3 x 20 mL) and brine (10 mL). The resulting solution was dried over anhydrous magnesium sulfate, filtered under gravity and concentrated under reduced pressure to give the title compound as a colourless oil (100 mg, 90%). The product was judged by ^{1}H NMR spectroscopy to be sufficiently pure to carry forward without further purification.

^{1}H NMR (500 MHz, $CDCl_3$): δ 5.51 (1 H, t, $J_{H,H}$ = 8.5, CC<u>H</u>CH_2Br), 5.26 (1 H, t, $J_{H,H}$ = 7.0, CC<u>H</u>CH_2), 5.12-5.04 (1 H, m, CC<u>H</u>CH_2), 4.01 (2 H, d, $J_{H,H}$ = 8.5, C<u>H</u>$_2$Br), 3.75 (2 H, d, $J_{H,H}$ = 5.5, NHC<u>H</u>$_2$), 2.25-1.97 (8 H, m, 2 x CCHC<u>H</u>$_2$C<u>H</u>$_2$), 2.00 (3 H, s, NHCC<u>H</u>$_3$), 1.71, 1.60 and 1.58 (3 x 3 H, 3 x s, 3 x CH_2CC<u>H</u>$_3$).

(2*E*, 6*E*, 10*E*)-12-Acetamido-3, 7, 11-trimethyl dodeca-2, 6, 10-trien-1-yl diphosphate (184)

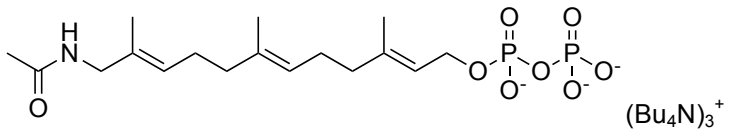

To a stirred solution of **193** (0.10 g, 0.30 mmol) in anhydrous acetonitrile (5 mL) was added **121** (0.50 g, 0.60 mmol). The reaction was left for 48 h to stir under nitrogen. The solvent was removed under reduced pressure and the resulting crude oil was purified by flash chromatography on silica gel (6:2.5:0.5, isopropanol: water: ammonium hydroxide). Fractions that contained the diphosphate as judged by comparison with an authentic FDP standard by TLC (6:3:1, isopropanol: water: ammonium hydroxide) were collected. The isopropanol was removed under reduced

pressure and the remaining solution was lyophilized to give the title compound as colourless oil (30 mg, 9%).

^{1}H NMR (500 MHz, D_2O): δ 5.41 (1 H, m, CC<u>H</u>CH_2), 5.24 (1 H, m, CC<u>H</u>CH_2), 5.15 (1 H, m, CC<u>H</u>CH_2), 4.42 (2 H, m, C<u>H</u>$_2$O), 3.62 (2 H, s, NHC<u>H</u>$_2$), 2.11-1.94 (8 H, m, 2 x CHC<u>H</u>$_2$C<u>H</u>$_2$), 1.96 (3 H, s, NCC<u>H</u>$_3$), 1.68 (3 H, s, CH_2CC<u>H</u>$_3$), 1.57 (3 H, s, CH_2CC<u>H</u>$_3$), 1.55 (3 H, s, CH_2CC<u>H</u>$_3$).

^{31}P NMR (243 MHz, D_2O): δ -8.5 (m), -10.69 (d, $J_{P,P}$ = 22).

LRMS (ES^-) *m/z*: 438.14 (100%, $[M - H]^-$), 411.13 (62), 339.22 (43).

HRMS (ES^-): calculated for $(C_{17}H_{30}O_8NP_2 - [H])^-$: 438.1447, found: 438.1453.

7.2.15 Preparation of 12-amino farnesyl diphosphate (12-Amino FDP, 185)

(9H-Fluoren-9-yl) methyl ((2*E*, 6*E*, 10*E*)-2, 6, 10-trimethyl-12-((tetrahydro-2H-pyran-2-yl) oxy) dodeca-2, 6, 10-trien-1-yl) carbamate (196)

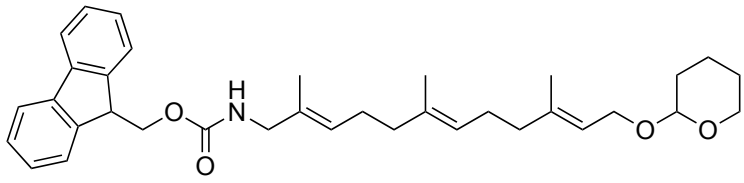

To a stirred solution of **187** (0.12 g, 0.40 mmol) in dioxane (10 mL), was added Fmoc chloride (120 mg, 0.6 mmol) and sodium bicarbonate (50 mg, 0.60 mmol). The reaction mixture was left to stir at room temperature for 24 h. The dioxane was removed under reduced pressure and the residual oil was dissolved in ether (2 mL). The crude oil was purified by flash chromatography on silica gel (95:5, hexane: ethyl acetate) to give the title compound as a colourless oil (870 mg, 74%).

^{1}H NMR (500 MHz, $CDCl_3$): δ 7.77 (2 H, d, $J_{H,H}$ = 7.5, 2 x CC<u>H</u>CH), 7.60 (2 H, d, $J_{H,H}$ = 7.5, 2 x CC<u>H</u>CH), 7.40 (2 H, t, $J_{H,H}$ = 7.5, 2 x CCHC<u>H</u>), 7.31 (2 H, t, $J_{H,H}$ = 7.5, 2 x CCHC<u>H</u>), 5.36 (1 H, t, $J_{H,H}$ = 6.0, CC<u>H</u>CH_2CH_2), 5.28 (1 H, t, $J_{H,H}$ = 7.0, CC<u>H</u>CH_2CH_2), 5.11 (1 H, t, $J_{H,H}$ = 6.5, CC<u>H</u>CH_2CH_2), 4.62 (1 H, t, $J_{H,H}$ = 4.0, OC<u>H</u>CH_2CH_2), 4.43 (2 H, d, $J_{H,H}$ = 7.0, NCOC<u>H</u>$_2$), 4.25-4.21 (2 H, m, C<u>H</u>CH_2OCN and CCHC<u>H</u>$_A$O), 3.91-3.49 (1 H, dd, $J_{H,H}$ = 12.0 and 7.5, CCHC<u>H</u>$_B$O), 3.72 (2 H, d, $J_{H,H}$ = 5.5, NHC<u>H</u>$_2$), 2.13-1.98 (8 H, m, 2 x CCHC<u>H</u>$_2$C<u>H</u>$_2$), 1.74-1.50 (6 H, m, OC<u>H</u>$_2$C<u>H</u>$_2$C<u>H</u>$_2$), 1.67, 1.60 and 1.59 (3 x 3 H, 3 x s, 3 x C<u>H</u>$_3$).

^{13}C NMR (125 MHz, $CDCl_3$): δ 156.5 (2 x N<u>C</u>O), 144.0 and 141.4 (4 x <u>C</u>CHCH), 140.0, 134.8 and 134.0 (3 x CH_3<u>C</u>CH), 127.6 and 127.0 (4 x CCH<u>C</u>H), 126.5 (C<u>C</u>HCH_2CH_2), 125.2 (2 x C<u>C</u>HCH), 124.3 (C<u>C</u>HCH_2CH_2), 120.8 (C<u>C</u>HCH_2CH_2), 112.0 (2 x C<u>C</u>HCH), 97.78 (O<u>C</u>HCH_2), 66.57 (NCO<u>C</u>H_2), 63.64 and 62.27 (<u>C</u>H_2OCHCH_2), 48.85 (NHC<u>H</u>$_2$), 47.37 (<u>C</u>HCH_2OCN), 39.58 and 39.48 (2 x CCHCH_2<u>C</u>H_2), 30.73 (OCH<u>C</u>H_2), 26.36 and

26.27 (2 x CCH$\underline{C}H_2CH_2$), 25.52 (OCH$_2\underline{C}H_2CH_2$), 19.62 (OCH$_2CH_2\underline{C}H_2$), 16.41, 16.00 and 14.31 (3 x C$\underline{C}H_3$).

LRMS (AP$^+$) *m/z*: 566.32 (100%, M + Na$^+$).

HRMS (AP$^+$): calculated for ($C_{35}H_{45}O_4N$+[Na]) $^+$: 566.3246, found: 566.3230.

(9H-Fluoren-9-yl) methyl ((2*E*, 6*E*, 10*E*)-12-hydroxy-2, 6, 10-trimethyl dodeca-2, 6, 10-trien-1-yl) carbamate (197)

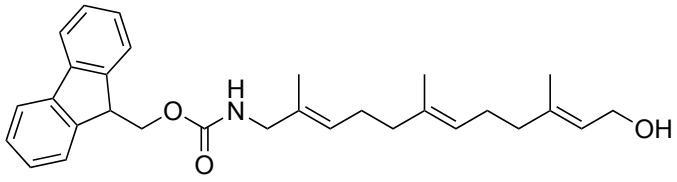

To a stirred solution of **196** (0.87 g, 1.6 mmol) in methanol (10 mL) was added *p*-toluenesulfonic acid (30 mg, 0.16 mmol) and stirred at room temperature for 1 h. The solvent was removed under reduced pressure and the residual oil was dissolved with diethyl ether (10 mL) and washed with saturated aqueous sodium bicarbonate solution (3 x 10 mL) and brine (10 mL). The resulting solution was dried over anhydrous magnesium sulfate, filtered under gravity and concentrated under reduced pressure to give the title compound as a colourless oil (630 mg, 86%). The product was judged by ^{1}H NMR spectroscopy to be sufficiently pure to carry forward without further purification.

^{1}H NMR (500 MHz, $CDCl_3$): δ 7.76 (2 H, d, $J_{H,H}$ = 7.5, 2 x CC$\underline{H}$CH), 7.59 (2 H, d, $J_{H,H}$ = 7.5, 2 x CC$\underline{H}$CH), 7.40 (2 H, t, $J_{H,H}$ = 7.5, 2 x CCHC$\underline{H}$), 7.31 (2 H, t, $J_{H,H}$ = 7.5, 2 x CCHC$\underline{H}$), 5.39 (1 H, t, $J_{H,H}$ = 7.0, CC$\underline{H}CH_2CH_2$), 5.27 (1 H, t, $J_{H,H}$ = 6.5, CC$\underline{H}CH_2CH_2$), 5.10 (1 H, m, CC$\underline{H}CH_2CH_2$), 4.42 (2 H, d, $J_{H,H}$ = 7.0, NCOC$\underline{H}_2$), 4.22 (1 H, m, C$\underline{H}CH_2$OCN), 4.12 (2 H, m, C$\underline{H}_2$OH), 3.71 (2 H, d, $J_{H,H}$ = 5.5, NHC$\underline{H}_2$), 2.17-1.99 (8 H, m, 2 x CCHC$\underline{H}_2$C$\underline{H}_2$), 1.66, 1.61 and 1.60 (3 x 3 H, 3 x s, 3 x C$\underline{H}_3$).

^{13}C NMR (125 MHz, $CDCl_3$): δ 156.7 (2 x N$\underline{C}$O), 144.2 and 141.5 (4 x $\underline{C}$CHCH), 139.7, 135.1 and 132.3 (3 x $CH_3\underline{C}$CH), 127.8 and 127.2 (4 x CCH$\underline{C}$H), 126.6 (C$\underline{C}HCH_2CH_2$), 125.2 (2 x C$\underline{C}$HCH), 124.3 (C$\underline{C}HCH_2CH_2$), 123.7 (C$\underline{C}HCH_2CH_2$), 120.2 (2 x C$\underline{C}$HCH), 66.72 (NCO$\underline{C}H_2$), 60.56 ($\underline{C}H_2$OH), 47.56 ($\underline{C}HCH_2$OCN), 39.64 and 39.40 (2 x CCHCH$_2\underline{C}H_2$), 26.43 and 26.38 (2 x CCH$\underline{C}H_2CH_2$), 16.44, 16.19, 14.53 (3 x $\underline{C}H_3$).

LRMS (AP$^+$) *m/z*: 482.27 (100%, M + Na$^+$), 442.27 (11, M$^+$).

HRMS (AP$^+$): calculated for ($C_{30}H_{37}O_3N$ + [Na])$^+$: 482.2671, found: 482.2679.

(9H-Fluoren-9-yl) methyl ((2*E*, 6*E*, 10*E*)-12-bromo-2, 6, 10-trimethyl dodeca-2, 6, 10-trien-1-yl) carbamate (198)

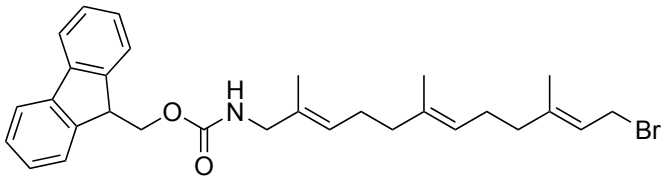

To a stirred solution of **197** (0.62 g, 1.3 mmol) in anhydrous THF (10 mL) at -10 °C, was added phosphorous tribromide (0.64 mL, 0.70 mmol), and this was left to stir for 1 h. The phosphorous tribromide and THF were removed under reduced pressure. The residual product was diluted in diethyl ether (10 mL) and washed with saturated aqueous ammonium bicarbonate solution (3 x 20 mL) and brine (10 mL). The resulting solution was dried over anhydrous magnesium sulfate, filtered under gravity and concentrated under reduced pressure to give the title compound as a colourless oil (630 mg, 89%). The product was judged by ^{1}H NMR spectroscopy to be sufficiently pure to carry forward without further purification.

^{1}H NMR (500 MHz, $CDCl_3$): δ 7.77 (2 H, d, $J_{H,H}$ = 7.5, 2 x CC<u>H</u>CH), 7.60 (2 H, d, $J_{H,H}$ = 7.5, 2 x CC<u>H</u>CH), 7.41 (2 H, t, $J_{H,H}$ = 7.5, 2 x CCHC<u>H</u>), 7.31 (2 H, t, $J_{H,H}$ = 7.5, 2 x CCHC<u>H</u>), 5.52 (1 H, t, $J_{H,H}$ = 8.5, CC<u>H</u>CH_2Br), 5.28 (1 H, t, $J_{H,H}$ = 7.0, CC<u>H</u>CH_2CH_2), 5.09 (1 H, m, CC<u>H</u>CH_2CH_2), 4.42 (2 H, d, $J_{H,H}$ = 7.0, NCO$C\underline{H}_2$), 4.23 (1 H, t, $J_{H,H}$ = 6.5, C<u>H</u>CH_2OCN), 4.02 (2 H, d, $J_{H,H}$ = 8.5, $C\underline{H}_2$Br), 3.73 (2 H, m, NH$C\underline{H}_2$), 2.19-1.97 (8 H, m, 2 x CCH$C\underline{H}_2C\underline{H}_2$), 1.72, 1.62 and 1.60 (3 x 3 H, 3 x s, 3 x $C\underline{H}_3$).

(2*E*, 6*E*, 10*E*)-12-Amino-3, 7, 11-trimethyl dodeca-2, 6, 10-trien-1-yl diphosphate (185)

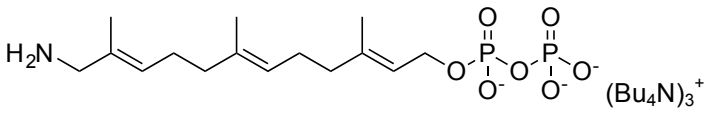

To a stirred solution of **198** (0.63 g, 1.2 mmol) in anhydrous acetonitrile (5 mL) was added **121** (2.2 g, 2.4 mmol). The reaction was left for 48 h to stir under nitrogen. The solvent was removed and the resulting crude oil was purified by flash chromatography on silica gel (6:2.5:0.5, isopropanol: water: ammonium hydroxide). Fractions that contained the diphosphate as judged by comparison with an authentic FDP standard by TLC (6:3:1, isopropanol: water: ammonium hydroxide), were collected. The isopropanol was removed under reduced pressure and the remaining solution was lyophilized to give the title compound as colourless oil (120 mg, 22%).

^{1}H NMR (500 MHz, $CDCl_3$): δ 5.38-5.26 (2 H, m, 2 x CC<u>H</u>CH_2), 5.08 (1 H, m, CC<u>H</u>CH_2), 4.48 (2 H, m, $CHC\underline{H_2}O$), 3.66 (2 H, s, $NH_2C\underline{H_2}$), 3.38-3.35 (36 H, m, 18 x $NC\underline{H_2}CH_2CH_2CH_3$), 2.09-1.95 (8 H, m, 2 x $CCHC\underline{H_2}C\underline{H_2}$), 1.65 (45 H, m, 18 x $NCH_2C\underline{H_2}CH_2CH_3$ and 3 x $CC\underline{H_3}$), 1.44-1.43 (36 H, m, 18 x $NCH_2CH_2C\underline{H_2}CH_3$), 0.97-0.95 (54 H, m, 18 x $NCH_2CH_2CH_2C\underline{H_3}$)

^{31}P NMR (243 MHz, $CDCl_3$): δ -7.71 (m).

LRMS (ES^-) *m/z*: 396.13 (55%, M – H^-), 375.22 (56), 339.27 (100), 312.23 (30).

HRMS (ES^-): calculated for $(C_{15}H_{29}O_7NP_2$ - [H]$)^-$: 396.1341, found: 396.1331.

7.2.16 Preparation of ethyl 2-(bis (2, 2, 2 trifluoroethoxy) phosphoryl) propanoate (141)

<u>Method 1:</u>

Ethyl 2-(diethoxyphosphoryl) propanoate (144)

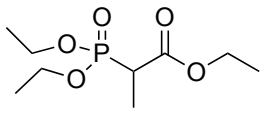

Ethyl 2-bromopropionate (14 mL, 0.10 mol) was preheated to 140 °C before triethyl phosphite (21 mL, 0.12 mol) was added drop-wise. The temperature was raised to 180 °C and the reaction was left to reflux for 24 h. The resulting oil was cooled down and fractionally distilled under reduced pressure. After confirmation by NMR analysis and GC-MS, it was determined that the fraction that distilled above 170 °C gave the title compound (18.3 g, 65%) as a yellow oil.

^{1}H NMR (300 MHz, $CDCl_3$): δ 4.24-4.11 (6 H, m, 3 x $OC\underline{H_2}CH_3$), 3.01 (1 H, dq, $J_{P,H}$ = 23.5 and $J_{H,H}$ = 7.5, PC<u>H</u>), 1.44 (3 H, dd, $J_{P,H}$ = 18 and $J_{H,H}$ = 7.5, $PCHC\underline{H_3}$), 1.33, 1.32 and 1.27 (9 H, 3 x t, $J_{H,H}$ = 7.0, 3 x CH_2CH_3).

^{13}C NMR (125 MHz, $CDCl_3$): δ 169.9 (O<u>C</u>O), 62.87 and 62.82 (2 x $\underline{C}H_2OP$), 61.57 ($\underline{C}H_2OC$), 40.16 (<u>C</u>HP), 16.60 and 16.57 (2 x $\underline{C}H_3CH_2OP$), 14.29 ($\underline{C}H_3CH_2OC$), 11.93 ($CH\underline{C}H_3$).

^{31}P NMR (121 MHz, $CDCl_3$): δ 23.9.

LRMS (EI^+) *m/z*: 238.10 (22%, $[M]^+$), 211.07 (25, $[M\text{-}C_2H_3]^+$), 193.06 (79), 165.05 (100), 109.01 (46).

HRMS (EI^+): calculated for $C_9H_{19}O_5P^+$: 238.0970, found: 238.0969.

Ethyl 2-(dichlorophosphoryl) propanoate (145)

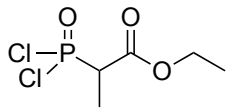

Phosphorous pentachloride (51.1 g, 250 mmol) was added in small portions to an ice cooled **144** (23.0 g, 100 mmol). After stirring for 1 h at room temperature, the solution was heated to 80 °C for 24 h. Once the reaction mixture was cooled and concentrated under reduced pressure, the residue was fractionally distilled. The fraction above 140 °C gave the title compound (13.3 g, 61%) as a yellow oil.

^{1}H NMR (300 MHz, $CDCl_3$): δ 4.34-4.24 (2 H, m, $OC\underline{H}_2CH_3$), 3.66 (1 H, dq, $J_{P,H}$ = 18.5 and $J_{P,H}$ = 7.0, $PC\underline{H}$), 1.68 (3 H, dd, $J_{P,H}$ = 27.5 and $J_{H,H}$ = 7.0, $PCHC\underline{H}_3$), 1.32 (3 H, t, $J_{H,H}$ = 7.0, $OCH_2C\underline{H}_3$).

^{31}P NMR (121 MHz, $CDCl_3$): δ 44.28 (s).

HRMS (EI^+): calculated for $C_5H_9O_3PCl_2^+$: 217.9666, found: 217.9673.

Ethyl 2-(bis (2,2,2-trifluoroethoxy) phosphoryl) propanoate (141)

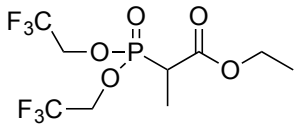

To a stirred solution of **145** (13 g, 60 mmol) in toluene (100 mL) at 0 °C was added a solution of trifluoroethanol (12.6 g, 130 mmol) and diisopropylethylamine (16.2 g, 130 mmol) in toluene (100 mL) that had been cooled to 0 °C prior to addition. The reaction mixture was then left to stir at room temperature for 6 h. After concentrating under reduced pressure, the resulting oil was fractionally distilled under reduced pressure. The fraction boiling at 150-160 °C gave the title compound (4.6 g, 22%) as a colourless oil.

^{1}H NMR (300 MHz, $CDCl_3$): δ 4.49-4.38 (4 H, m, 2 x $C\underline{H}_2CF_3$), 4.23 (2 H, q, $J_{H,H}$ = 7.0, $C\underline{H}_2CH_3$), 3.20 (1 H, dq, $J_{P,H}$ = 22.5 and $J_{H,H}$ = 7.5, $PC\underline{H}$), 1.52 (3 H, dd, $J_{P,H}$ = 19.5 and $J_{H,H}$ 7.5, $PCHC\underline{H}_3$), 1.29 (3 H, t, $J_{H,H}$ = 7.0, $CH_2C\underline{H}_3$).

^{13}C NMR (125 MHz, $CDCl_3$): δ 168.7 ($O\underline{C}O$), 122.6 (2 x $\underline{C}F_3$), 62.77 (2 x $CF_3\underline{C}H_2$), 62.41 ($\underline{C}H_2OC$), 40.29 ($\underline{C}HP$), 14.13 ($\underline{C}H_3CH_2OC$), 11.80 ($CH\underline{C}H_3$).

^{31}P NMR (121 MHz, $CDCl_3$): δ 27.3.

HRMS (EI^+): calculated for $C_9H_{13}O_5PF_6^+$: 346.0405, found: 346.0406.

Method 2:

Ethyl 2-(bis ((trimethylsilyl) oxy) phosphoryl) propanoate (146)

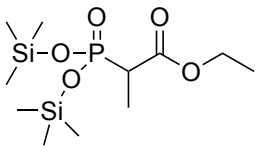

Triethyl 2-phosphonopropionate (6.60 mL, 27.7 mmol) and trimethylsilyl chloride (19.2 mL, 177 mmol) were combined in 3 pressure tubes, initially flushed with argon. The solutions were heated to 100 °C and left to stir for 7 days. The solutions were combined and concentrated under reduced pressure to give the title compound (9.9 g) as a yellow oil.

^{1}H NMR (500 MHz, $CDCl_3$): δ 4.20-4.16 (2 H, m, OCH_2), 2.99-2.86 (1 H, m, PCH), 1.40 (3 H, dd, $J_{P,H}$ = 19 and $J_{H,H}$ 7.5, $PCHCH_3$), 1.28 (3 H, t, $J_{H,H}$ = 7, CH_2CH_3), 0.30 (18 H, s, 6 x $SiCH_3$).

^{31}P NMR (121 MHz, D_2O): δ 4.75.

LRMS (ES^+) *m/z*: 327.12 (100%, M + H^+), 283.12 (17), 255.08 (92), 241.07 (26).

HRMS (ES^+): calculated for $(C_{11}H_{27}O_5PSi_2 + [H])^+$: 327.1213, found: 327.1199.

Ethyl 2-(dichlorophosphoryl) propanoate (145)

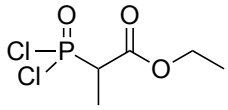

To a stirred solution of **146** (10.5 g, 32.2 mmol) in DCM (100 mL) was added DMF (1 mL). Oxalyl chloride (6.8 mL, 80 mmol) was added gradually over a period of 10 minutes and the reaction was left to stir for 1 h. The solvent was removed under reduced pressure to give the crude title compound (6.8 g).

^{1}H NMR (300 MHz, $CDCl_3$): δ 4.34-4.24 (2 H, m, CH_2CH_3), 3.66 (1 H, dq, $J_{P,H}$ = 18.5 and $J_{H,H}$ = 7, PCH), 1.68 (3 H, dd, $J_{P,H}$ = 27.5 and $J_{H,H}$ 7.0, $PCHCH_3$), 1.32 (3 H, t, $J_{H,H}$ = 7.0, CH_2CH_3).

^{31}P NMR (121 MHz, $CDCl_3$): δ 44.28.

HRMS (EI^+): calculated for $C_5H_9O_3P^{35}Cl_2^+$: 217.9666, found: 217.9673.

Ethyl 2-(bis (2,2,2-trifluoroethoxy) phosphoryl) propanoate (141)

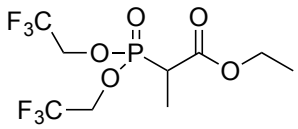

To stirred solution of **145** (6.80 g, 31.2 mmol) in DCM (50 mL) at 0 °C was added a solution of triethylamine (22.7 mL, 163 mmol) and 2,2,2-trifluoroethanol (7.90 mL, 109 mmol) in DCM (50 mL), drop-wise. 4-*N,N*-Dimethylaminopyridine (66 mg, 0.50 mmol) was then added and the resulting solution was left to stir for 24 h. The reaction was diluted with DCM (50 mL), washed with brine (3 x 50 mL), dried over anhydrous magnesium sulfate, filtered under gravity and concentrated under reduced pressure. The crude oil was purified by flash chromatography on silica gel (2:1, hexane: ethyl acetate) to give the title compound as a colourless oil (9.1 g, 84%).

^{1}H NMR (300 MHz, $CDCl_3$): δ 4.49-4.38 (4 H, m, 2 x $C\underline{H}_2CF_3$), 4.23 (2 H, q, $J_{H,H}$ = 7.0, $C\underline{H}_2CH_3$), 3.20 (1 H, dq, $J_{P,H}$ = 22.5 and $J_{H,H}$ = 7.5, PC<u>H</u>), 1.52 (3 H, dd, $J_{P,H}$ = 19.5 and $J_{H,H}$ = 7.5, PCHC$\underline{H}_3$), 1.29 (3 H, t, $J_{H,H}$= 7, $CH_2C\underline{H}_3$).

^{13}C NMR (125 MHz, $CDCl_3$): δ 168.7 (O<u>C</u>O), 122.6 (2 x $\underline{C}F_3$), 62.77 (2 x $CF_3\underline{C}H_2$), 62.41 ($\underline{C}H_2OC$), 40.29 (<u>C</u>HP), 14.13 ($\underline{C}H_3CH_2OC$), 11.80 ($CH\underline{C}H_3$).

^{31}P NMR (121 MHz, $CDCl_3$): δ 27.3.

^{19}F NMR (470 MHz, $CDCl_3$): δ -75.38.

LRMS (EI^+) *m/z*: 346.04 (22%, M^+), 319.02 (20), 301.00 (100), 274.02 (72), 245.99 (67).

HRMS (EI^+): calculated for $C_9H_{13}O_5PF_6^+$: 346.0405, found: 346.0406.

7.2.17 Preparation of (2*E*, 6*E*)-3, 7, 11-trimethyldodeca-2, 6, 10-trienal (279)

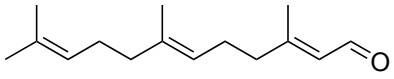

To a stirred solution of (2*E*, 6*E*)-Farnesol (50.0 mg, 227 μmol) in hexane (5 mL) was added manganese dioxide (500 mg, 5.75 mmol). This solution was left to stir for 48 h. After TLC analysis (8:2, hexane: ethyl acetate) showed complete consumption of the starting material, the solution was diluted with hexane (20 mL) and passed through a celite plug. The celite was washed with ethyl acetate (2 x 10 mL) and the combined organic extracts were concentrated under reduced pressure to give the title compound as a colourless oil (35 mg, 70%).

^{1}H NMR (500 MHz, $CDCl_3$): δ 9.96 (1 H, d, $J_{H,H}$ = 8.0, CHCHO), 5.86 (1 H, d, $J_{H,H}$ = 8.0, CHCHO), 5.08-5.01 (2 H, m, 2 x C=CH), 2.24-1.92 (8 H, m, 2 x CH_2CH_2), 2.14, 1.64, 1.57 and 1.56 (4 x 3 H, 4 x s, 4 x CH_3).

^{13}C NMR (125 MHz, $CDCl_3$): δ 191.5 (CHO), 164.2 (CCHCHO), 136.7 and 131.7 (2 x $CCHCH_2$), 127.6 (CCHCHO), 124.3 and 122.6 (2 x $CCHCH_2$), 40.78 and 39.79 (2 x $CHCH_2CH_2$), 26.77 and 25.87 (2 x $CHCH_2CH_2$), 25.83, 17.86, 17.78 and 16.23 (4 x CH_3).

LRMS (EI^+) *m/z*: 220.18 (10%, M^+), 202.17 (37), 187.15 (39), 173.13 (13), 159.12 (40), 145.10 (36), 119.08 (54), 93.06 (100), 67.05 (90).

HRMS (EI^+): calculated for $C_{15}H_{24}O^+$: 220.1827, found: 220.1827.

7.2.18 Preparation of methyl (*R*)-2-((1*R*, 4*R*, 4a*S*, 8a*S*)-4, 7-dimethyl-1, 2, 3, 4, 4a, 5, 6, 8a-octahydronaphthalen-1-yl) propanoate (11*R*-88)

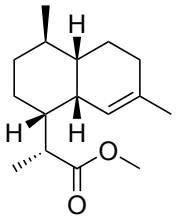

To a stirred solution of (11*R*)-**50** (25 mg, 0.10 mmol) in toluene (2 mL) was added *N,N*-dimethylformamide (10 μL, 0.69 μmol). The reaction was stirred at 0 °C while oxalyl chloride (9.4 mL, 0.11 mmol) was added drop-wise. The solution was left to stir for 30 min before a mixture of triethylamine (100 μL) and methanol (900 μL) was added drop-wise over 10 min. The mixture was stirred for 1 h and then the excess methanol was removed under reduced pressure. The toluene suspension was washed with water (2 x 5 mL), dried over anhydrous sodium sulfate, filtered under gravity and concentrated under reduced pressure. The crude oil was purified by flash chromatography on silica gel (9:1, hexane: ethyl acetate) to give the title compound as a colourless oil (14 mg, 78%).

^{1}H NMR (500 MHz, $CDCl_3$): δ 5.12 (1 H, bs, $CH_3C=CH$), 3.67 (3 H, s, CH_3OC), 2.50 (2 H, m, OCCHCHCH), 1.97-1.78 (3 H, m, $CH_3CCH_2CH_b$), 1.63 (3 H, s, $CH=CCH_3$), 1.63-1.55 (3 H, m, $CH_3CCH_2CH_a$ and OCCHCH and CH_3CHCH_b), 1.41 (1 H, m, CH_3CHCH_2), 1.26 (2 H, m, $OCCHCHCH_a$ and $CH=CCH_2CH_2CH$), 1.13 (3 H, d, *J* = 7.0, $CHCH_3$), 1.09-0.92 (2 H, m, $CH_3CHCH_aCH_b$), 0.86 (3 H, d, *J* = 6.5, $CHCH_3$).

^{13}C NMR (125 MHz, $CDCl_3$): δ 178.2 (OCO), 136.1 ($CH=CCH_3$), 119.7 ($CH=CCH_3$), 51.62 ($COCH_3$), 44.19 (CHCHCO), 43.27 (CHCHCO), 41.94 ($CHCH_2CH_2C=CH$), 36.63 ($CH=CCH_3$), 35.48 ($CH_3CHCH_2CH_2$), 27.89 ($CH_3CHCH_2CH_2$), 27.68 ($CH_3CHCH_2CH_2$),

26.84 ($CH_2\underline{C}H_2C$=CH), 25.99 ($\underline{C}H_2CH_2C$=CH), 24.05 ($\underline{C}H_3CHCH_2$), 19.92 (CH=C$\underline{C}H_3$), 15.34 ($\underline{C}H_3CHCO$).

LRMS (EI^+) *m/z*: 250.19 (1.4%, M^+), 219.17 (2.8), 201.16 (3.4), 162.13 (100), 147.11 (35.2), 121.10 (11.7), 91.05 (19.3), 79.05 (16.5).

HRMS (EI^+): calculated for $C_{16}H_{26}O_2^+$: 250.1933, found: 250.1930.

7.2.19 Preparation of (*R*)-2-((1*R*, 4*R*, 4a*S*, 8a*S*)-4, 7-dimethyl-1, 2, 3, 4, 4a, 5, 6, 8a-octahydronaphthalen-1-yl) propanal (11*R*-49)

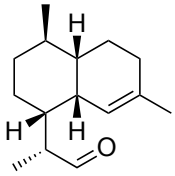

To a stirred solution of **88** (11 mg, 44 μmol) in anhydrous THF (1 mL) at -78 °C was added DIBAL-H (1 M in toluene, 44 μL, 44 μmol), drop-wise, and the reaction was left to stir for 30 min. The reaction was quenched by addition of saturated aqueous sodium bicarbonate solution (5 mL) and left to stir for 1 h. The layers were separated and the aqueous layer was extracted with diethyl ether (3 x 5 mL). The pooled organic extracts were washed with brine (10 mL) and dried over anhydrous sodium sulfate before being filtered under gravity and concentrated under reduced pressure. The crude oil was purified by flash chromatography on silica gel (19:1, hexane: ethyl acetate) to give the title compound as a colourless oil (3 mg, 31%).

^{1}H NMR (500 MHz, $CDCl_3$): δ 9.57 (1 H, d, *J* = 3.5, C$\underline{H}$O), 5.12 (1 H, bs, CH_3C=C$\underline{H}$), 2.48 (1 H, m, C=CHC$\underline{H}$), 2.37 (1 H, m, OCHC$\underline{H}$), 1.98-1.79 (3 H, m, $CH_3C\underline{C}H_2\underline{C}H_b$), 1.64 (3 H, s, $C\underline{C}H_3$), 1.63-1.56 (3 H, m, $CH_3CCH_2\underline{C}H_a$ and OCHCHC$\underline{H}$ and $CH_3CHC\underline{H}_b$), 1.41 (2 H, m, $CH_3C\underline{H}CH_2$ and OCHCHCHC$\underline{H}_a$), 1.29 (1 H, m, CH=C$\underline{C}H_2CH_2C\underline{H}$), 1.13 (1 H, dd, *J* = 13.0 and 3.0, OCHCHCHC$\underline{H}_b$), 1.07 (3 H, d, *J* = 7.0, OCHCHC$\underline{H}_3$), 0.96 (1 H, ddd, J = 24.5, 13.0 and 3.0, $CH_3CHC\underline{H}_2$), 0.88 (3 H, d, *J* = 6.5, CHC$\underline{H}_3$).

^{13}C NMR (125 MHz, $CDCl_3$): δ 206.3 ($\underline{C}$HO), 136.3 (CH=$\underline{C}CH_3$), 119.8 ($\underline{C}$H=CCH_3), 48.65 (OCH$\underline{C}$H), 42.06 ($CH_3\underline{C}CH_2CH_2\underline{C}H$), 41.69 (OCHCH$\underline{C}$H), 36.80 (C=CH$\underline{C}$H), 35.47 ($CH_3CH\underline{C}H_2CH_2$), 27.92 ($CH_3\underline{C}HCH_2CH_2$), 27.55 ($CH_3CHCH_2\underline{C}H_2$), 26.79 ($CH_2\underline{C}H_2C$=CH), 25.96 ($\underline{C}H_2CH_2C$=CH), 24.04 ($\underline{C}H_3C$=CH), 19.91 ($CH_2CH\underline{C}H_3$), 11.96 ($\underline{C}H_3CHCHO$).

LRMS (EI^+) *m/z*: 220.18 (29.3%, M^+), 202.17 (40.9), 187.15 (77.2), 162.14 (100), 147.12 (46.8), 131.10 (25.5), 91.06 (46.5), 79.06 (38.1).

HRMS (EI^+): calculated for $C_{15}H_{24}O^+$: 220.1827, found: 220.1830.

7.2.20 General procedures for incubations of ADS with FDP or FDP analogues

Analytical incubations

FDP (or FDP analogue, 0.4 mM) was combined with ADS (1 μM) in an incubation buffer (250 μL) (Buffer composition is given in Section 7.1.4). The incubation was overlaid with pentane (1 mL) and left to gently shake overnight at room temperature. The next day, the organic layer was extracted and analysed by GC-MS.

Preparative scale incubations

To minimize losses of volatile sesquiterpenoid products during incubation and workup, reactions were performed in sealed Schott bottles containing incubation buffer with FDP (or FDP analogue, 0.2 - 0.4 mM) and enzyme (1 μM). The incubation was overlaid with pentane (10-20% of incubation volume). Each incubation solution was gently agitated (24 h, RT) after which the pentane layer was separated using a separating funnel. The aqueous layer was extracted with additional pentane (3 x 10 mL). Each extraction was separated by first, freezing the emulsion formed by mixing both layers in liquid nitrogen. Upon thawing, the pentane trapped in the emulsion was freed and collected. The pooled pentane extracts were concentrated under reduced pressure to yield the product as a yellow oil.

Amorphadiene (45)

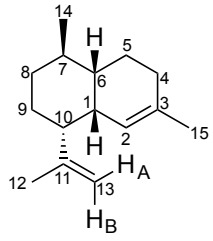

^{1}H NMR (500 MHz, $CDCl_3$): δ (ppm) 5.05 (1 H, bs, C<u>H</u>=CCH$_3$), 4.87 (1 H, bs, C=C<u>H</u>$_A$), 4.64 (1 H, bs, C=C<u>H</u>$_B$), 2.55 (1 H, m, CH$_2$CCHC<u>H</u>), 1.96-0.89 (11 H, m, (C<u>H</u>$_2$)$_2$C<u>H</u>C<u>H</u>(C<u>H</u>$_2$)$_2$C<u>H</u>), 1.74 (3 H, s, CH$_2$=CC<u>H</u>$_3$), 1.60 (3 H, s, CH=CC<u>H</u>$_3$), 0.88 (3 H, d, *J* = 6.5, CH$_2$CHC<u>H</u>$_3$).

^{13}C NMR (125 MHz, CDCl3): δ 148.2 (CH$_3$<u>C</u>=CH$_2$), 134.8 (CH$_3$<u>C</u>=CH), 121.1 (CH$_3$C=<u>C</u>H), 110.0 (CH$_3$C=<u>C</u>H$_2$), 47.85 (CH2=C<u>C</u>H), 42.02 (CH$_3$CCH$_2$CH$_2$<u>C</u>H), 37.84 (C=CH<u>C</u>H), 35.61 (CH$_3$CH<u>C</u>H$_2$), 26.68 (CH$_3$C<u>C</u>H$_2$), 26.01 (CH$_3$CHCH$_2$<u>C</u>H$_2$), 23.83 (<u>C</u>H$_3$C=CH), 22.77 (<u>C</u>H$_3$C=CH$_2$), 20.03 (<u>C</u>H$_3$CHCH$_2$).

LRMS (EI$^+$) *m/z*: 204.19 (63.5%, M$^+$), 189.16 (88.6), 175.15 (16.8), 162.14 (41.3), 147.12 (33.5), 133.10 (28.8), 119.08 (100), 105.07 (47.0), 93.07 (69.9), 79.05 (45.5), 67.05 (12.3).

14-Methyl amorphadiene (211)

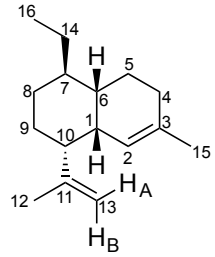

^{1}H NMR (500 MHz, $CDCl_3$): δ (ppm) 5.06 (1 H, bs, C<u>H</u>=CCH$_3$), 4.87 (1 H, bs, CH$_3$C=C<u>H$_A$</u>), 4.64 (1 H, bs, CH$_3$C=C<u>H$_B$</u>), 2.57 (1 H, m, CH$_2$=CCHC<u>H</u>), 1.74 (3 H, s, CH$_2$=CC<u>H$_3$</u>), 1.60 (3 H, s, CH=CC<u>H$_3$</u>), 0.88 (3 H, d, *J* = 6.5, CH$_2$CHC<u>H$_3$</u>).

LRMS (EI$^+$) *m/z*: 218.20 (53.6%, M$^+$), 203.18 (45.3), 189.16 (100), 175.15 (17.2), 162.14 (22.3), 147.12 (25.4), 133.10 (59.9), 119.09 (20.1), 105.07 (60.7), 93.07 (43.8), 79.05 (33.7).

Dihydroartemisinic aldehyde (mixture of 11-*R* and 11-*S* epimers) (11*R*-49 and 11*S*- 49)

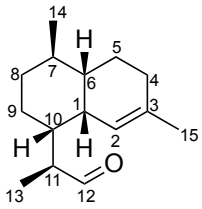

11*S*-49

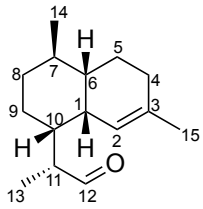

11*R*-49

^{1}H NMR (500 MHz, $CDCl_3$): δ (ppm) 9.62 (1 H, d, *J* = 3.5, C<u>H</u>O, (11*S*)), 9.57 (1 H, d, *J* = 3.5, C<u>H</u>O, (11*R*)), 5.26 (1 H, bs, CH$_3$C=C<u>H</u>, (11*S*)), 5.12 (1 H, bs, CH$_3$C=C<u>H</u>, (11*R*)), 2.48 (2 H, m, 2 x C=CHC<u>H</u>, (11*R*) and (11*S*)), 2.39 (2 H, m, 2 x OCHC<u>H</u>, (11*S*) and (11*R*)), 1.91-1.25 (20 H, m, 2 x (C<u>H$_2$</u>)$_2$C<u>H</u>C<u>H</u>(C<u>H$_2$</u>)$_2$, (11*R*) and (11*S*)), 1.63 (6 H, s, 2 x CC<u>H$_3$</u>), 1.08 (3 H, d, *J* = 7.0, OCHCHC<u>H$_3$</u>, (11*R*)), 1.06 (3 H, d, *J* = 7.0, OCHCHC<u>H$_3$</u>, (11*S*)), 0.87 (6 H, d, *J* = 6.5, 2 x CHC<u>H$_3$</u>, (11*R*) and (11*S*)).

^{13}C NMR (125MHz, CDCl3): δ 206.3 (<u>C</u>HO), 136.3 (CH=<u>C</u>CH$_3$), 119.8 (<u>C</u>H=CCH$_3$), 48.65 (OCH<u>C</u>H), 42.06 (CH$_3$<u>C</u>CH$_2$CH$_2$CH), 41.69 (OCHCH<u>C</u>H), 36.80 (C=CH<u>C</u>H), 35.47 (CH$_3$CH<u>C</u>H$_2$CH$_2$), 27.92 (CH$_3$<u>C</u>HCH$_2$CH$_2$), 27.55 (CH$_3$CHCH$_2$<u>C</u>H$_2$), 26.79 (CH$_2$<u>C</u>H$_2$C=CH), 25.96 (<u>C</u>H$_2$CH$_2$C=CH), 24.04 (<u>C</u>H$_3$C=CH), 19.91 (CH$_2$CH<u>C</u>H$_3$), 11.96 (<u>C</u>H$_3$CHCHO).

LRMS (EI$^+$) *m/z*: 220.18 (21.6%, [11*R*-49]$^+$), 202.17 (39.9), 187.15 (68.6), 162.14 (100), 147.12 (43.3), 131.09 (18.24), 105.07 (20.4), 91.05 (21.2), 79.05 (16.8).

LRMS (EI$^+$) *m/z*: 220.18 (20.9%, [11*S*-49]$^+$), 202.17 (58.4), 187.15 (100), 162.14 (81.4), 145.10 (52.2), 131.09 (28.1), 105.07 (25.7), 91.06 (25.4), 79.05 (15.6).

11*S*-Dihydroartemisinic aldehyde

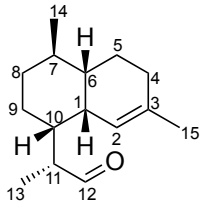

11*R*-49

^{1}H NMR (500 MHz, $CDCl_3$): δ (ppm) 9.62 (1 H, d, *J* = 3.5, C<u>H</u>O), C<u>H</u>O, 5.26 (1 H, bs, CH_3C=C<u>H</u>), 2.48 (1 H, m, C=CHC<u>H</u>), 2.39 (1 H, m, OCHC<u>H</u>), 1.91-1.25 (10 H, m, (C<u>H</u>$_2$)$_2$C<u>H</u>C<u>H</u>(C<u>H</u>$_2$)$_2$), 1.63 (6 H, s, 2 x CC<u>H</u>$_3$), 1.06 (3 H, d, *J* = 7.0, OCHCHC<u>H</u>$_3$), 0.87 (3 H, d, *J* = 6.5, CHC<u>H</u>$_3$).

8-Methoxy-γ-humulene (262)

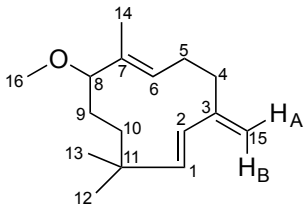

^{1}H NMR (500 MHz, $CDCl_3$): δ (ppm) 5.88 (1 H, d, *J* = 6.0, CH=C<u>H</u>), 5.52 (1 H, t, *J* = 8.0, CH_3C=C<u>H</u>C<u>H</u>$_2$), 5.48 (1 H, d, *J* = 6.0, C<u>H</u>=CH), 4.89 (1 H, d, *J* = 2.0, C<u>H</u>$_A$=C), 4.81 (1 H, d, *J* = 2.0, C<u>H</u>$_B$=C), 3.30 (1 H, dd, *J* = 2.5 and 9.0, OC<u>H</u>), 3.10 (3 H, s, OC<u>H</u>$_3$), 1.71-1.25 (8 H, m, 2 x C<u>H</u>$_2$C<u>H</u>$_2$), 1.37 (3 H, s, OCHCC<u>H</u>$_3$) 0.97 and 0.96 (2 x 3 H, 2 x s, 2 x CH_3CC<u>H</u>$_3$).

^{13}C NMR (125 MHz, CDCl3): δ 148.8 (<u>C</u>=CH$_2$), 143.0 (CH_3<u>C</u>=CH), 135.9 (CH_3C=<u>C</u>H), 129.4 and 125.5 (<u>C</u>H=<u>C</u>H), 113.5 (C=<u>C</u>H$_2$), 90.28 (<u>C</u>HO), 55.65 (O<u>C</u>H$_3$), 41.36 (<u>C</u>CH$_3$)$_2$), 36.41 and 32.78 (2 x CCH$_2$), 31.33 and 30.29 (<u>C</u>H$_3$C<u>C</u>H$_3$), 28.33 (<u>C</u>H$_2$CH=C), 18.15 (O<u>C</u>H$_3$), 10.75 (OCH<u>C</u>H$_2$).

LRMS (EI$^+$) *m/z*: 234.20 (6.4%, M$^+$), 219.18 (4.2), 202.17 (86.3), 187.15 (100), 173.13 (33.2), 159.12 (83.1), 145.10 (51.5), 131.09 (88.5), 119.09 (45.8), 105.07 (76.5), 91.05 (96.7), 79.05 (52.6), 67.05 (14.5).

Chapter 8. References

[1] World Health Organization, *World Malaria Report 2015*, World Health Organization, **2015**.

[2] UNICEF, World Health Organisation, *The Global Malaria Burden*, **2000**.

[3] L. F. Haas, *J. Neurol. Neurosurg. Psychiatry* **1999**, *67*, 520.

[4] World Health Organization, *Global Technical Strategy for Malaria 2016-2030*, **2015**.

[5] J. L. Gallup, J. D. Sachs, *The Economic Burden of Malaria*, American Society Of Tropical Medicine And Hygiene, **2001**.

[6] D. A. Macleod, A. P. Morse, *Sci. Rep.* **2014**, *4*, 1–7.

[7] Centers for disease control and prevention, 'Malaria facts', can be found under http://www.cdc.gov/malaria/about/facts.html, **2015**.

[8] K. Haldar, N. Mohandas, *Am. Soc. Hematol.* **2010**, *1*, 87–93.

[9] L. Florens, M. P. Washburn, J. D. Raine, R. M. Anthony, M. Grainger, J. D. Haynes, J. K. Moch, N. Muster, J. B. Sacci, D. L. Tabb, et al., *Nature* **2002**, *419*, 520–526.

[10] M. A. Biamonte, J. Wanner, K. G. Le Roch, *Bioorg. Med. Chem. Lett.* **2013**, *23*, 2829–2843.

[11] National institue of Healths, 'Life Cycle of the Malaria Parasite', can be found under https://www.niaid.nih.gov/topics/Malaria/Pages/lifecycle.aspx, **2012**.

[12] S. R. Meshnick, M. J. Dobson, in *Antimalar. Chemother. Mech. Action, Resist. New Dir. Drug Discov.* (Ed.: P.J. Rosenthal), Humana Press Inc, **2001**, pp. 15–26.

[13] J. Achan, A. O. Talisuna, A. Erhart, A. Yeka, J. K. Tibenderana, F. N. Baliraine, P. J. Rosenthal, U. D'Alessandro, *Malar. J.* **2011**, *10*, 1–12.

[14] Committee on the Economics of Antimalarial Drugs, Institute of Medicine, Board on global health, *Saving Lives, Buying Time: Economics of Malaria Drugs in an Age of Resistance*, The National Academies Press, Washington, **2004**.

[15] D. J. Sullivan, I. Y. Gluzman, D. G. Russell, D. E. Goldberg, *Proc. Natl. Acad. Sci. U. S. A.* **1996**, *93*, 11865–11870.

[16] A. F. G. Slater, *Pharm. Ther.* **1993**, *57*, 203–235.

[17] D. Greenwood, *Antimicrobial Drugs: Chronicle of a Twentieth Century Medical Triumph*, OUP Oxford, **2008**.

[18] A. B. S. Sidhu, D. Verdier-Pinard, D. A. Fidock, *Science* **2002**, *298*, 210–203.

[19] D. J. Terlouw, J. M. Courval, M. S. Kolczak, O. S. Rosenberg, A. J. Oloo, P. A. Kager, A. A. Lal, B. L. Nahlen, F. O. ter Kuile, *J. Infect. Dis.* **2003**, *187*, 467–476.

[20] M. Takechi, M. Matsuo, C. Ziba, A. Macheso, D. Butao, I. L. Zungu, I. Chakanika, M. D. G. Bustos, *Trop. Med. Int. Heal.* **2001**, *6*, 429–434.

[21] A. Nzila, *J. Antimicrob. Chemother.* **2006**, *57*, 1043–1054.

[22] R. G. Ridley, *Nature* **2002**, *415*, 686–693.

[23] R. L. DeGowin, R. D. Powell, *World Heal. Organ.* **1965**, 1–16.

[24] M. L. Gatton, L. B. Martin, Q. Cheng, *Society* **2004**, *48*, 2116–2123.

[25] S. Wells, G. Diap, J. R. Kiechel, *Malar. J.* **2013**, *12*, 1–10.

[26] R. W. Snow, J.-F. Trape, K. Marsh, *Trends Parasitol.* **2001**, *17*, 593–597.

[27] E. A. Ashley, M. Dhorda, R. M. Fairhurst, C. Amaratunga, P. Lim, S. Suon, S. Sreng, J. M. Anderson, S. Mao, B. Sam, et al., *N. Engl. J. Med.* **2014**, *371*, 411–423.

[28] D. L. Klayman, *Science* **1985**, *228*, 1049–1055.

[29] L. H. Miller, X. Su, *Cell* **2011**, *146*, 855–858.

[30] T. Youyou, *Nat. Med.* **2011**, *17*, 1217–1220.

[31] C. Hao, *Lasker Award Rekindles Debate Over Artemisinin's Discovery*, **2011**.

[32] E. Callaway, D. Cyranoski, *Nature* **2015**, *526*, 174–175.

[33] J.-B. Jiang, G.-Q. Li, X.-B. Guo, Y. C. Kong, K. Arnold, *Lancet* **1982**, *8293*, 285–288.

[34] L. Cui, X. Su, *Expert Rev. Anti. Infect. Ther.* **2009**, *7*, 999–1013.

[35] S. R. Meshnick, T. E. Taylor, S. Kamchonwongpaisan, *Microbiol. Rev.* **1996**, *60*, 301–315.

[36] I. D'Acquarica, F. Gasparrini, D. Kotoni, M. Pierini, C. Villani, W. Cabri, M. Di Mattia, F. Giorgi, *Molecules* **2010**, *15*, 1309–1323.

[37] F. Nosten, N. J. White, *Am. J. Trop. Med. Hyg.* **2007**, *77*, 181–192.

[38] P. G. Kremsner, S. Krishna, *Lancet* **2004**, *364*, 285–294.

[39] Z. Chang, *Sci. China Life Sci.* **2015**, *59*, 1–8.

[40] World Health Organisation, *Guidelines for the Treatment of Malaria.*, WHO Press, **2015**.

[41] G. D. Brown, *Molecules* **2010**, *15*, 7603–7698.

[42] J. Wang, L. Huang, J. Li, Q. Fan, Y. Long, Y. Li, B. Zhou, *PLoS One* **2010**, *5*, 1–12.

[43] B. Zhou, *Sci. China Life Sci.* **2015**, *58*, 1151–1153.

[44] P. M. O'Neill, V. E. Barton, S. A. Ward, *Molecules* **2010**, *15*, 1705–1721.

[45] J. Wang, C.-J. Zhang, W. N. Chia, C. C. Y. Loh, Z. Li, Y. M. Lee, Y. He, L.-X. Yuan, T. K. Lim, M. Liu, et al., *Nat. Commun.* **2015**, *6*, 1–11.

[46] N. Edikpo, S. Ghasi, A. Elias, N. Oguanobi, *Mol. Cell. Pharmacol.* **2013**, *5*, 75–89.

[47] S. Krishna, L. Bustamante, R. K. Haynes, H. M. Staines, *Trends Pharmacol. Sci.* **2008**, *29*, 520–527.

[48] S. Sinha, B. Medhi, R. Sehgal, *Parasite* **2014**, *21*, 61–76.

[49] W. Brandt, L. Brauer, N. Gunnewich, J. Kufka, F. Rausch, D. Schulze, E.

Schulze, R. Weber, S. Zakharova, L. Wessjohann, *Phytochem.* **2009**, *70*, 1758–1775.

[50] S. Deng, T. Wei, K. Tan, M. Hu, F. Li, Y. Zhai, S. Ye, Y. Xiao, L. Hou, Y. Pei, et al., *Sci. China Life Sci.* **2016**, *59*, 183–193.

[51] G. E. Bartley, P. a Scolnik, *Plant Cell* **1995**, *7*, 1027–1038.

[52] F. Chen, D. Tholl, J. Bohlmann, E. Pichersky, *Plant J.* **2011**, *66*, 212–229.

[53] C. H. Wen, Y. H. Tseng, F. H. Chu, *Holzforschung* **2012**, *66*, 183–189.

[54] P. M. Bleeker, P. J. Diergaarde, K. Ament, S. Schutz, B. Johne, J. Dijkink, H. Hiemstra, R. De Gelder, M. T. J. De Both, M. W. Sabelis, et al., *Phytochem.* **2011**, *72*, 68–73.

[55] J. Stökl, J. Brodmann, A. Dafni, M. Ayasse, B. S. Hansson, *Proc. Biol. Sci.* **2011**, *278*, 1216–1222.

[56] D. J. Newman, G. M. Cragg, K. M. Snader, *Nat. Prod. Rep.* **2000**, *17*, 215–234.

[57] C. Sallaud, D. Rontein, S. Onillon, F. Jabès, P. Duffé, C. Giacalone, S. Thoraval, C. Escoffier, G. Herbette, N. Leonhardt, et al., *Plant Cell* **2009**, *21*, 301–317.

[58] R. Croteau, T. M. Kutchan, N. G. Lewis, *Natural Products. Secondary Metabolites*, American Society Of Plant Physiologists, **2000**.

[59] D. S. Seigler, *Plant Secondary Metabolism*, Springer Science & Business Media, **1998**.

[60] L. Ruzicka, *Experientia* **1953**, *9*, 357–367.

[61] G. Singh, *Chemistry of Terpenoids and Carotenoids, Volume 3*, Discovery Publishing House, **2007**.

[62] A. Hemmerlin, J. L. Harwood, T. J. Bach, *Prog. Lipid Res.* **2012**, *51*, 95–148.

[63] B. A. Kellogg, C. D. Poulter, *Curr. Opin. Chem. Biol.* **1997**, *1*, 570–578.

[64] D. J. McGarvey, R. Croteau, *Plant Cell* **1995**, *7*, 1015–1026.

[65] J. S. Dickschat, *Nat. Prod. Rep.* **2011**, *28*, 1917–1936.

[66] P. Liao, A. Hemmerlin, T. J. Bach, M.-L. Chye, *Biotechnol. Adv.* **2016**, DOI 10.1016/j.biotechadv.2016.03.005.

[67] H. M. Miziorko, *Arch. Biochem. Biophys.* **2011**, *505*, 131–143.

[68] W. Eisenreich, M. Schwarz, M. H. Zenk, A. Bacherl, A. Cartayrade, D. Arigoni, *Chem. Biol.* **1998**, *5*, 221–233.

[69] W. Eisenreich, F. Rohdich, A. Bacher, *Trends Plant Sci.* **2001**, *6*, 78–84.

[70] W. Wang, K. Wang, I. Span, J. Jauch, A. Bacher, M. Groll, E. Oldfield, *J. Am. Chem. Soc.* **2012**, *134*, 11225–11234.

[71] J. Chappell, *Plant Physiol.* **1995**, *107*, 1–6.

[72] D. J. Hosfield, Y. Zhang, D. R. Dougan, A. Broun, L. W. Tari, R. V Swanson, J. Finn, *J. Biol. Chem.* **2004**, *279*, 8526–8529.

[73] C. D. Poulter, H. C. Rilling, *Am. Chem. Soc.* **1978**, *11*, 307–313.

[74] J. Bohlmann, G. Meyer Gauen, R. Croteau, *Proc. Natl. Acad. Sci. U. S. A.* **1998**, *95*, 4126–4133.

[75] Z. Yoosuf-Aly, J. A. Faraldos, D. J. Miller, R. K. Allemann, *Chem. Commun.* **2012**, *48*, 7040–7042.

[76] M. A. Phillips, M. R. Wildung, D. C. Williams, D. C. Hyatt, R. Croteau, *Arch. Biochem. Biophys.* **2003**, *411*, 267–276.

[77] G. J. Blomquist, R. Figueroa Teran, M. Aw, M. Song, A. Gorzalski, N. L. Abbott, E. Chang, C. Tittiger, *Insect Biochem. Mol. Biol.* **2010**, *40*, 699–712.

[78] D. T. Nguyen, J. C. Göpfert, N. Ikezawa, G. Macnevin, M. Kathiresan, J. Conrad, O. Spring, D. K. Ro, *J. Biol. Chem.* **2010**, *285*, 16588–16598.

[79] J. W. De Kraker, M. C. R. Franssen, M. Joerink, A. De Groot, H. J. Bouwmeester, *Plant Physiol.* **2002**, *129*, 257–268.

[80] M. M. Ravn, R. J. Peters, R. M. Coates, R. Croteau, *J. Am. Chem. Soc.* **2002**, *124*, 6998–7006.

[81] M. A. González, *Nat. Prod. Rep.* **2015**, *32*, 684–704.

[82] C. W. Brandt, L. G. Neubauer, *J. Chem. Soc.* **1939**, 1031–1032.

[83] S. C. Trapp, R. B. Croteau, *Genetics* **2001**, *158*, 811–832.

[84] D. W. Christianson, *Curr. Opin. Chem. Biol.* **2008**, *12*, 141–150.

[85] J. Degenhardt, T. G. Köllner, J. Gershenzon, *Phytochem.* **2009**, *70*, 1621–1637.

[86] D. W. Christianson, *Chem. Rev.* **2006**, *106*, 3412–3442.

[87] S. Mecozzi, A. P. West, D. A. Dougherty, *Proc. Natl. Acad. Sci. U. S. A.* **1996**, *93*, 10566–10571.

[88] M. W. Huff, D. E. Telford, *Trends Pharmacol. Sci.* **2005**, *26*, 335–340.

[89] C. L. Steele, J. Crock, J. Bohlmann, R. Croteau, *J. Biol. Chem.* **1998**, *273*, 2078–2089.

[90] D. B. Little, R. B. Croteau, *Arch. Biochem. Biophys.* **2002**, *402*, 120–135.

[91] S. C. Hammer, P. O. Syrén, M. Seitz, B. M. Nestl, B. Hauer, *Curr. Opin. Chem. Biol.* **2013**, *17*, 293–300.

[92] Y. Gao, R. B. Honzatko, R. J. Peters, *Nat. Prod. Rep.* **2012**, *29*, 1153–75.

[93] R. D. Kersten, J. K. Diedrich, J. R. Yates, J. P. Noel, *ACS Chem. Biol.* **2015**, *10*, 2501–2511.

[94] S. Katoh, D. Hyatt, R. Croteau, *Arch. Biochem. Biophys.* **2004**, *425*, 65–76.

[95] K. Back, J. Chappell, *Proc. Natl. Acad. Sci. U. S. A.* **1996**, *93*, 6841–6845.

[96] V. González, D. J. Grundy, J. A. Faraldos, R. K. Allemann, *Org. Biomol. Chem.* **2016**, *14*, 7451–7454.

[97] D. J. Miller, R. K. Allemann, *Nat. Prod. Rep.* **2012**, *29*, 60–71.

[98] H. A. Gennadios, V. Gonzalez, L. Di Costanzo, A. Li, F. Yu, D. J. Miller, R. K. Allemann, D. W. Christianson, *Biochemistry* **2009**, *48*, 6175–6183.

[99] I. Prosser, I. G. Altug, A. L. Phillips, W. A. König, H. J. Bouwmeester, M. H. Beale, *Arch. Biochem. Biophys.* **2004**, *432*, 136–144.

[100] L. C. Tarshis, M. Yan, C. D. Poulter, J. C. Sacchettini, *Biochemistry* **1994**, *33*, 10871–10877.

[101] J. P. Noel, N. Dellas, J. A. Faraldos, M. Zhao, B. A. Hess, J. L. Smentek, R. M. Coates, P. E. O'Maille, *ACS Chem. Biol.* **2010**, *5*, 377–392.

[102] P. Baer, P. Rabe, K. Fischer, C. A. Citron, T. A. Klapschinski, M. Groll, J. S. Dickschat, *Angew. Chem. Int. Ed.* **2014**, *53*, 7652–7656.

[103] E. Y. Shishova, L. Di Costanzo, D. E. Cane, D. W. Christianson, *Biochemistry* **2007**, *46*, 1941–1951.

[104] C. M. Starks, K. Back, J. Chappell, J. P. Noel, *Science* **1997**, *277*, 1815–1820.

[105] C. M. Bertea, J. R. Freije, H. van der Woude, F. W. Verstappen, L. Perk, V. Marquez, J. W. De Kraker, M. A. Posthumus, B. J. Jansen, A. de Groot, et al., *Planta Med.* **2005**, *71*, 40–47.

[106] T. E. Wallaart, H. J. Bouwmeester, J. Hille, L. Poppinga, N. C. A. Maijers, *Planta* **2001**, *212*, 460–465.

[107] J. Li, X. Fang, Q. Zhao, J. Ruan, C. Yang, L. Wang, D. J. Miller, J. A. Faraldos, R. K. Allemann, X. Chen, et al., *Biochem. J.* **2013**, *451*, 417–426.

[108] K. Arnold, L. Bordoli, J. Kopp, T. Schwede, *Bioinformatics* **2006**, *22*, 195–201.

[109] M. Biasini, S. Bienert, A. Waterhouse, K. Arnold, G. Studer, T. Schmidt, F. Kiefer, T. G. Cassarino, M. Bertoni, T. Bordoli, Lorenza Schwede, *Nucleic Acids Res.* **2014**, *42*, 252–258.

[110] P. Benkert, M. Biasini, T. Schwede, *Bioinformatics* **2011**, *27*, 343–350.

[111] L. Olofsson, A. Engström, A. Lundgren, P. E. Brodelius, *BMC Plant Biol.* **2011**, *11*, 45–57.

[112] G. D. Brown, L. K. Sy, *Tetrahedron* **2007**, *63*, 9548–9566.

[113] K. H. Teoh, D. R. Polichuk, D. W. Reed, P. S. Covello, *Botany* **2009**, *87*, 635–642.

[114] Y. Zhang, K. H. Teoh, D. W. Reed, L. Maes, A. Goossens, D. J. H. Olson, A. R. S. Ross, P. S. Covello, *J. Biol. Chem.* **2008**, *283*, 21501–21508.

[115] G. D. Brown, L. K. Sy, *Tetrahedron* **2004**, *60*, 1139–1159.

[116] G. D. Brown, L. K. Sy, *Tetrahedron* **2004**, *60*, 1125–1138.

[117] T. Wallaart, van Uden W, H. Lubberink, H. Woerdenbag, N. Pras, W. Quax, *J. Nat. Prod.* **1999**, *62*, 430–433.

[118] T. Wallaart, N. Pras, W. Quax, *J. Nat. Prod.* **1999**, *62*, 1160–1162.

[119] T. You You, N. Mu Yun, Z. Yu Rong, L. Lan Na, C. Shu Lian, Z. Mu Qun, W. Xiu Zhen, J. Zheng, L. Xiao Tian, *Planta Med.* **1982**, *44*, 143–145.

[120] A. Akhila, K. Rani, R. S. Thakur, *Phytochem.* **1990**, *29*, 2129–2132.

[121] F. Bohlmann, T. Gerke, J. Jakupovic, R. M. King, H. Robinson, *Phytochem.* **1984**, *23*, 1183–1184.

[122] J. A. Connolly, R. A. Hill, *Dictionary of Terpenoids*, Chapman And Hall/CRC Press, **1991**.

[123] H. J. Bouwmeester, T. E. Wallaart, M. H. a Janssen, B. Van Loo, B. J. M. Jansen, M. a. Posthumus, C. O. Schmidt, J. W. De Kraker, W. a. König, M. C. R. Franssen, *Phytochem.* **1999**, *52*, 843–854.

[124] Y. J. Chang, S. H. Song, S. H. Park, S. U. Kim, *Arch. Biochem. Biophys.* **2000**, *383*, 178–184.

[125] S. H. Kim, K. Heo, Y. J. Chang, S. H. Park, S. K. Rhee, S. U. Kim, *J. Nat. Prod.* **2006**, *69*, 758–762.

[126] P. Mercke, M. Bengtsson, H. J. Bouwmeester, M. a Posthumus, P. E. Brodelius, *Arch. Biochem. Biophys.* **2000**, *381*, 173–180.

[127] S. Picaud, L. Olofsson, M. Brodelius, P. E. Brodelius, *Arch. Biochem. Biophys.* **2005**, *436*, 215–226.

[128] S. Picaud, P. Mercke, X. He, O. Sterner, M. Brodelius, D. E. Cane, P. E. Brodelius, *Arch. Biochem. Biophys.* **2006**, *448*, 150–155.

[129] T. Townsend, V. Segura, G. Chigeza, T. Penfield, A. Rae, D. Harvey, D. Bowles, I. A. Graham, *PLoS One* **2013**, *8*, 1–11.

[130] T. R. Larson, C. Branigan, D. Harvey, T. Penfield, D. Bowles, I. A. Graham, *Ind. Crops Prod.* **2013**, *45*, 1–6.

[131] W. K. Milhous, P. J. Weina, *Science* **2010**, *327*, 279–280.

[132] I. A. Graham, K. Besser, S. Blumer, C. A. Branigan, T. Czechowski, L. Elias, I. Guterman, D. Harvey, P. G. Isaac, A. M. Khan, et al., *Science* **2010**, *327*, 328–331.

[133] J.-M. Kindermans, J. Pilloy, P. Olliaro, M. Gomes, *Malar. J.* **2007**, *6*, 125.

[134] R. Shretta, P. Yadav, *Malar. J.* **2012**, *11*, 399.

[135] J. S. Yadav, B. Thirupathaiah, P. Srihari, *Tetrahedron* **2010**, *66*, 2005–2009.

[136] M. A. Avery, W. K. M. Chong, C. Jennings-White, *J. Am. Chem. Soc.* **1992**, *114*, 974–979.

[137] P. J. Westfall, D. J. Pitera, J. R. Lenihan, D. Eng, F. X. Woolard, R. Regentin, T. Horning, H. Tsuruta, D. J. Melis, A. Owens, et al., *Proc. Natl. Acad. Sci. U. S. A.* **2012**, *109*, 111–118.

[138] D.-K. Ro, E. M. Paradise, M. Ouellet, K. J. Fisher, K. L. Newman, J. M. Ndungu, K. A. Ho, R. A. Eachus, T. S. Ham, J. Kirby, et al., *Nature* **2006**, *440*, 940–943.

[139] C. J. Paddon, P. J. Westfall, D. J. Pitera, K. Benjamin, K. Fisher, D. McPhee, M. D. Leavell, A. Tai, A. Main, D. Eng, et al., *Nature* **2013**, *496*, 528–532.

[140] J. A. Dietrich, Y. Yoshikuni, K. J. Fisher, F. X. Woolard, D. Ockey, D. J. McPhee,

N. S. Renninger, M. C. Y. Chang, D. Baker, J. D. Keasling, *ACS Chem. Biol.* **2009**, *4*, 261–267.

[141] F. Lévesque, P. H. Seeberger, *Angew. Chem. Int. Ed.* **2012**, *51*, 1706–1709.

[142] A. A. Frimer, *Chem. Rev.* **1979**, *79*, 359–387.

[143] O. Cascón, S. Touchet, D. J. Miller, V. Gonzalez, J. A. Faraldos, R. K. Allemann, *Chem. Commun.* **2012**, *48*, 9702–9704.

[144] W. S. Bowers, C. Nishino, M. E. Montgomery, L. R. Nault, M. W. Nielson, *Science* **1977**, *196*, 1121–1122.

[145] B. E. Maryanoff, A. B. Reitz, *Chem. Rev.* **1989**, *89*, 863–927.

[146] M. A. Birkett, S. A. Abassi, T. Kröber, K. Chamberlain, A. M. Hooper, P. M. Guerin, J. Pettersson, J. A. Pickett, R. Slade, L. J. Wadhams, *Phytochem.* **2008**, *69*, 1710–1715.

[147] R. Mozuraitis, M. Stranden, M. I. Ramirez, a-K. Borg-Karlson, H. Mustaparta, *Chem. Senses* **2002**, *27*, 505–9.

[148] K. A. Rising, C. M. Crenshaw, H. J. Koo, T. Subramanian, K. A. H. Chehade, C. Starks, K. D. Allen, D. A. Andres, H. P. Spielmann, J. P. Noel, et al., *ACS Chem. Biol.* **2015**, *10*, 1729–1736.

[149] N. J. White, *Trends Parasitol.* **2004**, *113*, 1084–1092.

[150] J. A. Faraldos, V. González, M. Senske, R. K. Allemann, D. E. Cane, P. C. Prabhakaran, E. J. Salaski, P. H. M. Harrison, H. Noguchi, B. J. Rawlings, et al., *Org. Biomol. Chem.* **2011**, *9*, 6920.

[151] H. Liu, J. H. Naismith, *BMC Biotechnol.* **2008**, *8*, 91.

[152] K. Mierzejewska, W. Siwek, H. Czapinska, M. Kaus-Drobek, M. Radlinska, K. Skowronek, J. M. Bujnicki, M. Dadlez, M. Bochtler, *Nucleic Acids Res.* **2014**, *42*, 8745–8754.

[153] B. R. Palmer, M. G. Marinus, *Gene* **1994**, *143*, 1–12.

[154] P. E. O'Maille, J. Chappell, J. P. Noel, *Anal. Biochem.* **2004**, *335*, 210–217.

[155] M. M. Bradford, *Anal. Biochem.* **1976**, *72*, 248–254.

[156] T. Zor, Z. Selinger, *Anal. Biochem.* **1996**, *236*, 302–308.

[157] E. J. Loveridge, R. J. Rodriguez, R. S. Swanwick, R. K. Allemann, *Biochemistry* **2009**, *48*, 5922–5933.

[158] G. Holzwarth, P. Doty, *J. Am. Chem. Soc.* **1965**, *87*, 218–228.

[159] C. A. Lesburg, *Science* **1997**, *277*, 1820–1824.

[160] N. Greenfield, *Nat. Protoc.* **2007**, *1*, 2876–2890.

[161] J. A. Faraldos, V. Gonzalez, A. Li, F. Yu, M. Koksal, D. W. Christianson, R. K. Allemann, *J. Am. Chem. Soc.* **2012**, *134*, 20844–20848.

[162] P. Muangphrom, M. Suzuki, H. Seki, E. O. Fukushima, T. Muranaka, *Plant Biotechnol.* **2014**, *31*, 483–491.

[163] D. a Whittington, M. L. Wise, M. Urbansky, R. M. Coates, R. B. Croteau, D. W. Christianson, *Proc. Natl. Acad. Sci. U. S. A.* **2002**, *99*, 15375–15380.

[164] J. Crock, M. Wildung, R. Croteau, *Proc. Natl. Acad. Sci. U. S. A.* **1997**, *94*, 12833–12838.

[165] J. A. Faraldos, D. J. Miller, V. González, Z. Yoosuf-Aly, O. Cascón, A. Li, R. K. Allemann, *J. Am. Chem. Soc.* **2012**, *134*, 5900–5908.

[166] D. E. Cane, H. T. Chiu, P. H. Liang, K. S. Anderson, *Biochemistry* **1997**, *36*, 8332–8339.

[167] E. W. Collington, A. I. Meyers, *J. Org. Chem.* **1971**, *36*, 3044–3045.

[168] S. R. Choi, M. Breugst, K. N. Houk, C. D. Poulter, *J. Org. Chem.* **2014**, *79*, 3572–3580.

[169] V. J. Davisson, A. B. Woodside, T. R. Neal, K. E. Stremler, M. Muehlbacher, C. D. Poulter, *J. Org. Chem.* **1986**, *51*, 4768–4779.

[170] R. K. Keller, R. Thompson, *J. Chromatogr.* **1993**, *645*, 161–167.

[171] O. Cascón, G. Richter, R. K. Allemann, T. Wirth, *Chempluschem* **2013**, *78*, 1334–1337.

[172] P. G. M. Wuts, T. W. Greene, *Greene's Protective Groups in Organic Synthesis*, John Wiley And Sons, Inc, **2007**.

[173] K. B. Sharpless, T. R. Verhoeven, *Aldrichimica Acta* **1979**, *12*, 69–70.

[174] M. A. Umbreit, K. B. Sharpless, *J. Am. Chem. Soc.* **1977**, *99*, 5526–5528.

[175] K. A. Parker, T. Iqbal, *J. Org. Chem.* **1987**, *52*, 4369–4377.

[176] J. P. Candlin, A. R. Oldham, *Discuss. Faraday Soc.* **1968**, *46*, 60–72.

[177] J. Bergueiro, J. Montenegro, C. Saa, S. Lopez, *Chem. A Eur. J.* **2012**, *18*, 14100–141107.

[178] K. Surendra, E. J. Corey, *J. Am. Chem. Soc.* **2008**, *130*, 8865–8869.

[179] K. Surendra, W. Qiu, E. J. Corey, *J. Am. Chem. Soc.* **2011**, *133*, 9724–9726.

[180] W. S. Wadsworth, W. D. Emmons, *J. Am. Chem. Soc.* **1961**, *83*, 1733–1738.

[181] W. C. Still, C. Gennari, *Tetrahedron Lett.* **1983**, *24*, 4405–4408.

[182] A. Bhattacharya, G. Thyagarajan, *Chem. Rev.* **1981**, *81*, 415–430.

[183] K. Borszeky, T. Mallat, A. Baiker, *Tetrahedron: Asymmetry* **1997**, *8*, 3745–3753.

[184] K. Mori, *Tetrahedron: Asymmetry* **2007**, *18*, 838–846.

[185] J. D. Moore, P. R. Hanson, *Tetrahedron: Asymmetry* **2003**, *14*, 873–880.

[186] F. Messik, M. Oberthur, *Synth.* **2013**, *45*, 167–170.

[187] S. Fortin, F. Dupont, P. Deslongchamps, *J. Org. Chem.* **2002**, *67*, 5437–5439.

[188] K. Ando, *J. Org. Chem.* **1997**, *62*, 1934–1939.

[189] R. Martin, G. Islas, A. Moyano, M. Pericas, A. Riera, *Tetrahedron* **2001**, *57*, 6367–6374.

[190] V. J. Davisson, D. R. Davis, V. M. Dixit, C. D. Poulter, *J. Org. Chem.* **1987**, *52*,

1794–1801.

[191] D. S. Rawat, R. A. Gibbs, *Org. Lett.* **2002**, *4*, 3027–3030.

[192] F. Sum, L. Weiler, *Can. J. Chem.* **1979**, *57*, 1431–1441.

[193] R. A. Gibbs, U. Krishnan, J. M. Dolence, C. D. Poulter, *J. Org. Chem.* **1995**, *60*, 7821–7829.

[194] T. J. Zahn, C. Weinbaum, R. A. Gibbs, *Bioorganic Med. Chem. Lett.* **2000**, *10*, 1763–1766.

[195] R. C. D. Brown, C. J. Bataille, R. M. Hughes, A. Kenney, T. J. Luker, *J. Org. Chem.* **2002**, *67*, 8079–8085.

[196] X. Dong, X. Wang, M. Lin, H. Sun, X. Yang, Z. Guo, *Inorg. Chem.* **2010**, *49*, 2541–2549.

[197] M. Nagaki, M. Nakada, T. Musashi, J. Kawakami, N. Ohya, M. Kurihara, Y. Maki, T. Nishino, T. Koyama, *Biosci. Biotechnol. Biochem.* **2007**, *71*, 1657–1662.

[198] J. A. Marco, J. Garcia-Pla, M. Carda, J. Murga, E. Falomir, C. Trigili, S. Notararigo, J. F. Diaz, I. Barasoain, *Eur. J. Med. Chem.* **2011**, *46*, 1630–1637.

[199] T. S. Feng, E. M. Guantai, M. J. Nell, C. E. J. Van Rensburg, H. C. Hoppe, K. Chibale, *Bioorganic Med. Chem. Lett.* **2011**, *21*, 2882–2886.

[200] T. Nguyen Le, W. M. De Borggraeve, P. Grellier, V. C. Pham, W. Dehaen, V. H. Nguyen, *Tetrahedron Lett.* **2014**, *55*, 4892–4894.

[201] G. R. Labadie, R. Viswanathan, C. D. Poulter, *J. Org. Chem.* **2007**, *72*, 9291–9297.

[202] K. Janthawornpong, S. Krasutsky, P. Chaignon, M. Rohmer, D. Poulter, M. Seemann, *J. Am. Chem. Soc.* **2014**, *135*, 1–52.

[203] K. Tago, E. Minami, K. Masuda, T. Akiyama, H. Kogen, *Bioorganic Med. Chem.* **2001**, *9*, 1781–1791.

[204] T. C. Turek, I. Gaon, D. Gamache, M. D. Distefano, *Bioorganic Med. Chem. Lett.* **1997**, *7*, 2125–2130.

[205] R. Pelagalli, I. Chiarotto, M. Feroci, S. Vecchio, *Green Chem.* **2012**, *14*, 2251–2255.

[206] P. J. Linstrom, W. G. Mallard, *NIST Chemistry WebBook, NIST Standard Reference Database Number 69*, National Institute Of Standards And Technology, Gaithersburg MD, 20899, **2016**.

[207] J. Faraldos, V. Gonzalez, A. Li, *J. Am. Chem. Soc.* **2012**, *134*, 20844–20848.

[208] S. Green, E. N. Friel, A. Matich, L. L. Beuning, J. M. Cooney, D. D. Rowan, E. MacRae, *Phytochem.* **2007**, *68*, 176–188.

[209] F. K. Davies, V. H. Work, A. S. Beliaev, M. C. Posewitz, *Front. Bioeng. Biotechnol.* **2014**, *2*, 21.

[210] L. K. Sy, G. D. Brown, *Magn. Reson. Chem.* **1990**, *35*, 424–425.

[211] W. Kreiser, F. Körner, *Helv. Chim. Acta* **1999**, *82*, 1427–1433.

[212] M. Tori, M. Aoki, Y. Asakawa, *Phytochem.* **1994**, *36*, 73–76.

[213] C. Walsh, *Tetrahedron* **1982**, *38*, 871–909.

[214] D. E. Cane, C. Bryant, *J. Am. Chem. Soc.* **1994**, *116*, 12063–12064.

[215] M. Peplow, *Nature* **2016**, *530*, 389–390.

[216] M. W. Rose, N. D. Rose, J. Boggs, S. Lenevich, J. Xu, G. Barany, M. D. Distefano, *J. Pept. Res.* **2005**, *65*, 529–537.

[217] V. J. Davisson, A. B. Woodside, T. R. Neal, K. E. Stremler, M. Muehlbacher, C. D. Poulter, *J. Org. Chem.* **1986**, *51*, 4768–4779.

[218] V. Birault, G. Pozzi, N. Plobeck, S. Eifler, M. Schmutz, T. Palanché, J. Raya, A. Brisson, Y. Nakatani, G. Ourisson, *Chem. - A Eur. J.* **1996**, *2*, 789–799.

[219] S. Touchet, K. Chamberlain, C. M. Woodcock, D. J. Miller, M. A. Birkett, J. A. Pickett, R. K. Allemann, *Chem. Commun.* **2015**, *51*, 7550–7553.

[220] V. Koppaka, D. C. Thompson, Y. Chen, M. Ellermann, K. C. Nicolaou, R. O. Juvonen, D. Petersen, R. A. Deitrich, T. D. Hurley, V. Vasiliou, *Pharmacol. Rev.* **2012**, *64*, 520–539.

[221] H. E. N. Bergmans, I. M. Van Die, W. P. M. Hoekstra, *J. Bacteriol.* **1981**, *146*, 564–570.

[222] G. Bertani, *J. Bacteriol.* **1951**, *62*, 293–300.

[223] J. A. Meyers, D. Sanchez, L. P. Elwell, S. Falkow, *J. Bacteriol.* **1976**, *127*, 1529–1537.

[224] J. A. Bornhorst, J. J. Falke, *Methods Enzymol.* **2000**, 245–254.

[225] A. L. Shapiro, E. Viñuela, J. V. Maizel, *Biochem. Biophys. Res. Commun.* **1967**, *28*, 815–820.

[226] R. J. Ritchie, T. Prvan, *Biochem. Educ.* **1996**, *24*, 196–206.

[227] H. Lineweaver, D. Burk, *J. Am. Chem. Soc.* **1934**, *56*, 658–666.

[228] K. Johnson, R. Goody, *Biochemistry* **2012**, *50*, 8264–8269.